SANDIA REPORT
SAND86–2527 • UC–70
Unlimited Release
Printed May 1987

Subseabed Disposal Project Annual Report, FY85 to Termination of Project: Physical Oceanography and Water Column Geochemistry Studies October 1984 Through May 1986

S. L. Kupferman, Editor

Prepared by
Sandia National Laboratories
Albuquerque, New Mexico 87185 and Livermore, California 94550
for the United States Department of Energy
under Contract DE-AC04-76DP00789

Issued by Sandia National Laboratories, operated for the United States Department of Energy by Sandia Corporation.

Printed in the United States of America
Available from
National Technical Information Service
U.S. Department of Commerce
5285 Port Royal Road
Springfield, VA 22161

NTIS price codes
Printed copy: A15
Microfiche copy: A01

SAND86-2527
Unlimited Release

Distribution
Category UC-70

SUBSEABED DISPOSAL PROJECT ANNUAL REPORT, FY85 TO TERMINATION OF PROJECT: PHYSICAL OCEANOGRAPHY AND WATER COLUMN GEOCHEMISTRY STUDIES OCTOBER 1984 THROUGH May 1986

S. L. Kupferman, Editor

ABSTRACT

This report covers the work of the Physical Oceanography and Water Column Geochemistry (POWCG) Studies Group of the Subseabed Disposal Project (SDP) from October 1984 to termination of the project in May 1986. The overview of the work includes an introduction, general descriptions of the activities, and a summary. Detailed discussions are included as appendices. During the period of this report the POWCG Studies Group held a meeting to develop a long-term research plan for the Nares Abyssal Plain, which was recently designated as a study area for the Environmental Study Group of the SDP. The POWCG Studies Group has also planned and participated in two interdisciplinary oceanographic missions to the Nares which have resulted in the acquisition of data and samples which can be used to begin to understand the workings of the ecosystem at the site, and for developing a preliminary site assessment.

ACKNOWLEDGEMENT

I want to thank J. K. Cochran, J. Dymond, E. P. Laine, H. D. Livingston, R. D. Pillsbury, and S. C. Riser, principal investigators for the Physical Oceanography and Water Column Geochemistry Studies Group, and their staffs, for their cooperation and dedication. I also thank the following persons for their cooperation and dedication: L. S. Gomez and M. G. Marietta, my SNLA collegues in the Environmental Studies Group; A. R. Robinson, principal physical oceanography consultant; D. P. Garber, technical writer. It was a pleasure to work with all of them.

CONTENTS

CONTENTS (Continued)

ILLUSTRATION

SUBSEABED DISPOSAL PROJECT ANNUAL REPORT, FY85 TO TERMINATION OF PROJECT: PHYSICAL OCEANOGRAPHY AND WATER COLUMN GEOCHEMISTRY STUDIES OCTOBER 1984 THROUGH MAY 1986

Introduction

This is the report of the Physical Oceanography and Water Column Geochemistry (POWCG) Studies Group of the Subseabed Disposal Project (SDP) for FY85 (October 1984 through September 1985) to termination of the POWCG contractors' work in May 1986.

During the period of this report the POWCG has

- Analyzed samples and data collected during the Nares I Mission to the Nares Abyssal Plain (Figure 1)

- Held a planning meeting to develop a six-year research plan for the Nares Abyssal Plain

- Planned and staged a second interdisciplinary (physical oceanography, water column geochemistry, environmental modeling, and biology) mission (November 1985) to the Nares Abyssal Plain (current meter results are discussed in Appendix E and radon results in Appendix H).

The POWCG Studies Group, the Biological Oceanography (BO) Group, and the Environmental Modeling (EM) Group comprise the Environmental Studies Group, whose area of responsibility is the environmental characterization of the world's oceans as they relate to subseabed disposal.

The three components of the Environmental Studies Group work together to provide data required to assess radiological impact of seabed disposal on the ecosystem in general and on human beings in particular. A functioning subseabed repository could have

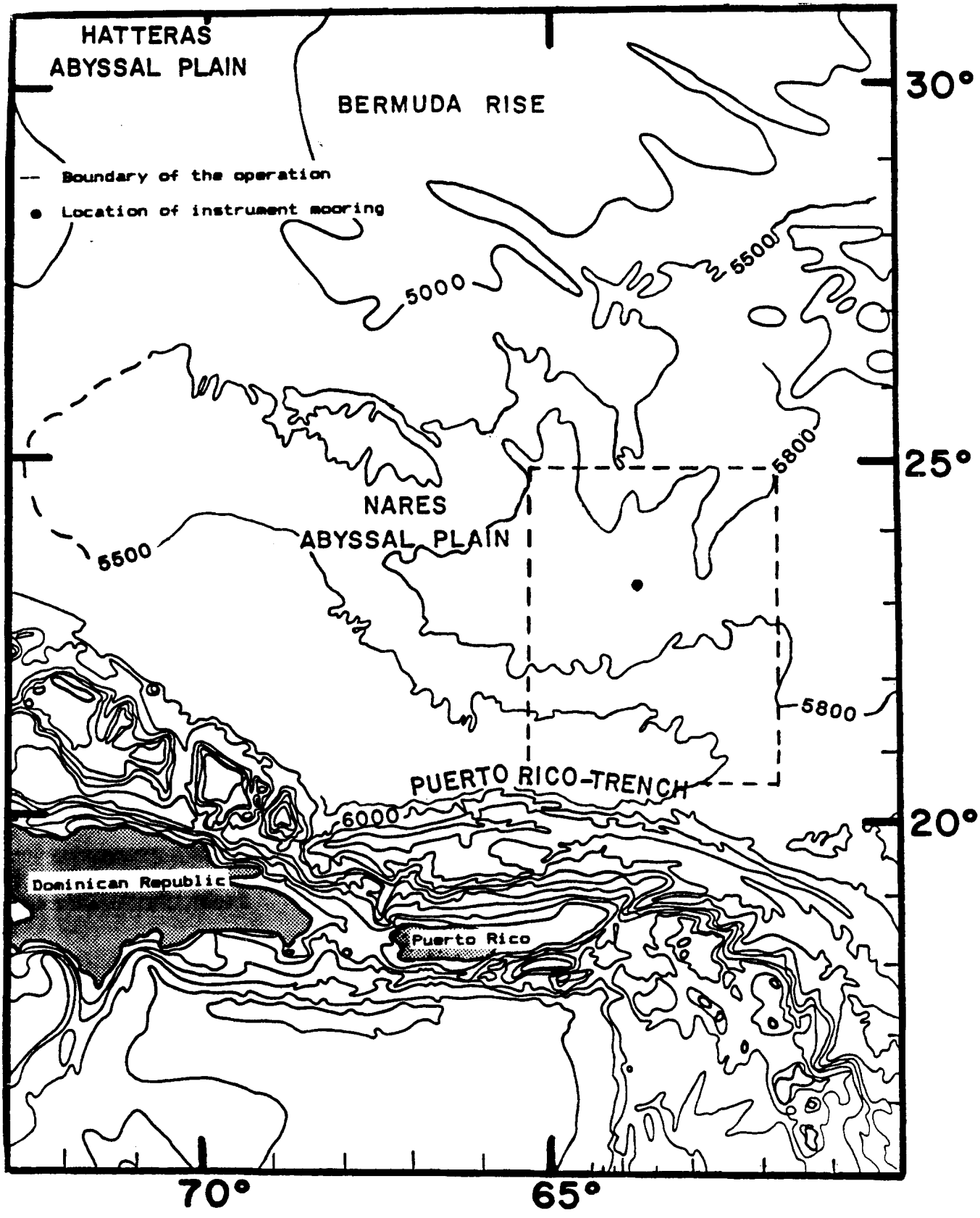

Figure 1. Location map of the second interdisciplinary mission to the Nares (depths in meters)

radiological impact on the ecosystem in a number of ways. Even a repository that completely satisfies all its performance criteria could eventually release small amounts of radioactive material into the surrounding ocean environment. Moreover, a few waste canisters could be improperly emplaced or the hole over an emplaced canister might not close properly. A low-probability accident involving a canister or a transport ship could result in leakage from canisters lying on the deep seafloor (It is assumed economically feasible to remove canisters accidentally placed in shallow water). In each of these cases, the environment would be affected through seawater contamination.

The EM Group is responsible for developing ocean transport models to reliably predict the impact of releases on the environment and humans. The POWCG and BO groups provide basic data that contribute to model development and validation, and which provide necessary information for characterizing potential sites. The POWCG and BO groups also study, or promote the study of, important processes that control movement of bottom-source tracers back to humans; the objective is to obtain a sufficiently complete understanding of the physics, chemistry, and biology of these processes to be able to determine under what circumstances they should be included in our ocean transport models and site characterizations. An example of a complex of such processes is the transport characteristics of deep western boundary currents and their exchange with the ocean interior. Such currents could provide a potential avenue for rapid transport to the deeply mixed waters of the Antarctic ocean.

The ocean transport models are for the most part up and running in their basic versions, and more advanced versions are being developed. Areas where sufficient data are available have been selected to validate the models. Also, site-specific application of the models has begun at locations chosen for their scientific or site interest. At one such location, the Nares Abyssal Plain in the western North Atlantic ocean, the SDP has established a long-term

observation program to characterize the mean flow, deep dispersion, and water column geochemical properties of the Nares region. The international Seabed Working Group (SWG) is sponsoring a similar study just east of Great Meteor Seamount (west of the Canary Islands). This work is in addition to the continuing international observation program at the present low-level dump site in the eastern North Atlantic. Exchange of physical oceanographic data among members of the SWG for model-model intercomparison is also in progress.

Activities

Planning Meeting for the Nares Abyssal Plain Long-Term Reasearch Plan

Sandia National Laboratories' (SNLA) staff, contractors, and consultants met in Albuquerque, NM, on March 14 and 15, 1985, to develop plans for a six-year interdisciplinary research program at the Nares Abyssal Plain. The Nares has been selected as the site at which the SDP will validate environmental models and perform a site characterization for the 1990 status document. In addition, the Nares work will be structured so that it can be used to develop techniques and tools to efficiently and cost-effectively produce a reliable risk assessment and site characterization (including model validation) for any location likely to be selected as a potential repository site. Results of this meeting are summarized in Appendix A.

Analysis of Data and Samples from the Nares I Oceanographic Mission

The purpose of this mission (September 19 to October 1, 1984) was to conduct an interdisciplinary reconnaissance of the Nares Region, which had at that time recently been designated a study area for the Environmental Studies Group. A summary of the work aboard ship is in last year's annual report (Kupferman, 1987). The following is an overview of the results of sample and data analysis contained in the appendices and references of this report. The

information obtained on the Nares Mission, along with a historical summary and synthesis of the physical oceanographic observations in the region, was used as background material for developing the Nares Abyssal Plain long-term research plan discussed in Appendix A.

The work on this mission consisted of a mooring recovery and deployment, hydrography, in-situ pumping and large-volume water sampling, coring, and exercising the onboard, real-time prediction system, using the Harvard open-ocean, regional-eddy-resolving model. The results and significance of this work are summarized below. Additional material is in the references and appendices.

Mooring work--A current-meter, sediment-trap transmissometer mooring deployed in August 1983 was recovered and replaced with a similar mooring containing more sediment traps for better definition of vertical particle fluxes.

The current meter data significantly increased information available about currents in the region (Pillsbury et al., 1986). The mean direction of flow was toward the northeast at all measured depths, which were between 725 m and 5800 m (the latter was 50 m above the bottom). Mean velocities were on the order of 1 cm/sec, while mean speeds were about 5 cm/sec. Maximum speeds observed in the deep water (2950 m and below) were about 10 cm/sec over the 400-day period that the mooring was in place. In the deep water, vertical coherence was very high at low frequency (i.e., less than 0.1 cycle/day). Most of the variance in the current meter records occurs at periods greater than 50 days. The major tidal energy is at the semi-diurnal frequency (at 5800 m, semi-major axis of m_2 component, 1 cm/sec at 12.42 hour period; S_2 component, 0.4 cm/sec at 12.00 hr period) with significant energy at the diurnal frequency (K_1 component, 0.3 cm/sec at 23.93 hr period) (Pillsbury, 1986).

All information supports initial suppositions that the Nares Abyssal Plain is a relatively inactive region where nontidal current patterns are dominated by intermittant, low-frequency (mesoscale)

activity. Measurements of at least several years' duration will be required to establish stable, mean-current-velocity values. This conclusion is supported by Nares II moorings results, which are discussed below and in Appendix E.

A quick look at data from the recovered sediment traps reported last year (Kupferman, 1987) showed that both upward and downward biogenic bulk fluxes were relatively low for an open ocean site, reflecting the low primary productivity at this central gyre location. This year the sediment trap samples were analyzed for mass, organic carbon, nitrogen, phosphores, calcium carbonate, opal, and other major and minor elements (see Appendix B). Subsamples were subjected to radiochemical analyses (see Appendices C and D).

The biogenic particle flux at Nares is lower than that near Bermuda by nearly a factor of two, implying very low biological productivity. Seasonal flux varies by a factor of two and the maximum flux is associated with high biological production in the spring and summer. Most flux values covary in the upper (1500-m) and lower (4800-m) traps, reflecting the rapid transport of surface-derived material to the deep ocean. There is also evidence that the horizontal transport of sediments from other depositional environments is occurring. The Nares Abyssal Plain lies directly beneath the trajectory of dust carried from the Sahara on the northeast trade winds; thus, the total fraction and net flux of terrigenous components are relatively high.

The upward flux of material collected by the inverted sediment trap at 4865 m was very low (typically three orders of magnitude less than fluxes downward) and lower than upward fluxes measured at other sites. This may be a consequence of the lower productivity at this site, which supports fewer abyssal organisms that produce buoyant particles. No apparent relationship exists between the downward organic carbon flux and the upward bulk flux. Buoyant particles do not appear to provide a significant upward transport vector at the Nares site (see Appendix B).

Hydrography--The hydrographic work consisted of conductivity, temperature, depth (CTD) profiles, along with simultaneous light-transmission and dissolved-oxygen profiles. These CTD/light-transmission/dissolved-oxygen profiles will be referred to hereafter as CTD profiles. Measurements are made in real time and transmitted by cable to the ship's laboratory.

During the profiles, water samplers on the profiling instrument are tripped remotely to collect point water samples (typically 12 to 24) for calibration of the CTD and to measure compounds such as silicate, for which chemical analyses must be conducted aboard ship. All information is used to analyze the property structure of water in a particular region, in order to characterize sources of water found in the region and the long-term water circulation patterns (years to hundreds of years). CTD data are also used to calculate water density as a function of depth, and this information can be used at successive measurement stations in the geostrophic approximation to calculate short-term currents in a region. The results of these dynamical calculations were used for initializing and validating mesoscale models. Knowledge of the current-field and long-term circulation in a region through hydrographic and current-meter measurements is important for interpreting geochemical and biological data and is thus an important first step in providing background for understanding the dynamics of a region's ecosystem.

It was originally planned to obtain ten CTD profiles and 22 XBT* profiles in a 90-km-per-side square grid centered at the mooring. These data, in conjunction with the geostrophic approximation, would be used to calculate currents for initializing the regional-eddy-

*The Expendable Bathythermograph is an expendable profiling instrument to measure temperature as a function of depth, typically to a depth of 750 m, to supplement CTD data for dynamical calculations and other purposes. XBTs save time because measurements can be made while the ship is underway. The ship must be stopped to take CTD profiles, which require five to six hours in the 6000-m Nares region depths.

resolving model. The CDT and XBT profiles were to be repeated after several days to check the accuracy of the model predictions. Unfortunately, the CTD cable experienced irreparable electrical failure after six CTDs, so it was impossible to carry out the program as planned. The initial grid pattern was completed using XBTs. It was decided that the most effective use of remaining time would be to examine the deep water mass structure south of the mooring in an attempt to locate the western boundary undercurrent and to determine the water types moving through the general area.

This program could be carried out with the nonconducting, hydrographic wire and water sampling equipment on board. Since the SDP is primarily concerned with bottom sources, sampling was concentrated in the deep water column from 4000 m to the bottom (about 6000 m).

Temperature salinity (θ-S) plots from CTD data were compared to a standard θ-S curve (Armi and Bray, 1982) for the western North Atlantic (see Laine, 1985). Our θ-S curves closely tracked the standard curve with slight deviations at 7°C and 5.4°C (about 950 m and 1150 m, respectively), due to slightly stronger admixtures of fresher Antarctic intermediate water at 7°C and saltier Mediterranian outflow water at 5.4°C. These water mass signals were about as expected for this location. Bottom mixed layers were observed in all CTDs for which near-bottom data were available (five out of six). These layers were very weak; the temperature signal was only a few millidegrees and the layer thicknesses ranged between 30 m and 65 m. Usually, the layers were most clearly evident in the light-transmission vs. depth plots.

A possible explanation for the weakness of the bottom mixed layers is that currents in the deep water were very weak at the time of the Nares mission, as indicated by the records from the recovered current meters (Pillsbury et al., 1986). Thus, any intrusion of bottom water from outside the region would have been slow, and there would not have been much kinetic energy available in the bottom

currents to convert to turbulence for vertically mixing the near-bottom waters.

By examining near-bottom water characteristics for temperature, salinity, silica, and oxygen data (see Laine, 1985) we hoped to discern the presence of the western boundary undercurrent, which is thought to flow to the east through the southern portion of the study area. A clear-cut indication of its presence was not found, presumably due to the complexity of the flow field in the region and to the wide station spacing (40 km) in the southern part of the region.

Pumping and large-volume water sampling--Pumping and large-volume water sampling are a part of the water column geochemistry program. The program's objectives are to develop and validate geochemical transport models and to assist in producing a site characterization for the Nares region.

In-situ pumps are used to sample large volumes of seawater (order of 1000 ℓ) for reactive chemical species, specifically, naturally-occurring thorium isotopes and the artificial radionuclides Pu and ^{241}Am. The concentration of these species is low in seawater; the pumps allow more accurate and precise analyses through the collection of larger samples than is possible by the collection and onboard processing of bulk water samples.

The pumps force water through a 1-micron filter cartridge and then through two identical cartridges previously coated with manganese dioxide (MnO_2). The first cartridge functions as a prefilter to collect suspended particulates and the two MnO_2 cartridges absorb the nuclides of interest from seawater. Analysis of both MnO_2 cartridges determines the chemical extraction efficiency and, coupled with the measured volume pumped, the concentration of radionuclide in solution.

The pumps are self contained and battery powered. Several pumps are lowered to different depths on the ship's hydrographic wire and left in place for several hours in order to collect samples. Timers turn the pumps on and off at sampling depth. A similar system with an onboard pump is available for collecting near-surface samples on station or when the ship is underway.

Large-volume water samples (60ℓ) are collected to determine dissolved Pu, ^{137}Cs, and ^{90}Sr (which are not efficiently absorbed by the MnO_2 cartridges) and for backup samples for the pumped radioisotope samples.

Pumping and large-volume water sampling are the responsibility of J. K. Cochran and H. D. Livingston, who are also working with radioisotopes in the sediment trap samples and in bottom sediments. After additional sampling, their work will result in a comprehensive picture of the distribution of thorium isotopes, ^{210}Pb, fallout transuranics, and ^{137}Cs in the water column (including particle-associated phases) and sediments at the Nares site.

The significance to the SDP is that this information can be used to define several parameters necessary to build a geochemical scavenging component into the physical modeling effort. These parameters are not restricted to the specific nuclides involved. The suite of nuclides studied spans a range of chemical reactivities with respect to scavenging; in many instances, these are critical radionuclides in high-level waste forms--or represent very close chemical relatives of critical nuclides. Thus the data set will be applicable to the selection of geochemical modeling parameters which are relevant, realistic, and based on real oceanic measurements as opposed to laboratory experiment extrapolations.

Fallout radionuclides also appear to be useful deep-water tracers for studying interaction of the deep western boundary current with the ocean interior at the Nares site. This interaction is a key component of the deep mixing processes which disperse a

waste signal introduced to the bottom water in the ocean interior from a site on the western side of an ocean basin. Tracers, which can establish the rates of such processes, will provide highly relevant input to the deep circulation modeling effort. This work is discussed in Appendices C and D.

Core Samples--The 1.8 m gravity core was analyzed for chemical composition (Appendix B) and for ^{238}U, ^{234}U, ^{232}Th, and ^{230}Th (Appendix C). The depth distribution of unsupported ^{230}Th, the isotope normally used to measure sediment accumulation rates, does not decrease regularly with depth, but shows alternating zones of high and low activity. No meaningful accumulation rate can be derived from these results. These data are similar to data of Thompson et al. (1984) in cores from the Nares, which led them to conclude that turbidite sedimentation strongly affects the stratigraphy of the site. The Nares core supports this conclusion and fosters belief that as much as 170 cm (of the 180 cm) of sediment found in the core must have been deposited relatively rapidly (over about ten thousand years), perhaps as a series of turbidite deposits separated by poorly defined periods of pelagic sedimentationn (a detailed discussion of these matters is contained in an addenda to Appendix H).

The pelagic sedimentation rate derived from the slowly accumulating "red clay" sequences studied by Thompson et al. (1984) was 0.3-0.7 mg/cm^2y. This "base" value is consistent with the range of terrigenous fluxes collected by the sediment traps (Appendix B).

^{241}Am analyses were completed on surficial sections of the sediment cores collected by the Research Vessel Tyro from the Nares site for which $^{239,240}Pu$, ^{137}Cs, and ^{210}Pb data were reported in the FY84 annual report (Kupferman, 1987). Concentrations and, consequently, sediment nuclide inventories are very low. Thus, the picture of the Nares area as a sedimentary regime receiving a very small flux of material from the surface ocean holds for ^{241}Am, as

well as for the other, less reactive fallout nuclides and the biogenic flux. The fact that the mean $^{241}Am/^{239,240}Pu$ ratio is elevated two to three times over that which would characterize integrated global fallout supplied to the surface ocean results from the supply of ^{241}Am-enriched, large sinking particles. The sediments are, however, still a very minor sink for the fallout transuranic inventory (Appendix D).

Mesoscale Modeling--Modelers from SNLA and Harvard University participated in the Nares mission. Their purpose was to assimilate XBT and CTD data into the Harvard-developed, regional-eddy model and forecast the current field in real time. Real-time modeling is important for monitoring, planning, and conducting biological and other types of experiments, and for model validation.

If the current field is known when data are being collected, critical areas for measuring can be inferred which will produce the most efficient monitoring and/or experimental plan, and the best model validation.

In spite of the CTD problem that made it impossible to initialize the model to predict deep current flow, it was possible to assimilate both CTD and XBT data into the shipboard computer in real time and to initialize the model to make predictions of current flow in the upper portion of the water column (less than 750 m depth). These results are discussed in Marietta and Simmons (1986).

The Nares II Oceanographic Mission (November 9 to 27, 1985)

The objective of the mission was to obtain information required to complete the data set for a preliminary ecological assessment of the Nares Abyssal Plain study area. Previous work at the site provided information about the physical oceanographic and water column geochemical structure of the region. The Nares II mission gathered analogous information about important biological features such as primary productivity, zooplankton activity, water column

biological fluxes, population densities of demersal scavangers, microbiology, amino acid concentration, and sediment biological activity--as well as supporting physical and geochemical data. A current-meter, sediment-trap mooring (Nares II) was recovered, extending the record length to 26 months. A similar mooring (Nares III) was deployed in approximately the same location. All information will be used by the SNLA environmental modeling group in developing ocean transport models to predict potential doses of radioactivity from a repository to humans. Biological data will also provide information for the biological carbon model used to verify the consistancy of the experimentally measured and estimated biological fluxes used in ecosystem models.

Planning for the mission took into account recommendations of the meeting for the Nares Abyssal Plain long-term research plan (Appendix A).

The mission had two legs. The first, scheduled for November 9 to 16, was to be primarily devoted to physical geochemical and modeling work; the second, November 17 to 27, primarily to biological and geophysical work. High seas from Hurricane Kate made it impossible to do much of the work planned for the first leg and led to the loss of a critical piece of equipment, the CTD/Rosette/Transmissometer System. As a result of these difficulties, the scientific party's makeup and work plan for the second leg were modified to insure that the critical task of recovering the mooring was accomplished, while maintaining the integrity of the biological work plan. Although bad weather delayed the second-leg departure for two days, the dedication and cooperation of the scientific parties of both legs made it possible to accomplish most of the mission objectives, although the abbreviated time schedule was a serious constraint that impacted all areas of work. The preliminary results of the shipboard work will be discussed briefly below. A more detailed discussion is in the cruise report by the chief scientists for the mission (Shephard and Laine, 1987).

Funding for the Atlantic Ocean field program was terminated shortly after the completion of the cruise; as a result the laboratory analysis of data and samples was limited. Work that was accomplished is reported here and in the appendices. Individual principal investigators are expected to analyze samples and data with funding from other sources and to publish their results in the open scientific literature.

Hydrography--Two deep CTDs in the vicinity of the mooring and 85 (750-m) XBTs were taken during the mission; 64 of the XBTs were collected in a grid pattern around the mooring. The original plan was to initialize the regional-eddy-resolving model with them and seven deep CTDs. This proved impossible because of the loss of the CTD and the bad weather, which made it inadvisable to deploy the backup CTD. The remaining 21 XBTs were collected on a transect from San Juan, Puerto Rico, to the study area. An examination of the XBT data indicated very little mesoscale activity in the upper water column (0 - 750 m), either along the transect or around the mooring early in Leg I.

In Situ Pumping--The in-situ pumps sample large volumes of seawater for reactive chemical species, particularly the isotopes Pu, ^{241}Am, and ^{137}Cs. Seawater is pumped through a cartridge prefilter to collect suspended particulates and then through chemically treated cartridges which extract dissolved radionuclides. Goals for the pumping were: 1) to compare retention of particles on membrane, cotton, and polypropylene fiber prefilters; 2) to assess the efficiency of extracting Pu from solution onto different manganese oxide substrates and at different flow rates; 3) to add to the pumping system a cartridge designed to scavenge dissolved ^{137}Cs. Nine subsurface samples were collected using battery-powered, in-situ pumps at depths between 350 and 5720 m. Five surface-water samples were collected using an onboard pumping system. The geochemical field work is discussed further in Appendix F.

Mooring Operations--The Nares-II mooring, installed September 21, 1984, was recovered with all instrumentation on November 21, 1985 at 23°14.76'N, 64°01.75'W. The recovery required 6.5 hours, due to the complexity of the mooring and moderately rough weather.

Instruments recovered were upright sediment traps at 735, 1435, 2885, 3800, 4785, and 5785 m, plus inverted sediment traps at 2915 and 4815 m, and five current meters located at 750, 1450, 2900, 4800, and 5800 m.

The current meters at 750, 1450, 2900, and 4800 m appear to have operated properly. The transmissometer at 4800 m also seems to have operated satisfactorily. The transmissometer at 2900 m malfunctioned and the data probably degrade rapidly after deployment. The transmissometer at 5800 m was modified for extra deep deployment, but doesn't seem to have survived. Its data are probably contaminated. Its failure caused the current meter to which it was attached to leak and eventually stop collecting data. The dual release system functioned properly.

The Nares-III mooring was deployed on November 22 at 23°15.07'N, 64°02.07. This mooring contains the following instrumentation:

- 5 current meters at 750, 1450, 2900, 4800, and 5800 m
- 2 upright sediment traps at 1435 and 4785 m
- 1 inverted sediment trap at 4835 m
- 7 passive chemical monitors (an experimental system for long-term radionuclide collection by absorption in situ, developed at Woods Hole Oceanographic Institution) at 750, 1285, 2000, 2900, 3900, 4635, and 5800 m)
- 3 transmissometers at 1450, 4800, and 5800 m.

This mooring was recovered on November 3, 1986 (see Appendix I). Summaries of data from the Nares-II current meters are

in Appendix E. Sediment trap work is discussed further in Appendix G.

Radon Analysis--The level of excess ^{222}Rn in near-bottom waters was measured as an index of the vertical diffusivity in the benthic mixed layer. ^{222}Rn, an inert, naturally-occurring radioactive gas, is produced from the decay of ^{226}Ra in sediment and seawater. Near the bottom, concentrations of ^{222}Rn are above those attributable to decay of dissolved Ra because of radon diffusion from the bottom sediments. The distribution of this excess radon can be used to calculate the rate of vertical mixing of bottom waters.

Samples were to have been obtained on Leg I, but due to rough weather and loss of the rosette sampler, the work was shifted to Leg II. Radon was extracted from seawater onto charcoal columns at dry ice temperatures and measured aboard ship using alpha scintillation counting. Some samples were also drawn for tritium analysis.

Biological Measurements Program*--The flux of organic carbon to the sediment was estimated using short-term moored sediment traps located 10 m and 95 m above the sediment surface. Sediment particles were obtained from these traps for gravimetric, elemental, and isotopic analyses. These analyses will provide data about the total flux of material to the sediment and also the organic carbon and total nitrogen flux to the sediment.

Two box cores were obtained which were used to provide: (1) pore water nutrient** and dissolved free amino acid content; (2) down core profiles of organic carbon and nitrogen; (3) bacterial

*Material on the biological measurements program is excerpted from the Cruise Report (Shephard and Laine, 1987).

**Pore water nutrient data were obtained on board using a computerized Technican Auto Analyzer system. Data on phosphate, silicate, nitrate, nitrite, and ammonia were obtained.

counts and growth rates; (4) down core meiofaunal biomass and sensitivities; (5) down core water content. Pore waters were extracted by squeezing sediments in a nitrogen atmosphere using Reebaugh squeezers. Down core sampling was performed by sectioning each box core horizontally using stainless steel "cookie sheets." Each section was subsequently subsampled.

Floating sediment traps were to be used to determine the flux of organic carbon and total nitrogen from the photic zone. Weather and time constraints prohibited this deployment.

Amphipod population densitites were to be determined using amphipod traps. As with the floating sediment traps, weather and time considerations prevented deployment.

Four primary productivity stations were made to determine the rate at which organic material is photosynthetically produced by phytoplankton in the waters surrounding the Nares Abyssal Plain study area. These measurements, in conjunction with chlorophyll biomass estimates, phytoplankton densities, and particulate carbon/nitrogen determinations, allow assessment of primary production and carbon inputs at the base of marine food webs. During the cruise, experiments were also designed to examine possible methodological problems in determining productivity in oligotrophic waters and to assess nutrient limitations of primary productivity in the Nares region.

Zooplankton studies were also conducted during the cruise. Any carbon model of water column processes must include an accounting of the effects of feeding by microscopic organisms. On attempt was made during this cruise to specify the vertical distribution of biomass and species of planktonic organisms in the area of the Nares Abyssal Plain over the upper 3,000 m, but with special emphasis on the upper 500 m. Feeding by zooplankton inhabiting various strata in the deep sea, and their growth and reproduction, determine the form (fecal pellets, eggs, live organisms, carcasses) in which

carbon reaches adjacent strata. Knowledge of the numbers, sizes, and types of deep-sea plankton can be used to predict their contributions to carbon cycling.

Lack of time and of an appropriate conducting cable precluded using an electronic opening-closing net system. Mechanical opening-closing nets were successfully used to sample these strata: 3000-2000 m, 2000-1000 m, 1000-500 m, 500-200 m, 200-100 m, and 500-0 m. In addition, several series of standard oblique net hauls covering the upper 500 m (500-0 m , 200-0 m, 100-0 m and 50-0 m) were performed to determine variance in plankton abundance in these upper layers. The nets were standard 1-m rings fitted with 149-μmesh nets and General Oceanics flowmeters. Towing speed was 2 knots. Samples were preserved in 5% neutral formalin-seawater solution for subsequent laboratory analysis.

There were no technical problems with the equipment used, which required only a hydrowinch. However, to adequately assess the role of zooplankton in water column carbon cycling, more sophisticated equipment and much more ship-time are necessary. The present study was a minimal, exploratory, and preliminary sampling effort.

Coordinated fish trapping and camera studies were conducted. Initially, there were two scientific objectives of the camera and trapping studies. The first was to repeat an experiment done elsewhere in June 1984 aboard the Research Vessel Columbus Iselin. This experiment used baited fish traps and a baited camera to study the composition of nekto-benthic fauna and their food search strategies, and tested a new method for estimating their populations without travel data. The second objective was to determine the distance from which organisms were attracted to the bait, to determine effects of changes in food abundance at a location. However, due to the loss of ship time from bad weather, time for the proposed experiments was insufficient for the original plan. Instead of setting the camera for six days and the traps nine times, the camera was set for three days and the traps three times. This

modification allowed capture of specimens for taxonomic identification and radio analysis, and for photography of nekton coming to the camera bait in order to relate their abundances and behavior to existing near-bottom water currents. The baited camera mooring included a current meter 6 m above the bottom. See Appendix E for a summary of the current meter record.

The camera and trapping stations were located along a heading of 327°, corresponding to the average direction of the bottom current during the same period in 1984. This proved to be a reasonable assumption for these deployments (see Appendix E). One trap was set 3 km in the assumed up-current direction from the camera, one was 3 km down-current, and the last was 6 km down-current of the camera. The camera was deployed for three days, but each trap fished for only 24 hours. The distances and fishing times for the traps were based upon the distance traveled in 24 hours by the bottom current at an average of 3.5 cm/sec. Upon retrieval, the exposed film was removed from the camera, to be developed after the cruise. Trap catches were preserved in formaldehyde-seawater (fish) or frozen (amphipods) after samples were removed for radioisotope analysis.

The photographs will be analyzed for identities of taxa, time of occurrence, direction of approach to the bait, and sizes. The trapped animals will be identified and measured, and, if possible, gastro-intestinal contents and reproductive state determined.

Microbiological studies were conducted to determine: (1) distribution and abundance of bacteria in the abysso-benthic boundary layer of the Nares abyssal plain; (2) origin of the bacteria present in that region (are most surface-water forms in abyssal depths via sinking particulates or uniquely-adapted deep-sea forms?); (3) ability of bacteria in abyssal waters and sediments to respond to nutrient enrichment of their environment.

To attain these objectives, samples of abyssal seawater, sediment, and sinking particulates from a sediment trap 10 m off the

bottom were collected and analyzed. Samples were fixed immediately in 2% formaldehyde for subsequent examination by epifluorescence microscopy to determine total bacterial abundance and distribution. Additional samples, retrieved and processed at in-situ temperature as best as possible, were repressurized to in-situ pressure following additions of ^{14}C glutamic acid, ^{14}C amino acid mixture, yeast extract, or (unlabeled) amino acids. Utilization of ^{14}C compounds was monitored at periodic intervals during a 48-hour incubation period. Bacterial response to additions of yeast extract or amino acids will be monitored at periodic intervals during a 12-day incubation period (cold, pressurized samples will be shipped to Chesapeake Bay Institute to continue the studies). Replicate samples incubated at sea-surface conditions and cold temperature, but atmospheric pressure, will indicate the presence of surface-water bacteria in the deep-sea samples, just as results of incubation studies at in-situ temperature and pressure will indicate the activities of the deep-sea bacteria themselves. Concentration of added nutrients (labeled and unlabeled) was varied at in-situ temperature and pressure to determine response of deep-sea bacteria to nutrient enrichment.

Onboard analysis was conducted of amino acid composition of pore water and seawaters from box core stations. Onboard analysis is needed to prevent loss of sample integrity due to freezing and transport. Also performed on board was an experiment to estimate the size of the plume from tuna used as bait for both the camera and fish trap arrays. Plumes from fish bait are highly dependent upon temperature and the surface area of the bait exposed to seawater. Pore waters were squeezed using latex membranes under nitrogen. Amino acids were determined using HPLC ion exchange with OPA as a post-column derivitization reagent with a fluoresence detector. Interstitial amino acid concentrations appear to be similar in magnitude to those observed in the Hatteras Abyssal Plain and Puerto Rico Trench.

Summary

This report period, October 1984 to termination of the project in May 1986, has been a fruitful one for the POWCG Studies Group. After last year's designation of the Nares Abyssal Plain as a long-term study area (Kupferman, 1987), a field program was developed to provide key information that would have by 1990 enabled the environmental program to demonstrate that the knowledge and capability exist to assess a site and that a validated ocean transport model and data are available to permit a relatively detailed assessment of physical and biological transport through the water column at the Nares site.

Two interdisciplinary (Physical Oceanography, Water Column Geochemistry, Biology, and Environmental Modeling) missions to the Nares have been completed. A major portion of the first year of the Nares Field Research Program outlined in Appendix A has been carried out. After further analysis, the data and samples obtained can be used to begin understanding the workings of the ecosystem at the site and developing a preliminary site assessment.

If future SDP work is carried out at the Nares, the greatest need will be for high-precision, deep-CTD data (along with supporting current meter data) to permit eddy-resolving models to be run on the site. Because of equipment and weather problems, it has not been possible on either of the two Nares missions to obtain a complete set of initialization data. The model, when run in real time, will be very useful for optimizing experimental plans aboard ship and for taking advantage of unforeseen scientific opportunities, as they arise. Laboratory simulation using these models will be useful for future ecoystem and site assessment work. The three years of moored current-meter data and the available hydrographic data will probably be adequate for first efforts in these areas.

The data collected thus far offer a unique opportunity for understanding transport processes in a deep ocean ecosystem. It is hoped that project principal investigators will continue to analyze samples and data using other funding sources and that they will continue to collaborate in investigating the dynamics of the site ecosystem.

References

Armi, L. and N. A. Bray, "A Standard Analytic Curve of Potential Temperature versus Salinity for the Western North Atlantic," J. Phys. Oceanog. 12, 1982, pp. 384-387.

Kupferman, S. L., ed., 1984 Subseabed Disposal Program Annual Report: Physical Oceanography and Water Column Geochemistry Studies, October 1983 through September 1984, SAND86-2526 (Albuquerque: Sandia National Laboratories, 1987).

Laine, E. P., Endeavor Cruise EN-121 Leg II, September 18-October 1, 1984, Nares Abyssal Plain, SAND85-7172 (Albuquerque: Sandia National Laboratories, 1985).

Marietta, M. G. and W. F. Simmons, Subseabed Disposal Project Annual Report: Ocean Modeling Studies, October 1983 through September 1984, SAND86-0929 (Albuquerque: Sandia National Laboratories, 1986).

Pillsbury, R. D. et al., Data Report for Current Meters on Mooring Nares-1, 1983-84; Nares Abyssal Plain, SAND85-7215 (Albuquerque: Sandia National Laboratories, 1986).

Shephard, L. E. and E. P. Laine, Endeavor Cruise EN137, 1985, Nares Abyssal Plain SAND86-2803 (Albuquerque: Sandia National Laboratories, in preparation).

Thomson, J. et al., "Metal Accumulation Rates in Northwest Atlantic Pelagic Sediments," Geochim. et Cosmochim. Acta 48, 1984, pp. 1935-1948.

APPENDIX A

OVERVIEW OF NARES ABYSSAL PLAIN ENVIRONMENTAL PROGRAM PLANNING MEETING

Appendix A

OVERVIEW OF NARES ABYSSAL PLAIN ENVIRONMENTAL PROGRAM PLANNING MEETING

The meeting was held in Albuquerque, NM, on March 14 and 15, 1985, and was attended by Sandia National Laboratories' (SNL) staff, contractors, and consultants (Table 1) to develop plans for a six-year interdisciplinary research program at the Nares Abyssal Plain and to discuss arrangements for the fall 1985 oceanographic mission to the Nares Abyssal Plain.

The six-year term of this phase of the research program was set by the date of the next Go/No Go Subseabed Disposal Project (SDP) program gate in 1990. At the very least and in spite of funding constraints, by 1990 we should have been able to demonstrate that we had developed the knowledge and capabilities necessary to assess a site. By 1990 refocusing of effort and improved coordination among program coordinators and principal investigators should also have permitted formulation of necessary models and acquisition of an adequate data set for a relatively detailed assessment of the physical and biological transport through the water column at the Nares.

The meeting agenda is shown in Table 2. The meeting attendees were presented with a strawman work plan (Table 3), based on a preliminininary assessment of the oceanographic missions and

major tasks that would have to be carried out (and which could be supported financially) to insure that the 1990 program gate requirements would be met.

Participants were provided with copies of a review of available physical oceanographic data for the Nares (Riser, 1985) and a cruise report of the September-October, SNL-sponsored oceanographic mission to the Nares Abyssal Plain (Laine, 1985). Speakers reviewed in detail the results of the Nares mission* and introduced additional biological, physical, and geochemical data relating to the Nares Study Area. A six-year work plan was formulated and is presented in Table 4. The schedule, in essence, follows the timing of the cruises and tasks specified in the strawman plan (Table 3). Cost and ship-time requirements are summarized in Table 5.

There was not sufficient time available for the detailed planning of the fall 1985 oceanographic mission. This work was the subject of continuing informal discussions and was completed at a meeting held in July 1985.

---

*This information is contained in Appendices B, C, D, and E of the 1984 progress report (Kupferman, 1987) and in Appendices B, C, and D of this volume.

Table 1

ATTENDEES

D. R. Anderson	Sandia National Laboratories
L. H. Brush	Sandia National Laboratories
J. K. Cochran	State University of New York
J. Dymond	Oregon State University
W. O. Forster	Department of Energy
L. S. Gomez	Sandia National Laboratories
C. L. Ingram	Scripps Inst. of Oceanography
D. W. Jackson	Scientific Info. Management, Inc.
R. D. Klett	Sandia National Laboratories
S. L. Kupferman	Sandia National Laboratories
E. P. Laine	University of Rhode Island
H. D. Livingston	Woods Hole Oceanographic Inst.
M. G. Marietta	Sandia National Laboratories
R. D. Pillsbury	Oregon State University
S. C. Riser	University of Washington
A. R. Robinson	Harvard University
G. T. Rowe	Brookhaven National Laboratory
W. F. Simmons	Woods Hole, Massachusetts
L. E. Shephard	Sandia National Laboratories
K. L. Smith	Scripps Inst. of Oceanography
G. L. Weatherly	Florida State University
A. A. Yayanos	Scripps Inst. Of Oceanography

Table 2

NARES ABYSSAL PLAIN RESEARCH PLANNING MEETING
AGENDA

Thursday, March 14, - 8:30 a.m.

Charge to the meeting	D. R. Anderson	(15)
General Overview	S. L. Kupferman	(15)
Modeling Overview	M. G. Marietta	(15)
Nares Biological Data Needs	G. T. Rowe	(15)
Details of Nares Circulation	S. C. Riser	(15)
Break		(15)

Discussion of Nares objectives and components of the research program to include measurements, components and schedules both long-term and for the October 1985 cruise. During this period there will be opportunity for formal statements of up to 10-15 minutes by individuals. This discussion will be led and moderated by A. R. Robinson (3 hours) (Will be interrupted for 1 hour at noon for lunch, to be served in the meeting room.)

Charge to the working groups	S. L. Kupferman	(15)
Break into working groups to discuss overall philosophy and general approach	2 hours	
Short statements by group leaders and discussion	S. L. Kupferman (1 hour)	

Friday, March 15 - 8:30 a.m..

Individual group planning meetings (exchange of individuals between groups is encouraged)	(3 1/2 hours)	
Lunch	(1 1/2 hours)	
Presentation of detailed group reports and discussion	S. L. Kupferman (3 1/2 hours)	

TABLE 3

STRAWMAN SIX YEAR PLAN

FY1986	October 1985 cruise: deploy Nares 3, recover Nares 2, integrate biology.
FY1987	October 1986 cruise: deploy scale determining array, recover Nares 3, deploy deep drifters. (Possible ship of opportunity launch of deep drifters.)
FY1988	October 1987 cruise: deploy single mooring, recover array. Analysis of array data for FY89 experiment.
FY1989	October 1988 cruise: deploy full array and dispersion experiment, recover single mooring.
FY1990	October 1989 cruise: recover array, continue to track drifters, deploy single mooring. Analyze data for status report.
FY1991	Continue data analysis and modeling. Begin historical research and planning for work at a new site and/or consider follow-up work at Nares.

TABLE 4
NARES FIELD RESEARCH PROGRAM

October 1985	FY1985		All in 1985 Dollars
PO & GC	Ship Time	Total Cost	Purpose
Recover & Deploy Mooring	1/2 D	75K	Long Term Variability & Statistics
Hydrographic Studies*	4 D	50 K	Regional Exploration, Modeling Support
Drifters (5 pop-ups)	-	30 K	Float Exploration
ODPS**	7 D	6 K	Model Initialization & Check
Pumping	2 D	120 K	Water Column Nuclides & Scavenging
Sediment Traps	-	190K	Fluxes & Scavenging
Radiochemistry	-	80 K	Analysis of Trap Samples
Gravity Cores (2 ea.)	1/3 D	30K	Accumulation Rates Planning
Bottom Boundary Layer	-	-	Planning
Radon (2 Profiles)	-	10 K	Definie BBL†
Tritium (100 Samples)	-	20 K	Characterize WBUC††
	13.83 D	611 K	

*Includes Silica
**ODPS - Ocean Description Prediction System
†BBL - bottom boundary layer
††WBUC - Western Boundary Undercurrent

NARES FIELD RESEARCH PROGRAM

October 1985	FY1985		All in 1985 Dollars
Biology	Ship Time	Total Cost	Purpose
(Characterize Standing Stocks)			
Box Cores (6 ea., 6 people)	3 D	153K	Carbon Model Validation Cf's* Bioturbation
Upper Water Column (1 person)	1/2 D	25 K	Source of Biogenic Particles
Zooplankton (2 people)	1 D	60 K	Deep Tows, Characterize Reprocessing
Fish Trapping(1 person)	1 D	80 K	Carbon Model, Cf's
Amphipod Trapping (2 people)	1/2 D	4K	Carbon Model
Baited Camera, Time Lapse	1/8 D	25K	Carbon Model
Stereo Camera Sled (1 person)	1 D	4 K	Carbon Model
Radiochemical Analysis	-	24 K	Organism Radioactivity
	8.125 D	375 K	
Meeting		25 K	

*Cf - concentration factors

NARES FIELD RESEARCH PROGRAM

October 1986	FY1987		All in 1985 Dollars
PO & GC	Ship Time	Total Cost	Purpose
Recover & Deploy Scale Array	1 D	350 K	Determine Scales of Motion
Hydrographic Studies	10 D	100 K	Modeling Support, Mooring Support
RAFOS* Floats & Sound Sources	3 D	275 K	Currents & Dispersion
ODPS	7 D	6 K	Model Initialization
Pumping & Chemical Monitoring	2 D	1110 K	Water Column Nuclides & Scavenging. WBUC Exchange
New Pump Construction	-	20 K	
Sediment traps	-	146 K	Horizontal Gradients in Fluxes & Scavenging
Radiochemistry	-0	80 K	Analysis of Trap Samples
Radon (Six Profiles	-	30 K	Test BBL Model Dynamics
BBL	-	150 K	Model Validation, BBL, Characterization
Tritium (250 Samples)	-	50 K	WBUC - Interior Studies
	23 D	1317 K	

*Variant of neutrally buoyant SOFAR (Sound Fixing and Ranging) floats, RAFOS is SOFAR spelled backwards.

NARES FIELD RESEARCH PROGRAM

October 1986	FY1987		All in 1985 Dollars
Biology	Ship Time	Total Cost	Purpose
(Characterize Some Rates of Processes)			
Box Cores	As Needed		
Upper Water Column (1 person)	1/2 D	25 K	Source of Biogenic Particles
Zooplankton (2 people)	2 D	60 K	Characterize Reprocessing
Fish Trapping (1 Person)	1 D	80 K	Carbon Model
Amphipod Trapping (2 people)	1/2 D	4 K	Carbon Model
Benthic Respirometer (2 people)	a D	-	Carbon Model Rates
Free Vehicles A^4 (2 people)	1 D	10 K	Carbon Model Rates
Radiochemical Analysis	-	27 K	Organism Radioactivity
	6 D	231 K	
Meeting		25K	

Need bigger ship and US port (free vehicles, sound sources).

NARES FIELD RESEARCH PROGRAM

October 1987	FY1988		All in 1985 Dollars
PO & GC	Ship Time	Total Cost	Purpose
Recover Array, Deploy	1 1/2D	75 K	Long Term Variability and Statistics
Hydrographic Studies	10 D	130 K	Model RAFOS, Support Residence Time Work
RAFOS Floats (30 ea.)	5 D	250 K	Deploy Float Clusters
ODPS	7 D	6 K	Simulation Studies
Pumping & Chemical Montoring	2 D	130 K	Water Column Nuclides & Scavenging & WBUC Exchange
Sediment Traps	-	195 K	Scavenging & Horizontal Processes
Radiochemistry	-	30 K	Same as Above
Radon (6 Profiles)	-	30 K	Test BBL Model Dynamics
BBL	-	45 K	Analysis
Tritium	-	17 K	Analysis
	25.5D	1038 K	

NARES FIELD RESEARCH PROGRAM

October 1987	FY1988		All in 1985 Dollars
Biology	Shiptime	Total Cost	Purpose
(Fill in Holes)			
Box Cores	As Needed		
Upper Water Column (1 person)	1/2 D	25 K	Source of Biogenic Particles
Zooplankton (2 people)	2 D	60 K	Characterize reprocessing
Fish Trapping (1 person)	1 D	80 K	Carbon Model
Amphipod Trapping	1/2 D	4 K	Carbon Model
Benthic Respirometer (2 people)	1 D	-	Carbon Model Rates
Move Free Vehicle A[4] Higher in Water Column (2 people)	1 D	10 K	Carbon Model Rates
Respiration Rate (2 people)	-	-	Carbon Model Rates
Intensive Radio-Chemical Anal.	-	40 K	Organism Radioactivity
Floating Sediment Trap (2 people)	-	25 K	Fluxes
	6 D	244 K	
Meeting		25 K	

Need Large Ship

NARES FIELD RESEARCH PROGRAM

October 1986	FY1989		All in 1985 Dollars
PO & GC	Ship Time	Total Cost	Purpose
Recover, Deploy Array	2 D	455 K	Dispersion Expt., Model Validation
Hydrographic Studies (50 CTD's)	10 D	130 K	Model, Mooring, RAFOS Support
RAFOS (45 Floats & Extra Sound Sources)	-	375 K	Dispersion Expt., Model Validation
ODPS	7 D	6 K	Simulation Studies
Pumping & Chemical Monitoring	2 D	145 K	Water Column Nuclides & Scavenging, WBUC Exchange
Sediment Traps	-	197 K	Scavenging & Horizontal Processes
Radiochemistry	-	80 K	Scavenging
Radon (6 profiles)	-	30 K	Test BBL Model Dynamics
BBL	-	200 K	Model Validation, BBL Escapement
Tritium (250 Samples)	-	50 K	WBUC-Interior Studies
	21 D	1668 K	

NARES FIELD RESEARCH PROGRAM

October 1988	FY1989	All in 1985 Dollars
Biology	**Ship Time**	**Total Cost**	**Purpose**
Net Tows		200 K (& Dedicated Ship)	Model Validation
Free Vehicle A^4	-	-	Carbon Model Rates
Carbon Model, Radioactivity Model Validation		100 K	Validation
Intensive Radio Chemistry	-	40 K	Organism Radioactivity
	7 D	340 K	
Meeting		25 K	

Need large ship.

NARES FIELD RESEARCH PROGRAM

October 1989	FY1990		All in 1985 Dollars
PO & GC	Ship Time	Total Cost	Purpose
Recover Array,	2 1/2 D	75 K	Long Term Variability & Statistics
Hydrographic Studies (50 CTD)	10 D	130 K	Model, Mooring, RAFOS Support
RAFOS (Recover Sources)	-	120 K	Analysis
ODPS	7 D	6 K	Simulation Studies
Plumbing and Chemical Monitoring	2 D	160 K	Water Column Nuclides & Scavenging, WBUC Exchange
Sediment Traps	-	60 K	Scavenging & Horizontal Processes
Radiochemistry	-	240 K	Scavenging
Radon (6 profiles)	-	30 K	Test BBL Model Dynamics
BBL	-	55 K	Analysis
Tritium	-	20 K	Analysis of Data
	21.5 D	1096 K	

NARES FIELD RESEARCH PROGRAM

October 1989	FY1990		All in 1985 Dollars
Biology	Ship Time	Total Cost	Purpose
Horizontal Varience In Biological Field	-	250 K	Exploration, Model Validation
Radiochemistry, Cores	-	50 K	Model Validation
Radiochemistry, Organisms	-	15 K	Model Validation
	7 D	315 K	
Meeting		25 K	

NARES FIELD RESEARCH PROGRAM

October 1990	FY1991		All in 1985 Dollars
PO & GC	Ship Time	Total Cost	Purpose
Recover Mooring	1/3 D	40 K	Long Term Variability & Statistics
Hydrographic Studies	3 D	40 K	Model Support
RAFOS	-	75 K	Analysis
ODPS	-	-	Simulation studies
Pumping & Chemical Monitoring	-	50 K	Analysis
Sediment Traps	-	130 K	Scavenging Processes
Radiochemistry	-	80K	Scavenging
BBL	-	30 K	Analysis
Synthesis of Geochemistry	-	50 K	Analysis & Reports
		485 K	
Biology			
Synthesis of Biology	-	60 K	Analysis & Reports
Meeting		25 K	

TABLE 5

NARES FIELD RESEARCH PROGRAM

COST AND SHIP TIME SUMMARY

NOTES:

Have added 7D for Transit Time to each mission.

Have charged 10K/Day for ship days, Add to PO and GC.

Have added costs for meetings to PO and GC.

Fiscal Year	Total Ship Days	Total PO & GC (K)	Total Biology (K)
1986	29	926	375
1987	36	1702	231
1988	39	1453	244
1989	35	2043	340
1990	36	1481	315
1991	10	620	60

Costs in 1985 $.

APPENDIX A

REFERENCES

Kupferman, S. L., Ed., 1987, 1984 Subseabed Disposal Program Annual Report: Physical Oceanography and Water Column Geochemistry Studies, October, 1983 through September, 1984, SAND86-2526, Sandia National Laboratories, Albuquerque, NM.

Laine, E. P., 1985, Endeavor Cruise EN-121 Leg 11, September 18-October 1, 1985, Nares Abyssal Plain, SAND85-7272, Contractor Report, Sandia National Laboratories, Albuquerque, NM.

Riser., S. C., 1985, Physical Oceanographic Characteristics of the Nares Plain Region of the Western North Atlantic, SAND 85-7186, Contractor Report, Sandia National Laboratories, Albuquerque, NM.

APPENDIX B

NARES ABYSSAL PLAIN SEDIMENT FLUX STUDIES, FY1985 ANNUAL REPORT

J. DYMOND AND W. R. COLLIER

1985 ANNUAL REPORT

SUBSEABED DISPOSAL PROGRAM

Contract 25-8715

with

Sandia National Laboratories

Albuquerque, New Mexico

Jack Dymond and Robert Collier
College of Oceanography
Oregon State University
Corvallis, OR 97331

April, 1986

NARES ABYSSAL PLAIN SEDIMENT FLUX STUDIES

I. SUMMARY OF FIELD ACTIVITIES (FY85)

Mooring NAP-1.

On 20 Sept. 1984, during cruise EN-121 of the R/V ENDEAVOR, the sediment trap mooring designated NAP-1 was recovered. The mooring had been deployed on 15 August 1983, and contained two upward-looking sediment traps (@1463m, 4832m) and one downward-facing trap (@4862m) of the standard 5-cup OSU design (Moser et al., 1986). The mooring was located in the Nares Abyssal Plain at 23°12.0'N, 63°58.9'W (bottom depth 5847 meters). The microprocessor timer was set to sequence samples every 78 days (cups 2-5). On 28 June 1984, the collector returned to its deployment position (cup 1) where it remained until recovery (84 days). Although we will present the data for this last subsample, the quality of the sample is in question because of potential contamination or loss of material during recovery (see below). A quantitative recovery of the azide solution (preservative) in cup 1 of the 1463m trap suggests that this sample was probably intact whereas cup 1 on the 4832m trap was abnormally depleted in azide and probably lost material during recovery.

These particulate matter samples were analyzed for mass, organic carbon, nitrogen, phosphorus, calcium carbonate, opal, and other major and minor elements. Subsamples of these were also provided to Drs. K. Cochran (SUNY) and H. Livingston (WHOI) for radiochemical analyses.

Mooring NAP-2.

On 21 September 1984 (during the same cruise), another mooring was deployed at 23°14.5'N, 64°02.1'W with a bottom depth of 5835 meters. This complex mooring contained 6 upward-looking traps (@720, 1420, 2870, 3785, 4770, 5780 meters) and two inverted traps (@2900, 4800 meters). [This mooring was successfully recovered on 21 November 1985.]

Sediments.

During EN-121, a gravity core (GC #1) was collected near the mooring site by Dr. K. Cochran. We have analyzed subsamples of this core for the same suite of elements characterized in the traps and these results are also reported in this document.

II. RESULTS - SEDIMENT TRAP FLUXES

A. Bulk fluxes.

The bulk mass fluxes and the chemical fluxes collected by NAP-1 are given in Table 1A & 1B and the average flux for the deployment is shown in Figure 1. Also plotted (hexagon) is the average flux for the <37μm fraction of particles collected in the Sargasso Sea near Bermuda at 3200 m depth (Deuser et al., 1981). The particle flux (and biological productivity) at Nares is lower by nearly a factor of 2 compared to that near Bermuda. As commonly observed elsewhere, the flux increases between the upper and lower trap (Honjo et al., 1982; Dymond and Collier, 1986; Walsh et al., submitted). This observation is not fully understood but it is probably due to zooplankton feeding dynamics in the upper water column and deep horizontal tranport of material from other sedimentary environments. Seasonal variations in flux range by a factor of 2 and the maximum flux is associated with high biological production in the spring and summer. Most signals are seen to covary in the upper and lower traps reflecting the rapid transport of surface-derived material to the deep ocean.

The bulk flux can be broken down into the contributions of organic matter, carbonate, opal and terrigenous material (Table 2). These estimates are of varying quality: $CaCO_3$ is actually measured through both Ca and carbonate carbon; "organic matter" is only crudely estimated based on ash weights and total organic carbon content. In spite of the inaccuracy of these classifications, essentially 100% of the particle mass is accounted for by this method. It can be seen that the flux is approximately 50% biogenic and 50% lithogenous. The biogenic component is dominated by calcium carbonate production and the contribution of opal is very small (and inaccurately estimated by this method).

B. Biogenic Fluxes.

The fluxes of organic carbon and carbonate carbon are shown in Figure 2 and the mean fluxes for the deployment are displayed in Figure 3. The same seasonal signal detected in the bulk flux is seen for the individual components since the biogenic flux generally drives the total flux even in this low productivity region. However, the large pulse of carbonate and organic carbon collected in the deep trap, cup 5, was not seen as strongly in the shallow trap. Since this pulse was also associated with a strong aluminum input, horizontal transport of recently deposited sediments into the trap is suggested (see below). Figure 4 demonstrates the dominance of carbonate productivity in this region. The ratio of organic/carbonate carbon is seen to be slightly less than 1. This ratio is common to low productivity environments - e.g. diatom vs. coccolithophorid production - and regional variations in this ratio are significant to models of the global cycle of carbon (Dymond and Lyle, 1985).

C. Terrigenous Materials.

The total fraction and net flux of terrigenous components are higher at the NAP-1 mooring than at any other pelagic site we have sampled. The Al fluxes (Figure 5) are as much as 2 to 10 times higher than those measured in the tropical Pacific and there is a significant increase in the flux between the upper and lower traps. These fluxes are supported by high surface inputs and by active nepheloid transport processes in the deep Atlantic.

The Nares Abyssal Plain lies directly beneath the trajectory of the famous Saharan dust storms which transport more than 2×10^8 tons of mineral dust per year on the NE trades (Prospero and Nees, 1977; Schütz et al., 1981). Although good deposition measurements do not exist for this open ocean region, washout models coupled with air concentration measurements from Barbados suggest an aluminum deposition flux of 20-30 $\mu g/cm^2/yr$. This is entirely consistent with the fluxes collected by the upper trap at NAP-1 (Figure 5). The Saharan transport is also seasonal with more than an order of magnitude increase during the summer. Although this is also roughly consistent with the timing of the aluminum flux changes in the traps, the downward transport of this small-diameter terrigenous material is primarily driven by the production and downward flux of biogenic material (Figure 6; Deuser et al., 1981). However, because of this strong atmospheric input,

the covariation of Al and organic carbon is not nearly as tight as that observed near Bermuda (dotted line on Fig. 6) and there is much more Al transported.

The deep trap at NAP-1 collects nearly twice as much Al as the 1464m trap due to the horizontal transport of sediments from other depositional environments. This may also be seen by the fact that the variation in flux (Figure 5) at the deep trap is not as clearly related to the surface variations. The common terrigenous origin of the aluminum, iron and silicon in both the upper and lower traps is very clearly demonstrated in Figure 7. The Fe/Al ratio is 0.55 (±.01) and the Si/Al ratio is 3.0 (±.1). The Fe/Al ratio in the sediment trap material is somewhat lower than that in the Saharan dust (0.62; Buat-Menard and Chesselet, 1979; Rahn et al., 1979). This may indicate that some of the Fe (~10%) is mobilized upon deposition (Rueter and Stallings, 1985) or that the trapped material is largely resuspended sediments (see below).

D. Upward (Buoyant) Particle Fluxes.

The flux of material collected by the inverted sediment trap at 4865m was very low at the NAP-1 mooring (Table 3). [Notice that the units of the bulk and elemental fluxes are three orders of magnitude smaller than those for the downward fluxes given in Table 1.] The buoyant fluxes, commonly enriched in lipids and other labile organic compounds (Simoneit et al., 1986), are lower at NAP-1 than those measured at the "EN" and "WN" sites (Figure 8). This may be a consequence of the lower productivity at this site which supports fewer abyssal organisms that can produce lipid-rich particles. The relatively high concentration of Ca in the N-1 inverted trap may suggest a contribution from benthic foraminifera. There is no apparent relationship between the downward and upward flux of aluminum (Figure 9) or between the downward organic carbon flux and the upward bulk flux (Figure 10). This process does not appear to provide a significant upward transport vector at the Nares site.

E. Trap Fluxes vs. Sediment Composition and Accumulation.

The chemical composition of the gravity core from the N-1 site is presented in Table 4. We can usually gain insight to the rates and types of diagenetic processes occurring at the seafloor by comparing the flux of material in the traps to the accumulation rate of the same components in sediment cores. This is effective in an ideal one-dimensional (vertical) system but is especially difficult at Nares where significant horizontal transport occurs. Alternating periods of slow deposition and turbidite flows occur in the region (Thomson et al., 1984) and the gravity core collected at NAP-1 shows these rapidly-deposited discontinuities (Cochran, pers. comm.). Thomson et al. (1984) suggest that both the rapidly and slowly deposited sections have similar detrital chemical compositions (and sources?) which allows us to make first-order comparisons between these sediments and the trap material.

The sedimentation rate derived from the slowly accumulating "red clay" sequences studied by Thomson et al. (1984) was 0.3-0.7 $mg/cm^2/yr$. This value is consistent with the range of terrigenous fluxes collected by the traps (Table 2). At all other pelagic sites studied to date, the flux of Al in traps matches its accumulation rate in the sediments (Dymond, 1984). Even though we do not have a valid sedimentation rate for the gravity core from N-1, we can make sediment flux comparisons with the trap based on the assumption that the Al in the trap is associated with terrigenous material and that it is completely preserved in the sediments. In this way, we have estimated the relative accumulation rates of components in the sediment core and compared these to the fluxes into the lower trap (Figure 11). Elements falling along the center diagonal are accumulating at the same rate they are collected by the trap. For the most part, these include the terrigenous components discussed previously (Fe, Ti, Mg, inorganic P, and Si which is mostly detrital in these traps). Manganese is accumulating slightly more rapidly than the flux collected by the trap. This is commonly observed and is probably due to authigenic deposition of excess Mn from water column and hydrothermal sources. All other biogenic components are regenerated at the seafloor such that less than 10% of these phases are preserved (organic carbon, calcium carbonate, organic P, and Sr).

III. SUMMARY

The sediment trap NAP-1 was successfully recovered and the materials have been analyzed for a set of bio- and geochemical components. The trap mooring NAP-2 was deployed and recovered but no analyses have been completed. The bulk fluxes are relatively low at this site and are approximately 50% biogenic and 50% terrigenous. The flux of terrigenous material is very high due to primary atmospheric inputs and horizontal transport of resuspended sediments. The buoyant particle fluxes are also extremely low. The accumulation of material in the sediments reflects the crustal nature of the vertical flux and also shows the normal loss of labile biogenic phases.

REFERENCES

Buat-Menard, P. and R. Chesselet, 1979. Variable influence of the atmospheric flux on the trace metal chemistry of oceanic suspended matter. Earth Planet. Sci. Lett. 42:399-411.

Deuser, W.G., E.H. Ross and R.F. Anderson, 1981. Seasonality in the supply of sediment to the deep Sargasso Sea and the implications for the rapid transfer of matter to the deep ocean. Deep-Sea Res. 28A:495-505.

Dymond, J., 1984. Sediment traps, particle fluxes, and benthic boundary layer processes. In Proceedings of a Workshop, Global Ocean Flux Study, Woods Hole, MA., Nat. Acad. Press., pp 260-284.

Dymond, J. and R. Collier, 1986. Biogenic particle fluxes in the Equatorial Pacific: Evidence for both high and low productivity El Niño effects. Submitted to Nature.

Dymond, J. and M. Lyle, 1985. Flux comparisons between sediments and sediment traps in the eastern tropical Pacific: Implications for atmospheric CO_2 variations during the Pleistocene. Limnol. Oceanogr. 30:699-712.

Honjo, S., S.J. Manganini and J.J. Cole, 1982. Sedimentation of biogenic matter in the deep ocean. Deep-Sea Res. 29:609-625.

Moser, J.C., J. Dymond and K. Fischer, 1986. Multiple sampling OSU sediment trap: Technical design and function. Submitted to Limnol. Oceanogr.

Prospero, J.M. and R.T. Nees, 1977. Dust concentration in the atmosphere of the Equatorial North Atlantic: Possible Relationship to the Sahelian Drought. Science 196:1196-1198.

Rahn, K.A., R.D. Borys, G.E. Shaw, L. Shutz and R. Jaenicke, 1979. Long-range impact of desert aerosolon atmospheric chemistry: two examples. In Saharan Dust, Morales (ed.), Wiley, pp 243-266.

Rueter, J.G. and C. Stallings, 1985. Stimulation of photosynthesis in two cyanophyte species by iron. EOS 66:1266 (abstract).

Schutz, L., R. Jaenicke and H. Pietrek, 1981. Saharan dust transport over the North Atlantic Ocean. Geol. Soc. Amer., Special Paper 186:87-100.

Simoneit, B.R.T., J.O. Grimalt, K. Fischer and J. Dymond, 1986. Upward and downward flux of particulate organic material in abyssal waters of the Pacific Ocean. Submitted to Nature.

Thomson, J., M.S.N. Carpenter, S. Colley, T.R.S. Wilson, H. Elderfield and H. Kennedy, 1984. Metal accumulation rates in northwest Atlantic pelagic sediments. Geochim. Cosmochim. Acta. 48:1935-1948.

Walsh, I., J. Dymond and R. Collier, 1986. Rates of recycling of biogenic components of fast settling particles derived from sediment trap experiments. Submitted to J. Mar. Res.

TABLE 1A. NARES ABYSSAL PLAIN SEDIMENT TRAP FLUXES (downward, mooring NAP-I)

Depth	Cup	Total days	Date cup opened	Bulk flux mg/cm²/y	C_{carb} µg/cm²/y	C_{org}	N	P_T	P_{inorg}	P_{org}	Al	Ca	Fe	Si
1464m	C2	78	21AUG83	1.418	69.8	92.0	12.3	1.86	1.32	.54	55.7	238.5	30.3	174.2
	C3	78	7NOV83	.834	49.8	37.4	4.5	.50	.28	.22	29.8	163.6	16.5	96.9
	C4	78	24JAN84	.626	42.1	32.1	3.9	.43	.25	.18	16.8	138.5	9.5	62.7
	C5	78	11APR84	.768	52.0	47.8	5.6	.48	.23	.25	16.9	170.0	9.6	70.8
	C1	7+84-91	28JUN84	.422	26.2	24.2	2.9	.33	.18	.15	13.1	84.3	7.3	45.6
average flux	(C2+C1)			.801	47.3	46.0	5.7	.71	.44	.26	26.0	156.6	14.4	88.6
	(C2+C5)			.912	53.4	52.3	6.6	.82	.52	.30	29.8	177.7	16.5	101.2
4832m	C2	78	21AUG83	1.194	57.9	61.7	6.6	.62	.29	.33	50.3	191.6	28.0	164.5
	C3	78	7NOV83	.850	42.6	34.8	4.1	.46	.23	.23	37.4	143.1	21.0	118.2
	C4	78	24JAN84	.806	41.0	30.7	3.7	.43	.22	.22	35.6	135.9	20.1	111.9
	C5	78	11APR84	1.624	86.0	69.7	8.6	.96	.47	.49	65.4	277.6	36.7	216.5
	C1	7+84-91	28JUN84	.989	50.4	42.7	4.8	.55	.25	.30	42.4	163.8	24.4	138.2
average flux	(C2+C1)			1.089	55.4	47.8	5.5	.60	.29	.31	46.1	181.8	25.9	149.5
	(C2+C5)			1.119	56.9	49.2	5.8	.62	.30	.32	47.2	187.1	26.5	152.8

TABLE 1B.

Depth	Cup	Ba µg/cm²/yr	Cu	Mg	Mn	Ni	Sr	Ti	Zn	Li	V	I	Br
1464m	C2	1.12	.069	13.5	.326	.05	2.1	3.8	.13	.03	.083	.16	.41
	C3	.78	.055	8.2	.293	.03	1.4	2.3	.07	.02	.055	.11	.20
	C4	.55	.042	5.4	.177	.03	1.1	1.1	.04	.01	.028	.10	.20
	C5	.63	.043	6.2	.172	.03	1.3	1.3	.04	.01	.029	.13	.25
	C1	.34	.020	3.4	.069	.015	.6	.9	.03	.01	.018	.059	.15
average flux	(C2-C1)	.67	.044	7.2	.202	.03	1.2	1.9	.06	.02	.042	.11	.24
	(C2-C5)	.77	.052	8.6	.242	.04	1.5	2.1	.07	.02	.049	.13	.27
4832m	C2	.98	.11	11.6	.621	.05	1.4	3.3	.08	.03	.087	.13	.26
	C3	.72	.08	8.4	.495	.04	1.0	2.1	.06	.02	.069	.10	.12
	C4	.71	.08	8.1	.522	.03	.95	2.2	.07	.02	.068	.10	.13
	C5	1.45	.16	15.5	1.173	.07	2.05	3.9	.11	.04	.135	.22	.42
	C1	.86	.094	9.5	.718	.04	1.2	2.7	.61	.03	.080	.14	.18
average flux	(C2-C1)	.94	.11	10.6	.707	.04	1.31	2.8		.03	.087	.14	.22
	(C2-C5)	.97	.11	11.2	.702	.05	1.35	2.9	.08	.03	.090	.14	.23

TABLE 2. NARES ABYSSAL PLAIN - COMPONENTS OF BULK DOWNWARD FLUXES

Bulk fluxes - component estimates

depth	cup	mg/cm²/yr bulk flux (measured)	Organic[1] (estimates →	$CaCO_3$[2]	Opal[3]	Terrig.[4])	Σ%[5]
1464 m	C2	1.418	.166	.581	.018	.635	99%
	C3	.834	.067	.415	.020	.340	101%
	C4	.626	.058	.351	.032	.191	101%
	C5	.768	.086	.433	.052	.193	99%
	C1	.422	.044	.218	.016	.149	101%
4832 m	C2	1.194	.111	.482	.036	.573	101%
	C3	.850	.063	.355	.015	.426	101%
	C4	.806	.055	.342	.013	.406	101%
	C5	1.624	.125	.716	.054	.745	101%
	C1	.989	.077	.420	.028	.483	102%

[1] Organic matter = $1.8 \cdot C_{org}$ (Wefer, Suess and Ungerer, 1986)

[2] $CaCO_3 = 8.33 \cdot C_{carb}$

[3] Opal = $2.61 \cdot (Si - 3.0 \cdot Al)$ -- subtract out detrital Si.

[4] Terrigenous = $11.4 \cdot Al$ -- using Al content of local sediments - 8.8%

[5] Total bulk flux accounted for by sum of estimated components

TABLE 3. INVERTED TRAP FLUXES (4865m):

Cup	Total days	Date cup opened	Bulk flux µg/cm²/y	Al ng/cm²/y	Ca	Ti	Mn	V	I	Br	Ba
C2	78	21AUG83	.8	11.2	17.3	1.4	.025	.006	.085	1.53	.9
C3	78	7NOV83	1.5	5.8	79.6	-	.034	.012	.18	2.76	-
C4	78	24JAN84	.95	7.7	27.1	1.7	.062	.027	.070	2.21	-
C5	78	11APR84	.52	6.0	28.2	-	.048	.008	.003	.32	-
C1	7+84=91	28JUN84	3.2	35.5	44.2	6.2	7.1	.091	.21	5.2	1.6
average flux(C2→C1)			1.5	14.1	24.4	-	.19	.029	.120	2.0	-
(C2→C5)			.94	7.7	38.1	-	.042	.021	.084	1.7	-

TABLE 4. CRUISE EN-121 GRAVITY CORE 1

Depth (cm)	ash	C_{carb} %	C_{org}	Si	Al	Fe	Ca	K	Mg	Ti	Li ppm	Sr	Ba	Mn	Cu	Ni	Zn	P_T	P_{inorg}	P_{org}
7.5	.9526	.26	.32	23.2	9.96	5.76	.988	3.315	2.10	.54	81.9	140	545	1605	61	46	130	599	516	83
20	.9300	.52	.31	22.8	9.65	5.24	2.685	3.23	2.02	.55	79.9	160	535	2845	45	45	121	520	482	38
30	.8418	1.05	.30	21.5	8.99	5.25	4.53	3.06	1.95	.49	77.4	250	560	873	34	42	112	486	471	15
40	.9461	.87	.26	23.3	8.17	4.09	-	2.735	1.78	.53	73.4	225	515	463	59	52	97	560	529	31
58	.8981	.15	.24	23.1	9.55	5.98	-	3.22	1.98	.53	82.5	120	520	878	28	34	116	557	515	42
75	.9405	.68	.28	27.2	7.28	3.70	2.595	2.54	1.52	.52	54.5	160	445	640	53	22	76	513	487	26
88	.9297	.27	.44	22.7	9.99	5.65	1.115	3.56	2.02	.54	88.0	120	515	780	32	40	110	503	462	41
98	.9138	.83	.34	26.1	7.60	3.58	2.59	2.47	1.70	.52	59.5	140	460	640	88	44	82	463	442	21
118	.9371	.54	.13	28.2	7.22	3.48	2.325	2.42	1.46	.54	48.0	160	505	610	14	22	68	563	574	0
135	.8973	.63	.29	25.5	8.58	4.15	2.475	2.915	1.76	.51	63.0	160	540	730	15	31	91	462	474	0
151	.9263	.58	.31	22.9	8.96	5.04	1.94	3.42	2.35	.51	77.8	140	515	996	25	44	114	542	512	30
167	.9265	.47	.26	22.9	9.26	5.58	1.695	3.46	2.41	.52	78.5	140	530	1155	41	51	121	590	555	35
175	.9495	.50	.32	24.4	8.58	4.68	1.95	2.865	2.04	.50	66.5	160	495	908	39	44	108	572	515	57
185	.9226	.49	.24	22.5	9.08	5.30	1.495	3.35	2.46	.50	74.0	160	560	1425	68	44	124	610	576	34

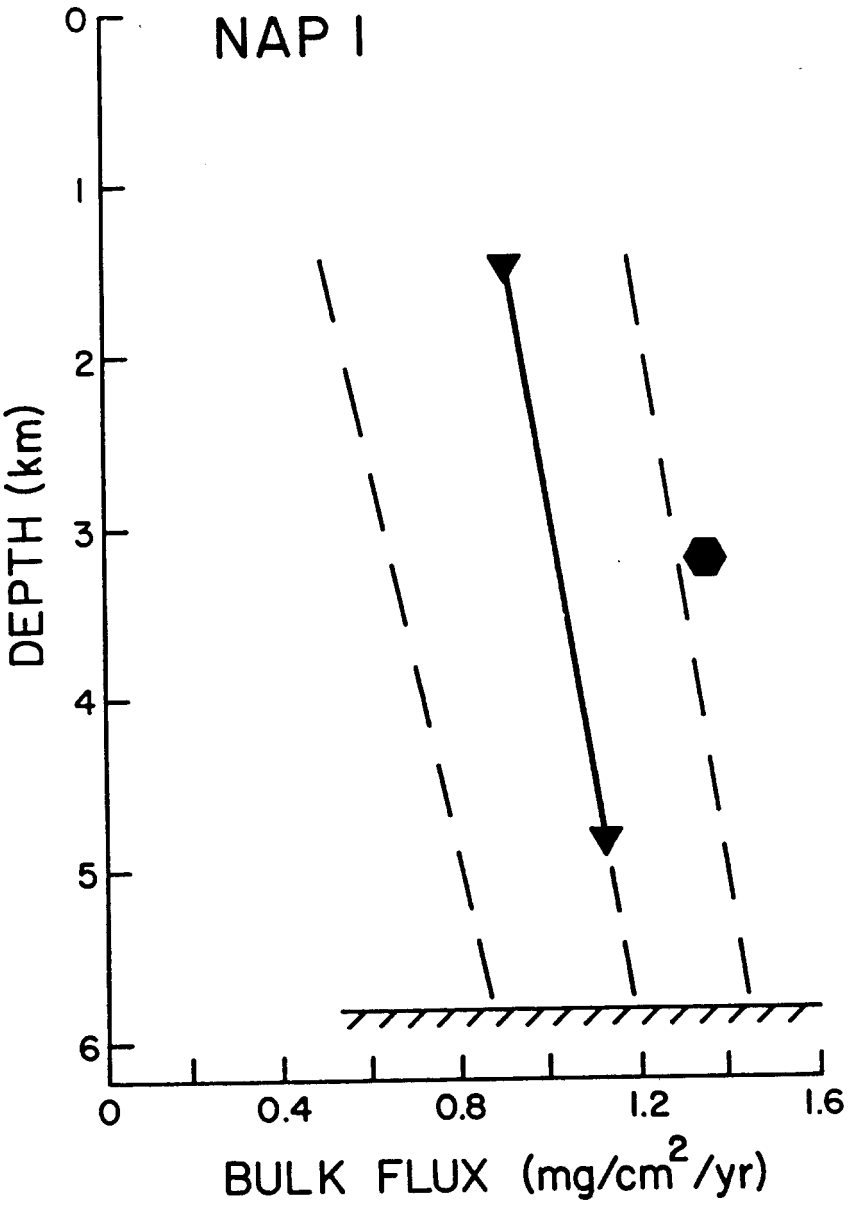

Figure 1. Average bulk particle flux (triangles) collected by mooring NAP1 (cups 2-5). Dashed lines represend the range of individual cup fluxes. Mass flux reported by Dueser et al. (1981) from the Sargasso Sea is also shown for comparison (octagon).

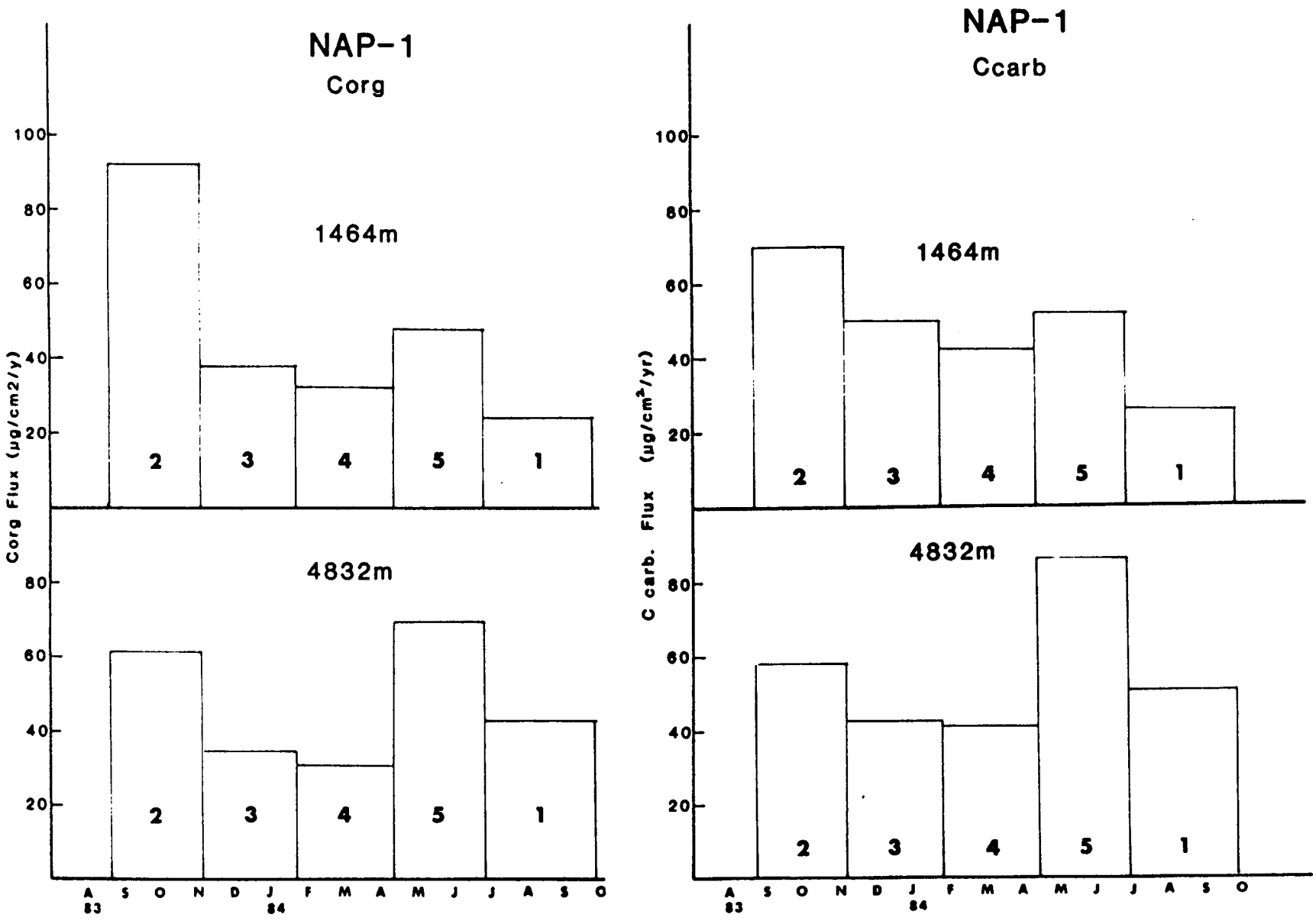

Figure 2. Vertical flux of organic carbon and carbon associated with calcium carbonate in each collecting cup (2-5, 1) between August 1983 and October 1984.

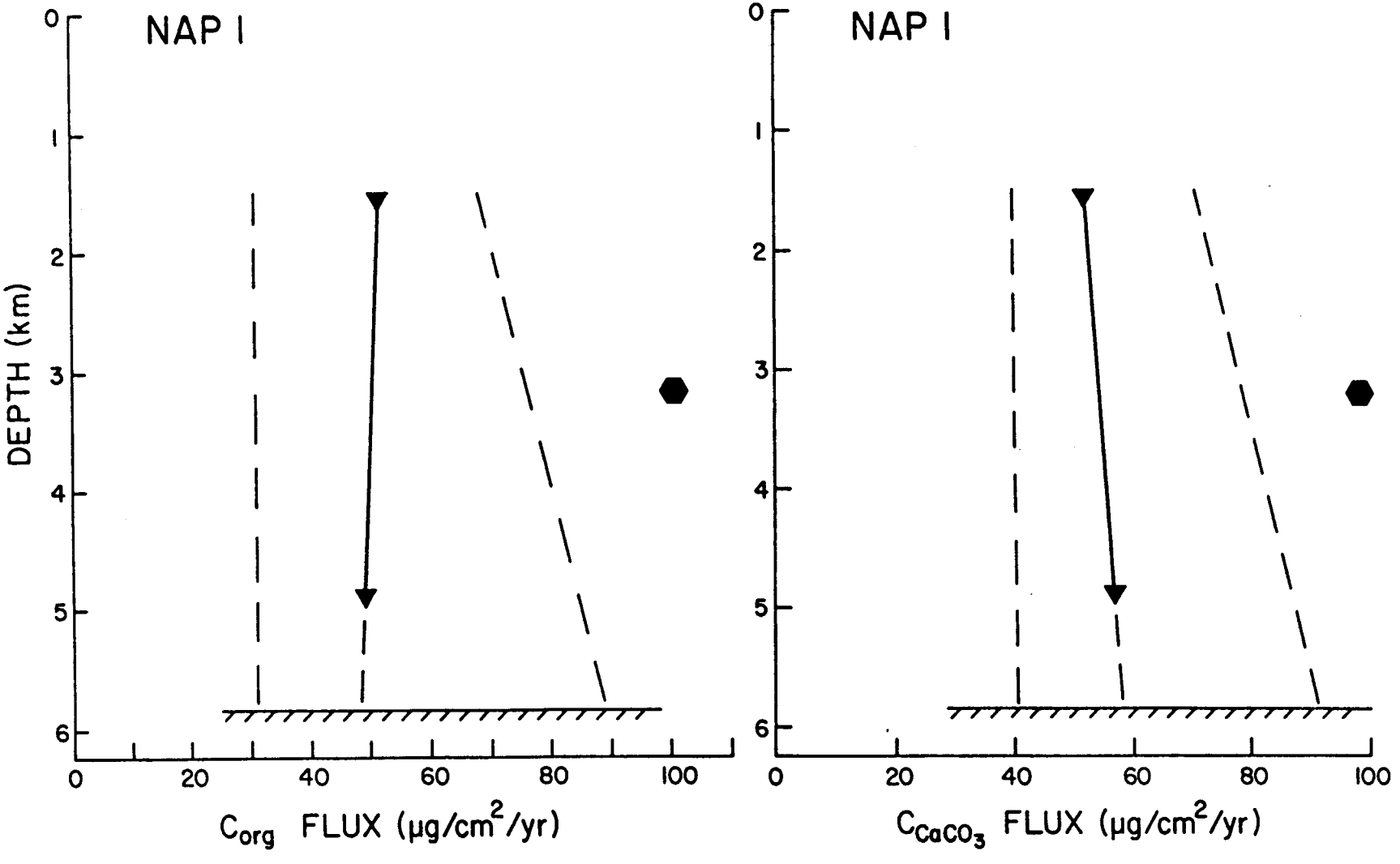

Figure 3. Average vertical (downward) flux of organic carbon and calcium carbonate carbon. Comparative values from Dueser et al. (1981) are shown as before. While the bulk flux increase with depth (Fig. 1) the organic carbon flux decreases.

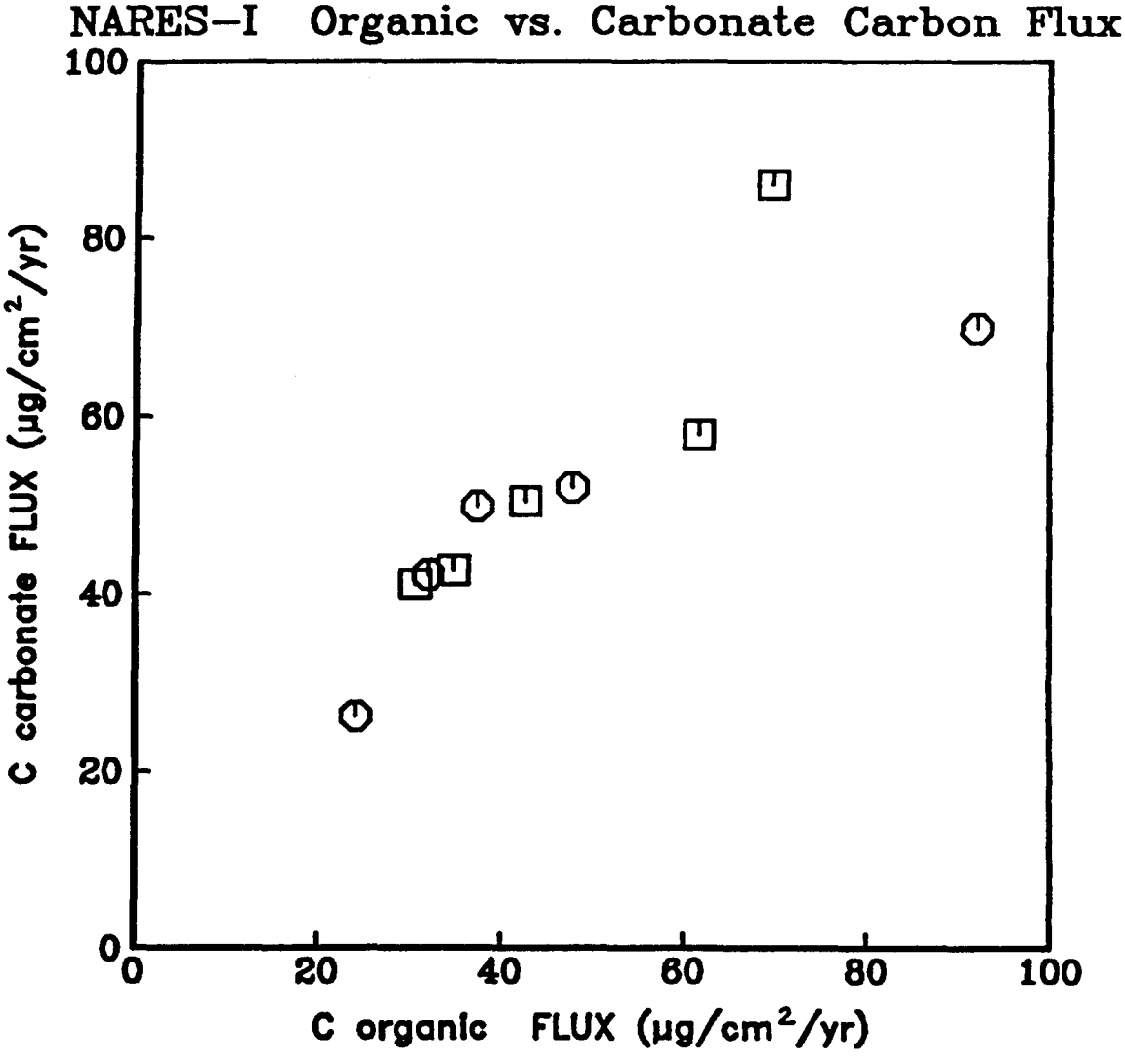

Figure 4. Flux of calcium carbonate carbon vs. organic carbon for all cups. Most of the biogenic particle flux at the Nares site is associated with carbonate production (coccolithophorid and foraminifa).

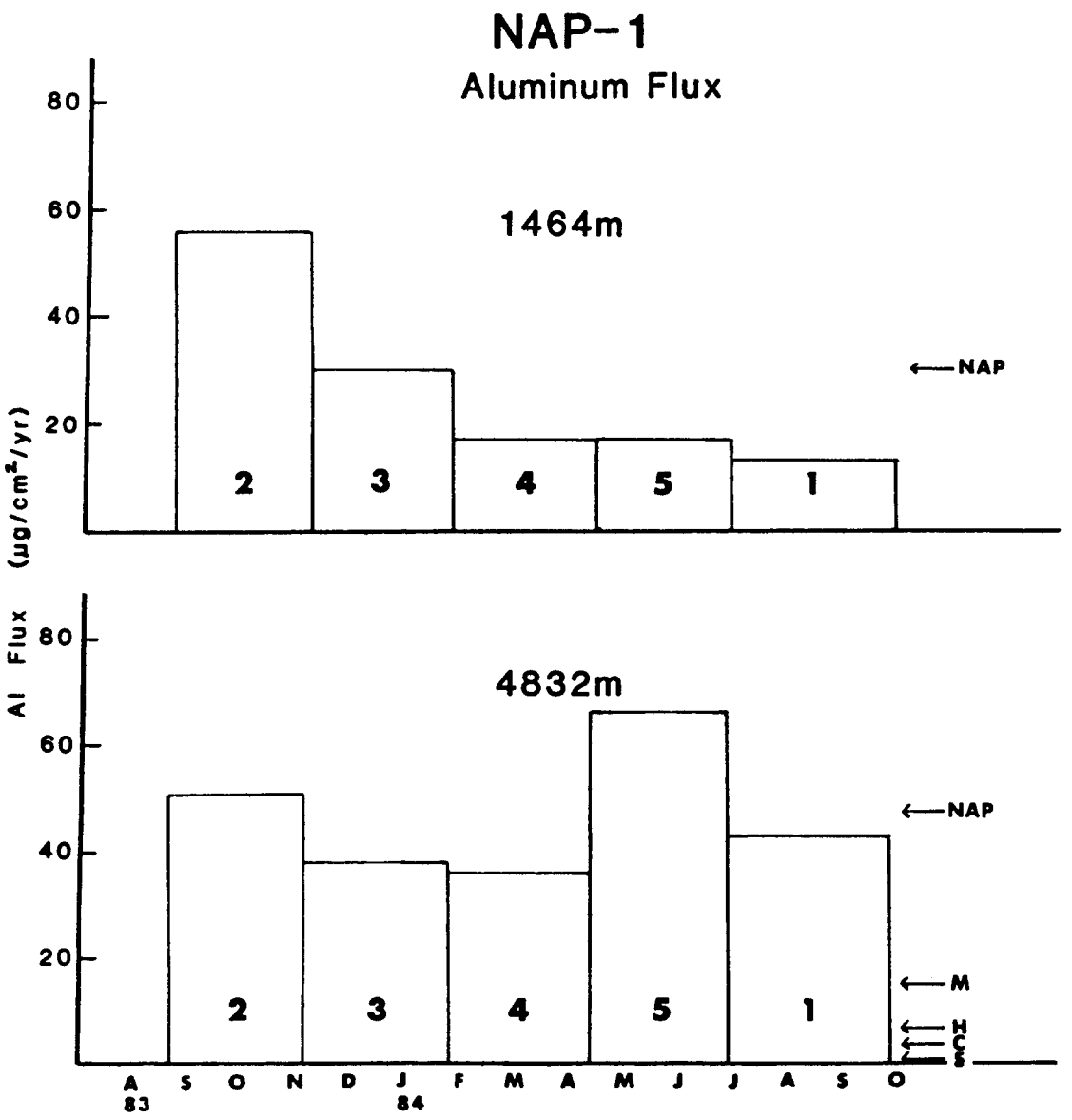

Figure 5. Vertical flux of aluminum at NAP-1. The average value at NAP-1 (arrow) is compared with averages in the deep Pacific (Manop sites M,H,C, and S). The flux at Nares is the highest pelagic value we have ever measured.

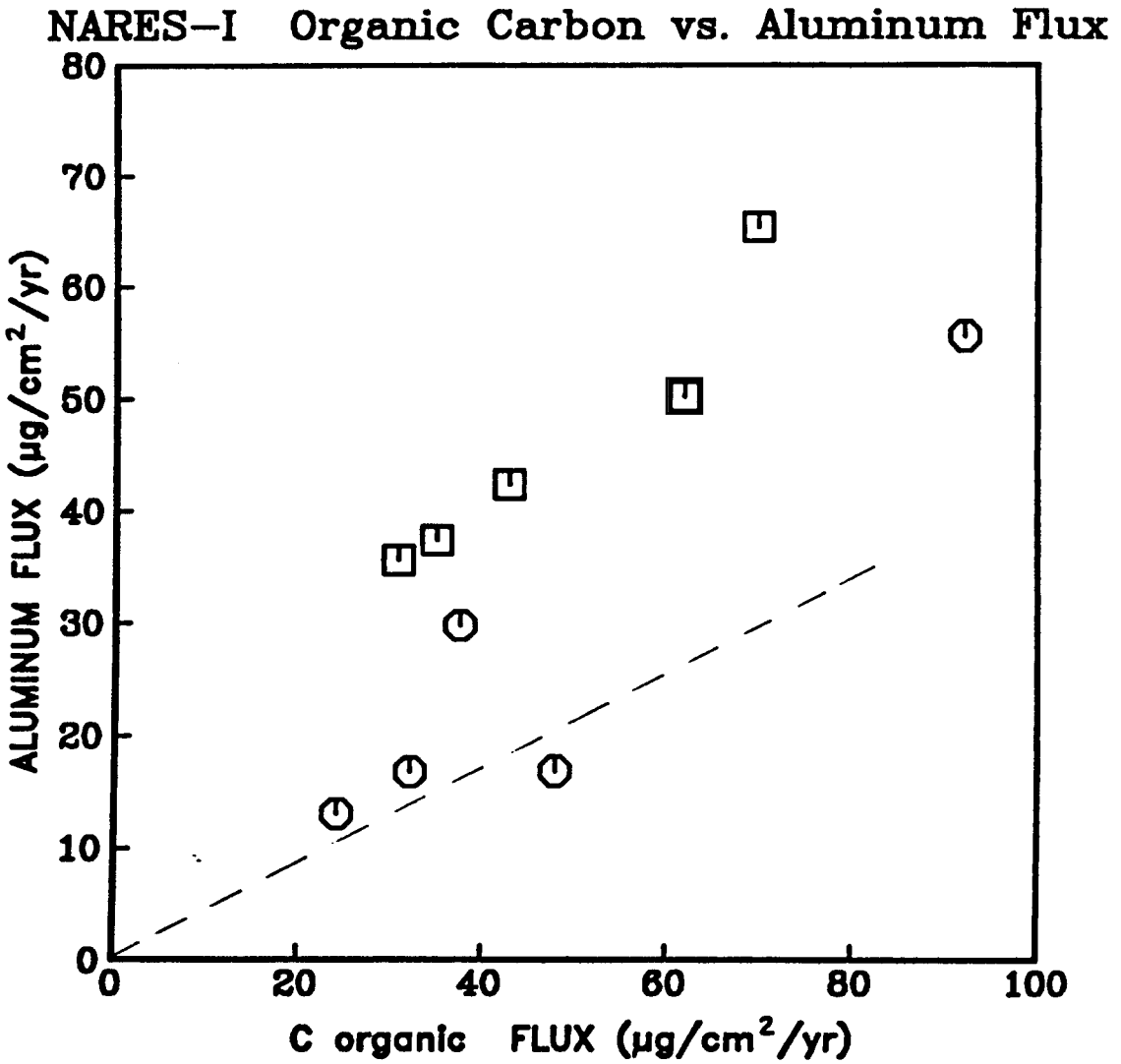

Figure 6. Flux of aluminum vs. organic carbon. The transport of the fine-grained terrigenous material has been shown to depend on the biogenic particle flux which settles rapidly through the water column (Dueser et al., 1981; Dymond, 1984). The relationship seen in the Sargasso (Dueser et al., 1981) is shown with the dotted line.

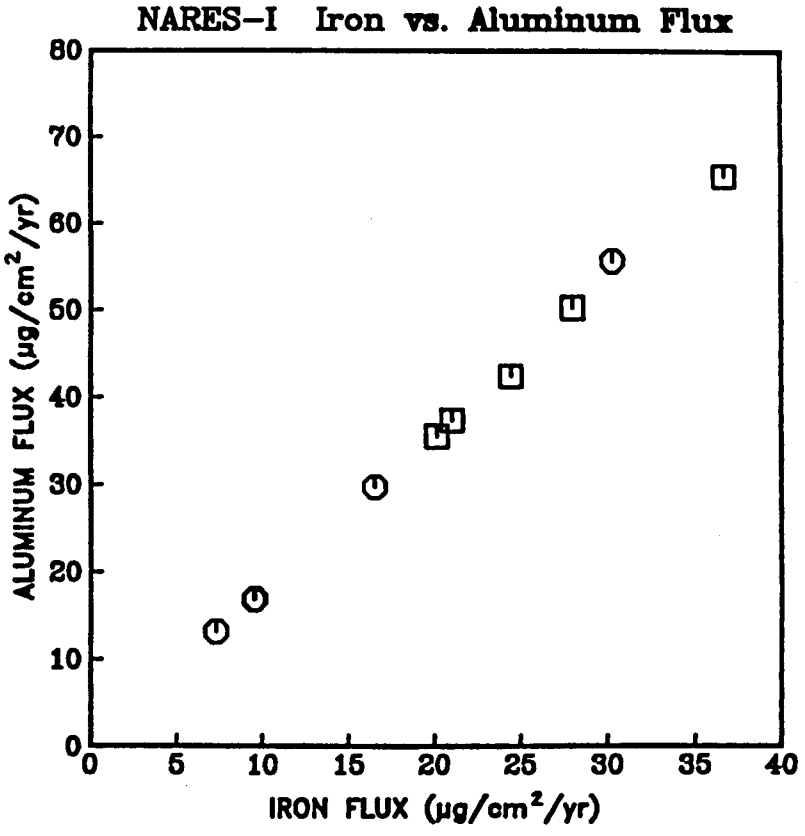

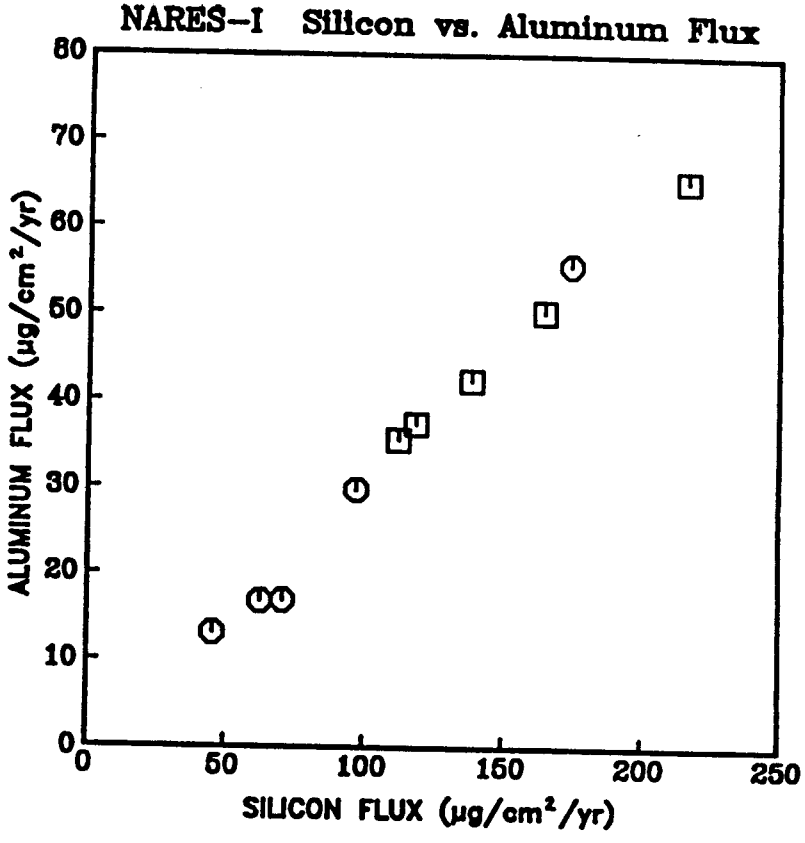

Figure 7. The flux of aluminum, iron and silicon in all cups at NAP-1. The constant crustal composition of this terrigenous end member drives all three of these elements.

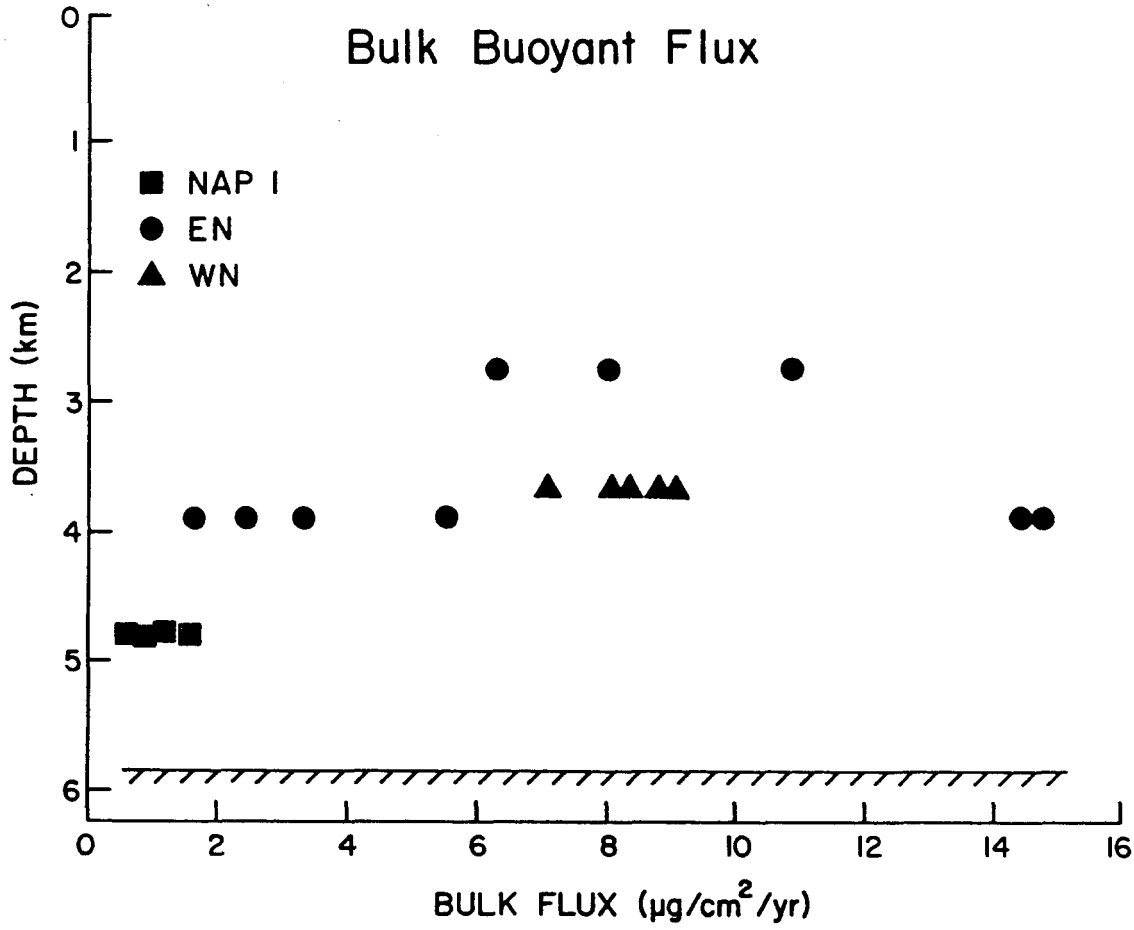

Figure 8. The flux of buoyant particulate matter collected by an inverted sediment trap at 4865 m depth (squares). For comparison the significantly higher buoyant fluxes collected at sites "EN" and "WN" are shown (circles and triangles).

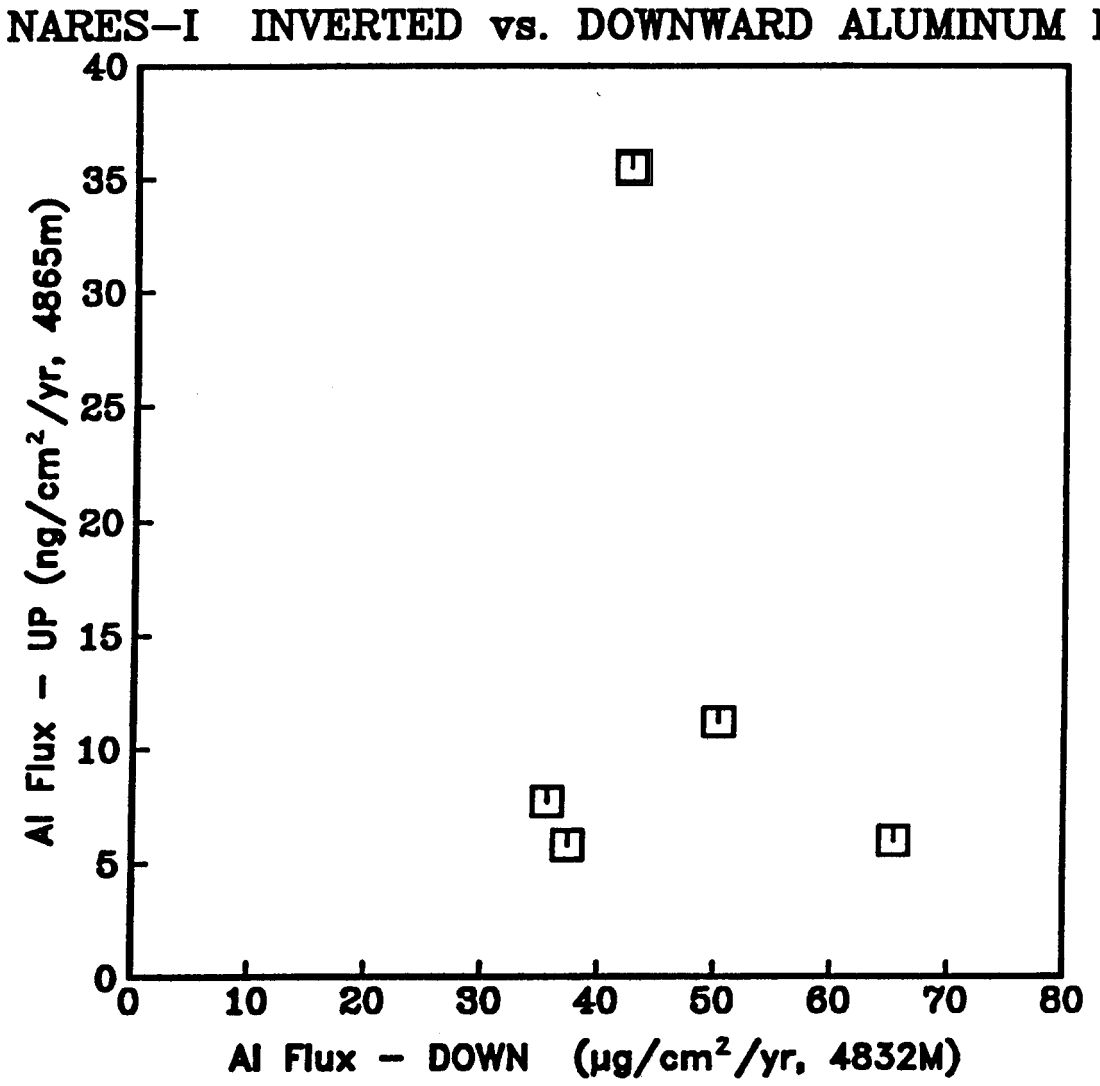

Figure 9. The downward and upward flux of aluminum at NAP-1. The upward flux is < 0.1% of the downward flux and its variations are not related to the downward flux magnitude.

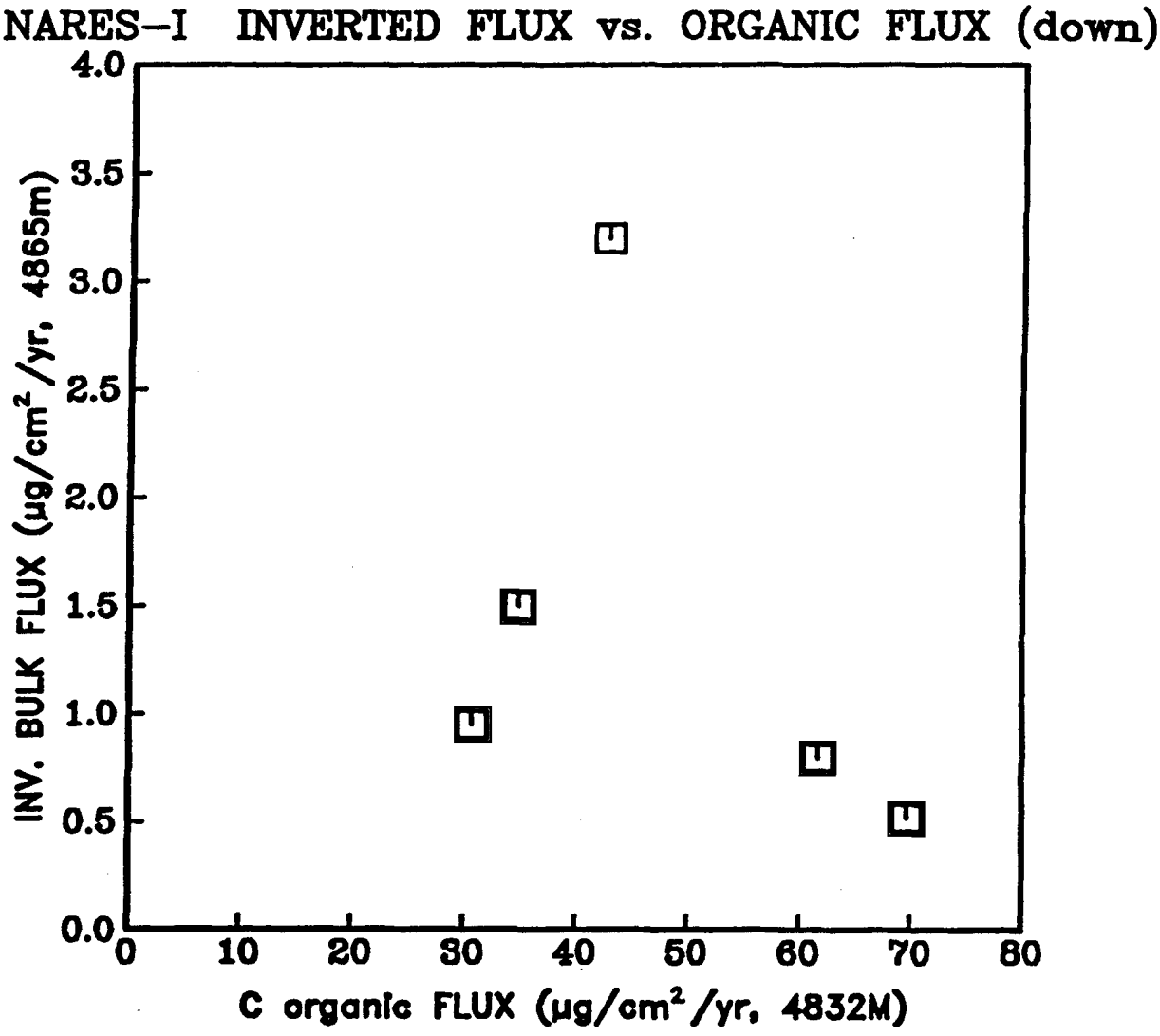

Figure 10. The bulk flux of buoyant particles vs. the downward flux of organic carbon. The upward fluxes at NAP-1 are very low which may be related to the low productivity of the surface waters. As was the case for Al there is no specific relationship between organic carbon and buoyant flux.

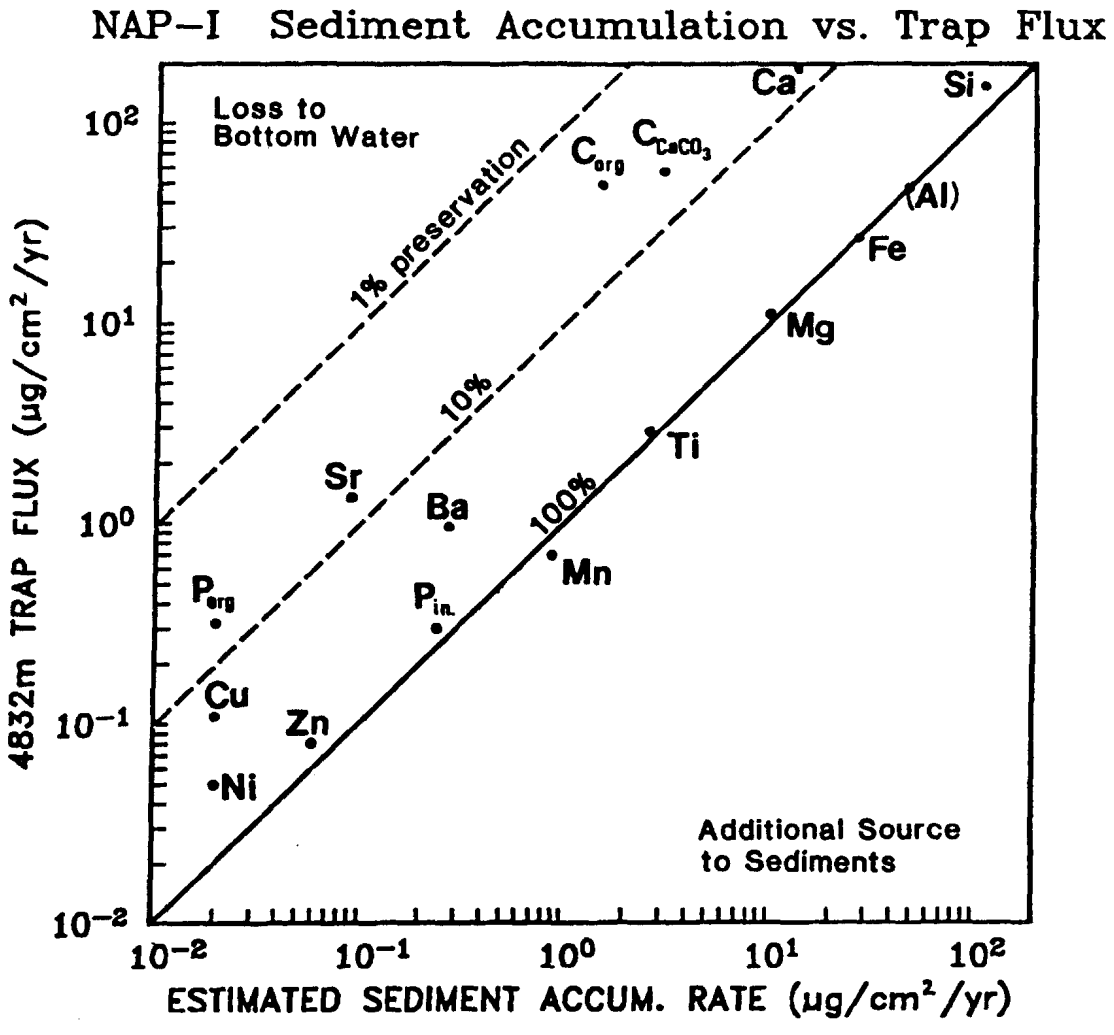

Figure 11. The vertical flux of elements at 4832 m compared to an estimate of the non-turbidite sedimentation rate for the same elements. Components in the upper left half of this log-log plot are not accumulating as rapidly as they are settling. Components on the lower right require an additional source to balance their accumulation rate.

APPENDIX C

RADIOCHEMICAL STUDIES AT THE NARES ABYSSAL PLAIN: NATURAL RADIONUCLIDE RESULTS

J. K. COCHRAN AND D. J. HIRSCHBERG

1985

Annual Report

Sandia Contract 25-8717

Radiochemical Studies at the Nares Abyssal Plain: Natural Radionuclide Results

J. Kirk Cochran
and
David J. Hirschberg

Marine Sciences Research Center
State University of New York
Stony Brook, New York 11794-5000

Table of Contents

List of Tables

List of Figures

I. Introduction

This report describes work accomplished during FY 1986 on samples of sea water, suspended particles, sediment trap material and bottom sediments collected from the Nares Abyssal Plain. The sample collection during the September 1984 cruise EN-121 of the R/V Endeavor was described in last year's report. Our work on natural radionuclides is complementary to Dr. Hugh Livingston's studies of artificial radionuclides on the same samples.

The geochemical field program at Nares is designed to provide information needed for the MkA scavenging model being developed by the Physical Oceanography Task Group of the Seabed Working Group. The model requires information on the partitioning of reactive radionuclides between solution and suspended particles and on fluxes of radionuclides through the water column. Data on the former are provided through samples taken with an in situ pumping system. Information on the latter has come from samples from sediment traps deployed at Nares (designated Nares-1, location 23°16.3'N, 63°55.4'W) by Dr. Jack Dymond's group at Oregon State University. Box cores and a gravity core have also been recovered at Nares and enable us to calculate the inventories of scavenged radionuclides which are present in bottom sediments.

II. Sample Collection and Analysis

A. Water Samples

Water samples were collected by the WHOI in situ pumping system (Winget et al. 1982) which filters large volumes of water through a Microwynd 1 μm polypropylene cartridge prefilter and two identical MnO_2-coated cartridges. Because the cartridges had been treated with a surfactant to prevent wetting, they were prepared for the MnO_2 by successive soaking in soap, NaOH and HCl baths before being placed in a warm saturated $KMnO_4$ solution

for 24 hours. The latter portion of the treatment is essentially that used by Moore (1976) for acrylic fibers. Flow rates of water through the cartridges were 3-8 liters/min and ~2000 liters were filtered during a typical cast.

Prior to radiochemical analysis, each cartridge was ignited at 450°C in a muffle furnace for ~24 hours. Radiochemical analysis was performed on the ash, with initial dissolution and radiochemical separation being done at WHOI for half the samples and at SUNY-Stony Brook for the remaining half. The ash was dissolved in ~200 ml 8N HNO_3 in the presence of ^{229}Th, ^{243}Am and ^{242}Pu tracers. A small amount of $NaNO_2$ was added to ensure that the Pu was all in the +4 oxidation state. The sample solution was passed through a 20 ml anion exchange column (Biorad AG1x8 50-100 mesh). U, Ra and ^{241}Am passed through the column while Th and Pu were retained. Th was eluted with concentrated HCl and Pu was eluted with concentrated HCl + NH_4I. Subsequent purification of Th involved a smaller HNO_3 anion exchange column. Pu and Am were purified as described in Livingston et al. (1975). Mounts for alpha spectrometry were prepared by electroplating the purified Th, Am and Pu fractions in $(NH_4)_2SO_4$ solution (Livingston et al. 1975). Final purification and plating was done at SUNY for all Th fractions and at WHOI for all Pu and Am fractions. The solution remaining after the Am separation from the effluent of the first anion exchange column contains Ra and has been reserved for later analysis of ^{228}Ra by ^{228}Th in growth.

B. Sediment Trap Samples

Approximately 100 mg of material from seasonal sediment trap samples were analyzed for ^{210}Pb, Th and Pu isotopes and ^{137}Cs. The sample was dissolved in small amounts of HCl, HNO_3 and HF in the presence of ^{229}Th, ^{243}Am and ^{242}Pu tracers. An aliquot consisting of ~5% of the sample was set aside for ^{210}Pb analysis by ^{210}Po. ^{208}Po tracer was added to this fraction and Po

was plated onto silver disks following the method of Flynn (1968). Subsequent separation and plating of the Th, Am and Pu fractions followed the procedure for the cartridges outlined above.

C. Sediment Samples

Known volumes of wet sediment were dried to determine percent water and dry bulk density. Subsequent radiochemical analyses followed the procedure of Livingston et al. (1975) for the artificial radionuclides and of Cochran and Krishnaswami (1980) and Cochran (1985) for ^{210}Pb, ^{226}Ra, Th and U isotopes. Unlike the cartridges and sediment trap samples, different aliquots of the sediment samples were analyzed for the man-made and natural radionuclides. This was necessitated by the different sample size requirements for the procedures (50 g for the artificial radionuclides vs. 0.5 g for the natural radionuclides) and by the fundamental difference of leaching the sediment in the artificial radionuclide procedure and total dissolution for the natural radionuclide analyses.

III. Results

A. Water Column Data

The low Th isotope activities of sea water make blank corrections important even for relatively large sample volumes. Blank cartridges (including ones impregnated with MnO_2) were analyzed by the same procedure used for samples and the results are given in Table 1. Blank contributions were negligible for Pu and ^{241}Am but not for Th. Higher values for ^{230}Th and ^{228}Th relative to ^{232}Th are related to small amounts of ^{228}Th in the ^{229}Th tracer and to contributions from the ^{229}Th tracer peak, which comprises a broad multiple energy peak lying between the ^{230}Th and ^{228}Th peaks. All cartridge data were corrected for these blank values and the results are presented in Tables 2-4.

Table 1. Polypropylene cartridge blanks.

	^{232}Th (dpm)	^{230}Th (dpm)	^{228}Th (dpm)
Pretreated with soap, NaOH, HCl; loaded with MnO_2	.018 ±.003	.037 ±.008	.066 ±.020
Pretreated with soap, NaOH, HCl; loaded with MnO_2	.022 ±.005	.051 ±.004	.108 ±.019
Pretreated with soap, NaOH, HCl	.024 ±.011	.059 ±.002	.099 ±.008
Mean ± 1σ	.022 ±.003	.037 ±.011	.091 ±.022

Table 2. Extraction efficiency of MnO_2 cartridge series for Th isotopes (Nares-1).

Depth (m)	Volume Filtered (ℓ)	Flow Rate (ℓ/min)	Cartridge Efficiency (%) ^{232}Th	^{230}Th	^{228}Th
surface	2315.3	6.4	72.2 ±4.7	87.0 ±9.3	74.9 ±1.5
400	1622.5	6.8	-	84.2 ±5.6	90.1 ±5.9
800	1575.3	6.6	-	85.6 ±4.5	87.1 ±1.6
1464	1234.0	5.1	-	80.0 ±3.2	78.7 ±3.4
2540	1831.3	7.6	-	86.1 ±1.8	83.4 ±2.8
3750	1783.0	7.4	-	84.6 ±1.9	84.6 ±1.5
5695	1708.0	7.1	-	84.0 ±1.8	77.9 ±1.4
5785	1064.0	4.3	-	97.5 ±1.5	88.1 ±1.4

Table 3. Concentrations of Th isotopes on filtered particles and water from Nares-1.

Depth (m)	^{232}Th Part	^{232}Th Diss (dpm/1000ℓ)	^{232}Th Total	^{230}Th Part	^{230}Th Diss (dpm/1000ℓ)	^{230}Th Total	^{228}Th Part	^{228}Th Diss (dpm/1000ℓ)	^{228}Th Total
Surface	.060 ±.005	.058 ±.006	.118 ±.008	.043 ±.006	.065 ±.011	.108 ±.013	0.90 ±.04	12.5 ±0.6	13.4 ±0.6
400	.007 ±.002	.007 ±.003	.014 ±.004	.034 ±.008	.176 ±.018	.210 ±.020	0.92 ±.06	9.17 ±.81	10.1 ±0.8
800	.010 ±.003	.007 ±.002	.017 ±.004	.062 ±.009	.201 ±.018	.263 ±.020	0.41 ±.03	1.33 ±.07	1.74 ±.08
1464	n.d.	n.d.	-	.032 ±.010	.496 ±.041	.528 ±.042	0.134 ±.011	0.851 ±.068	.985 ±.069
2540	.013 ±.002	.008 ±.002	.021 ±.003	.080 ±.009	.538 ±.030	.618 ±.031	0.164 ±.016	0.601 ±.040	.765 ±.043
3750	n.d.	.013 ±.003	.013 ±.004	.039 ±.007	.716 ±.049	.755 ±.049	0.074 ±.014	3.49 ±.21	3.56 ±.21
5695	.017 ±.002	.020 ±.003	.037 ±.004	.123 ±.011	.641 ±.036	.764 ±.038	0.51 ±.03	8.19 ±.40	8.70 ±.40
5785 (B-60)	.031 ±.006	.020 ±.008	.051 ±.010	.256 ±.024	.784 ±.103	1.04 ±.11	0.73 ±.05	9.47 ±1.03	10.2 ±1.1

n.d. - not detectable

Table 4. Fraction of Th isotopes collected on 1 μm cartridge prefilters (Nares-1).

Depth (m)	^{232}Th		^{230}Th		^{228}Th	
	% Part.	Cp/Cd	% Part.	Cp/Cd	% Part.	Cp/Cd
surface	51 ±6	1.0	40 ±7	.66	7 ±.4	.072
400	50 ±20	1.0	16 ±4	.19	9 ±1	.10
800	59 ±22	1.4	24 ±4	.31	24 ±2	.31
1464	-	-	6 ±2	.06	14 ±2	.16
2540	62 ±13	1.6	13 ±2	.15	21 ±2	.27
3750	-	-	5 ±1	.05	2 ±4	.02
5695	46 ±7	.85	16 ±2	.19	6 ±4	.06
5785	61 ±17	1.6	25 ±3	.33	7 ±1	.08
Mean				.24		.13

The activity of "dissolved" radionuclide is calculated from the activities on the two MnO_2 cartridges according to eq. 1 (Mann et al., 1984).

$$E = 1 - \frac{B}{A} \quad (1)$$

Where E = efficiency of chemical extraction of Th or Am from solution

B = activity on the second cartridge

A = activity on the first cartridge.

The efficiencies are given in Table 2. The value of B for ^{232}Th is in most cases close to the blank value making the efficiency subject to large uncertainty. The exception to this pattern is in surface water, in which the dissolved ^{232}Th activity is significantly greater than the blank value. Values calculated for the efficiency for ^{230}Th, ^{228}Th and ^{241}Am are generally greater than 80% and, for ^{230}Th and ^{228}Th, agree well with each other. This is a sensible result in that both thorium isotopes should behave chemically alike with respect to adsorption onto MnO_2.

The high values of the efficiency suggest that the in situ pumping system is an effective way to remove Th and Am from large volumes of sea water. It is interesting that Table 2 shows no clear correlation with flow rate and that flow rates as great as ~8ℓ/min produce high extraction efficiencies.

The activity of radionuclide on suspended particles is calculated from the prefilter as "dpm/ℓ water filtered". Because of the nature of the cartridge filters it was not practical to pre-weigh the filters and determine the mass of particles filtered. Dissolved activities were calculated from:

$$\text{Dissolved activity} = \frac{A}{E.V} \quad (2)$$

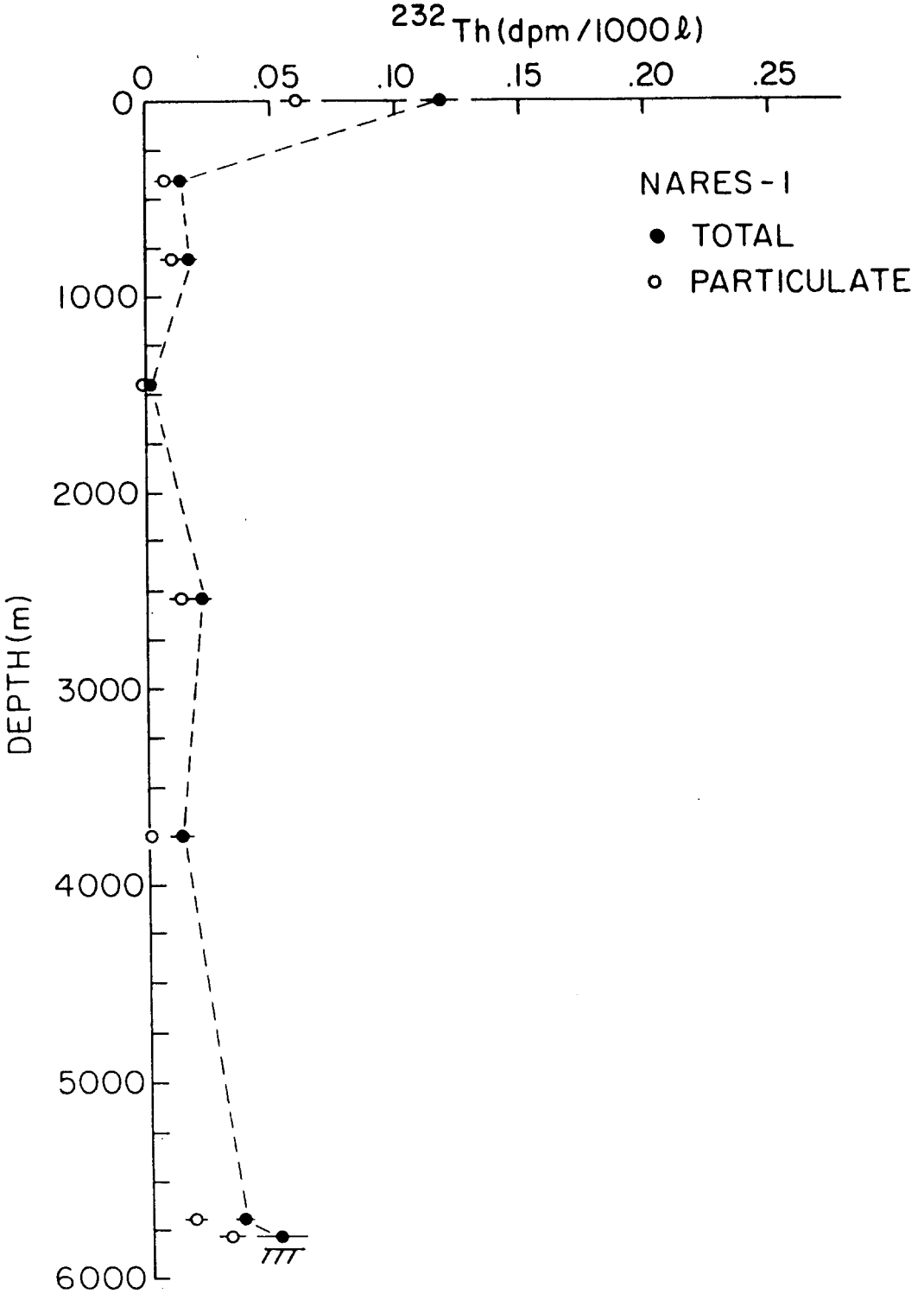

Figure 1. ^{232}Th activity vs. depth at Nares-1.
Solid circles = particulate + dissolved activity.
Open circles = particulate (1 μm cartridge filter) activity.

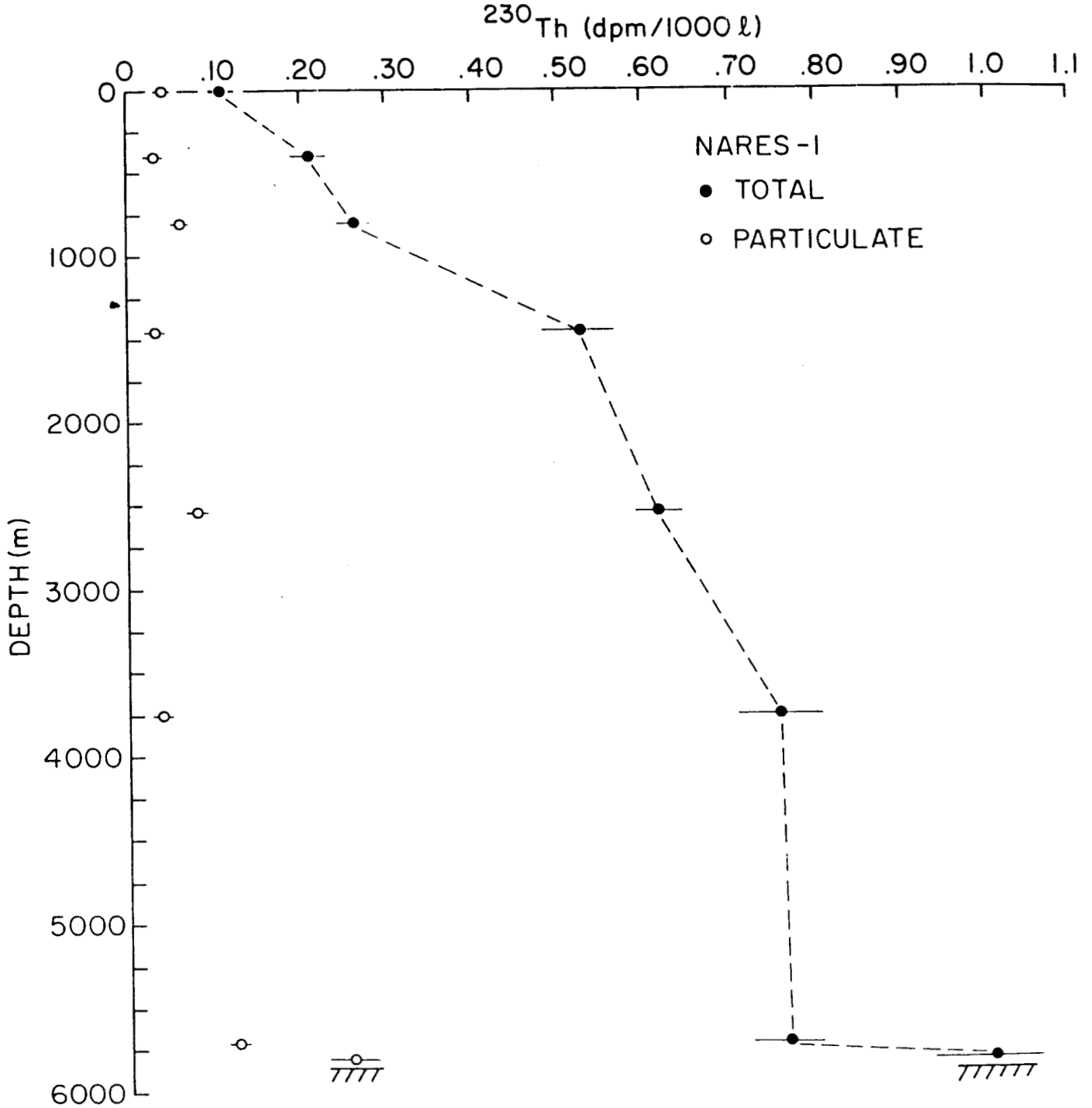

Figure 2. ^{230}Th activity vs. depth at Nares-1.
Solid circles = particulate + dissolved activity.
Open circles = particulate (1 μm cartridge filter) activity.

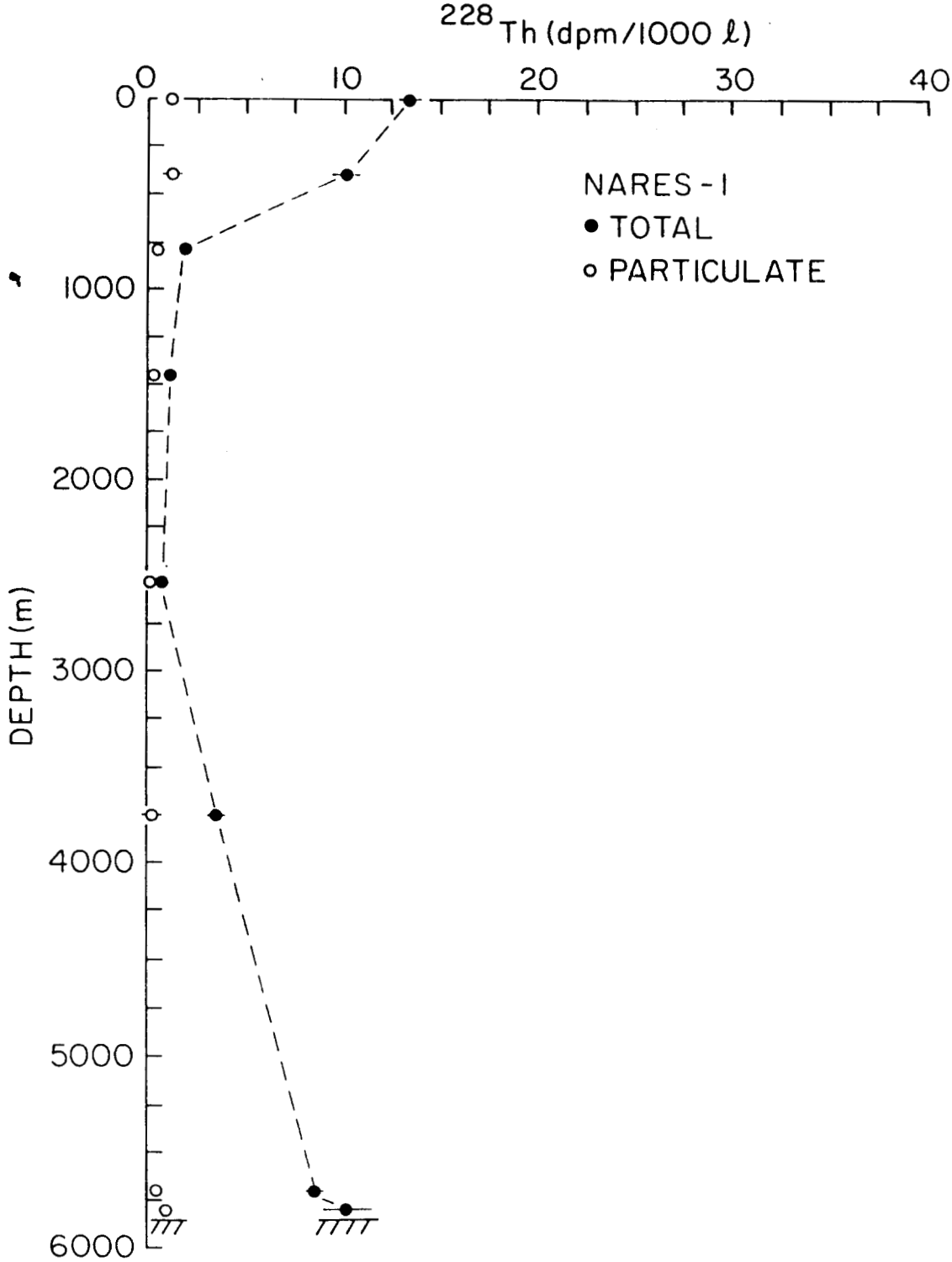

Figure 3. ^{228}Th activity vs. depth at Nares-1.
Solid circles = particulate + dissolved activity
Open circles = particulate (1 μm cartridge filter) activity.

Where A = activity on first MnO_2 cartridge

E = chemical extraction efficiency (eq. 1)

V = volume filtered.

These data are given in Table 3, and are plotted in Figs. 1-3, together with total activities calculated as the sum of the activities on the prefilter and in solution. We emphasize that our notation of "dissolved" and "particulate" activities are operational and are based on the 1 μm prefilter used. Unpublished data comparing a 1 μm cartridge filter with a 1 μm membrane filter (Livingston, pers. comm.) suggest that the former is more effective in filtering particles from sea water than is the latter. Thus it seems likely that the higher tortuosity of the cartridge filter is responsible for filtering particles of somewhat smaller diameter than 1 μm.

Using our operational definition of dissolved and particulate activities, the fraction of Th associated with filterable particles (calculated as % of total) is given in Table 4. Also given is the ratio of the activity on particles to that in solution. This latter value is of use in calculating scavenging rate constants for Th. (See discussion below).

B. Sediment Trap Data

Radionuclide activities in sediment trap material are given in Table 5 and activity fluxes, calculated from the specific activities and the bulk mass fluxes, are presented in Table 6. The specific activity is essentially constant with time at any depth despite variations in the bulk fluxes and variations in activity fluxes are thus produced by variations in bulk fluxes. This latter relationship is well demonstrated by Figs. 4-6.

C. Sediment Data

The gravity core data from Nares-1 are presented in Table 7 and Figure 7. Excess ^{230}Th is observed throughout the 170 cm core but the values

Table 5. Activities of Th isotopes and Pb-210 in Nares-1 sediment trap samples (23°16.3'N, 63°55.4'W, recovered 9/20/84).

Depth (m)	Cup	Collection Interval (days)	^{232}Th	^{230}Th	^{228}Th	^{210}Pb
			dpm/g			
1464	1	91	0.85±.19	3.13±.42	27.6±2.5	179±14
	2	78	0.45±.06	3.98±.39	33.4±2.4	206±14
	3	78	0.98±.14	3.45±.32	25.9±1.7	267±21
	4	78	1.46±.21	4.09±.42	33.3±2.4	260±20
	5	78	0.93±.09	2.87±.18	31.9±1.3	231±21
4832	1	91	1.51±.11	8.02±.36	29.3±1.1	454±29
	2	78	1.41±.11	7.83±.35	23.8±0.9	438±33
	3	78	1.51±.13	9.22±.45	25.8±1.1	388±25
	4	78	1.73±.22	10.2±0.8	27.5±2.0	499±31
	5	78	1.46±.21	10.6±.9	31.1±2.4	465±30

Table 6. Th isotope and Pb-210 fluxes at Nares-1
(23°16.3'N, 63°55.4'W, recovered 9/20/84).

Depth (m)	Cup	Mass Flux (mg/cm²y)	^{232}Th	^{230}Th* dpm/cm²ky	^{228}Th	^{210}Pb dpm/cm²y
1464	1	.425	.36	1.33	11.7	.076
	2	1.431	.64	5.70	47.8	.295
	3	.839	.82	2.89	21.7	.224
	4	.630	.92	3.43	27.9	.164
	5	.773	.72	2.22	24.6	.179
	Mean Annual Flux	.807	.68	3.06	26.3	.184
4832	1	1.003	1.51	8.04	29.4	.455
	2	1.207	1.70	9.45	28.7	.529
	3	.852	1.29	7.86	22.0	.331
	4	.809	1.40	8.25	22.2	.404
	5	1.639	2.39	17.4	51.0	.762
	Mean Annual Flux	1.10	1.65	10.1	30.6	.495

*Production from decay in water column
@1464 = 3.8 dpm/cm²ky
@4832 = 12.6 dpm/cm²ky

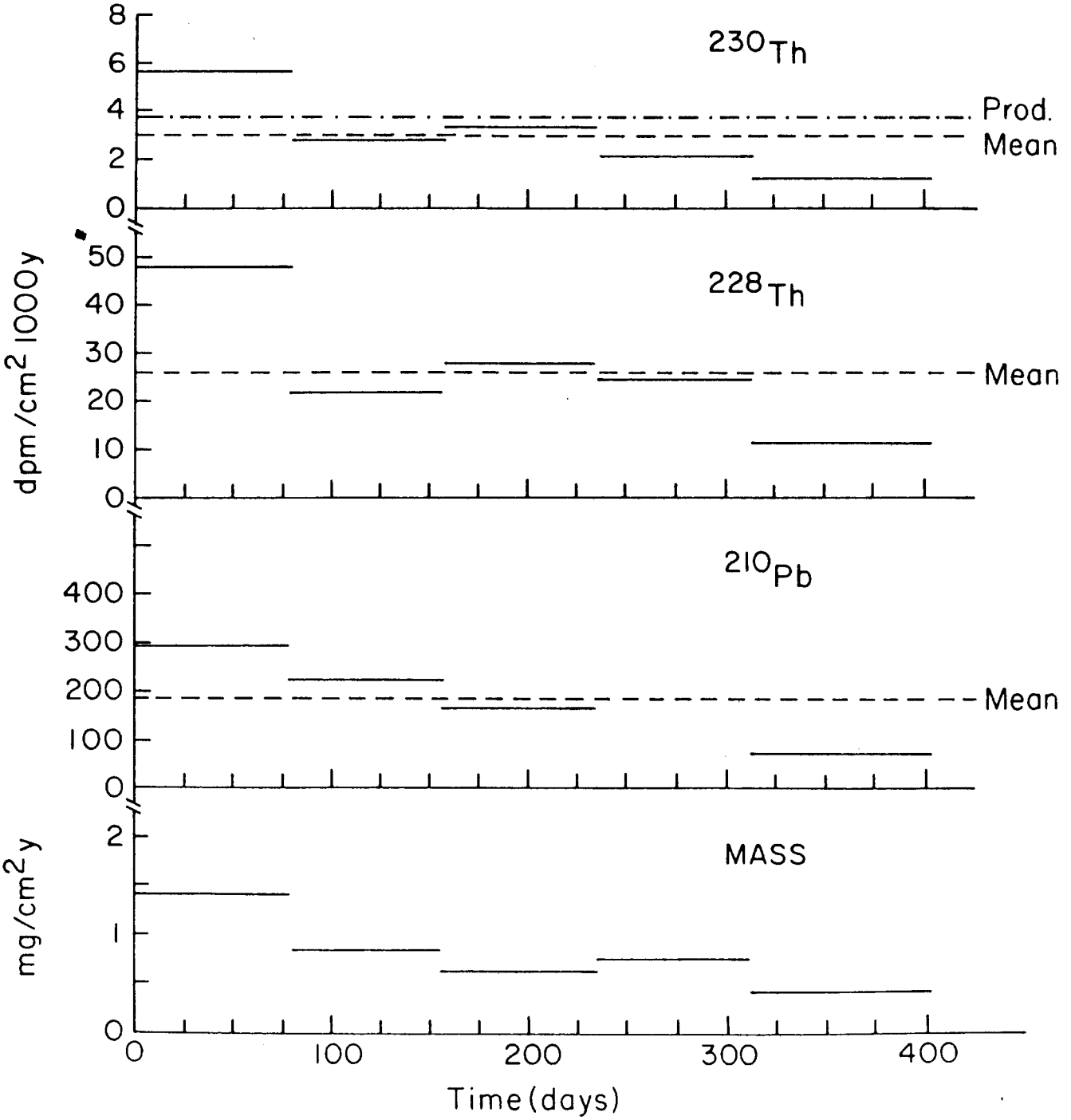

SEDIMENT TRAP NARES-I, 1464m
NARES ABYSSAL PLAIN

Figure 4. Radionuclide and bulk fluxes from sediment trap at 1464 m at Nares-1. Dashed lines indicate mass-weighted mean flux.

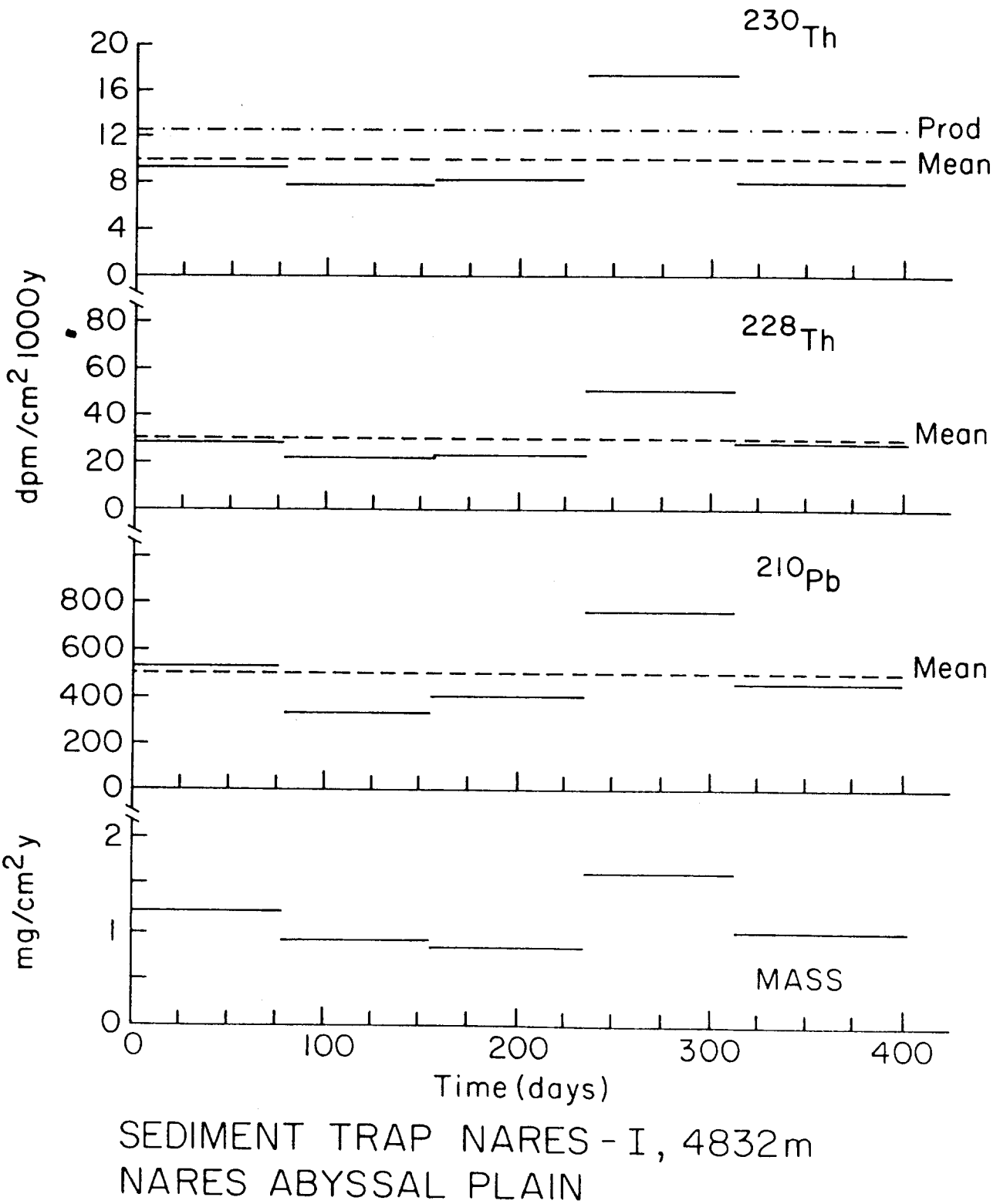

Figure 5. Radionuclide and bulk fluxes from sediment trap at 4832 m at Nares-1. Dashed lines indicates mass-weighted mean fluxes.

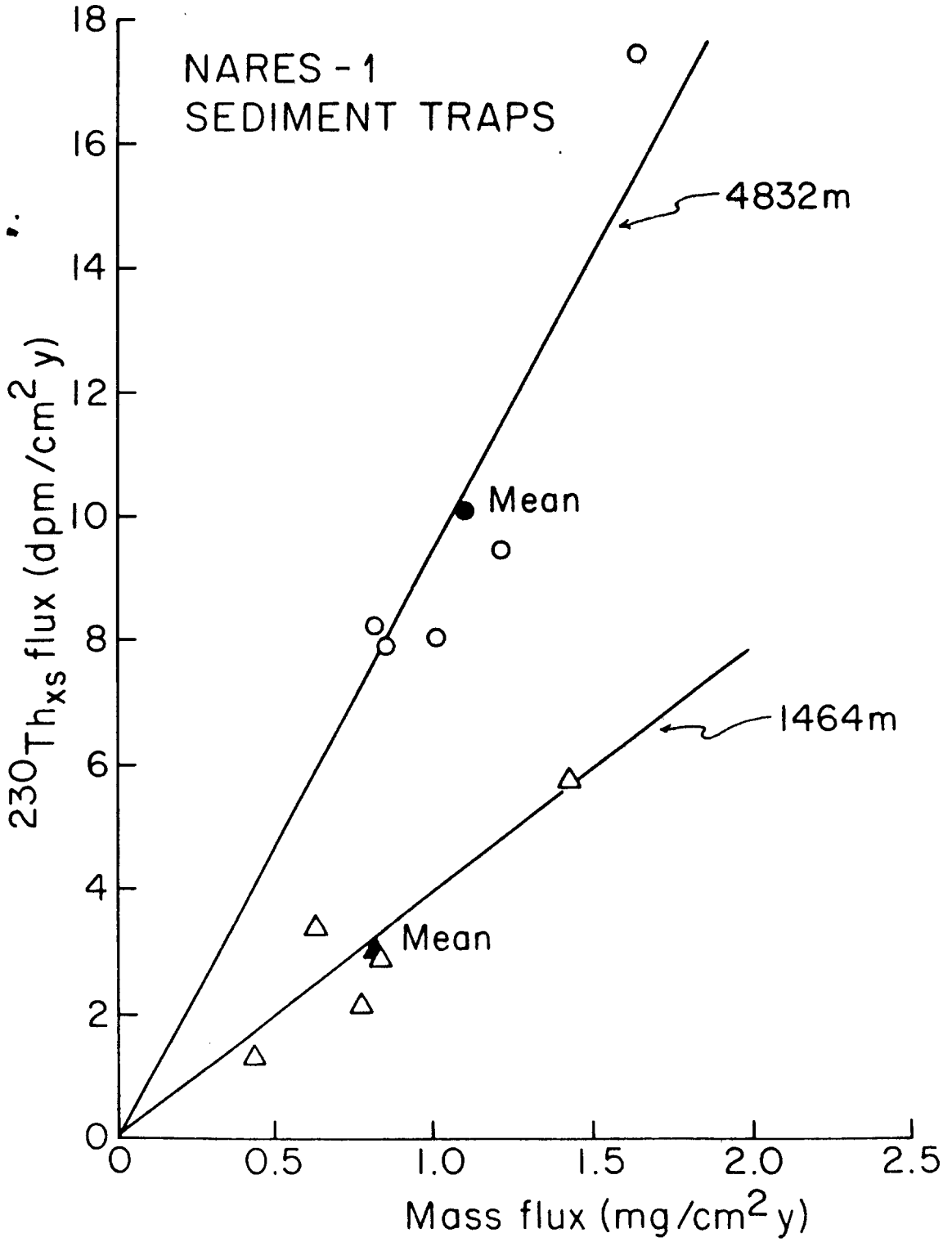

Figure 6. ^{230}Th flux vs. mass flux in Nares-1 sediment traps.

are low and the variation with depth is irregular. Water content values are also low for pelagic sediments and dry bulk densities are correspondingly large. The data are consistent with the presence of turbidite sedimentation in the Nares area (Thomson et al. 1984) and sediment accumulation rates cannot be reliably determined from Fig. 7.

IV. Discussion

A. Thorium Isotope Profiles

The thorium isotope profiles (Figs. 1-3) reflect the sources of each isotope to the oceans. ^{232}Th is not produced in situ but is added to the oceans by rivers and the atmosphere. Most of the ^{232}Th in sea water is associated with particles and dissolved ^{232}Th at Nares is <.02 dpm/1000 kg. This result is in agreement with Huh and Bacon's (1985) measurements of ^{232}Th in the Caribbean. A notable exception to this pattern is seen in the surface waters where the dissolved ^{232}Th is as great as 0.2 dpm/1000ℓ. The dissolved ^{232}Th seems to vary with location and is greater at the Hatteras E-N3 low level site than at Nares. The pattern of high dissolved ^{232}Th in surface waters also was observed by Huh and Bacon (1985). Both riverine and atmospheric sources undoubtedly contribute ^{232}Th to the surface ocean, with the former more important than the latter. Both the Hatteras and Nares sites show that dissolved ^{232}Th is rapidly removed from the surface ocean with values decreasing by about an order of magnitude between the surface and 400 m. At depth in the water column the ^{232}Th profiles show variations which are related to advective transport and to resuspension near the bottom. These features are apparent in the particulate ^{232}Th maxima at 700 and 4000 m at Hatteras and near the bottom at both sites. The increase in near-bottom particulate ^{232}Th is probably related to resuspension or near-bottom sediment transport, a process which is more active at Hatteras than at Nares (for example see sediment trap data from Cochran and Hirschberg, 1984).

Table 7. Radiochemical data for Nares sediments.
Core GC-1 (23°12.0'N, 63°58.5'W)

Depth in core (cm)	Dry bulk density (g/cm^3)	^{238}U	^{234}U	^{232}Th (dpm/g)	^{230}Th	$^{230}Th_{xs}$	$\frac{^{230}Th_{xs}}{^{232}Th}$ (dpm/dpm)
6.5-8.5	0.78	1.62 ±.30	1.47 ±.32	3.72 ±.24	7.98 ±.10	6.51 ±.34	1.75 ±.15
19-21	0.91	1.64 ±.38	1.78 ±.36	3.19 ±.14	4.47 ±.10	2.69 ±.37	0.84 ±.12
29-31	0.92	1.62 ±.38	1.30 ±.47	3.24 ±.38	5.21 ±.20	3.91 ±.51	1.21 ±.21
39-41	0.95	1.75 ±.31	1.45 ±.37	2.99 ±.39	3.70 ±.29	2.25 ±.47	0.75 ±.18
57-59	0.72	1.57 ±.23	1.65 ±.23	3.71 ±.44	5.73 ±.26	4.08 ±.35	1.10 ±.16
74-76	1.07	1.74 ±.31	1.82 ±.30	2.40 ±.19	3.02 ±.15	1.20 ±.34	0.50 ±.15
87-89	0.65	2.13 ±.21	1.84 ±.22	4.49 ±.16	6.59 ±.10	4.75 ±.24	1.06 ±.07
97-99	0.87	2.25 ±.16	2.23 ±.16	3.09 ±.24	8.28 ±.06	6.05 ±.17	1.96 ±.16
117-119	1.10	1.46 ±.32	1.38 ±.39	2.52 ±.16	2.13 ±.20	0.75 ±.44	0.30 ±.18
134-136	1.22	1.42 ±.36	1.19 ±.48	2.62 ±.15	2.31 ±.39	1.12 ±.62	0.43 ±.24
150-152	0.69	1.66 ±.31	1.35 ±.35	3.17 ±.25	3.25 ±.23	1.90 ±.42	0.60 ±.14
166-168	0.78	1.60 ±.37	1.36 ±.49	3.27 ±.16	4.67 ±.10	3.31 ±.50	1.01 ±.16

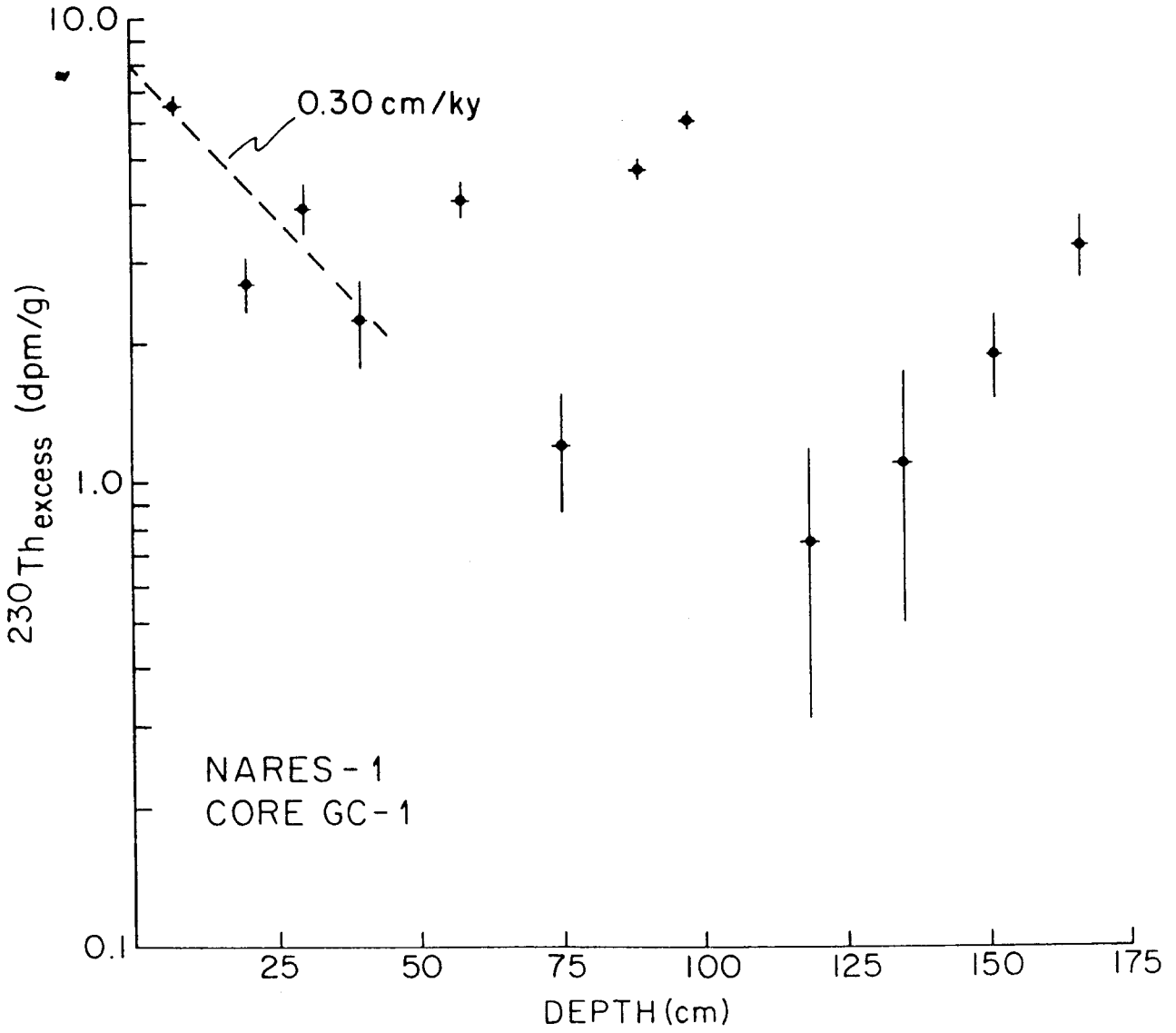

Figure 7. Excess ^{230}Th activity vs. depth in gravity core GC-1 from Nares-1.

Unlike the Pacific Ocean (Nozaki et al. 1981) there is no well defined increase in dissolved ^{232}Th near the bottom at our Atlantic sites. Instead the gradients in ^{232}Th seem strongly linked to particulate gradients.

Unlike ^{232}Th, ^{230}Th and ^{228}Th are both produced in situ from decay of soluble ^{234}U and ^{228}Ra, respectively. Their distributions (Figs. 2-3) reflect these sources. The production of ^{228}Th is greatest in the near surface and near bottom waters where the activities of ^{228}Ra are greatest. Indeed, the surface activity of ^{228}Ra decreases strongly away from the continental shelf (Broecker et al. 1973) and this, rather than variations in the ^{228}Th removal rate in surface waters, is probably the explanation for the greater surface ^{228}Th activities at the Hatteras site (E-N3). Because ^{232}Th activities of bottom sediments are similar at the two sites at Hatteras the bottom source of ^{228}Ra should be similar and this is reflected in the comparable near-bottom activities of ^{228}Th.

The production of ^{230}Th is uniform throughout the water column and is in part responsible for the shape of the ^{230}Th profile. Dissolved and particulate ^{230}Th generally increase with depth to highest values near the bottom. The increase is not, however, monotonic, and exceptions occur as in the surface water at Hatteras and the local particulate ^{230}Th maximum-dissolved ^{230}Th minimum at 4028 m at the same station. The latter coincides with a maximum in particulate ^{232}Th data and may be an advective feature. The ^{230}Th data do display significant differences from those of Nozaki et al. (1981) in the North Pacific. These include generally lower total ^{230}Th activities in the Atlantic ($\lesssim$1 dpm/1000 kg vs 2 dpm/1000 kg) and activities which are nearly constant (~0.6-0.7 dpm/1000kg) below ~2000 m. Increases in total ^{230}Th near the bottom are largely linked to increases in particulate ^{230}Th, possibly related to resuspension. Our ^{230}Th profiles at Hatteras and Nares are similar to that of

Bacon (1984) near Bermuda, so the features we observe seem to be general ones of the northwest Atlantic. In the opposite sense, lower ^{230}Th activities are observed in oceanic margin regions such as the eastern Atlantic (Mangini and Key, 1984) and Panama Basin (Bacon and Anderson, 1982).

B. Scavenging of Th Isotopes

Nozaki et al. (1981) and Bacon and Anderson (1982) have shown that the general increase in particulate and dissolved ^{230}Th with depth is consistent with a vertical scavenging model in which sinking particles progressively accumulate ^{230}Th as they sink but also maintain a sorption equilibrium with the solution. This approach is less valid in areas of the ocean in which isopycnal transport is occurring, and we have already suggested the possibility of such features in the Th profiles. However, sediment trap results (discussed further below) show that ~80% of the ^{230}Th produced in the water column at Hatteras or Nares is recovered in the traps, indicating that vertical processes are also quite important at these sites.

Assuming that the interactions between Th in solution and on particles is first order with respect to the Th concentration gives the equation:

$$\frac{dC_p}{dt} = k_1 Cd - (\lambda + k_2) C_p \qquad (3)$$

Where k_1 = rate constant for adsorption (y^{-1})

k_2 = rate constant for desorption

λ = decay constant

C_p = activity on particles (dpm/volume solution)

C_d = activity in solution (dpm/volume solution)

At steady state,

$$\frac{C_p}{C_d} = \frac{k_1}{\lambda + k_2} \qquad (4)$$

and for long lived radionuclides such that $k_2 >> \lambda$,

$$\frac{C_p}{C_d} = \frac{k_1}{k_2} \tag{5}$$

The rates C_p/C_d is related to the commonly measured geochemical distribution coefficient (K_d) as:

$$K_d = \frac{C_p/C_d}{P} \tag{6}$$

Where P = concentration of particles (g particles/cm³ solution).

Because the Th isotopes have markedly different half-lives, it is possible to determine k_1 and k_2 uniquely. This approach has been used successfully by Bacon and Anderson (1982) for ^{230}Th and ^{234}Th. For ^{230}Th and ^{228}Th, eq. 4 implies that the ratio of C_p/C_d for ^{228}Th should be less than or equal to that for ^{230}Th. Indeed, combining eq. 4 for ^{228}Th and eq. 5 for ^{230}Th produces:

$$(C_p/C_d)_{230} = (1 + \frac{\lambda_{228}}{k_2}) (C_p/C_d)_{228} \tag{7}$$

Values of C_p/C_d for ^{230}Th and ^{228}Th are tabulated in Table 4 and show that $(C_p/C_d)_{228} \lesssim (C_p/C_d)_{230}$ for surface and near-bottom water. Contrary to prediction, the relationship is reversed for mid-depths. A possible explanation for this feature is that whereas ^{230}Th is produced throughout the water column, ^{228}Th production is quite low at mid-depths due to the very low ^{228}Ra there (Moore et al. 1985). Thus the ^{228}Th in solution at mid-depths is almost completely derived from release from sinking particles. ^{230}Th in solution at mid-depths is derived both from sinking particles and from ^{234}U decay in solution.

Applying eq. 7 to depths below ~4000 m yields values for k_1 of .01-.04 at Nares and .06-.51 at Hatteras and values for k_2 of .12-.24 at Nares and .10-1.5

at Hatteras. The generally higher values at Hatteras may reflect more rapid scavenging due to a better developed bottom nepheloid layer at that site.

Values of K_d may be calculated from the C_p/C_d ratio for ^{230}Th and Table 8 shows these results. The values were calculated assuming a suspended particle concentration of ~10 µg/l. Also included are K_d values for ^{241}Am and $^{239,240}Pu$ calculated from Dr. Hugh Livingston's data. Th is characterized by a high Kd and the value for Am is similar. Both elements are distinctly more reactive than Pu. This sequence is consistent with the strong retention of Am and Th on the MnO_2 cartridges but only weak uptake of Pu.

C. Sediment Trap Activities and Fluxes

The sediment trap data given in Table 5 show that the specific activity of the radionuclides measured is nearly constant in trap samples collected at any given depth. This is so in spite of variations of a factor of 2-10 in bulk mass fluxes over time. Thus the activity flux is controlled by the bulk flux as shown for the two Nares traps in Fig. 6. A similar observation was made by Hugh Livingston for Am and Pu and by Bacon (1985) for trap samples from a station near Bermuda.

The specific activities of the sediment trap material also change in a sensible way with depth. ^{230}Th and ^{210}Pb activities increase as sinking particles continue to pick up these radionuclides which are produced throughout the water column. For the two Nares traps, the relative lack of change in ^{228}Th activity reflects the fact that these traps are out of the surface zone of high ^{228}Th production. Particles sinking from 1464 m to 4832 m are picking up little additional ^{228} Th from sea water.

A check on the ability of the traps to collect the particulate flux is provided by the measured fluxes of ^{230}Th. We know from the water column data that this isotope is almost completely scavenged from sea water and we also

Table 8. K_d values for Am, Pu and Th isotopes.

Nuclide	C_p/C_d [1]	K_d [2]
Nares (Nares-1)		
^{230}Th	.24	2.4×10^7
^{228}Th	.13	1.3×10^7
^{241}Am	.065	6.5×10^6
$^{239,240}Pu$	.016	1.6×10^6
Hatteras (E-N3)		
^{230}Th	.24	2.4×10^7
^{228}Th	.19	2.0×10^7
^{241}Am	.10	1.0×10^7
$^{239,240}Pu$	.009	8×10^5

1 Ratio of particulate (1 μm cartridge filter) to dissolved radionuclide. Am and Pu data are from Dr. Hugh Livingston (WHOI).

2 Calculated using particle concentration of 10 μg/kg measured by Dr. Jack Dymond.

know its rate of production from ^{234}U decay. As shown in Table 6, the traps recover about 80% of the ^{230}Th removed from sea water. If this removal is by vertical processes at the trap site then the traps are ~80% efficient at collecting the particulate flux. Alternatively some of the ^{230}Th may be transported horizontally and removed at sinks distant from the Nares Abyssal Plain as suggested by Anderson et al. (1983). A final check on the ^{230}Th balance at the Nares site is provided by comparing the trap fluxes with the ^{230}Th accumulation in the sediments there. The extensive emplacement of turbidites at the site prevents this comparison, however.

The observations of 1) nearly complete scavenging of ^{230}Th by the large, rapidly settling particles, 2) the constant specific activity of those particles and 3) the direct relationship between the activity flux and bulk flux can be explained by a two stage scavenging mechanism involving small suspended particles and large settling particles. Reactive nuclides become associated with the suspended particles by the sorption mechanism discussed earlier. The specific activity of these particles (not determined in our work) is set by the K_d of the radionuclide and the concentration of particles. These small particles and associated radionuclide are removed from the water column by incorporation into large rapidly sinking particle aggregates and this process may occur biologically through grazing and fecal pellet production or physically through the collision of large particles by small ones (McCave, 1984). If the large particles do not take up reactive radionuclides directly from solution do so but only through the incorporation of small particles, the specific activity of the large particles should remain constant at any given depth (provided each "large" particle incorporates a fixed amount of "small" particles). The greater the flux of large particles, the greater the uptake of small particles and thus the greater the flux of reactive radionuclides. This

scheme represents a modification of the MkA geochemical model in that the large particles seem to be serving only as collectors of small particles rather than sorbing radionuclides directly. It is important to note however that large particles such as tests or tissue may incorporate radionuclides as the particles form in surface waters. Such incorporation would not be seen with ^{230}Th which is produced mainly at depth.

D: Sediment chronologies

Figure 7 shows the results of excess ^{230}Th determinations on the long (~1.8 m) gravity core taken during the 1984 cruise to Nares. The data do not show regular decreases with depth but instead show alternating zones of high activity and low activity. No meaningful accumulation rate can be derived from these results and the data are similar to those of Thomson et al. (1984). The irregular ^{230}Th decreases observed by Thomson et al. (1984) in cores from the Nares area led them to conclude that turbidite sedimentation strongly affects the stratigraphy of the site. We concur in that conclusion and find that as much as 170 cm of sediment must have been deposited relatively rapidly, perhaps in series of turbidites separated by poorly defined periods of pelagic sedimentation.

References

Anderson, R. F., M. P. Bacon, P. G. Brewer (1983) Removal of Th-230 and Pa-231 from the open ocean. Earth Planet. Sci. Lett. 62, 7-23.

Bacon, M. P. and R. F. Anderson (1982) Distribution of thorium isotopes between dissolved and particulate forms in the deep-sea. J. Geophys. Res. 87, 2045-2056.

Bacon, M. P. (1984) Radionuclide fluxes in the ocean interior. In: Global Ocean Flux Study, Proc. of a Workshop, Nat. Acad. Press, Washington, D.C., pp 180-205.

Bacon, M. P. (1985) Seasonality in the flux of natural radionuclides and plutonium in the deep Sargasso Sea. Deep-Sea Res. 32, 273-286.

Broecker, W. S., A. Kaufman, R. M. Trier (1973) The residence time of thorium in surface sea water and its implications regarding the fate of reactive pollutants. Earth Planet. Sci. Lett. 20, 35-44.

Cochran, J. K. and S. Krishnaswami (1980) Radium, thorium, uranium and Pb-210 in deep-sea sediments and sediment pore waters from the North Equatorial Pacific. Am. J. Sci. 280, 849-889.

Cochran, J. K. and D. J. Hirschberg (1984) Radiochemical Studies in Support of the Low Level Waste Ocean Disposal Program (East Coast Site). Final Report, Sandia Contract 58-3521.

Cochran, J. K. (1985) Particle mixing rates in sediments of the eastern equatorial Pacific: Evidence from Pb-210, Pu-239,240 and Cs-137 distributions at MANOP sites. Geochim. Cosmochim. Acta 49, 1195-1210.

Huh, C. A. and M. P. Bacon (1985) Thorium-232 in the eastern Caribbean Sea. Nature 316, 718-721.

Livingston, H. D., D. R. Mann and V. T. Bowen (1975) Analytical procedures for transuranic elements in seawater and marine sediments. In: Analytical Methods in Oceanography (T.R.P. Gibb, ed.) Am. Chem. Society, pp. 124-138.

Mangini, A. and R. M. Key (1983) A Th-230 profile in the Atlantic Ocean. Earth Planet Sci. Lett. 62, 377-384.

McCave, I. N. (1984) Size spectra and aggregation of suspended particles in the deep ocean. Deep-Sea Res. 31, 329-352.

Moore, W. S. (1976) Sampling Ra-228 in the deep ocean. Deep-Sea Res. 23, 647-651.

Moore, W. S., R. M. Key and J. L. Sarmiento (1985) Techniques for precise mapping of Ra-226 and Ra-228 in the ocean. J. Geophys. Res. 90, 6983-6994.

Nozaki, Y., Y. Horibe and H. Tsubota (1981) The water column distributions of thorium isotopes in the western North Pacific. Earth Planet. Sci. Lett. 54, 203-215.

Thomson, J., M. S. N. Carpenter, S. Colley, T. R S. Wilson, H. Elderfield and H. Kennedy (1984) Metal accumulation rates in northwest Atlantic pelagic sediments. Geochim. Cosmochim. Acta 48, 1935-1948.

Winget, C. L., J. C. Burke, D. L. Schneider and D. R. Mann. (1982) A self-powered pumping system for in situ extraction of particulate and dissolved materials from large volumes of seawater. WHOI Technical Report, WHOI-82-8.

APPENDIX D

RADIOCHEMICAL STUDIES AT THE NARES ABYSSAL PLAIN: ANTHROPOGENIC RADIONUCLIDE RESULTS, FY1985 ANNUAL REPORT

H. D. LIVINGSTON

1985 ANNUAL PROGRESS REPORT

SUBSEABED DISPOSAL PROGRAM

Contract 25-8712

with

Sandia National Laboratories

Albuquerque, New Mexico

Hugh D. Livingston

Woods Hole Oceanographic Institution

Woods Hole, Massachusetts 02543

11/15/85

Introduction

In the past year, the major effort has involved analytical work on samples collected in the water column at the Nares Abyssal Plain study site for the Subseabed Disposal Program. These samples included large volume water samples, large volume filtered particulates and soluble phase concentrates collected by in-situ electrical pumps and sediment trap samples collected at the Nares-1 mooring in Dr. J. Dymond's traps. In addition, further radiochemical analyses were completed of the Nares sediment cores for which Pu, ^{137}Cs and ^{210}Pb data were reported last year. New data for surficial ^{241}Am concentrations were obtained.

All of these data describe in a comprehensive (albeit incomplete) manner, the distribution of fallout transuranics and ^{137}Cs in the water column (including particle-associated phases) and sediments at the Nares site. Their significance to the Subseabed Disposal Program is that they define several of the parameters necessary to build a geochemical scavenging component into the physical modelling effort of the program. These parameters are not restricted to the specific nuclides involved. Together with the natural series nuclides (Th and Pb) studied by Dr. J. K. Cochran at S.U.N.Y., the suite of nuclides studied span a range of chemical reactivities with respect to scavenging, and in many instances are critical radionuclides in high level waste forms - or represent very close chemical relatives of critical nuclides. So the data set will be applicable to the selection of geochemical modelling parameters which are realistic and based on real oceanic measurements as opposed to laboratory experiment extrapolations.

A recent, and somewhat surprising, development in the application of bomb fallout nuclide studies at the Nares site to the Subseabed Program, is in applicability of these measurements as deep water tracers of the interaction of the deep Western Boundary Current with the deep gyre interior at the Nares Site. As this interaction is a key component of the deep mixing processes responsible for dispersal of a waste signal introduced to the bottom water in the gyre interior, tracers which can set constraints on the rates of such processes will provide a highly relevant input to the deep circulation modelling effort. For several reasons, these fallout nuclear

measurements will be a highly significant addition to the set of tritium measurements planned to study the boundary current/gyre interior interaction. Firstly, our measurements of a deep water atmospheric advective tracer signal at the Nares site in 1984 represent the earliest unequivocal detection of such a signal there. Secondly, new techniques of measurement of a deep ^{137}Cs signal offer the potential for detecting low level tracer signals at sensitivities one to two orders of magnitude greater than have been used to date. This potential could be used to define the deep tracer distribution in the Nares region with significantly increased precision than will be possible from the tritium measurements.

Fallout Nuclides in the Water Column at Nares-1

1. Large Volume Water Samples

A general description of the distribution of fallout tracers in the water column at the Nares Abyssal Plain site comes from radiochemical analyses of the 60-liter samples collected with Niskin bottles on ENDEAVOR-121 cruise in September 1984. From these samples we have completed analyses for ^{137}Cs and $^{239,240}Pu$ (and a limited number of ^{90}Sr analyses). These data can be compared with the distribution of the various water masses which they characterize and are a basic data set to which the associated data on actinide associations with both fine and large particles are referenced. The radiochemical results are listed in Table 1 together with their associated hydrographic data. The depth distributions of the two radioelements are plotted in Figure 1. The major fraction of the inventories of both radioelements is in the water masses of the upper water column, i.e. above the deep water. 21% of the total ^{137}Cs and 31% of the $^{239,240}Pu$ is in the deep water. This distribution argues for advective supply of the deep ^{137}Cs tracer and of much of the $^{239,240}Pu$. The importance of this, as far as geochemical scavenging of Pu is concerned, is that its advective supply to the deep water is substantially more than the supply in association with sinking particulates.

Since this conclusion rests heavily on the reliability which can be attached to the determination of the deep ^{137}Cs signal, independent evidence

of the existence of a deep advective atmospheric signal was sought. Firstly, comparison of the temperature and salinities measured in the large volume Niskin samples with T-S characteristics of the Nares site - both measured in 1984 and historically - showed that no contamination of the samples with shallower, high tracer water had occurred. Secondly, ^{90}Sr measurements were made on some of the ENDEAVOR-121 deep water samples. As a fallout tracer with low particle reactivity, its presence in deep water would be clear confirmation of an advective supply. To facilitate the precision of the measurement of the very low concentration expected, the strontium isolates from the five deepest samples were combined for radiochemical analysis. The preliminary result of this analysis is a mean concentration of 0.8 dpm/100 Kg. This value seems consistent with the range of deep ^{137}Cs values in Table 1 (given the fallout $^{137}Cs/^{90}Sr$ ratio of 1.5).

A further piece of evidence which adds confidence to the detection of a deep advective signal comes from inspection of deep tritium values reported in the region from TTO samples collected in 1981 (Ostlund, University of Miami, Tritium Laboratory, Data Release #81-35). The distribution of a deep tritium signal in water of Western Boundary Undercurrent origin is confined to positions nearer the exterior of the gyre, near the Antilles Arc. The deep tritium data in the interior in 1981 - at the Nares study site - are represented by TTO Station 24 and are plotted in Figure 2. Only one sample, at 4584 m, contained enough tritium to be distinguishable from zero. To compare our measurements of deep ^{137}Cs concentrations to tritium, it is necessary to apply an appropriate conversion. Referenced to 1981, a ratio of 6 was used for the ratio ^{137}Cs (dpm/100 Kg)/Tritium Units (81 TU). This number characterized 1972 Greenland Sea Deepwater (GEOSECS Data Reports) and Denmark Strait Overflow in 1972 (Livingston et al., J. Geophys. Res. 90, 6971 (1985)). As such, it seems an appropriate value to use for water advected to the south by 1984. The solid circles and line in Figure 2 represent our 1984 ^{137}Cs data at Nares converted to tritium. Although the uncertainties in the data are not trivial, it seems clear that the average values in the deep water below 3000 m are elevated over those seen in 1981 but at a level consistent with that observed in 1981 at 4584 m. We plan further work on the 1985 cruise to confirm further, and document, this deep signal.

The data for the upper part of the Nares water column fallout tracers show two subsurface maxima - one in the 0-1000 m range and one in the 1000-2000 m range. The shallower maximum is clearly the expression at the Nares site of the tracer maximum at this density in the Sargasso Sea for Subtropical Mode water described by Jenkins (J. Mar. Res. 38, 533 (1980)). The deeper maximum, though usually associated with Mediterranean water, is believed by Jenkins to derive its tracer properties from a more northerly source. Certainly it is possible to produce its properties by suitable mixing of Labrador Sea water with Mediterranean outflow water from the eastern North Atlantic basin.

When the ^{137}Cs and Pu profiles in Figure 1 are compared, there is no immediate sense of Pu transport relative to ^{137}Cs - except for the slightly deeper Pu maximum in the upper 1000 m. Knowing the fallout $^{239,240}Pu/^{137}Cs$ ratio (0.019 referenced to 1984), it is possibly to convert the observed ^{137}Cs distribution to that which would obtain for $^{239,240}Pu$ if no preferential geochemical vertical transport were taking place. In Figure 3 the solid line is the plot of such a conversion. The measured values lie at substantially lower values in the upper 700 m indicating that scavenging has removed a substantial fraction of the upper ocean inventory. It is not clear from the limited data set whether this deficiency is balanced by an excess between 700 and 2000 m, although the 1464 m measured value does indicate an excess over the converted ^{137}Cs value. What does seem clear is that the deficiency is not transferred to the deep water as the deep water Pu inventory only marginally exceeds that obtained by conversion of the ^{137}Cs inventory.

This conclusion means that advection is being proposed as the major supply of $^{239,240}Pu$ to the deep water - together with ^{137}Cs and similar tracers. Arguments can be advanced which support this proposition by comparing the relative amounts of $^{239,240}Pu$ and ^{137}Cs in the deep water with those which would characterize the advective source waters. Denmark Strait overflow water sampled in 1972 at GEOSECS 11 was characterized with a mean $^{239,240}Pu/^{137}Cs$ ratio of 0.017 decay corrected to 1984 (Livingston et al., WHOI Tech. Rept. 85-19). Deep water sampled in 1980 close to the Western Boundary Undercurrent off Cape Hatteras had a mean ratio of 0.018 - from data from a station at the EN-2 site of the low-level waste ocean disposal program

(Livingston et al., 1983 Annual Report, Sandia Labs). The mean value in the deep water at the Nares site is 0.023. The fact that this value is only slightly greater than those which could be viewed to characterize the source water which is being advected into the gyre interior at the Nares site, suggests very strongly that vertical transport need account for a minor fraction of the deep Nares Pu inventory. As was indicated last year, the Nares sediments contain extremely low levels of fallout Pu and thus do not represent a sink for the upper water column deficiency. It seems, therefore, that the scavenging and vertical transport of fallout Pu is chiefly taking place in the main thermocline at present.

2. In Situ Pump Samples

a. Total ^{241}Am analyses

The very large (1000-2000 liter) samples obtained using our wire mounted, electrically-powered pumping systems permitted the analyses of nuclides associated with the filtered fine-particle phase and those in the soluble phase collected by the MnO_2 chemisorbers in series behind the filters. In addition to the Th isotope data reported by Dr. J. K. Cochran, we have completed analyses for ^{239,240}Pu and ^{241}Am in the particulate phases and of ^{241}Am in the soluble phase (Pu is not efficiently collected by this chemisorber). These results are listed in Table 2.

The total ^{241}Am concentrations represented by the sum of the filtered and soluble phase concentrations are plotted in Figure 4 for comparison with the ^{239,240}Pu data obtained from the Niskin bottle samples. The production of ^{241}Am is by radiogenic ingrowth of its parent ^{241}Pu decay. Accordingly, the general shape of the ^{241}Am profile broadly resembles that of ^{239,240}Pu. Closer examination of the data reveals evidence of the effects of higher scavenging rates for ^{241}Am compared to ^{239,240}Pu - due to its greater particle affinity. By 1984, ^{241}Pu decay in global fallout debris can be shown to have generated ^{241}Am to the extent that the ^{241}Am/^{239,240}Pu ratio would be 0.29 if no external geochemical fractionation was in effect. If Am and Pu had identical particle reactivities, the oceanic ^{241}Am profile would equal that of Pu multiplied by 0.29. In Figure 5 this hypothetical ^{241}Am is produced from the measured ^{239,240}Pu data and shown by the solid line. The

measured values in the upper water column lie at lower values than the non-fractionation predicted values. This shows that active differential scavenging has occurred transferring ^{241}Am more rapidly to deeper water. The sample spacings are not sufficient to identify the location of this scavenged ^{241}Am. It seems clear that the deep water contains insufficient ^{241}Am in excess of that associated with in-situ ingrowth; so, as with the scavenging of Pu discussed above, it seems probable that the upper water column deficiency must be balanced by an excess in the lower part of the main thermocline, i.e. at intermediate depths between 800 m and the upper deep water boundary. The sediment data reported later in this report show no evidence of the sediments being a sink accumulating enough ^{241}Am to balance the upper layer deficiency. So again, the geochemical scavenging of both fallout transuranics seems chiefly restricted to the upper water column over the timescales represented by fallout tracers.

b) Transuranics on filtered particulates

Table 2 lists the concentrations of $^{239,240}Pu$ and ^{241}Am measured on the fine-particle samples collected by filtration on the 1 μm polypropylene wound-fiber filter cartridges used in the in-situ pump systems. The depth profiles of these nuclides are plotted in Figures 6 and 7. Also shown are the comparable data obtained on the same cruise at the EN-3 study site at the Hatteras Abyssal Plain. Both transuranics show particulate profiles like those of the total concentrations, but at very much lower concentrations. Given moderately uniform concentrations of suspended particles, the partition between soluble and particulate phases seems correspondingly uniform for each radioelement - though different between them in line with the greater particle reactivity of ^{241}Am.

The partition of ^{241}Am observed at Nares is marginally less than observed at the Hatteras Abyssal Plain site. For the subsurface waters the mean ratio for the particle/dissolved concentration was 0.065 at Nares compared with 0.096 at the Hatteras site. For $^{239,240}Pu$, the mean value at the Hatteras site was 0.010. This may be a more meaningful estimate of the Pu partition, as the mean value at Nares of 0.016 is based on fewer measurements and biased by the high value (but high uncertainty) at 5785 m. At the very low concentrations involved, it seems better at present to use the

Hatteras value as the best estimate for North Atlantic Gyre water columns. The difference between the mean ^{241}Am values may reflect higher suspended particle concentrations at the Hatteras site. Certainly the large particle fluxes are higher there and it seems likely that this difference could well be associated with a corresponding fine-particle concentration difference.

The very low degree of particle association noted for $^{239,240}Pu$ is consistent with the conclusion above that little vertical transport of $^{239,240}Pu$ from the upper to the deep water layers has taken place at the Nares location since the arrival of fallout nuclides in the ocean. Advection is again the dominant process. The higher particle association characteristics of ^{241}Am leads to the greater expectation of vertical transport to the deep water being detectable. The precision of the deep water ^{241}Am data are not quite sensitive enough to resolve this question. However, the mean concentrations of both ^{241}Am and $^{239,240}Pu$ in the deep waters at the Hatteras and Nares sites, 0.009 and 0.025 dpm/100 Kg respectively, give a $^{241}Am/^{239,240}Pu$ ratio of 0.36. This exceeds the value of 0.29 for unfractionated fallout and may well reflect some vertical transport of ^{241}Am preferentially to deep water.

3. Sediment trap samples

Radiochemical analyses have been completed for transuranic nuclides on the seasonal series of settling particulate samples collected in the upward facing traps at 1464 m and 4832 m on the Nares-1 mooring. The concentrations of $^{239,240}Pu$ and ^{241}Am in the particulates are tabulated in Table 4 and plotted in Figure 8 by collection interval. The collection interval numbers refer to the fractions collected in the time series of cups which rotate under each trap. The final interval (#5) is recovered unsealed and is susceptible to material loss or contamination during recovery. This cup is also open for the first eight days of deployment.

The $^{239,240}Pu$ concentrations in both traps show remarkable uniformity over the first four collection intervals. The final interval concentrations are systematically lower than the others. Given the open nature of this collection during recovery, this suggests that it may be the result of an artifact - such as dilution with low activity material from the near surface water column. The four collection intervals span a time interval of almost

11 months beginning in late August and roughly correspond to fall, winter, spring, and summer seasons. The ^{241}Am concentrations follow a similar pattern to those of $^{239,240}Pu$ with systematic low values from the final collection interval. There is a slight departure from the uniformity of the observed concentrations in the third and fourth intervals - with the 1464 m trap showing slightly higher values than the 4832 m trap.

The similarity of the radionuclide composition and mass fluxes at the two trap depths is suggestive of limited transformation on the nature of sinking particles as they move from the lower thermocline towards the bottom waters. Given the much lower concentrations of transuranics on suspended particles in the deep water compared with those in the main thermocline, any significant disaggregation/aggregation which accompanies the sinking of large particles would tend to reduce the nuclide concentrations in the particles collected in the deep water. Since this is not observed, it may be that there is little exchange going on over these depth ranges.

The transuranic fluxes at the two trap depths are tabulated in Table 5 and plotted in Figure 9. Both the mass flux and the nuclide fluxes from the final collection interval (open during recovery) are systematically low and material loss during recovery cannot be eliminated. Accordingly, the mean annual fluxes in Table 5 are averages of the four seasonal traps only. There does not appear to be any strong seasonal variability in the nuclide fluxes correlated with surface productivity changes as has been observed further north in the Sargasso Sea (Bacon et al., Deep Sea Res. 32, 273 (1985)). It is possible, however, that the collection intervals are long enough to mask such seasonal signals. There is a strong suggestion in the data for the deeper trap nuclide fluxes, of systematically higher fluxes in the latter part of the sampling period, i.e. in spring and early summer of 1984. In collection interval 4, for example, the elevated nuclide fluxes in the deep trap do not reflect corresponding increases observed at the 1464 m trap depth. It is tempting to speculate on whether a deep advective process is contributing particles (such as sporadic turbidite import) to the bottom water.

The fluxes of both $^{239,240}Pu$ and ^{241}Am are very low in relation to the water column inventories. If integrated over the 30 years of fallout his-

tory, they represent total integrated fluxes amounting to about 10% of the total water and sediment inventories below the main thermocline. It seems likely that the major components of these nuclide fluxes in the upper water column are recycled with the organic matter - leaving only a minor fraction which survives into the deeper water layers. This small supply on sinking particles seems to be consistent with the arguments advanced earlier on advection being the major source of deep water fallout tracer supply.

Figures 10 and 11 show the correlations of the mass fluxes in the Nares trap samples with the $^{239,240}Pu$ and ^{241}Am fluxes respectively. Also shown are the corresponding data for a trap series from deployment at 4000 m in the Hatteras Abyssal Plain (E-N3) from mid-1983 to mid-1984 (at 32°46'N, 70°50'W). As has been observed by Bacon et al. (Deep Sea Res. 32, 273 (1985)), mass flux fluctuations in large particle fluxes appear to be a major control on nuclide fluxes. The Nares and Hatteras data show that this correlation holds up over depth ranges from 1500-5000 m and over sampling locations over 500 miles apart. The fact that the data from the two locations lie on essentially the same line is probably a consequence of a similarity in concentration of transuranics in the region of the water column where the large particle flux originates. Over this part of the North Atlantic gyre, similarity in the pattern of fallout nuclide concentrations with depth is not surprising. The mass fluxes, and corresponding nuclide fluxes are higher at the Hatteras site. Lacking the appropriate data on primary productivity differences between the two areas, it is only possible to speculate that the mass fluxes are correspondingly correlated.

4. ^{241}Am in Nares sediments

^{241}Am analyses were completed on the surficial sections of the sediment cores from the Nares site for which $^{239,240}Pu$, ^{137}Cs and ^{210}Pb data were reported last year. These data are listed in Table 6 together with the corresponding $^{241}Am/^{239,240}Pu$ ratio. The concentrations (and, consequently, sediment nuclide inventories) are very low. The picture of the Nares sediment as a sedimentary regime receiving a very small flux of material from the surface ocean holds, consequently, for ^{241}Am as well as the other, less reactive fallout nuclides. The fact that the mean $^{241}Am/^{239,240}Pu$ ratio is 2-3 times elevated over that which would characterize integrated global fallout supplied

to the surface ocean, results from the supply of ^{241}Am-enriched, large sinking particles. The mean ratios in the 1464 m trap and 4832 m trap samples were 1.5 and 1.9, respectively. The sediments are, however, a very minor sink still for the fallout transuranic inventory.

TABLE 1

Fallout ^{137}Cs and $^{239,240}Pu$ Concentrations at NARES-1
Nares Abyssal Plain; 23°11'N, 63°58'W; Collected 9/29/84; Bottom Depth 5840 m.

Sample Depth (m)	Salinity °/••	Potential Temperature °C	^{137}Cs* d.p.m./100 Kg	$^{239,240}Pu$ (collection date)
0	--	--	12.6±0.2	0.033±0.008
263	36.538	18.23	17.9±0.3	0.145±0.019
436	36.222	16.18	20.5±0.3	0.158±0.023
668	35.494	11.28	9.8±0.3	0.204±0.022
834	35.035	7.79	2.2±0.2	0.083±0.013
1060	35.020	6.00	1.8±0.2	0.035±0.006
1442	35.016	4.36	3.1±0.3	0.094±0.016
2550	34.958	2.85	0.2±0.2	0.009±0.007
3331	34.921	2.27	1.4±0.2	0.029±0.008
4124	34.904	1.974	0.6±0.2	0.027±0.008
4994	34.883	1.78	1.0±0.2	0.023±0.005
5681	34.850	1.527	1.8±0.2	0.022±0.006
5788	34.849	1.517	0.3±0.2	0.020±0.007
	Integrated activity** (mCi/Km^2)			
	0-5840m		79.7	1.19
	2000-5840m		16.0	0.37

* ^{137}Cs corrected for blank value of 0.3.
** Using interpolated 2000m values.

TABLE 2

Concentrations of Fallout Transuranics in Seawater and Filtered Particles at NARES-1

Depth	$^{239,240}Pu$			^{241}Am		
	Particles	Dissolved†	Total$^{\Delta}$	Particles	Dissolved	Total
(m)			d.p.m./1000 ℓ			
Surf.				0.005±0.003	0.015±0.008	0.022±0.009
400	0.005±0.002	1.495	1.50	0.010±0.004	0.176±0.009	0.194±0.010
800			1.07	0.021±0.006	0.285±0.020	0.306±0.021
1464	0.010±0.002	0.93	0.94	0.017±0.005	0.203±0.014	0.222±0.014
2540				0.002±0.002	0.062±0.009*	0.064±0.010*
3750	0.003±0.001	0.277	0.28	0.005±0.002	0.089±0.011	0.094±0.011
5695				0.004±0.002	0.057±0.029*	0.061±0.029*
5785	0.006±0.003	0.194	0.20	0.005±0.004	0.063±0.011	0.068±0.011

† = Total minus particulate concentration.
Δ = From large volume water samples.
* = Provisional values; longer counts being made.

TABLE 3

Fraction of Fallout Transuranics Collected
by 1 μm Cartridge Prefilters at NARES-1

Depth (m)	$^{239,240}Pu$ % Part.[1]	$^{239,240}Pu$ Cp/Cd[2]	^{241}Am % Part.[1]	^{241}Am Cp/Cd[2]
Surface			25±18	0.33
400	0.3±0.1	0.003	9.3±2.1	0.057
800			6.9±2.0	0.074
1464	1.1±0.2	0.011	7.7±2.3	0.084
2540			3.1±3.2[3]	0.032
3750	1.6±0.5	0.016	5.3±2.2	0.056
5695			6.5±4.5[3]	0.070
5785	3.2±1.6	0.033	7.4±6.0	0.079
Mean		0.016	6.6	0.065

1 = % of total activity on particles.
2 = Particulate activity (Cp) divided by dissolved activity (Cd).
3 = Provisional values.

TABLE 4

Concentrations of Fallout Transuranics in NARES-1 Trap Samples

Mooring and Trap Depth	Collection Interval (days)	Mass Flux $g/m^2/y$	$^{239,240}Pu$	^{238}Pu	^{241}Am
			d.p.m./g		
NARES-1, 1464m	8-86	14.31	0.41±0.04	n.d.	0.65±0.08
8/15/83-9/20/84	86-164	8.39	0.33±0.04	n.d.	0.60±0.13
23°16'N, 63°55'W	164-242	6.30	0.36±0.04	n.d.	0.91±0.10
	242-320	7.73	0.38±0.04	n.d.	0.69±0.09
	1-8, 320-404	4.25*	0.27±0.04*	n.d.	0.39±0.09*
NARES-1, 4832m	8-86	12.07	0.37±0.04	n.d.	0.58±0.08
8/15/83-9/20/84	86-164	8.52	0.44±0.05	n.d.	0.65±0.10
23°16'N, 63°55'W	164-242	8.09	0.42±0.05	n.d.	0.58±0.09
	242-320	16.39	0.38±0.04	n.d.	0.43±0.07
	1-8, 320-404	10.03*	0.25±0.03*	n.d.	0.41±0.07*

Seasonal trap (Day 8-320) mean concentrations

1464m trap	0.37	0.71
4832m trap	0.40	0.56

n.d. = not detected
* = open cup during trap retrieval

TABLE 5

Transuranic Fluxes in NARES-1 Traps

Mooring and Trap Depth	Collection Interval (days)	$g/m^2/y$	$^{239,240}Pu$ d.p.m. per m^2	^{241}Am per year
NARES-1, 1464m	8-86	14.31	5.9±0.6	9.3±1.1
8/15/83-9/20/84	86-164	8.39	2.8±0.3	5.1±1.1
23°16'N, 63°55'W	164-242	6.30	2.3±0.3	5.7±0.6
	242-320	7.73	2.9±0.3	5.3±0.7
	1-8, 320-404	4.25*	1.1+0.2*	1.7+0.4
Mean annual flux (seasonal trap average, day 8-320)		9.18	3.15	6.4
NARES-1, 4832m	8-86	12.07	4.5±0.5	7.0±1.0
8/15/83-9/20/84	86-164	8.52	3.7±0.4	5.5±0.9
23°16'N, 63°55'W	164-242	8.09	3.4±0.4	4.7±0.7
	242-320	16.39	6.2±0.7	7.0±1.1
	1-8, 320-404	10.03*	2.5+0.3*	4.1+0.7
Mean annual flux (seasonal trap average day 8-320)		11.26	4.5	6.1

* = open cup during retrieval.

TABLE 6

^{241}Am and $^{241}Am/^{239,240}Pu$ Ratios in
Surficial Nares Abyssal Plain Sediments

Colllection	Core No.	$^{241}Am^{*}$	$^{241}Am/^{239,240}Pu$
R/V TYRO	BC02	4.93±0.40	0.71±0.07
7-19 Feb. 1984	BC08	4.17±0.36	0.65±0.06
22°10' - 23°35'N,	BC09	2.12±0.25	0.63±0.09
63°15' - 64°45'W	BC15	1.05±0.20	0.60±0.03
5719 - 5779 m	BC18	0.67±0.14	0.74±0.14
	BC23	3.70±0.29	0.70±0.08
	BC25	1.71±0.24	0.78±0.13
	BC32	2.55±0.28	0.59±0.17

* = dpm/Kg (dry weight).

FIGURE 1

Fallout nuclides at Nares-1 : 9/29/84

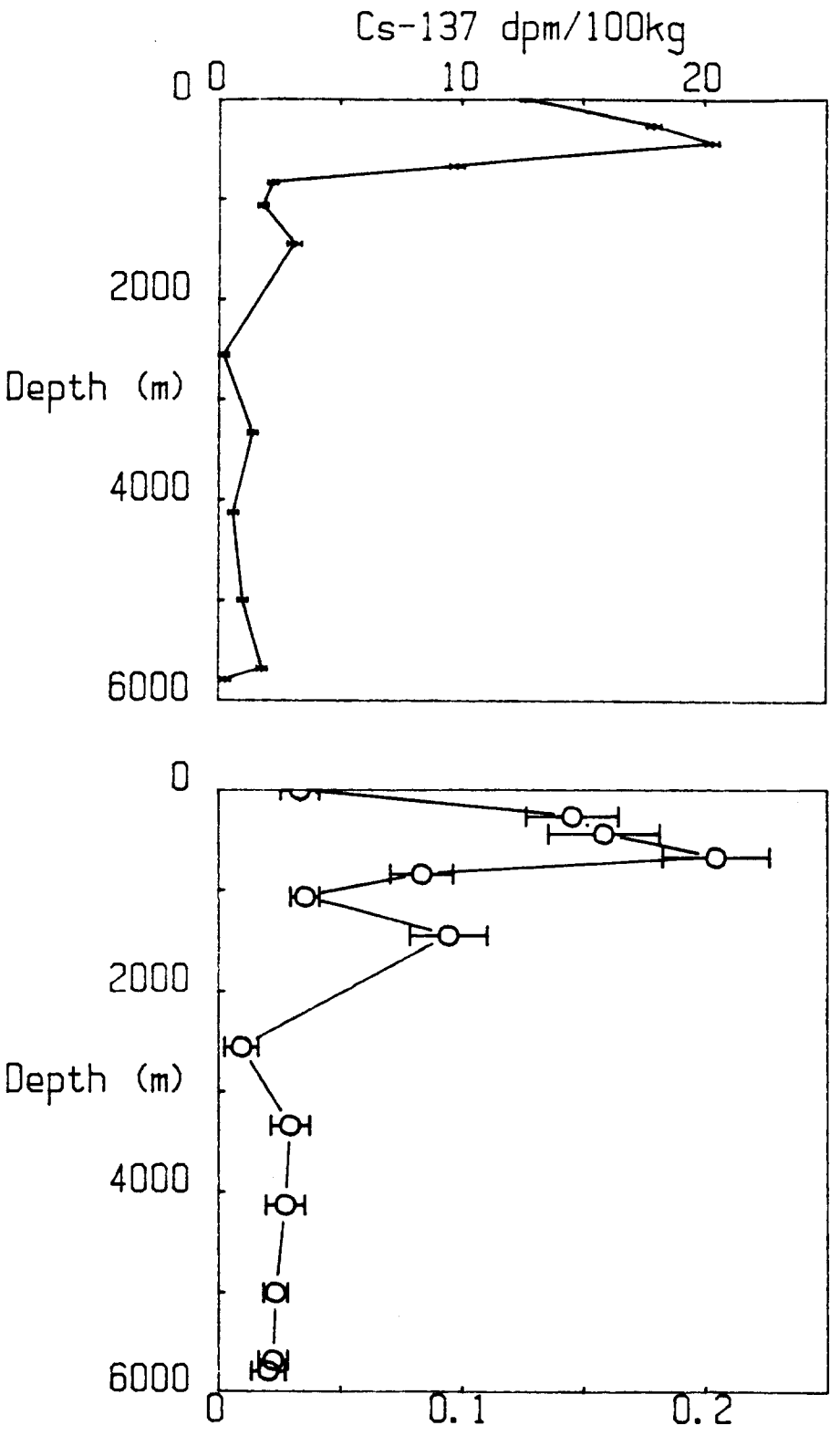

FIGURE 2

Deepwater tracer increase 1981-1984

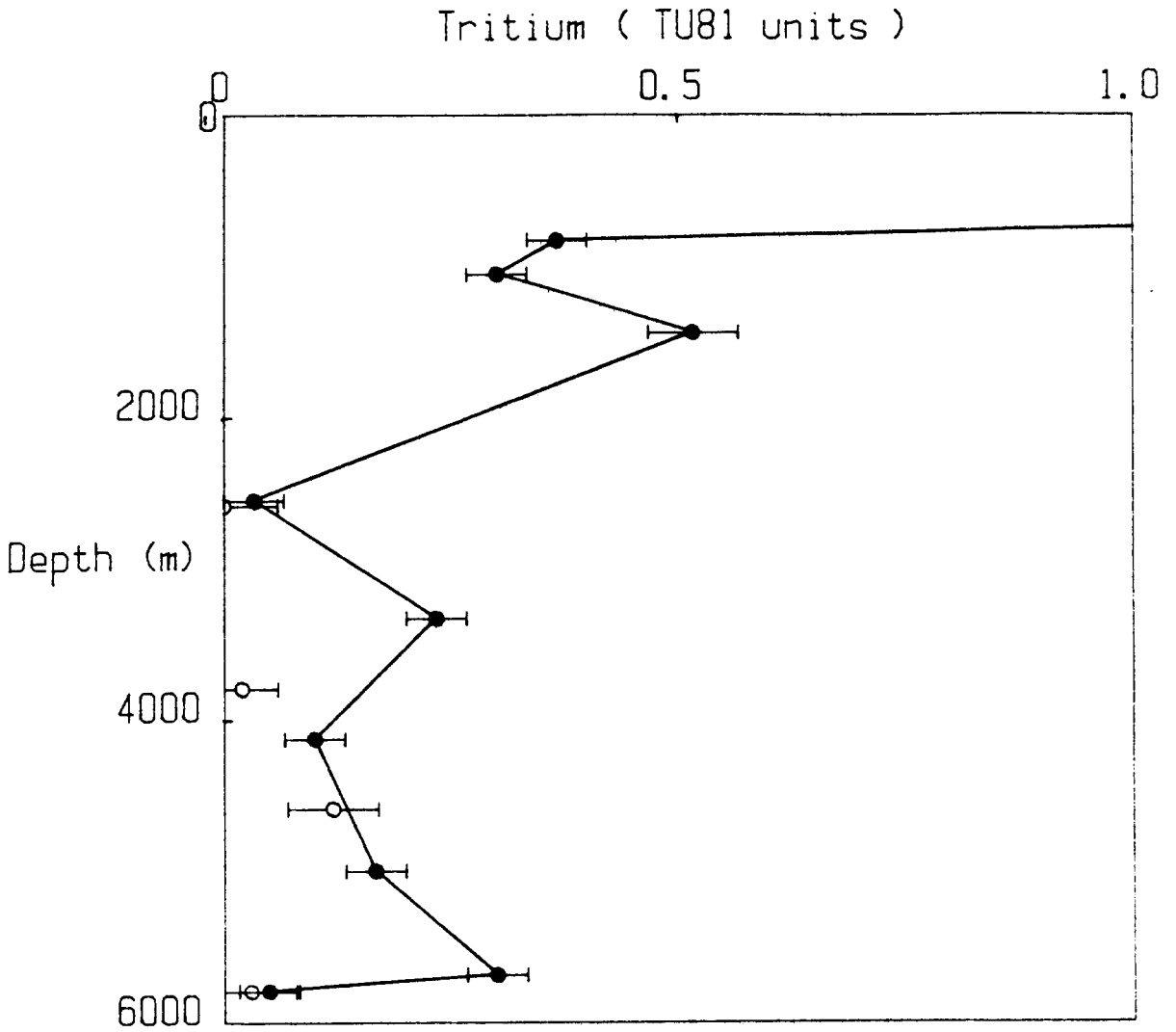

Open circles : TTO-24 measured tritium in 1981.

Solid circles : Nares-1 Cs137 converted to tritium.

FIGURE 3

Fallout Pu239,240 at Nares-I : 9/24/84

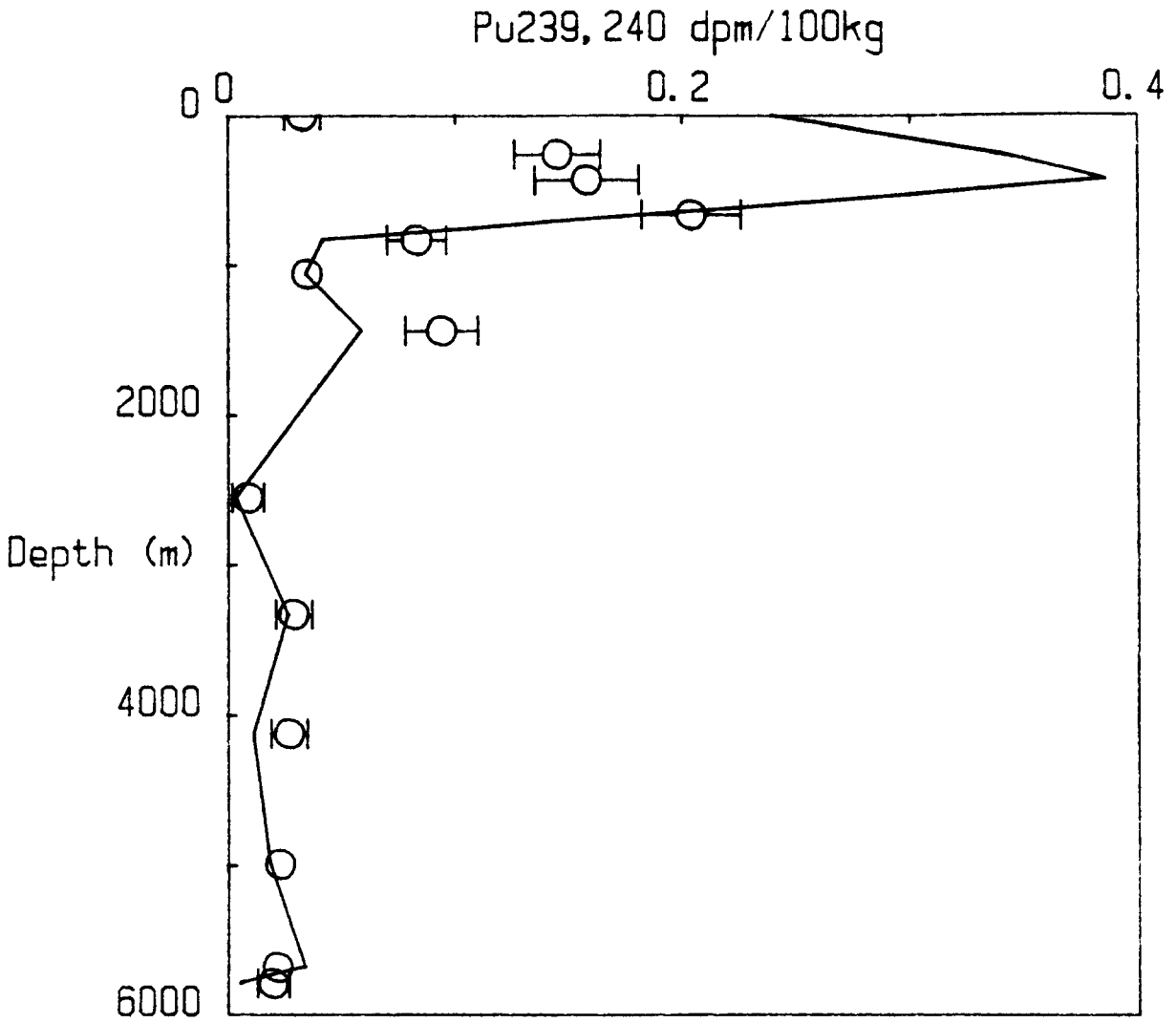

Open circles : Measured Pu concentration

Solid line : Pu predicted from Cs-137 profile (no particulate Pu transport)

FIGURE 4

Transuranics at Nares-1 9/24/84

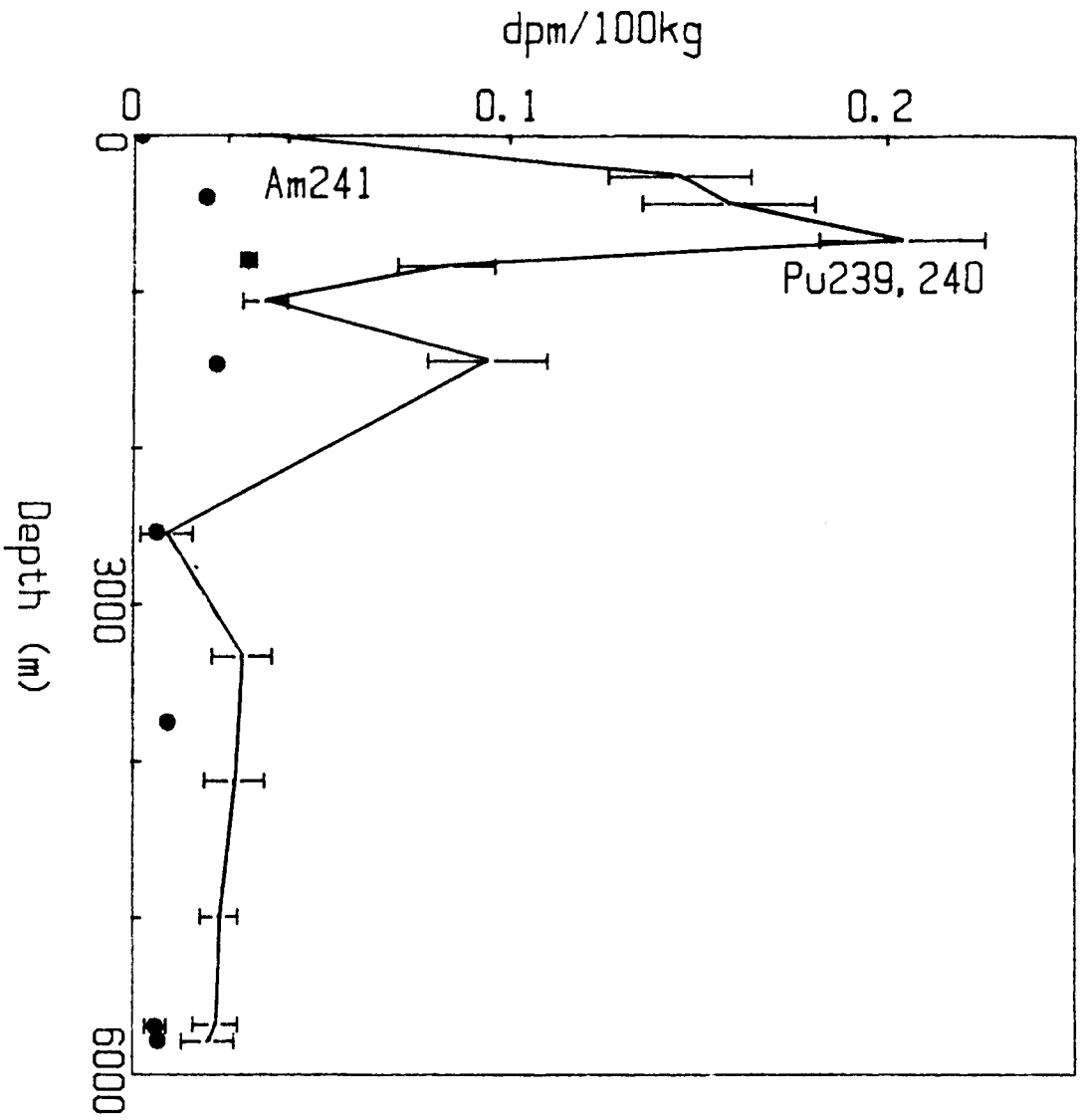

FIGURE 5

Fallout Am241 at Nares -1 ; 9/24/84

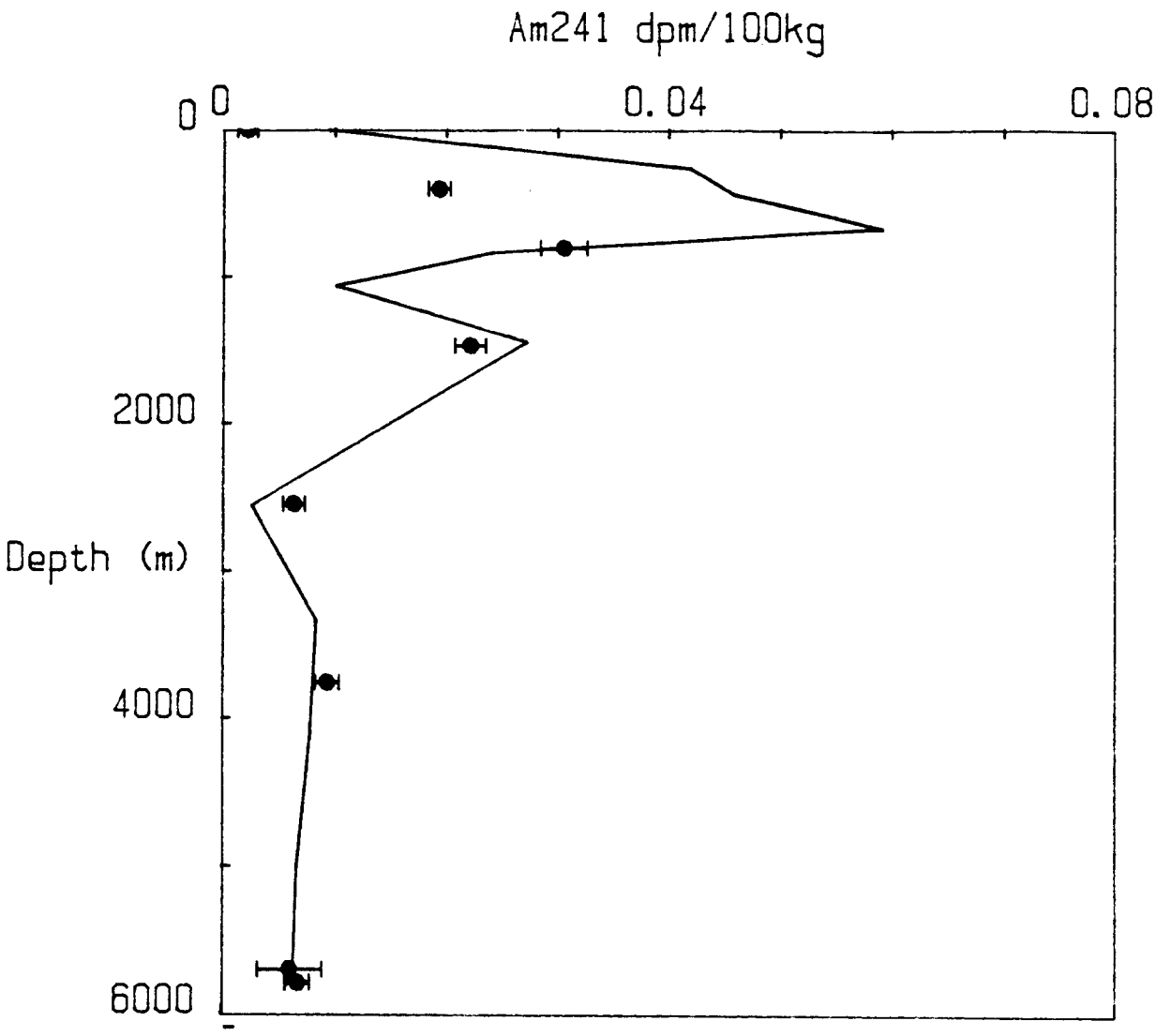

Solid circles : measured Am241 concentration

Solid line : Ingrowth of Am241 from Pu 241 decay

FIGURE 6

Fine particle Pu in Northwest Atlantic

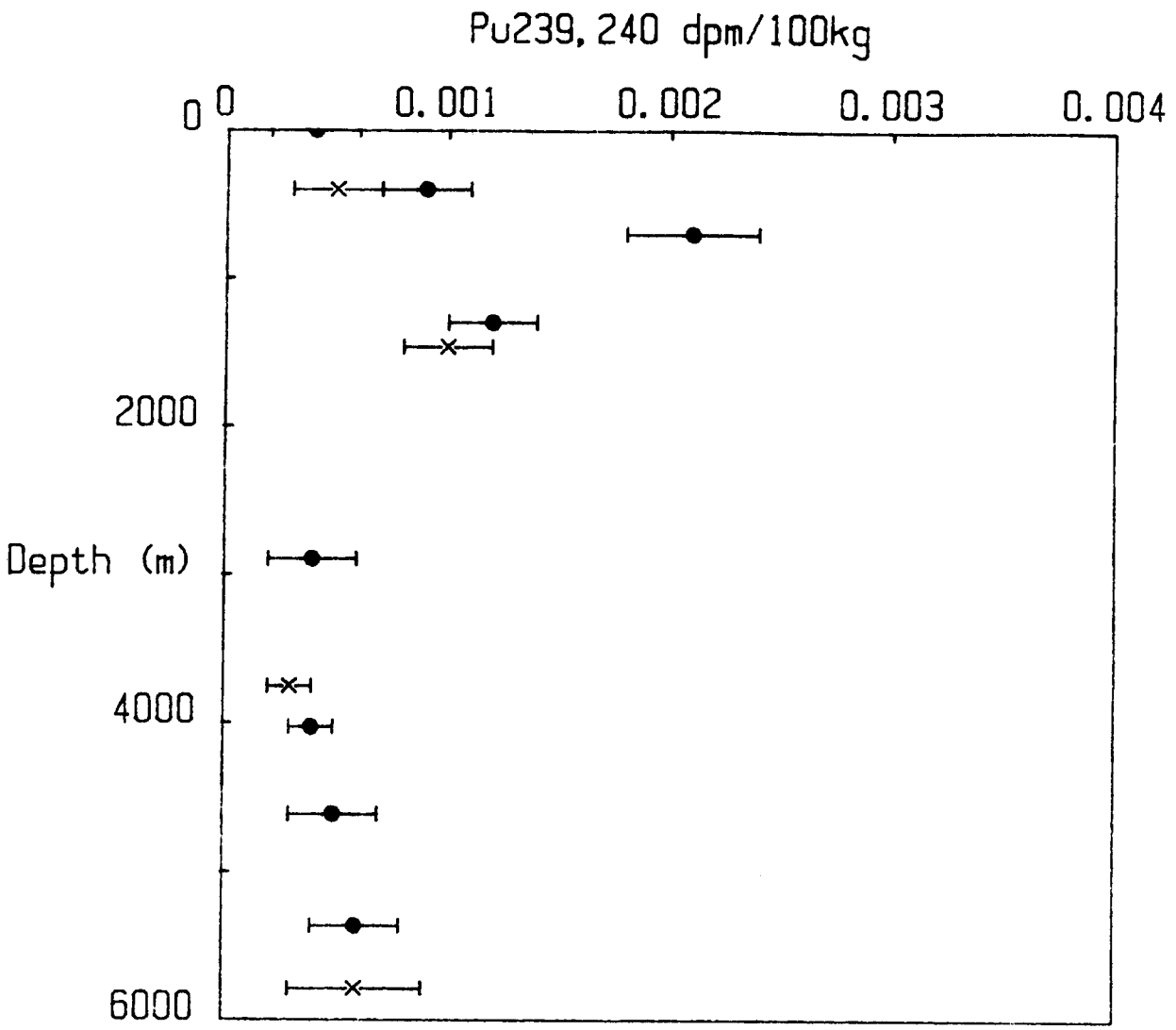

Solid circles : Hatteras Abyssal Plain (EN-3)

Crosses : Nares-1 9/24-84

FIGURE 7

Fine particle Am241 in Northwest Atlantic

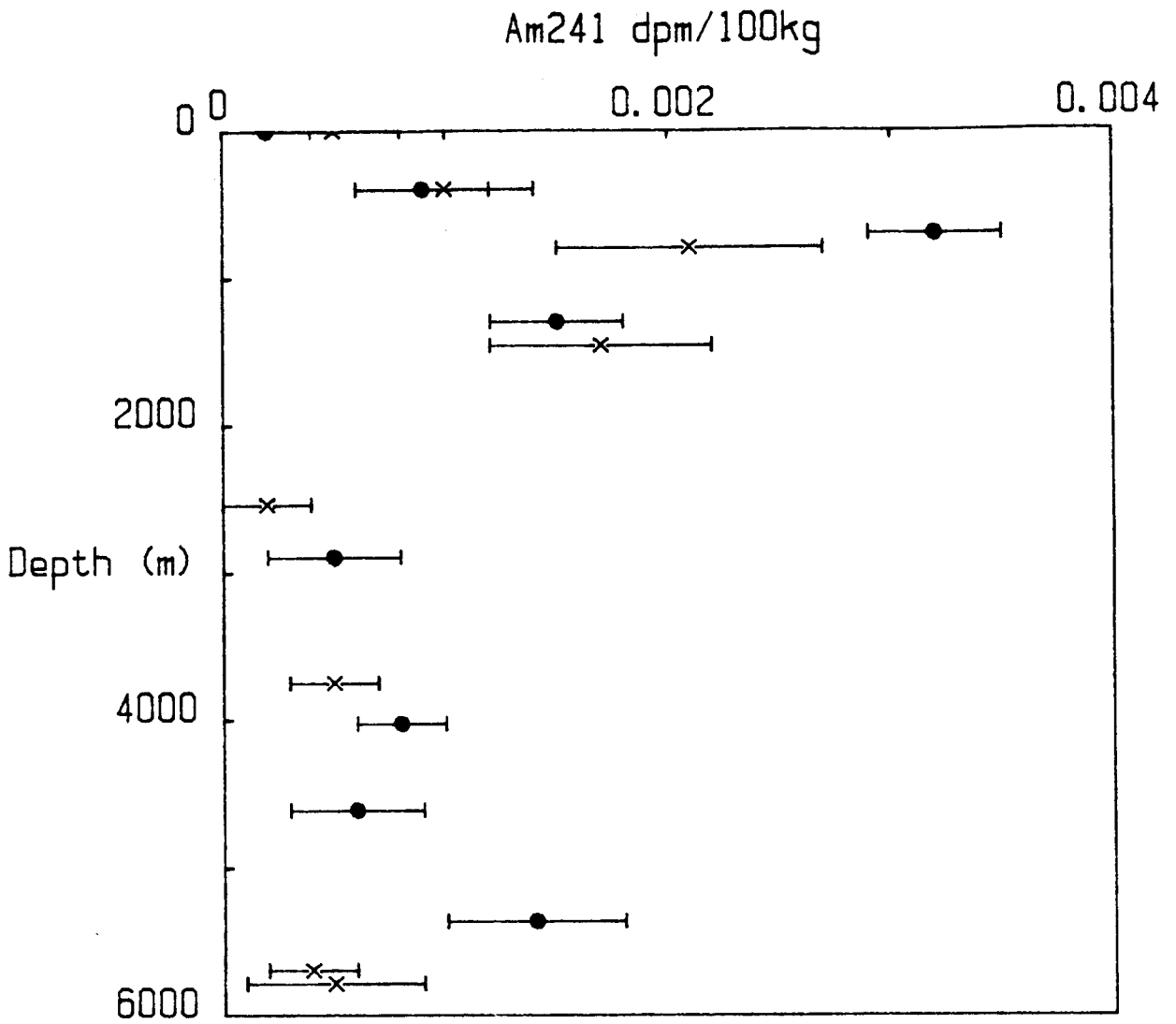

Solid circles : Hatteras Abyssal plain (EN-3)

Crosses : Nares-1 9/24/84

FIGURE 8

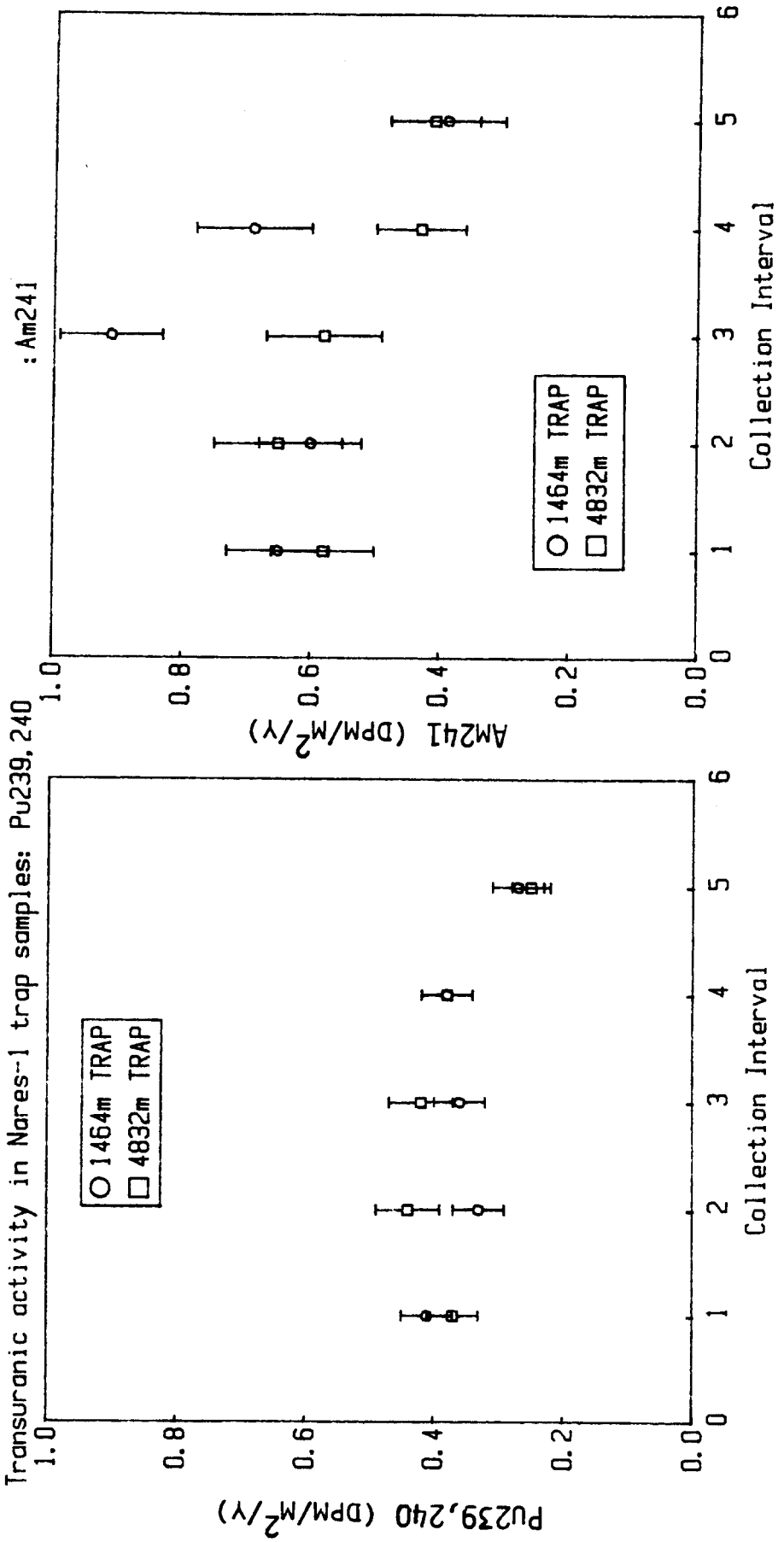
Transuranic activity in Nares-1 trap samples: Pu239,240
Pu239,240 (DPM/M²/y)
Collection Interval
1464m TRAP
4832m TRAP
: Am241
Am241 (DPM/M²/y)
Collection Interval
1464m TRAP
4832m TRAP

FIGURE 9

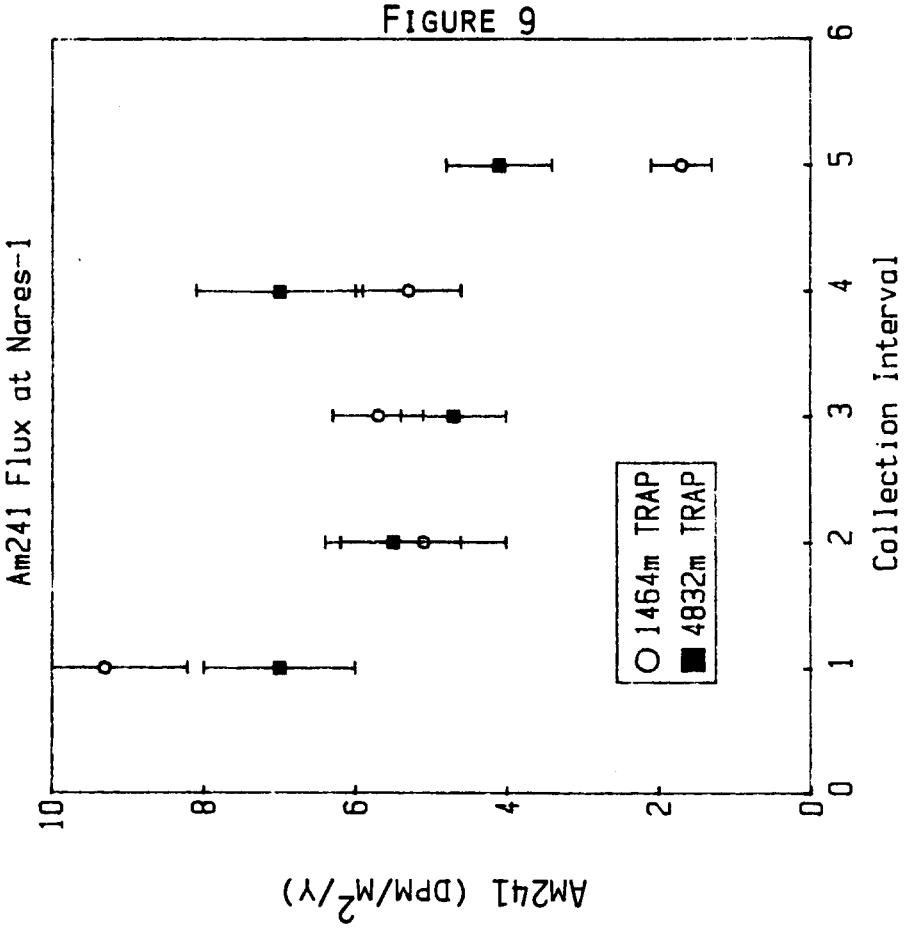
Am241 Flux at Nares-1
AM241 (DPM/M²/Y)
Collection Interval
1464m TRAP
4832m TRAP
0
2
4
6
8
10
0
1
2
3
4
5
6

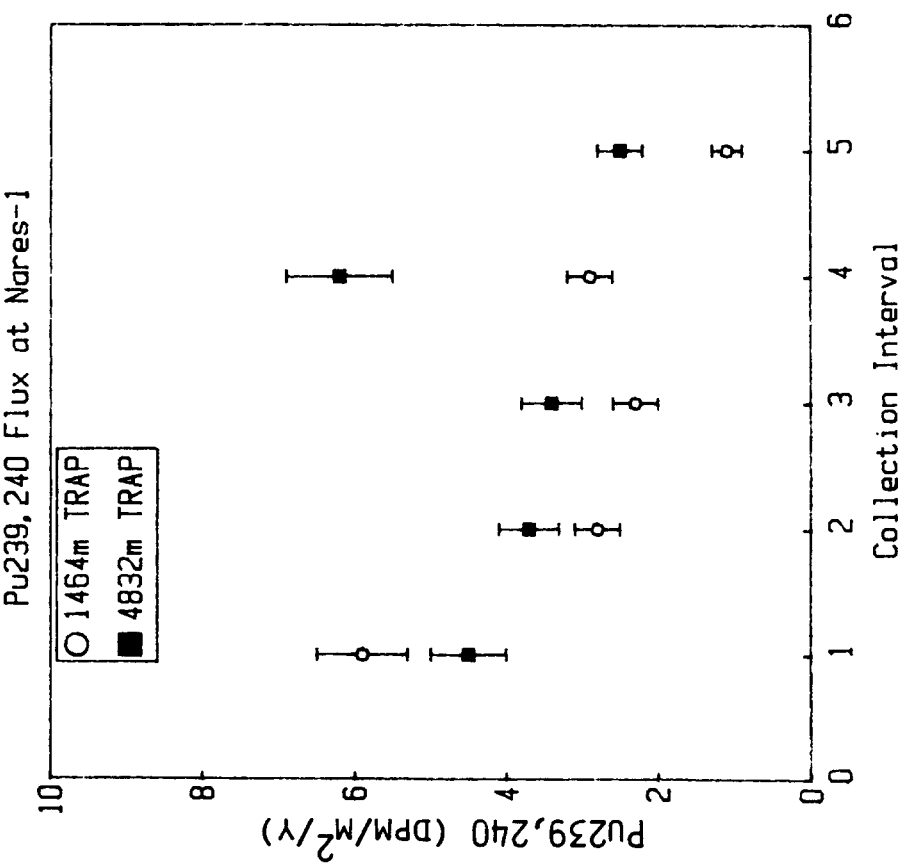
Pu239,240 Flux at Nares-1
PU239,240 (DPM/M²/Y)
Collection Interval
1464m TRAP
4832m TRAP
0
2
4
6
8
10
0
1
2
3
4
5
6

FIGURE 10

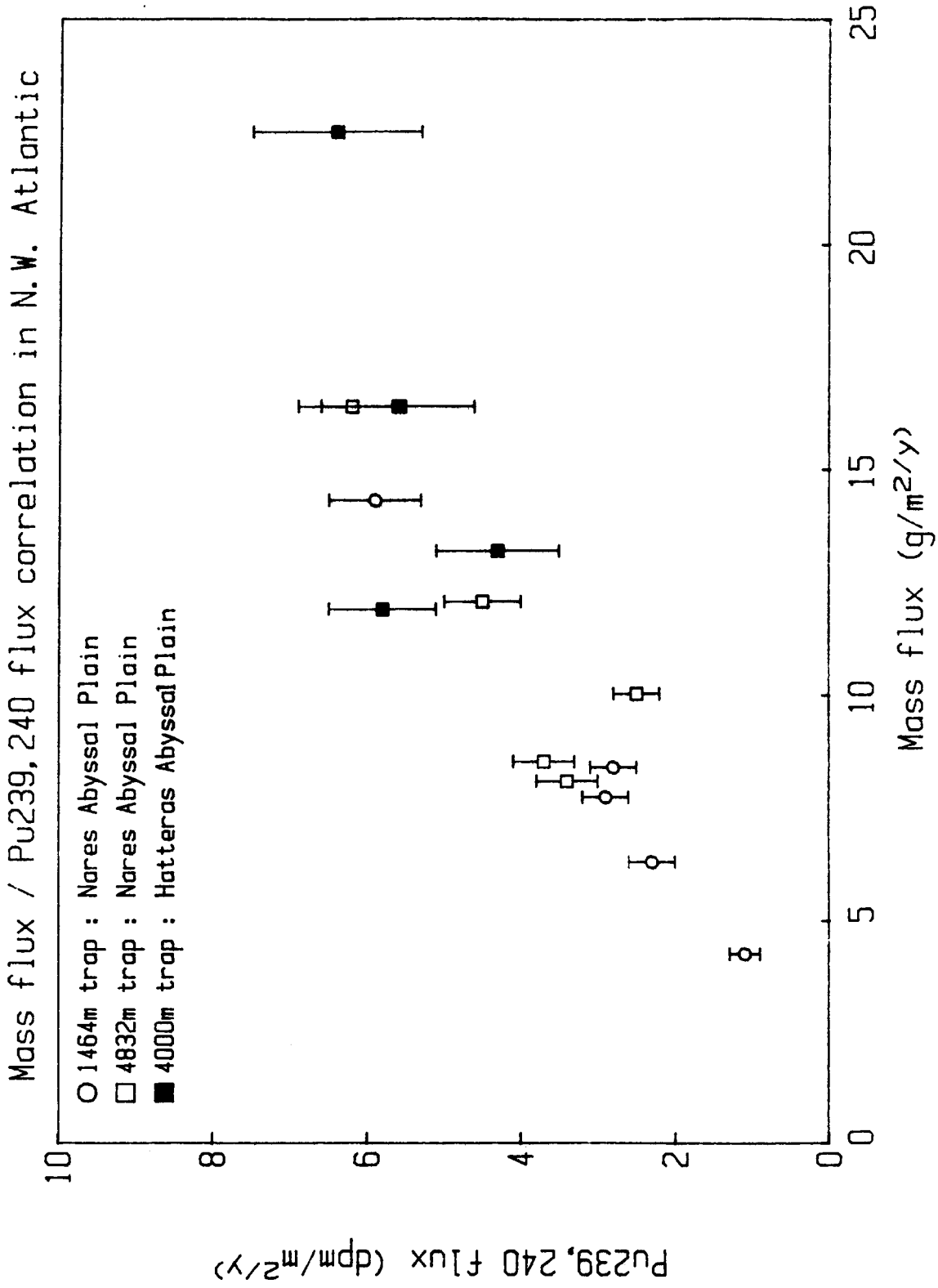
Mass flux / Pu239,240 flux correlation in N.W. Atlantic
○ 1464m trap : Nares Abyssal Plain
□ 4832m trap : Nares Abyssal Plain
■ 4000m trap : Hatteras Abyssal Plain
Pu239,240 flux (dpm/m2/y)
Mass flux (g/m2/y)
0
2
4
6
8
10
0
5
10
15
20
25

FIGURE 11

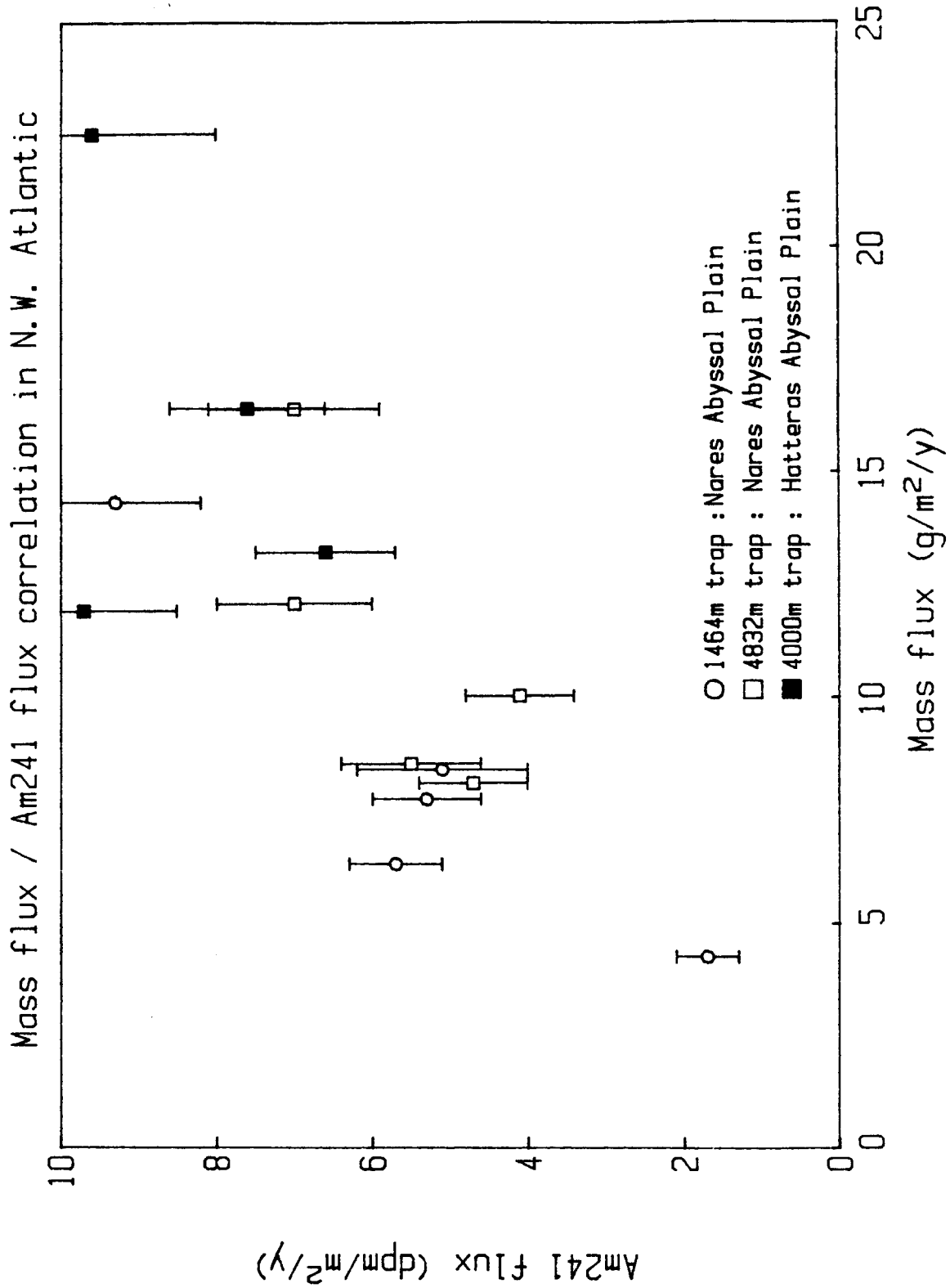
Mass flux / Am241 flux correlation in N.W. Atlantic
Am241 flux (dpm/m²/y)
Mass flux (g/m²/y)
0
2
4
6
8
10
0
5
10
15
20
25
O 1464m trap :Nares Abyssal Plain
□ 4832m trap : Nares Abyssal Plain
■ 4000m trap : Hatteras Abyssal Plain

APPENDIX E

PRELIMINARY DATA REPORT NARES II MOORING AND BAITED CAMERA MOORING: CURRENT METERS

R. D. PILLSBURY

APPENDIX E

Oregon State University Sediment Trap Group, Cruise Report,

Nares Abyssal Plain Mission, EN121, LEGII

Editor's Notes

Soon after the Subseabed Project phaseout began in early January 1986, funding for all Nares-related work was greatly reduced. This reduction, only six weeks after the completion of a major cruise, made it impossible to completely evaluate current-meter data from moorings recovered on the Nares II cruise. We thank R. D. Pillsbury and the Oregon State University (OSU) Current Meter Group for completing the Preliminary Data Report in Appendix E.

Two moorings containing current meters were recovered on the Nares II mission. One was the Nares-II current-meter sediment-trap mooring ($23^{o}14.5'N$, $64^{o}02.1'W$) deployed on the Nares-I mission in September 1984 (for a mooring diagram see Figure 1). The second, the baited camera mooring deployed for 53 hours ($23^{o}20.1'N$, $64^{o}058'W$), contained one current meter, 6 m above the bottom. For descriptions of the instruments and data analysis procedures see Pillsbury et al. (1986). Some notes relating to the preliminary data report follow.

The columns in the processed files, which contain the notations "FIRST 5 LINES" and "LAST 5 LINES," are (from left to right)

- Time (UCT)
- Day
- Month
- Year

- Current Speed (cm/sec)
- Current direction (degrees true or toward)
- U component of current (cm/sec)
- V component of current (cm/sec)
- Temperature (degrees centigrade)
- Pressure (decibars)
- Attenuation coefficient (1/m).

There are two data summary listings at each current meter depth. For example, the heading "DATA AT NARES -II, 776 METERS, LINE 1 THRU END OF FILE" is preceeded in one listing by a "P" and in the other by an "LLP". The summary listings preceded by a "P" were prepared from hourly data records. The summary listings preceded by "LLP" were prepared from records filtered to remove tides and inertial oscillations and sampled at six-hour intervals.

In progressive vector diagrams, the small squares mark the beginning of a new calendar month. Time increases from the 0, 0 point on the axis.

The processed file of the current meter at 1464 m is three cycles short (i.e., three hours worth of data are missing). The reason is unknown, but loss of this small portion of data should not significantly influence the data summaries or any potential uses of the data.

The processed data file of the current meter at 2900 is one cycle short. The consequences of this are slight. Also, the transmissometer channel was not processed, due to an instrument malfunction. Current speed is suspiciously low throughout most of the record compared to the deeper current meters and to the records from the Nares-I current meter at 2950 m. The reason is unknown. It would be informative to process the record to extract tidal amplitudes for comparison with those of the Nares-I 2900-m current meter.

The 5800-m current meter record is short, due to a leak which developed in one of the transmissometer electrical passthroughs. Evidently, the transmissometer underwater unit leaked at depth, which may account for the large offset in attenuation coefficient seen on 15 Mar 85. No corrections were applied to processed attenuation coefficient.

The 5800-m, 4800-m, and 2900-m records (excepting the latter's unexplained low speeds) appear to be highly correlated, as was the case for the Nares-I current meters. However, the Nares-II mean currents are toward the south, unlike those from Nares I, which were toward the west.

The brief (53-hour) record from the current meter (6 m above the bottom) on the baited camera mooring has been processed, and summaries are included here (Table 1, Figures 2 and 3). The flow is nearly all northward. The speed plot points out how useful a lower-threshold instrument would be for this near-bottom work.

The records for the Nares-I and Nares-II 4800-m current meters have been combined to produce a progressive Vector diagram 826 days in length (Figure 4). The record clearly shows that the Nares Abyssal Plain is a relatively inactive region where nontidal current patterns are dominated by intermittant low frequency (mesoscale) activity, and where measurements of at least several years' duration will be required to establish stable mean current velocity values.

The OSU Current Meter Group has provided Sandia National Laboratories with a data tape containing all current-meter data from the Nares-I and Nares-II moorings. This tape will be kept on file at Sandia. OSU will continue to archive the data, and will maintain the archive for several more years. Descriptions of the tape format and header records are included below for completeness.

Tape Format Description

The nine-track data tape was written in ASCII code at 1600 BPI with odd parity. The first record in each file contains header information and is 80 characters in length. It is followed by blocked data records which are generally 4000-characters long. Each 4000-character record contains 50 logical records of 80 characters each. The last data record in a file will usually contain fewer than 50 logical records and will hence be shorter than 4000 characters. Each file is terminated by a single file mark, except for the last file on the tape which is followed by two file marks.

Nares Data Tape Header Records

1.	725 METERS AT NARES-I,	AUG 83 - SEP 84.	TAPE 4409/19.
2	2950 METERS AT NARES-I.	AUG 83 - SEP 84.	TAPE 4411/18.
3	4800 METERS AT NARES-I.	AUG 83 - SEP 84.	TAPE 5862/7.
4	5800 METERS AT NARES-I.	AUG 83 - SEP 84.	TAPE 5884/3.
5	776 METERS AT NARES-II.	SEP 84 - NOV 85.	TAPE 5860/9.
6	1464 METERS AT NARES-II.	SEP 84 - NOV 85.	TAPE 5859/10.
7	2900 METERS AT NARES-II.	SEP 84 - NOV 85.	TAPE 4918/18.
8	4800 METERS AT NARES-II.	SEP 84 - NOV 85.	TAPE 7161/3.
9	5800 METERS AT NARES-II.	SEP 84 - AUG 85.	TAPE 4911/15.

Reference

Pillsbury, R. D. et al., Data Report for Current Meters on Mooring Nares-1, 1983-84; Nares Abyssal Plain, SAND85-7215 (Albuquerque: Sandia National Laboratories, 1986).

5840 METERS AT BAITED CAMERA. TAPE 5860/10.

FIRST 5 LINES:

1230 22 11 85	4.5	96	4.5	-0.5	2.10	1
1245 22 11 85	4.4	75	4.2	1.1	2.10	2
1300 22 11 85	4.1	62	3.6	1.9	2.10	3
1315 22 11 85	3.7	52	2.9	2.3	2.10	4
1330 22 11 85	3.8	74	3.7	1.1	2.10	5

LAST 5 LINES:

1630 24 11 85	3.8	21	1.4	3.5	2.10	209
1645 24 11 85	3.9	22	1.5	3.6	2.10	210
1700 24 11 85	4.0	23	1.6	3.7	2.10	211
1715 24 11 85	4.1	23	1.6	3.8	2.10	212
1730 24 11 85	4.2	22	1.6	3.9	2.10	213

	MIN	MEAN	MAX	SD
SPEED, CM/SEC	0.80	2.56	5.50	1.60
U, CM/SEC	-0.40	0.85	4.50	1.12
V, CM/SEC	-0.50	2.22	5.50	1.50
TEMP, DEG C	2.10	2.10	2.10	0.00

TABLE 1. Current Meter Data Summary
(6 m above bottom)

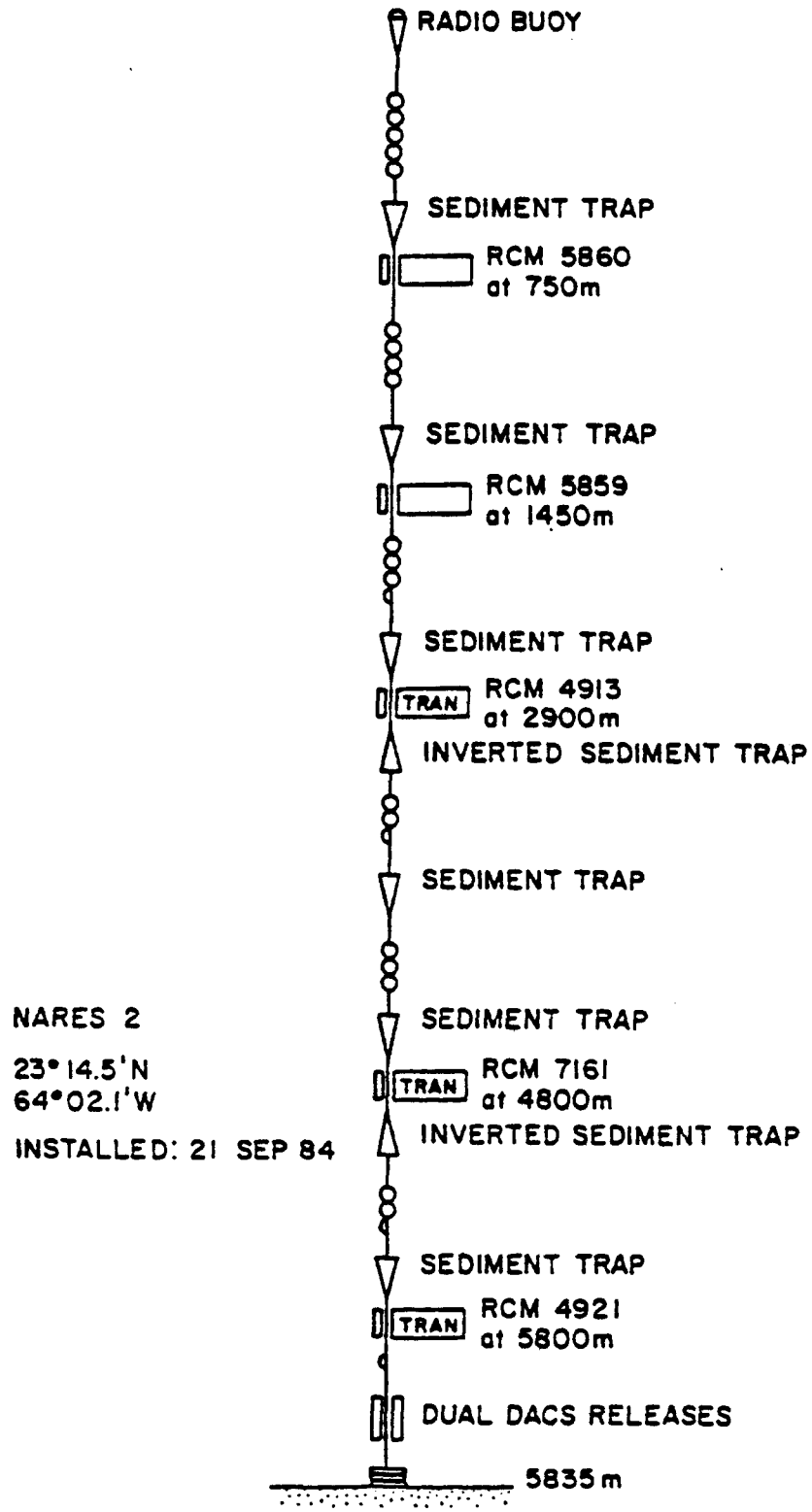

FIGURE 1. Current Meter Mooring Plan

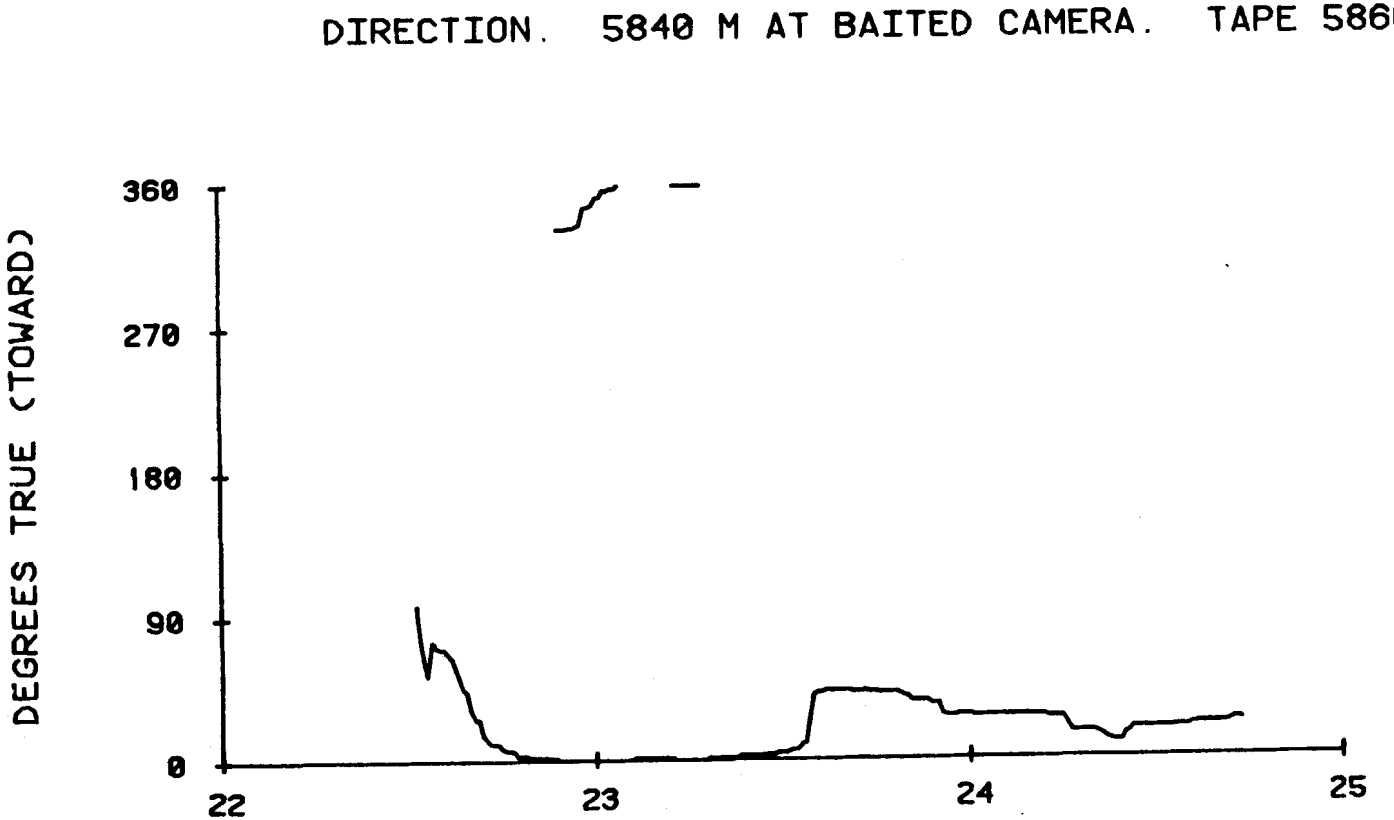

FIGURE 2. Current Meter
6 m above bottom

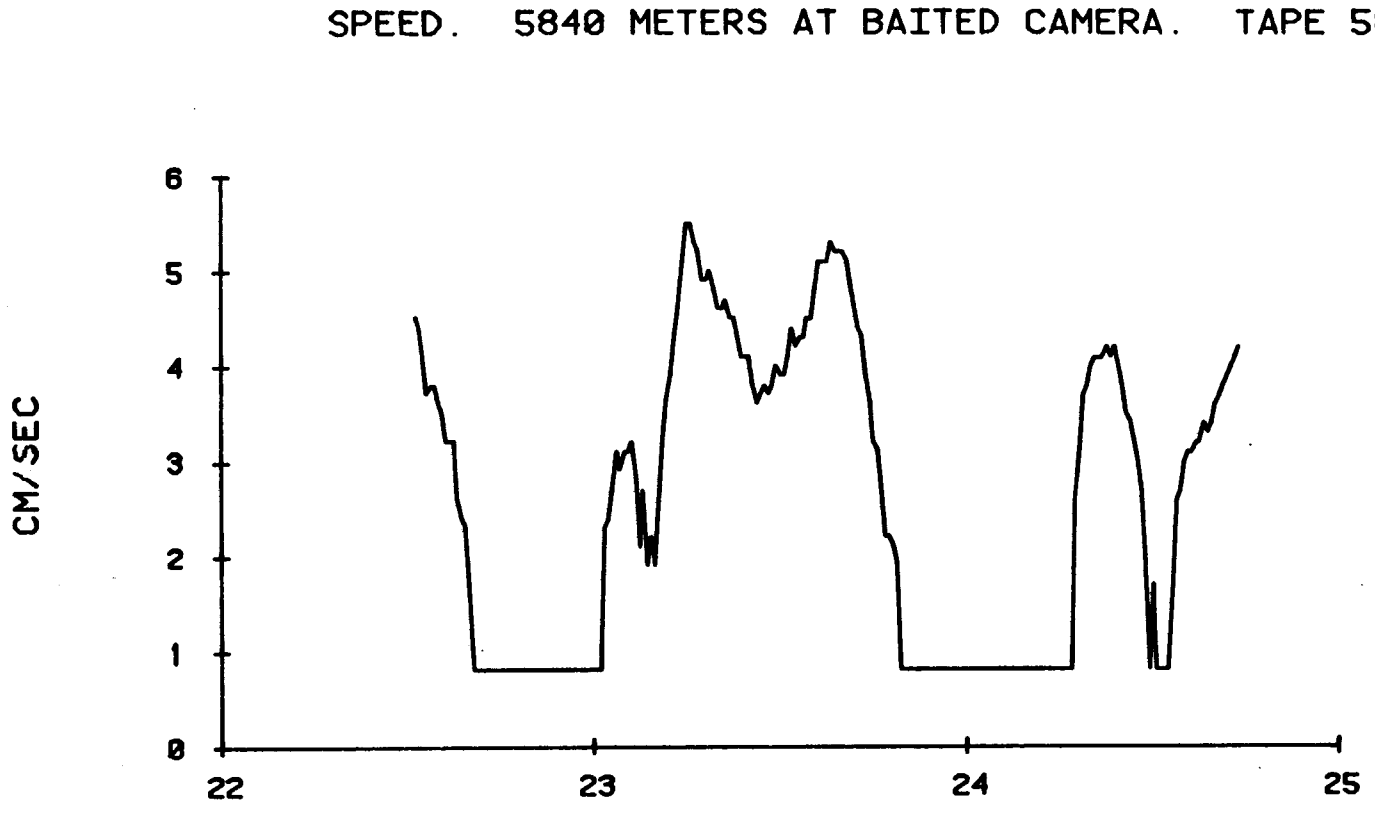

FIGURE 3. Current Meter
6 m above bottom

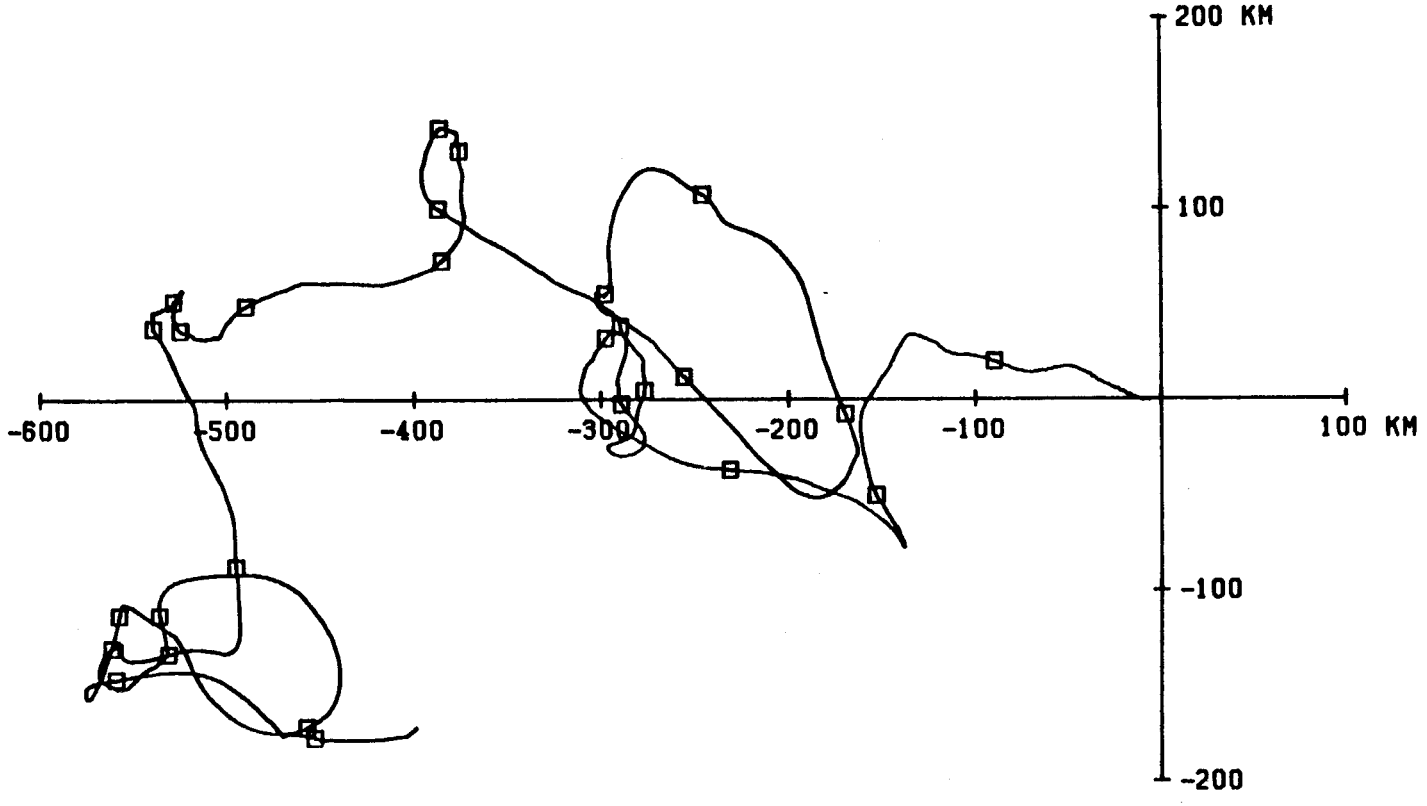

FIGURE 4. Progressive Vector Diagram, Squares are one month apart

Final Report on Contract 32-5717

Task 1.

The Nares 3 mooring was prepared. The cruise to recover Nares 2 and install Nares 3 was done in late November of 1985. No additional equipment has been prepared since all effort has been stopped on this task.

Task 2.

The recalibration of current meters recovered from the mooring Nares 2 was done. These calibrations were then used to convert the data collected by the Aanderaa current meters to standard oceanographic units. The data were recorded on magnetic tape and a copy of that tape is included as a portion of the final report. An analysis of the distribution of kinetic energy in the collected data from Nares 2 was done. That analysis showed about 70% of the eddy kinetic energy is in motions with a period longer than 50 days, a result nearly identical to that from the Nares 1 data.

Task 3. Deleted

Task 4. Deleted

NARES II Preliminary Data Report

.P DATA AT NARES-II, 776 METERS
LINE 1 THRU END OF FILE

	MEAN	SD	SKEWNESS	KURTOSIS	MIN	MAX	LENGTH
S	5.81	2.90	0.70	4.10	0.80	21.80	10215
U	-1.81	4.81	0.29	3.24	-18.60	19.70	10215
V	-0.37	3.96	0.17	2.91	-15.20	13.80	10215
T	9.42	0.44	0.63	2.77	8.39	10.76	10215
P	788.13	3.19	1.10	3.90	783.80	803.20	10215

EDDY KE =	19.40	10215 POINTS
HEAT FLUX U =	0.61	10215 POINTS
HEAT FLUX V =	-0.01	10215 POINTS
MOMENTUM FLUX =	-1.79	10215 POINTS

.LLP DATA AT NARES-II, 776 METERS
LINE 1 THRU END OF FILE

	MEAN	SD	SKEWNESS	KURTOSIS	MIN	MAX	LENGTH
U	-1.84	3.67	0.52	3.54	-13.31	10.30	1694
V	-0.36	2.42	0.20	2.62	-6.18	6.15	1694
T	9.42	0.41	0.79	2.74	8.73	10.55	1694
P	788.09	2.90	0.98	3.37	784.94	799.43	1694

EDDY KE =	9.65	1694 POINTS
HEAT FLUX U =	0.56	1694 POINTS
HEAT FLUX V =	-0.05	1694 POINTS
MOMENTUM FLUX =	-0.83	1694 POINTS

776 Meters at Nares-II. 21 Sep 84 - 21 Nov 85. Tape 5860/9.

FIRST 5 LINES:

2100	21	9	84	10.7	35	6.1	8.8	9.03	803.2	1
2200	21	9	84	5.2	106	5.0	-1.4	9.07	801.0	2
2300	21	9	84	3.6	126	3.0	-2.1	9.07	801.0	3
0	22	9	84	4.4	115	4.0	-1.9	8.96	801.0	4
100	22	9	84	4.7	128	3.7	-2.9	9.03	801.0	5

LAST 5 LINES:

700	21	11	85	9.4	159	3.4	-8.8	10.20	787.3	10211
800	21	11	85	8.3	156	3.4	-7.6	10.20	788.4	10212
900	21	11	85	5.5	158	2.0	-5.1	10.20	790.7	10213
1000	21	11	85	5.1	138	3.4	-3.8	10.11	791.8	10214
1100	21	11	85	3.1	72	2.9	1.0	10.06	793.0	10215

	MIN	MEAN	MAX	SD	NUM
SPEED, CM/SEC	0.80	5.81	21.80	2.90	10215
U, CM/SEC	-18.60	-1.81	19.70	4.81	10215
V, CM/SEC	-15.20	-0.37	13.80	3.96	10215
TEMP, DEG C	8.39	9.42	10.76	0.44	10215
PRESSURE, DB	783.80	788.13	803.20	3.19	10215

776 M at Nares-II. 21 Sep 84 - 21 Nov 85. Tape 5860/9.

FREQUENCY TABLE FOR CURRENT SPEED

LOWER BOUND	UPPER BOUND	FREQUENCY	RELATIVE FR.
0.00	2.00	842	0.082428
2.00	4.00	1907	0.186686
4.00	6.00	2921	0.285952
6.00	8.00	2426	0.237494
8.00	10.00	1304	0.127655
10.00	12.00	515	0.050416
12.00	14.00	191	0.018698
14.00	16.00	61	0.005972
16.00	18.00	30	0.002937
18.00	20.00	11	0.001077
20.00	22.00	7	0.000685
22.00	24.00	0	0.000000
24.00	26.00	0	0.000000
26.00	28.00	0	0.000000

MEAN	5.81235
STANDARD DEVIATION	2.90467

776 M at Nares-II. 21 Sep 84 - 21 Nov 85. Tape 5860/9.

FREQUENCY TABLE FOR CURRENT DIRECTION

LOWER BOUND	UPPER BOUND	FREQUENCY	RELATIVE FR.
0	10	183	0.017915
10	20	168	0.016446
20	30	144	0.014097
30	40	163	0.015957
40	50	129	0.012628
50	60	122	0.011943
60	70	162	0.015859
70	80	155	0.015174
80	90	212	0.020754
90	100	264	0.025844
100	110	225	0.022026
110	120	249	0.024376
120	130	189	0.018502
130	140	198	0.019383
140	150	181	0.017719
150	160	186	0.018209
160	170	200	0.019579
170	180	210	0.020558
180	190	275	0.026921
190	200	300	0.029369
200	210	382	0.037396
210	220	404	0.039550
220	230	461	0.045130
230	240	449	0.043955
240	250	467	0.045717
250	260	529	0.051787
260	270	580	0.056779
270	280	506	0.049535
280	290	469	0.045913
290	300	471	0.046109
300	310	335	0.032795
310	320	306	0.029956
320	330	250	0.024474
330	340	233	0.022810
340	350	267	0.026138
350	360	191	0.018698

776 M at Nares-II. 21 Sep 84 - 21 Nov 85. Tape 5860/9.

FREQUENCY TABLE FOR TEMPERATURE

LOWER BOUND	UPPER BOUND	FREQUENCY	RELATIVE FR.
8.00	8.10	0	0.000000
8.10	8.20	0	0.000000
8.20	8.30	0	0.000000
8.30	8.40	2	0.000196
8.40	8.50	15	0.001468
8.50	8.60	44	0.004307
8.60	8.70	82	0.008027
8.70	8.80	156	0.015272
8.80	8.90	529	0.051787
8.90	9.00	706	0.069114
9.00	9.10	979	0.095839
9.10	9.20	1273	0.124621
9.20	9.30	991	0.097014
9.30	9.40	1091	0.106804
9.40	9.50	667	0.065296
9.50	9.60	540	0.052863
9.60	9.70	561	0.054919
9.70	9.80	415	0.040627
9.80	9.90	440	0.043074
9.90	10.00	507	0.049633
10.00	10.10	338	0.033089
10.10	10.20	221	0.021635
10.20	10.30	223	0.021831
10.30	10.40	155	0.015174
10.40	10.50	135	0.013216
10.50	10.60	110	0.010768
10.60	10.70	28	0.002741
10.70	10.80	7	0.000685
10.80	10.90	0	0.000000
10.90	11.00	0	0.000000

MEAN	9.41750
STANDARD DEVIATION	0.43617

776 M at Nares-II. 21 Sep 84 - 21 Nov 85. Tape 5860/9.

FREQUENCY TABLE FOR PRESSURE

LOWER BOUND	UPPER BOUND	FREQUENCY	RELATIVE FR.
780.00	782.00	0	0.000000
782.00	784.00	1	0.000098
784.00	786.00	2960	0.289770
786.00	788.00	2767	0.270876
788.00	790.00	2123	0.207832
790.00	792.00	1149	0.112482
792.00	794.00	489	0.047871
794.00	796.00	464	0.045423
796.00	798.00	186	0.018209
798.00	800.00	52	0.005091
800.00	802.00	17	0.001664
802.00	804.00	7	0.000685
804.00	806.00	0	0.000000

MEAN	788.13507
STANDARD DEVIATION	3.18776

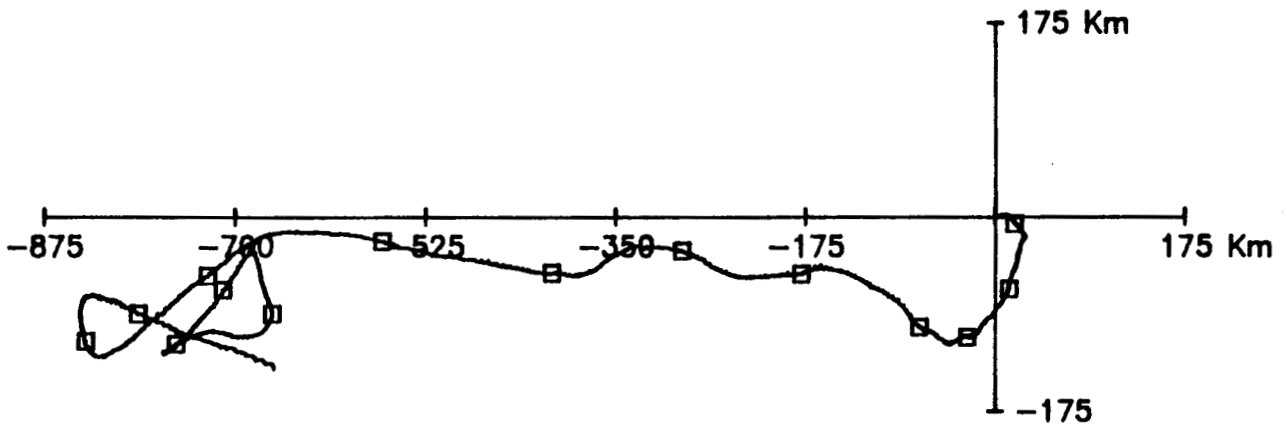

776 M at Nares—II. 425.6 days starting 2100 21 Sep 84.

776 M at Nares–II. 21 Sep 84 – 21 Nov 85. Tape 5860/9.

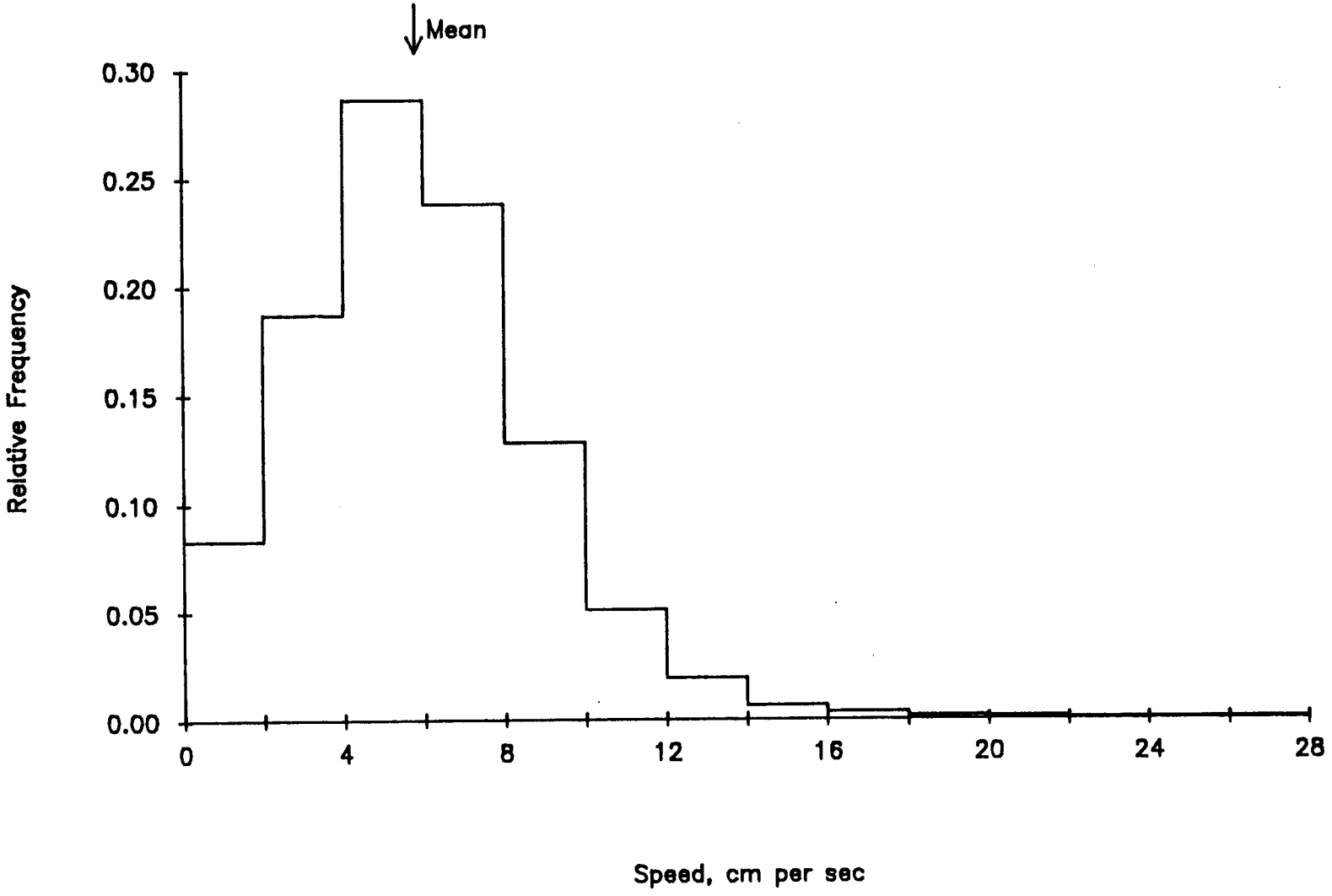

776 M at Nares–II. 21 Sep 84 – 21 Nov 85. Tape 5860/9.

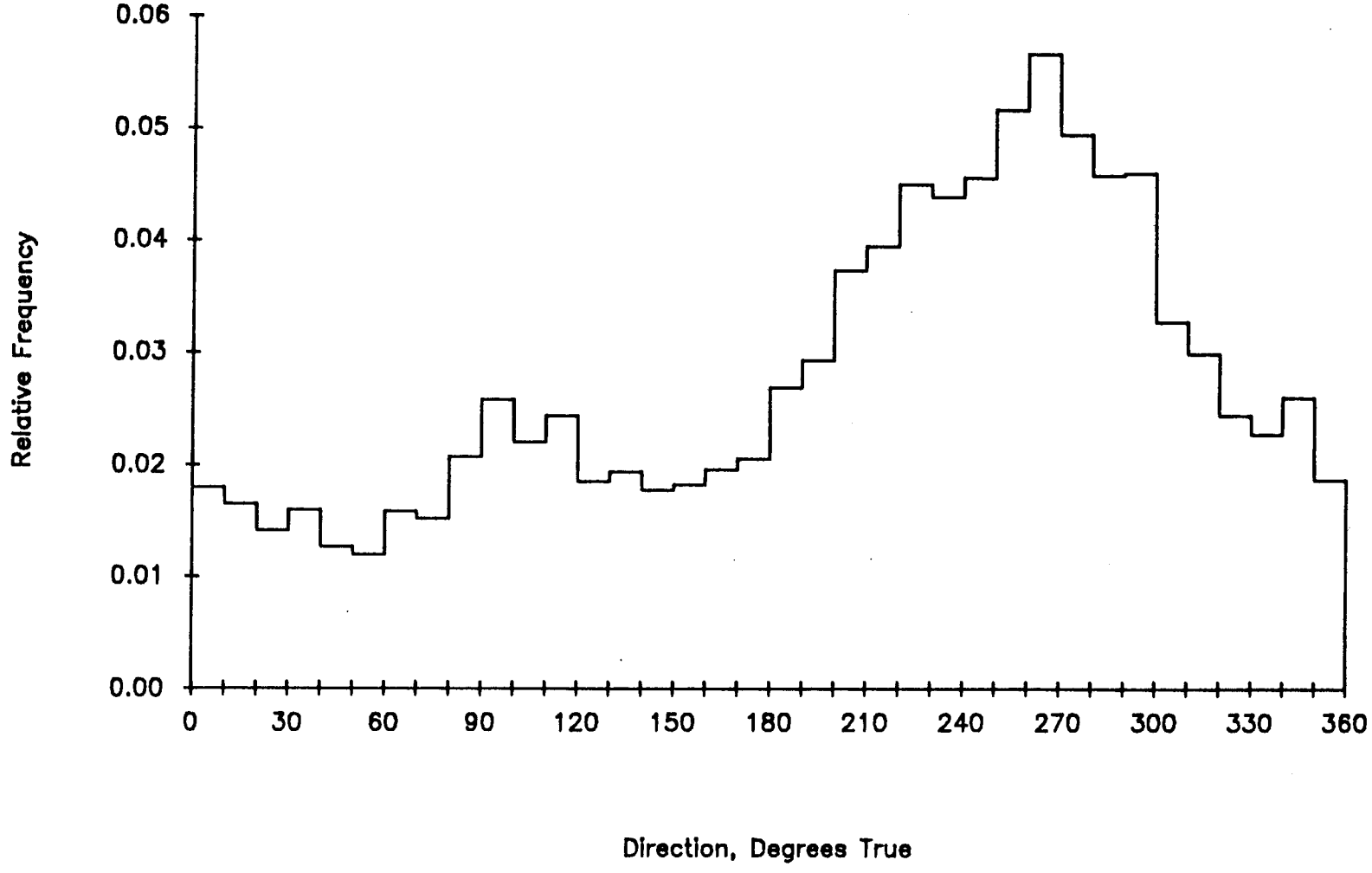

776 M at Nares–II. 21 Sep 84 – 21 Nov 85. Tape 5860/9.

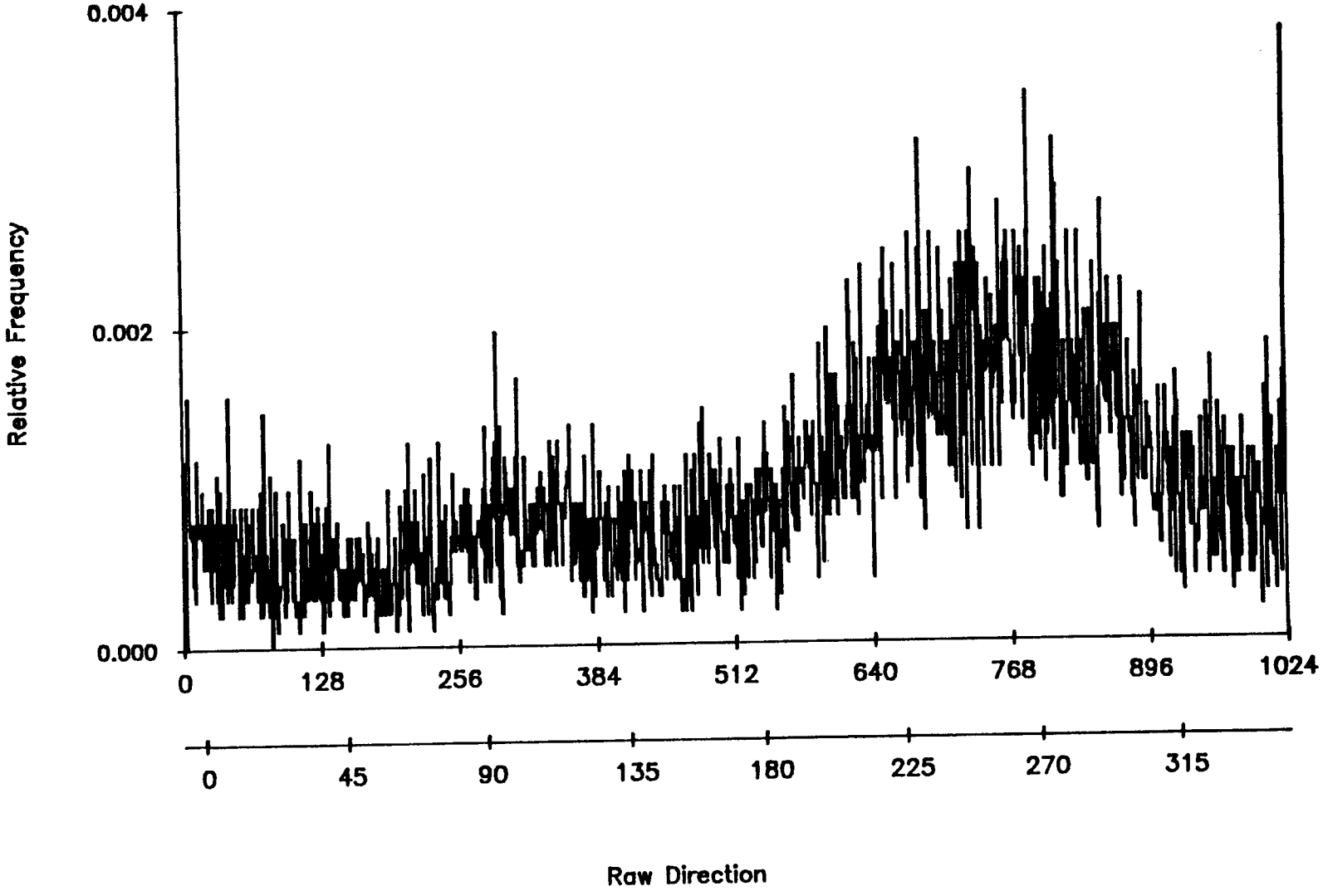

776 M at Nares–II. 21 Sep 84 – 21 Nov 85. Tape 5860/9.

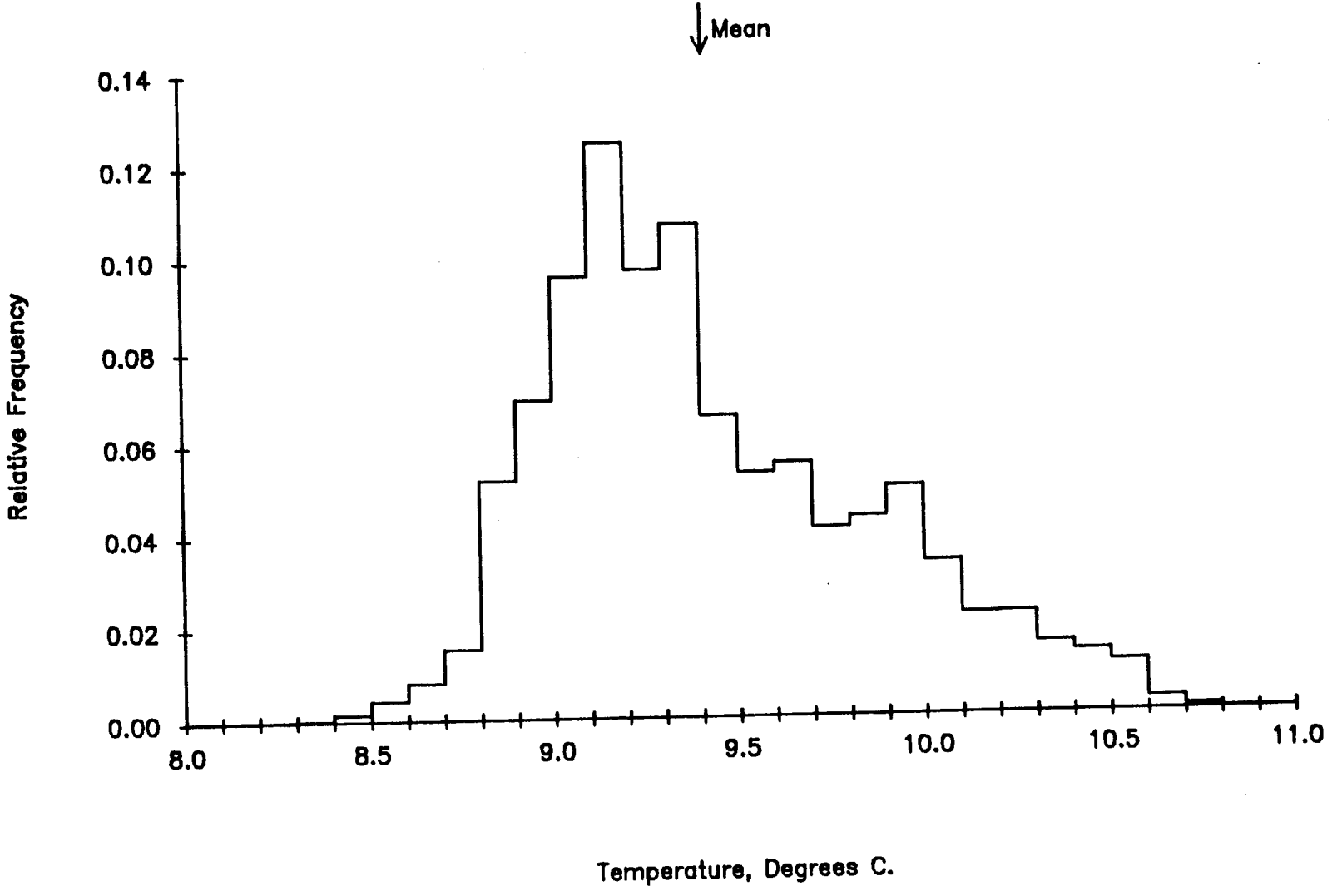

776 M at Nares–II. 21 Sep 84 – 21 Nov 85. Tape 5860/9.

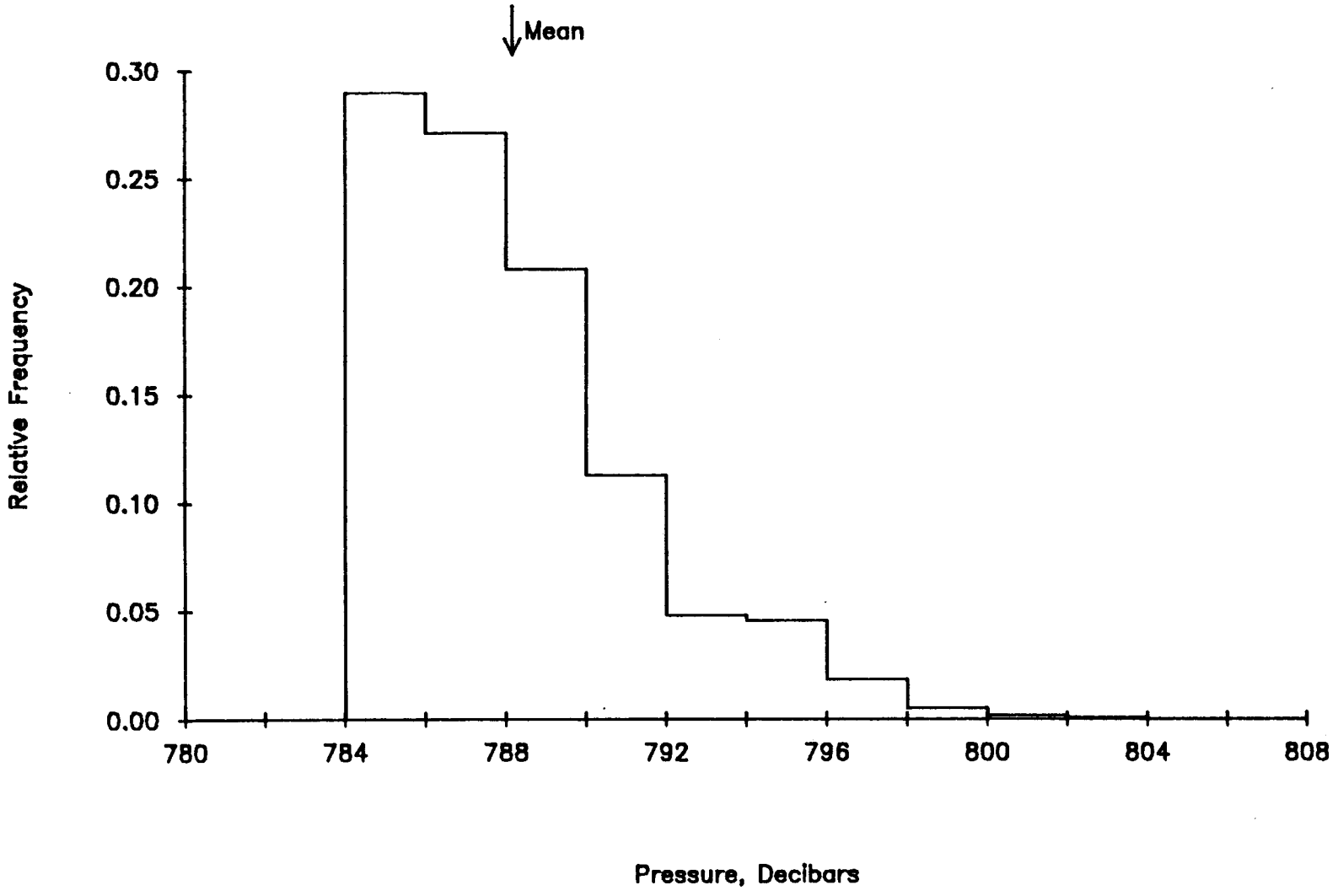

.P DATA AT NARES-II, 1464 METERS
LINE 1 THRU END OF FILE

	MEAN	SD	SKEWNESS	KURTOSIS	MIN	MAX	LENGTH
S	3.92	2.12	0.34	2.83	0.80	13.70	10211
U	0.16	3.50	0.38	2.72	-10.50	13.60	10211
V	-0.12	2.75	0.08	3.09	-9.00	9.70	10211
T	4.52	0.10	0.02	2.22	4.24	4.79	10211
P	1486.17	2.95	0.52	2.70	1479.80	1495.60	10211

EDDY KE	=	9.89	10211 POINTS
HEAT FLUX U	=	0.07	10211 POINTS
HEAT FLUX V	=	0.06	10211 POINTS
MOMENTUM FLUX	=	-0.93	10211 POINTS

.LLP DATA AT NARES-II, 1464 METERS
LINE 1 THRU END OF FILE

	MEAN	SD	SKEWNESS	KURTOSIS	MIN	MAX	LENGTH
U	0.13	2.96	0.61	2.57	-5.67	8.31	1693
V	-0.12	2.03	0.18	3.20	-5.58	6.48	1693
T	4.52	0.10	0.04	2.12	4.28	4.75	1693
P	1486.14	2.81	0.45	2.53	1481.99	1495.03	1693

EDDY KE = 6.42 1693 POINTS

HEAT FLUX U = 0.07 1693 POINTS

HEAT FLUX V = 0.06 1693 POINTS

MOMENTUM FLUX = -0.60 1693 POINTS

1464 Meters at Nares-II. 21 Sep 84 - 21 Nov 85. Tape 5859/10.

FIRST 5 LINES:

2200	21	9	84	1.7	205	-0.7	-1.6	4.44	1495.6	1
2300	21	9	84	1.9	213	-1.0	-1.6	4.41	1495.6	2
0	22	9	84	3.3	220	-2.1	-2.5	4.43	1495.6	3
100	22	9	84	3.0	227	-2.2	-2.0	4.43	1495.6	4
200	22	9	84	2.8	268	-2.8	-0.1	4.40	1495.6	5

LAST 5 LINES:

400	21	11	85	12.1	101	11.9	-2.3	4.51	1486.6	10207
500	21	11	85	10.4	108	9.9	-3.2	4.54	1486.6	10208
600	21	11	85	10.5	113	9.6	-4.1	4.55	1486.6	10209
700	21	11	85	10.0	110	9.4	-3.4	4.60	1486.6	10210
800	21	11	85	9.6	114	8.8	-3.9	4.58	1486.6	10211

	MIN	MEAN	MAX	SD	NUM
SPEED, CM/SEC	0.80	3.92	13.70	2.12	10211
U, CM/SEC	-10.50	0.16	13.60	3.50	10211
V, CM/SEC	-9.00	-0.12	9.70	2.75	10211
TEMP, DEG C	4.24	4.52	4.79	0.10	10211
PRESSURE, DB	1479.80	1486.17	1495.60	2.95	10211

The processed file is 3 cycles short.

1464 M at Nares-II. 21 Sep 84 - 21 Nov 85. Tape 5859/10.

FREQUENCY TABLE FOR CURRENT SPEED

LOWER BOUND	UPPER BOUND	FREQUENCY	RELATIVE FR.
0.00	2.00	2187	0.214181
2.00	4.00	3016	0.295368
4.00	6.00	3287	0.321908
6.00	8.00	1401	0.137205
8.00	10.00	268	0.026246
10.00	12.00	46	0.004505
12.00	14.00	6	0.000588
14.00	16.00	0	0.000000
16.00	18.00	0	0.000000
18.00	20.00	0	0.000000
20.00	22.00	0	0.000000
22.00	24.00	0	0.000000
24.00	26.00	0	0.000000
26.00	28.00	0	0.000000

MEAN	3.91888
STANDARD DEVIATION	2.11600

1464 M at Nares-II. 21 Sep 84 - 21 Nov 85. Tape 5859/10.

FREQUENCY TABLE FOR CURRENT DIRECTION

LOWER BOUND	UPPER BOUND	FREQUENCY	RELATIVE FR.
0	10	206	0.020174
10	20	161	0.015767
20	30	139	0.013613
30	40	133	0.013025
40	50	159	0.015571
50	60	218	0.021350
60	70	250	0.024483
70	80	296	0.028988
80	90	402	0.039369
90	100	386	0.037802
100	110	439	0.042993
110	120	397	0.038880
120	130	280	0.027421
130	140	236	0.023112
140	150	242	0.023700
150	160	223	0.021839
160	170	233	0.022819
170	180	251	0.024581
180	190	268	0.026246
190	200	245	0.023994
200	210	323	0.031633
210	220	283	0.027715
220	230	271	0.026540
230	240	315	0.030849
240	250	320	0.031339
250	260	406	0.039761
260	270	376	0.036823
270	280	411	0.040251
280	290	397	0.038880
290	300	340	0.033297
300	310	322	0.031535
310	320	285	0.027911
320	330	255	0.024973
330	340	253	0.024777
340	350	284	0.027813
350	360	206	0.020174

1464 M at Nares-II. 21 Sep 84 - 21 Nov 85. Tape 5859/10.

FREQUENCY TABLE FOR TEMPERATURE

LOWER BOUND	UPPER BOUND	FREQUENCY	RELATIVE FR.
4.10	4.15	0	0.000000
4.15	4.20	0	0.000000
4.20	4.25	5	0.000490
4.25	4.30	69	0.006757
4.30	4.35	158	0.015474
4.35	4.40	704	0.068945
4.40	4.45	1902	0.186270
4.45	4.50	1296	0.126922
4.50	4.55	1711	0.167564
4.55	4.60	1510	0.147880
4.60	4.65	1519	0.148761
4.65	4.70	938	0.091862
4.70	4.75	359	0.035158
4.75	4.80	40	0.003917
4.80	4.85	0	0.000000
4.85	4.90	0	0.000000

MEAN	4.52385
STANDARD DEVIATION	0.10128

1464 M at Nares-II. 21 Sep 84 - 21 Nov 85. Tape 5859/10.

FREQUENCY TABLE FOR PRESSURE

LOWER BOUND	UPPER BOUND	FREQUENCY	RELATIVE FR.
1475.00	1479.00	0	0.000000
1479.00	1483.00	1648	0.161395
1483.00	1487.00	5489	0.537558
1487.00	1491.00	1985	0.194398
1491.00	1495.00	1046	0.102439
1495.00	1499.00	43	0.004211

MEAN	1486.05078
STANDARD DEVIATION	2.95682

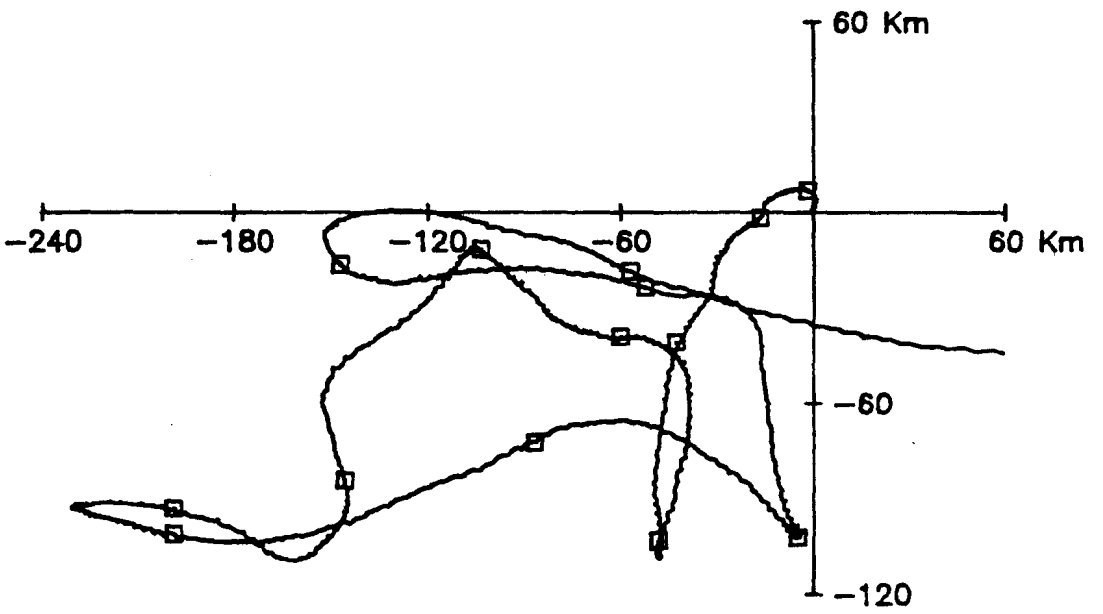

1464 M at Nares—II. 425.4 days starting 2200 21 Sep 84.

1464 M at Nares-II. 21 Sep 84 – 21 Nov 85. Tape 5859/10.

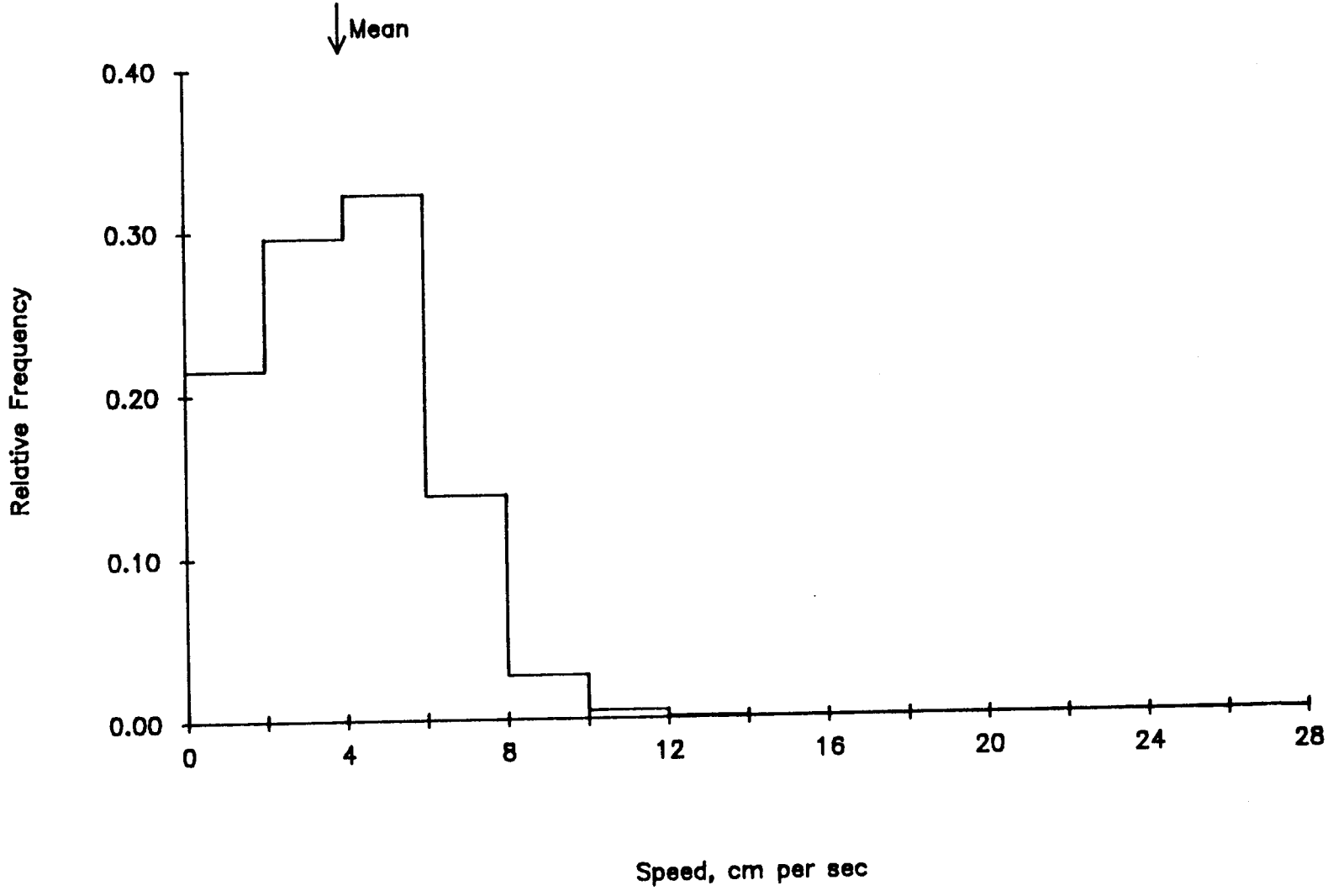

1464 M at Nares–II. 21 Sep 84 – 21 Nov 85. Tape 5859/10.

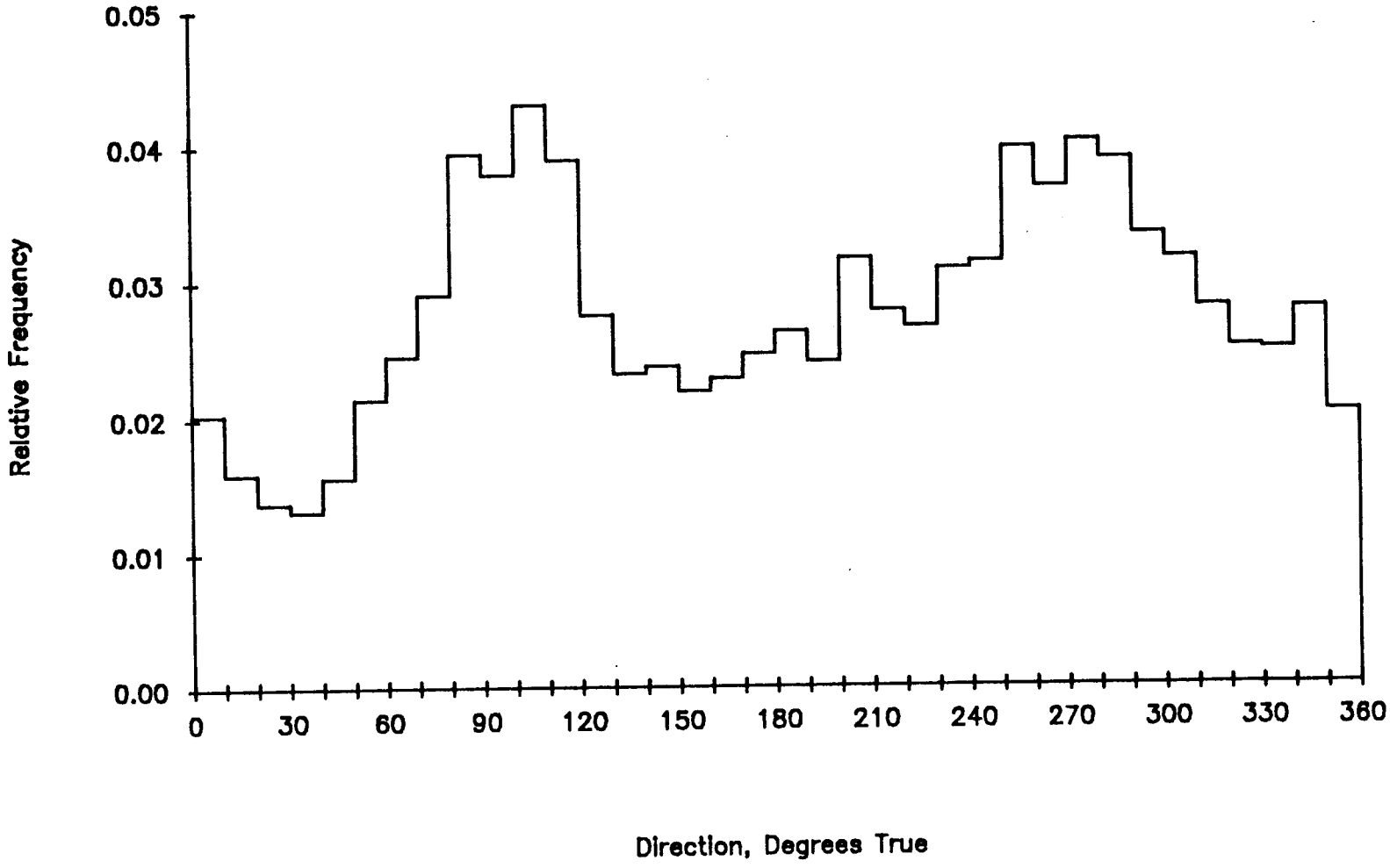

1464 M at Nares-II. 21 Sep 84 – 21 Nov 85. Tape 5859/10.

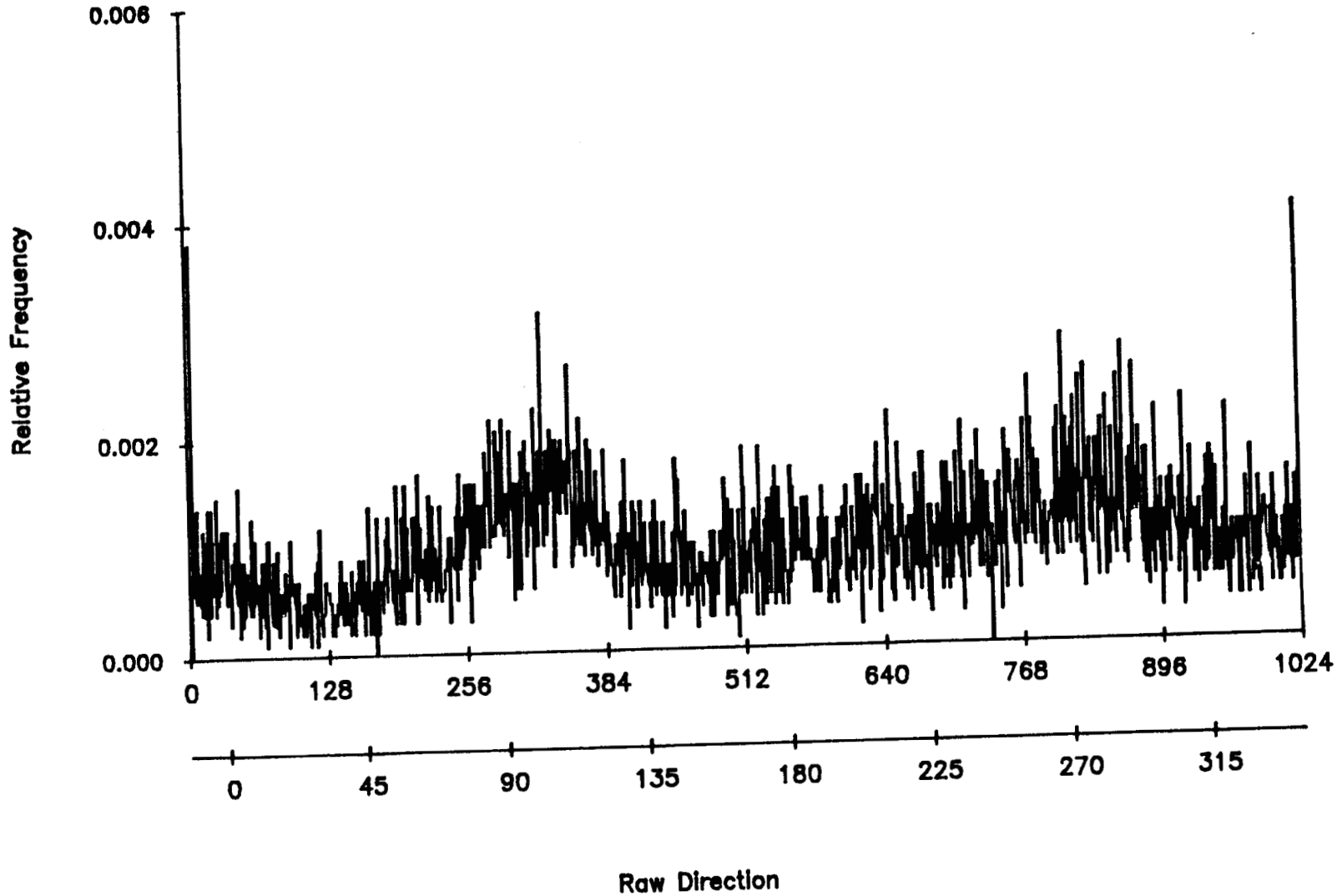

1464 M at Nares-II. 21 Sep 84 – 21 Nov 85. Tape 5859/10.

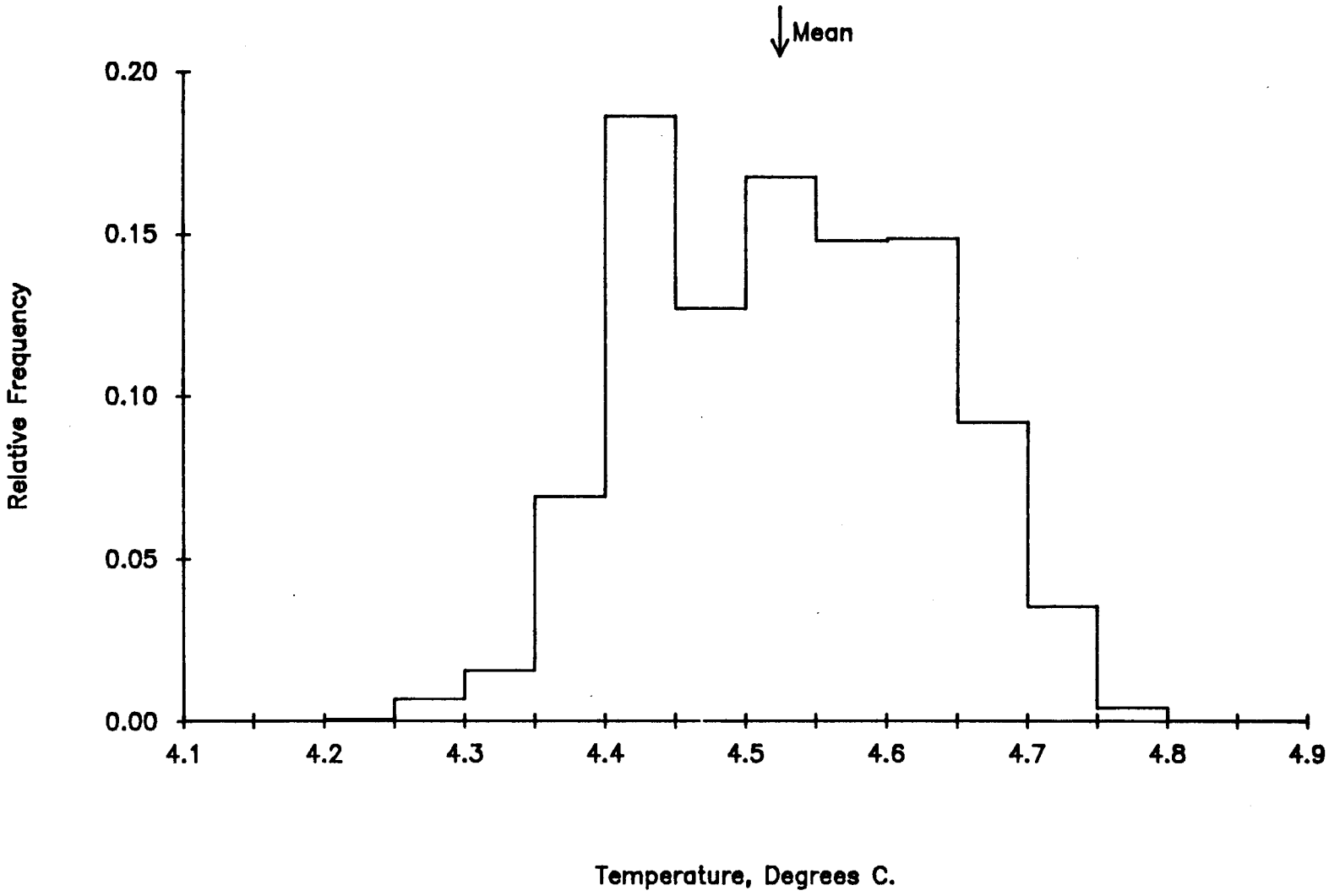

1464 M at Nares-II. 21 Sep 84 – 21 Nov 85. Tape 5859/10.

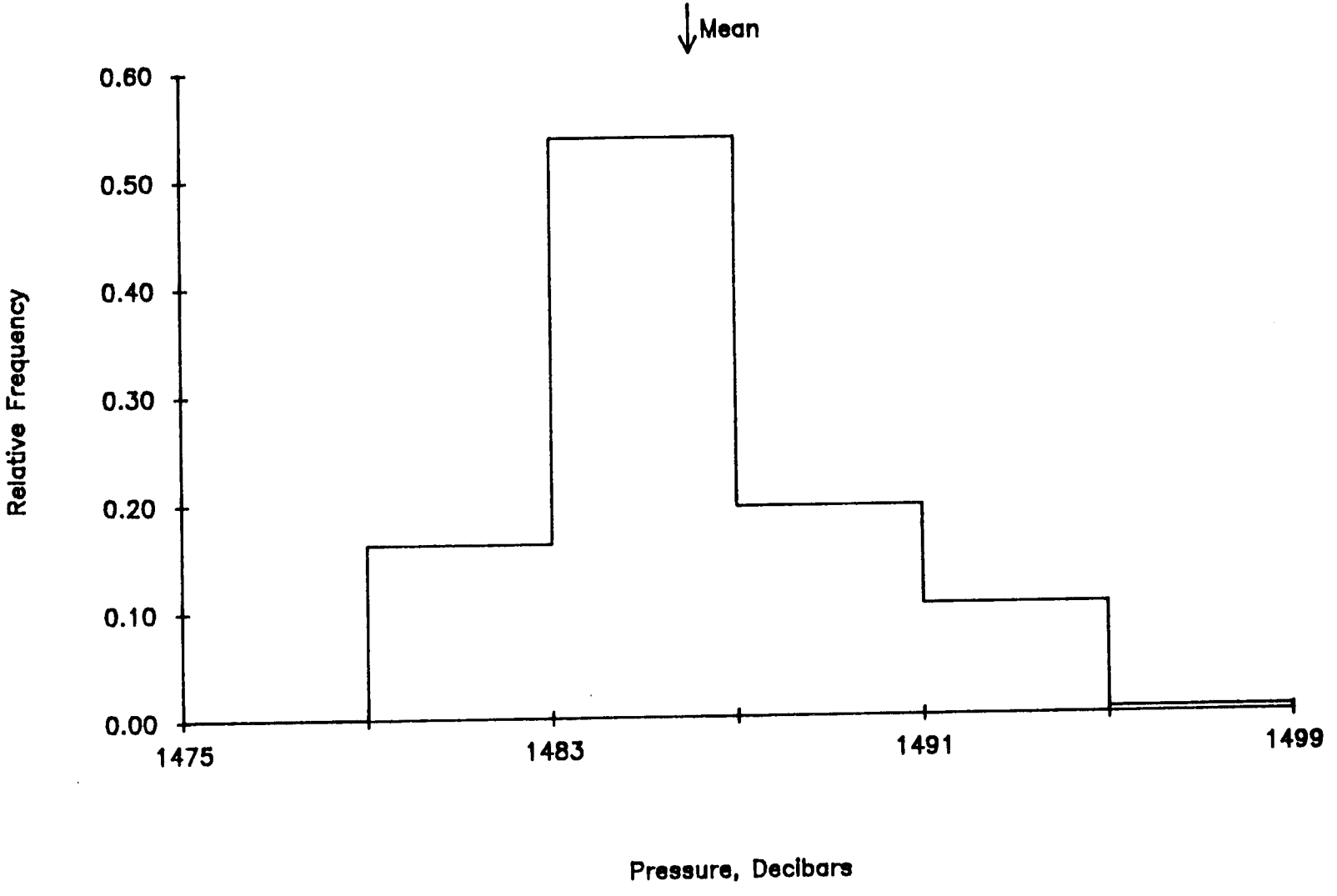

.P DATA AT NARES-II, 2900 METERS
LINE 1 THRU END OF FILE

	MEAN	SD	SKEWNESS	KURTOSIS	MIN	MAX	LENGTH
S	1.07	0.85	4.09	21.82	0.80	8.20	10213
U	-0.09	0.94	1.10	12.15	-5.60	8.20	10213
V	-0.14	0.93	-2.20	13.74	-8.00	4.70	10213
T	2.79	0.02	-0.07	3.01	2.69	2.88	10213

EDDY KE = 0.88 10213 POINTS

HEAT FLUX U = 0.00 10213 POINTS

HEAT FLUX V = -0.01 10213 POINTS

MOMENTUM FLUX = -0.11 10213 POINTS

.LLP DATA AT NARES-II, 2900 METERS
LINE 1 THRU END OF FILE

	MEAN	SD	SKEWNESS	KURTOSIS	MIN	MAX	LENGTH
U	-0.10	0.69	1.01	4.83	-2.00	2.87	1694
V	-0.15	0.73	-2.17	11.12	-4.30	1.79	1694
T	2.79	0.02	-0.10	2.71	2.74	2.85	1694

EDDY KE	=	0.51	1694 POINTS
HEAT FLUX U	=	0.00	1694 POINTS
HEAT FLUX V	=	-0.01	1694 POINTS
MOMENTUM FLUX	=	-0.05	1694 POINTS

2900 Meters at Nares-II. 21 Sep 84 - 21 Nov 85. Tape 4913/18.

FIRST 5 LINES:

2100	21	9	84	3.9	104	3.8	-0.9	2.80	1
2200	21	9	84	0.8	153	0.3	-0.7	2.79	2
2300	21	9	84	1.5	164	0.4	-1.5	2.79	3
0	22	9	84	1.8	165	0.5	-1.7	2.79	4
100	22	9	84	0.8	183	0.0	-0.7	2.77	5

LAST 5 LINES:

500	21	11	85	2.9	90	2.9	0.0	2.77	10209
600	21	11	85	2.0	88	2.0	0.1	2.77	10210
700	21	11	85	1.8	98	1.8	-0.2	2.77	10211
800	21	11	85	1.6	101	1.6	-0.3	2.77	10212
900	21	11	85	0.8	97	0.7	-0.1	2.76	10213

	MIN	MEAN	MAX	SD	NUM
SPEED, CM/SEC	0.80	1.07	8.20	0.85	10213
U, CM/SEC	-5.60	-0.09	8.20	0.94	10213
V, CM/SEC	-8.00	-0.14	4.70	0.93	10213
TEMP, DEG C	2.69	2.79	2.88	0.02	10213

The processed file is one cycle short.
The transmissometer channel was not processed due to an instrument malfunction.
Speed is suspiciously low throughout most of the record.

2900 M at Nares-II. 21 Sep 84 - 21 Nov 85. Tape 4913/18.

FREQUENCY TABLE FOR CURRENT SPEED

LOWER BOUND	UPPER BOUND	FREQUENCY	RELATIVE FR.
0.00	2.00	9417	0.922060
2.00	4.00	537	0.052580
4.00	6.00	213	0.020856
6.00	8.00	38	0.003721
8.00	10.00	8	0.000783
10.00	12.00	0	0.000000
12.00	14.00	0	0.000000
14.00	16.00	0	0.000000
16.00	18.00	0	0.000000
18.00	20.00	0	0.000000
20.00	22.00	0	0.000000
22.00	24.00	0	0.000000
24.00	26.00	0	0.000000
26.00	28.00	0	0.000000

MEAN	1.06550
STANDARD DEVIATION	0.85112

2900 M at Nares-II. 21 Sep 84 - 21 Nov 85. Tape 4913/18.

FREQUENCY TABLE FOR TEMPERATURE

LOWER BOUND	UPPER BOUND	FREQUENCY	RELATIVE FR.
2.40	2.45	0	0.000000
2.45	2.50	0	0.000000
2.50	2.55	0	0.000000
2.55	2.60	0	0.000000
2.60	2.65	0	0.000000
2.65	2.70	1	0.000098
2.70	2.75	282	0.027612
2.75	2.80	5193	0.508470
2.80	2.85	4601	0.450504
2.85	2.90	136	0.013316
2.90	2.95	0	0.000000
2.95	3.00	0	0.000000
3.00	3.05	0	0.000000
3.05	3.10	0	0.000000

MEAN	2.79062
STANDARD DEVIATION	0.02382

2900 M at Nares-II. 21 Sep 84 - 21 Nov 85. Tape 4913/18.

FREQUENCY TABLE FOR CURRENT DIRECTION

LOWER BOUND	UPPER BOUND	FREQUENCY	RELATIVE FR.
0	10	158	0.015470
10	20	144	0.014100
20	30	170	0.016645
30	40	154	0.015079
40	50	166	0.016254
50	60	189	0.018506
60	70	234	0.022912
70	80	259	0.025360
80	90	296	0.028983
90	100	389	0.038089
100	110	353	0.034564
110	120	241	0.023597
120	130	242	0.023695
130	140	214	0.020954
140	150	248	0.024283
150	160	251	0.024577
160	170	256	0.025066
170	180	237	0.023206
180	190	251	0.024577
190	200	296	0.028983
200	210	299	0.029276
210	220	309	0.030256
220	230	301	0.029472
230	240	394	0.038578
240	250	447	0.043768
250	260	524	0.051307
260	270	492	0.048174
270	280	474	0.046411
280	290	430	0.042103
290	300	400	0.039166
300	310	322	0.031528
310	320	269	0.026339
320	330	238	0.023304
330	340	220	0.021541
340	350	170	0.016645
350	360	176	0.017233

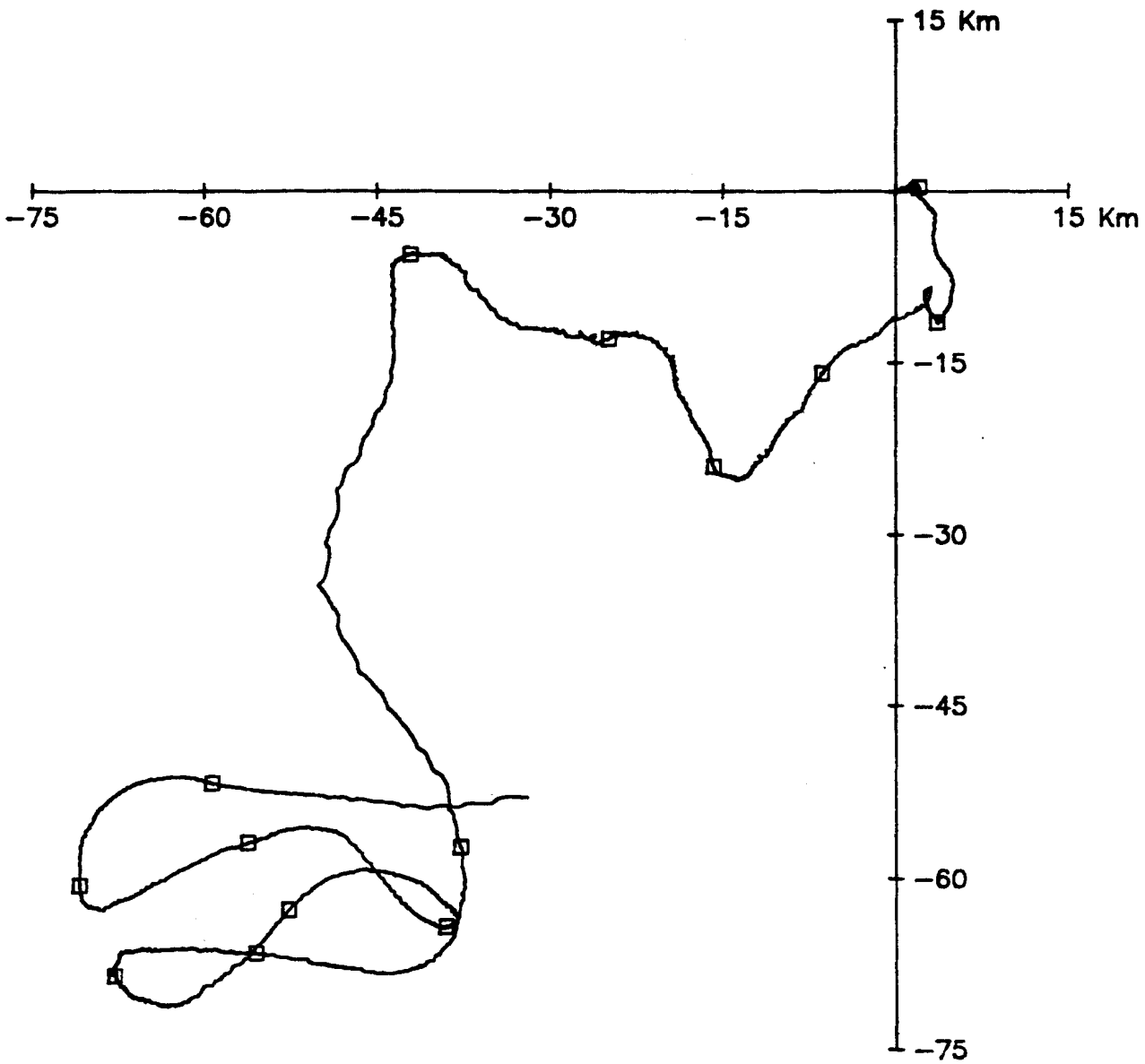

2900 M at Nares−II. 425.5 days starting 2100 21 Sep 84.

2900 M at Nares–II. 21 Sep 84 – 21 Nov 85. Tape 4913/18.

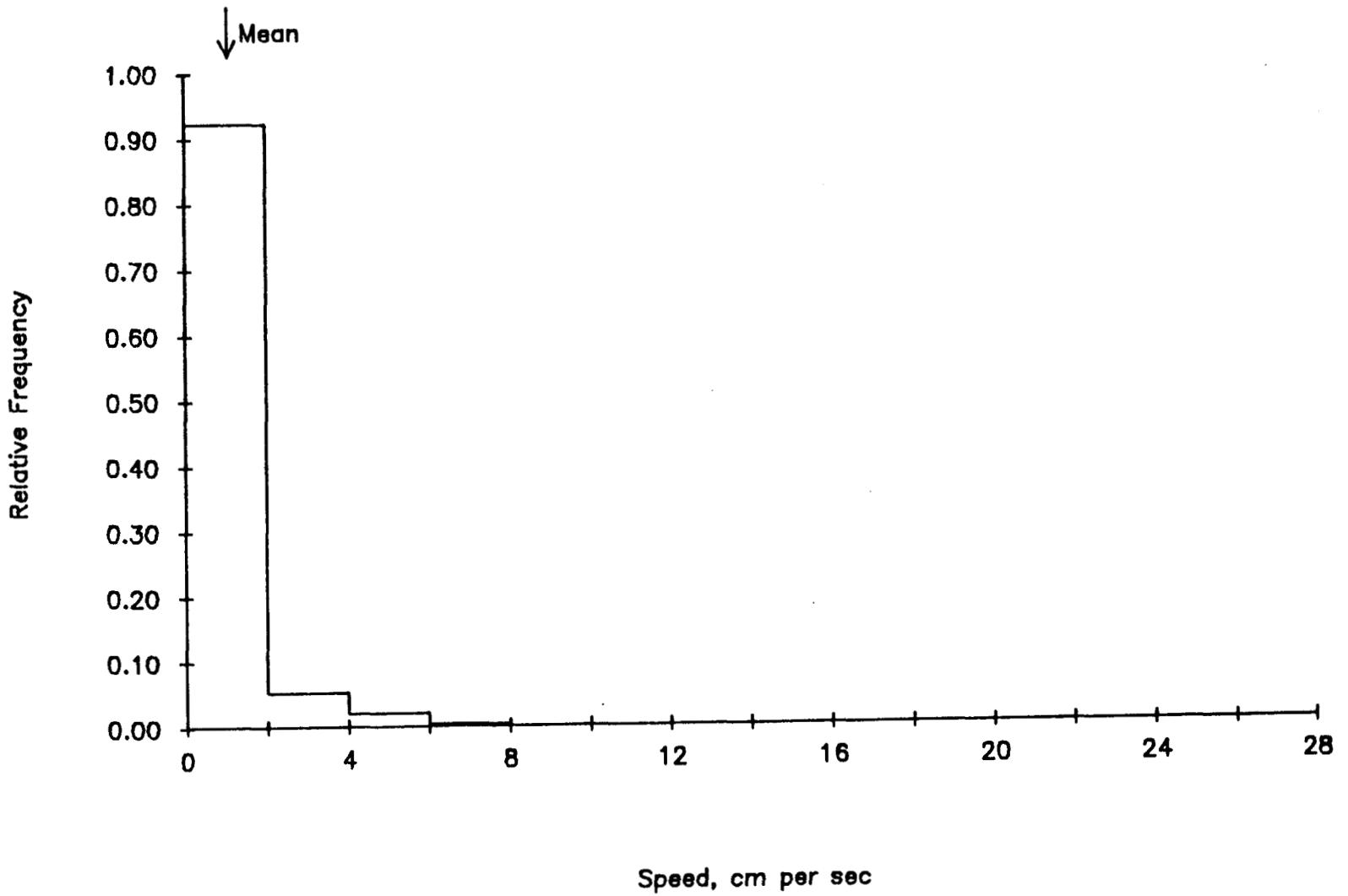

2900 M at Nares–II. 21 Sep 84 – 21 Nov 85. Tape 4913/18.

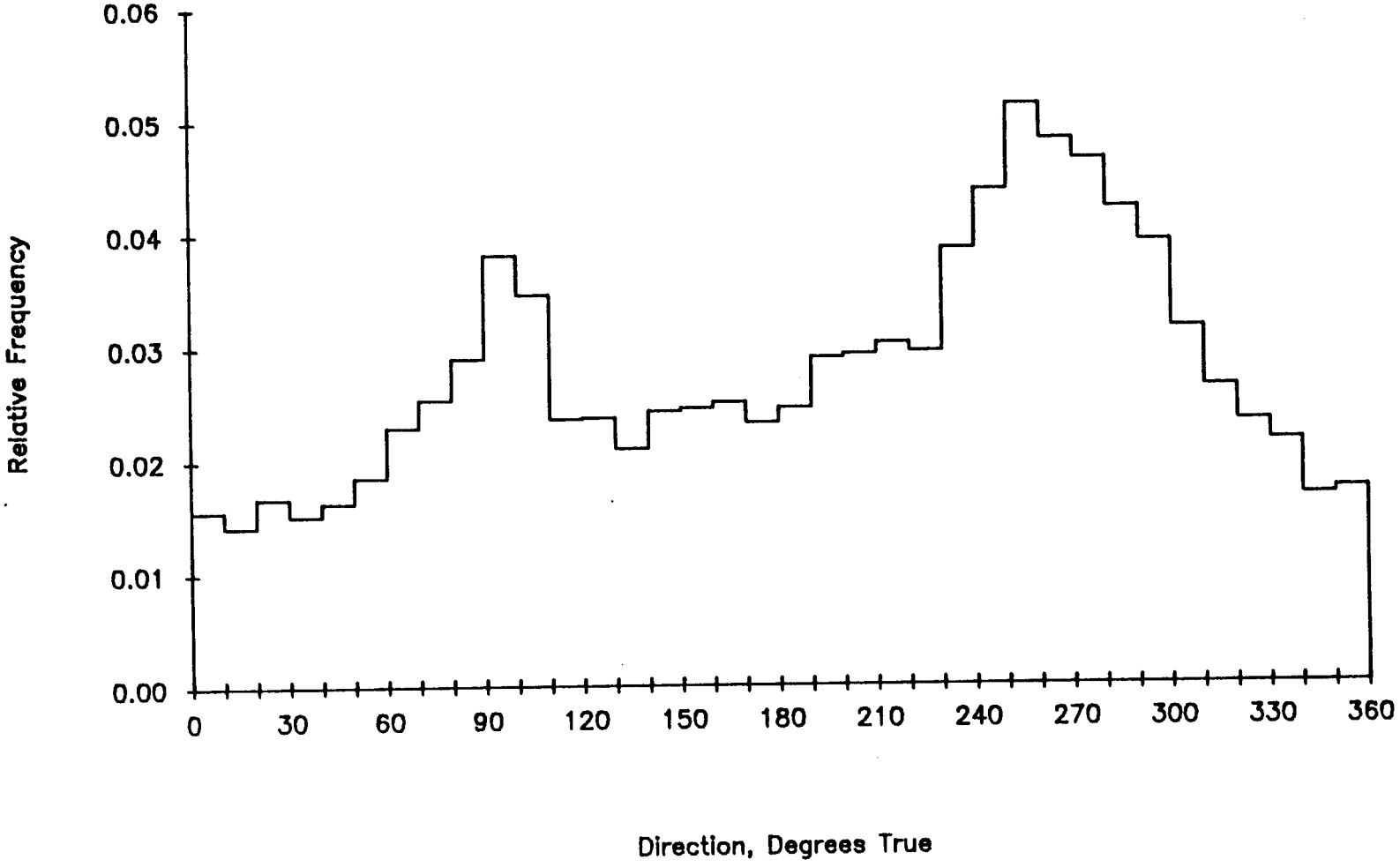

2900 M at Nares–II. 21 Sep 84 – 21 Nov 85. Tape 4913/18.

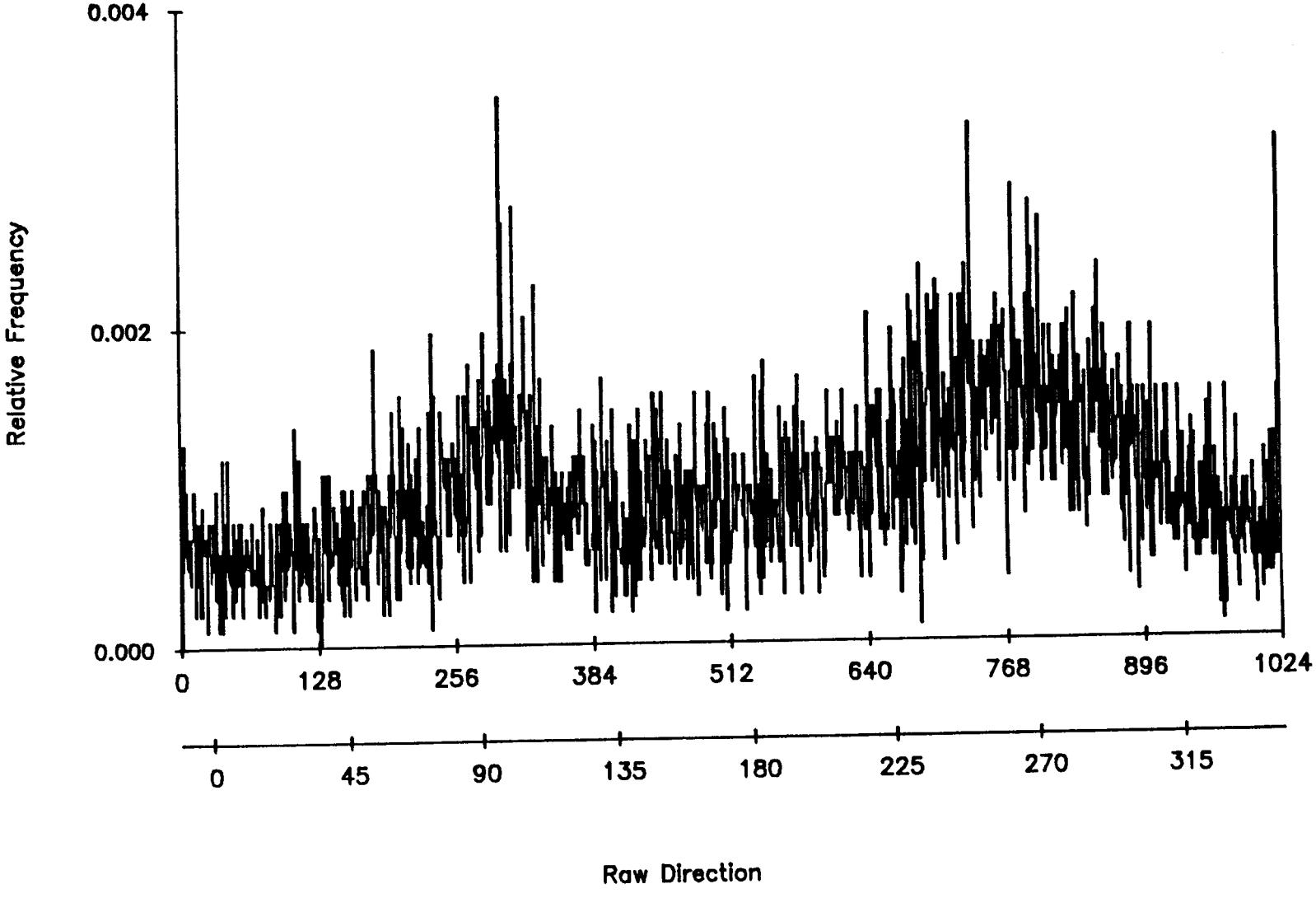

2900 M at Nares–II. 21 Sep 84 – 21 Nov 85. Tape 4913/18.

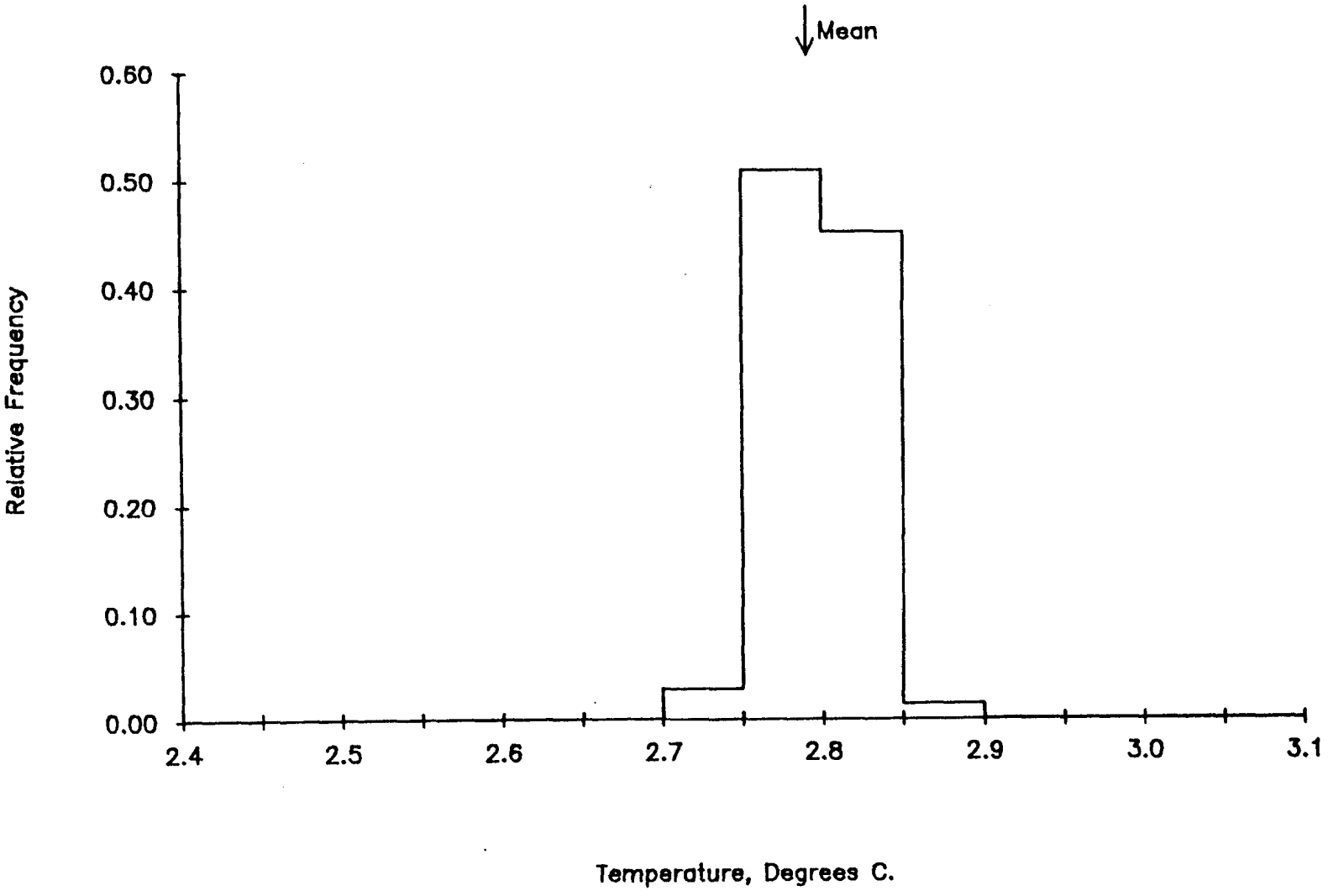

,F DATA AT NARES-II, 4800 METERS
LINE 1 THRU END OF FILE

	MEAN	SD	SKEWNESS	KURTOSIS	MIN	MAX	LENGTH
S	3.50	2.14	0.53	2.55	0.80	11.00	10215
U	-0.05	3.00	0.20	3.07	-9.30	9.40	10215
V	-0.83	2.68	-0.06	3.90	-10.70	9.10	10215
T	2.28	0.01	-1.35	7.51	2.21	2.37	10215
A	0.47	0.05	0.39	1.76	0.25	0.61	10215

EDDY KE =	8.07	10215 POINTS
HEAT FLUX U =	0.00	10215 POINTS
HEAT FLUX V =	0.01	10215 POINTS
MOMENTUM FLUX =	-1.23	10215 POINTS

.LLP DATA AT NARES-II, 4800 METERS
LINE 1 THRU END OF FILE

	MEAN	SD	SKEWNESS	KURTOSIS	MIN	MAX	LENGTH
U	-0.06	2.75	0.23	3.27	-7.36	7.69	1694
V	-0.84	2.43	-0.06	4.38	-8.14	7.39	1694
T	2.28	0.01	-2.13	8.74	2.21	2.31	1694
P	0.47	0.05	0.33	1.52	0.40	0.55	1694

EDDY KE = 6.76 1694 POINTS

HEAT FLUX U = 0.00 1694 POINTS

HEAT FLUX V = 0.01 1694 POINTS

MOMENTUM FLUX = -0.98 1694 POINTS

4800 Meters at Nares-II. 21 Sep 84 - 21 Nov 85. Tape 7161/3.

FIRST 5 LINES:

2100	21	9	84	0.8	53	0.6	0.5	2.31	0.0	0.406	1
2200	21	9	84	0.8	188	-0.1	-0.7	2.30	0.0	0.406	2
2300	21	9	84	0.8	161	0.2	-0.7	2.29	0.0	0.401	3
0	22	9	84	0.8	191	-0.1	-0.7	2.28	0.0	0.406	4
100	22	9	84	0.8	186	-0.1	-0.7	2.27	0.0	0.406	5

LAST 5 LINES:

700	21	11	85	3.6	46	2.6	2.5	2.29	0.0	0.498	10211
800	21	11	85	3.3	49	2.5	2.2	2.29	0.0	0.533	10212
900	21	11	85	3.3	58	2.8	1.8	2.30	0.0	0.533	10213
1000	21	11	85	4.2	72	4.0	1.3	2.29	0.0	0.538	10214
1100	21	11	85	4.2	72	4.0	1.3	2.30	0.0	0.462	10215

	MIN	MEAN	MAX	SD	NUM
SPEED, CM/SEC	0.80	3.50	11.00	2.14	10215
U, CM/SEC	-9.30	-0.05	9.40	3.00	10215
V, CM/SEC	-10.70	-0.83	9.10	2.68	10215
TEMP, DEG C	2.21	2.28	2.37	0.01	10215
ATTEN. C. 1/M	0.25	0.47	0.61	0.05	10215

4800 M at Nares-II. 21 Sep 84 - 21 Nov 85. Tape 7161/3.

FREQUENCY TABLE FOR CURRENT SPEED

LOWER BOUND	UPPER BOUND	FREQUENCY	RELATIVE FR.
0.00	2.00	2709	0.265198
2.00	4.00	3637	0.356045
4.00	6.00	2295	0.224670
6.00	8.00	1319	0.129124
8.00	10.00	235	0.023005
10.00	12.00	20	0.001958
12.00	14.00	0	0.000000
14.00	16.00	0	0.000000
16.00	18.00	0	0.000000
18.00	20.00	0	0.000000
20.00	22.00	0	0.000000
22.00	24.00	0	0.000000
24.00	26.00	0	0.000000
26.00	28.00	0	0.000000

MEAN	3.50195
STANDARD DEVIATION	2.13838

4800 M at Nares-II. 21 Sep 84 - 21 Nov 83. Tape 7161/3.

FREQUENCY TABLE FOR CURRENT DIRECTION

LOWER BOUND	UPPER BOUND	FREQUENCY	RELATIVE FR.
0	10	66	0.006461
10	20	67	0.006559
20	30	80	0.007832
30	40	105	0.010279
40	50	165	0.016153
50	60	180	0.017621
60	70	195	0.019090
70	80	270	0.026432
80	90	335	0.032795
90	100	330	0.032305
100	110	272	0.026628
110	120	197	0.019285
120	130	201	0.019677
130	140	243	0.023789
140	150	296	0.028977
150	160	433	0.042389
160	170	449	0.043955
170	180	460	0.045032
180	190	432	0.042291
190	200	415	0.040627
200	210	389	0.038081
210	220	364	0.035634
220	230	425	0.041605
230	240	456	0.044640
240	250	447	0.043759
250	260	485	0.047479
260	270	452	0.044249
270	280	362	0.035438
280	290	315	0.030837
290	300	273	0.026725
300	310	230	0.022516
310	320	220	0.021537
320	330	199	0.019481
330	340	148	0.014488
340	350	149	0.014586
350	360	110	0.010768

4800 M at Nares-II. 21 Sep 84 - 21 Nov 85. Tape 7161/3.

FREQUENCY TABLE FOR TEMPERATURE

LOWER BOUND	UPPER BOUND	FREQUENCY	RELATIVE FR.
1.90	1.95	0	0.000000
1.95	2.00	0	0.000000
2.00	2.05	0	0.000000
2.05	2.10	0	0.000000
2.10	2.15	0	0.000000
2.15	2.20	0	0.000000
2.20	2.25	274	0.026823
2.25	2.30	9386	0.918845
2.30	2.35	546	0.053451
2.35	2.40	9	0.000881
2.40	2.45	0	0.000000
2.45	2.50	0	0.000000
2.50	2.55	0	0.000000
2.55	2.60	0	0.000000
2.60	2.65	0	0.000000
2.65	2.70	0	0.000000

MEAN	2.28115
STANDARD DEVIATION	0.01467

4800 M at Nares-II. 21 Sep 84 - 21 Nov 85. Tape 7161/3.

FREQUENCY TABLE FOR ATTENUATION COEFFICIENT

LOWER BOUND	UPPER BOUND	FREQUENCY	RELATIVE FR.
0.10	0.15	0	0.000000
0.15	0.20	0	0.000000
0.20	0.25	0	0.000000
0.25	0.30	5	0.000489
0.30	0.35	6	0.000587
0.35	0.40	47	0.004601
0.40	0.45	5275	0.516397
0.45	0.50	1657	0.162212
0.50	0.55	2905	0.284386
0.55	0.60	317	0.031033
0.60	0.65	3	0.000294
0.65	0.70	0	0.000000
0.70	0.75	0	0.000000
0.75	0.80	0	0.000000

MEAN	0.46563
STANDARD DEVIATION	0.04947

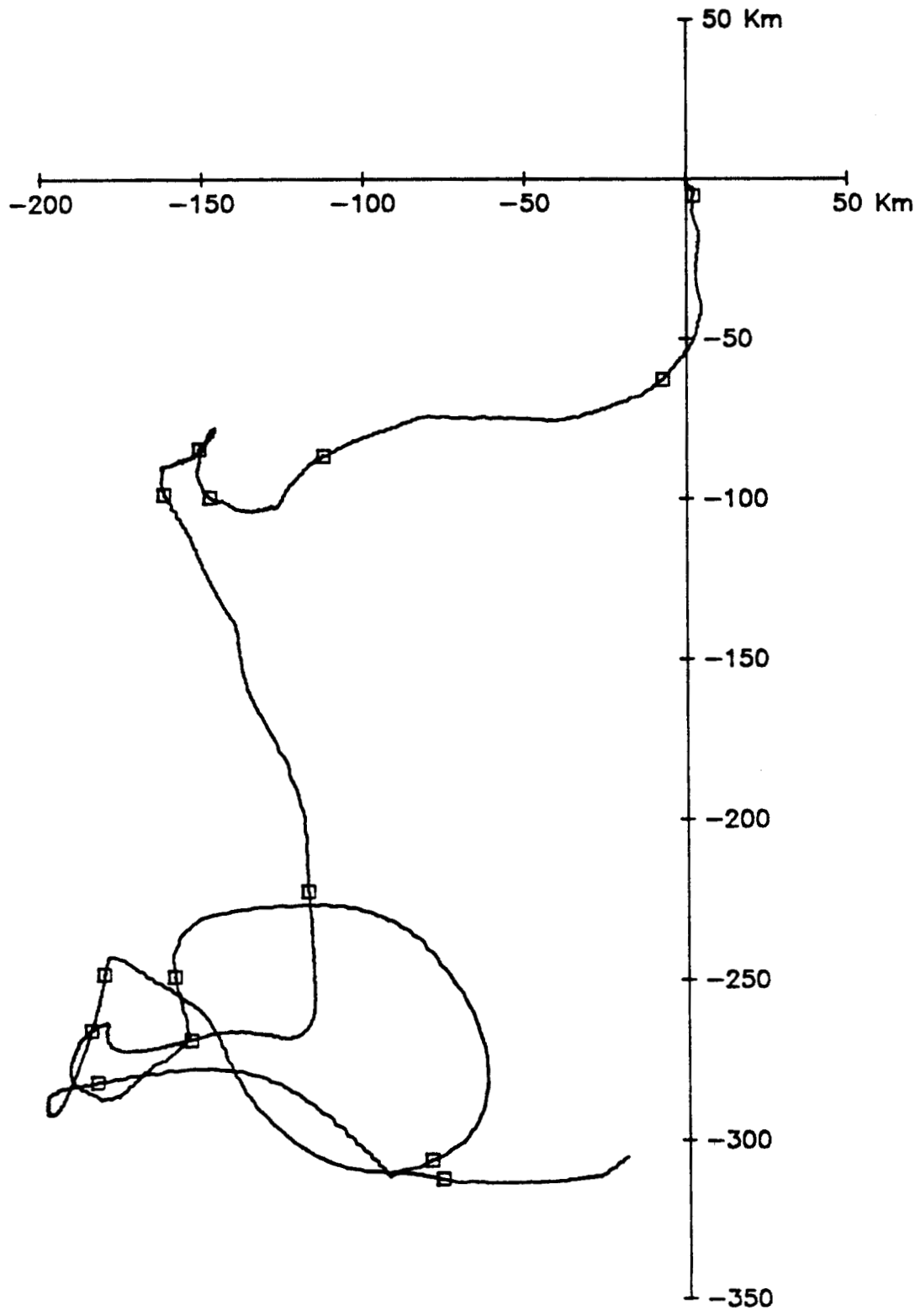

4800 M at Nares—II. 425.6 days starting 2100 21 Sep 84.

4800 M at Nares–II. 21 Sep 84 – 21 Nov 85. Tape 7161/3.

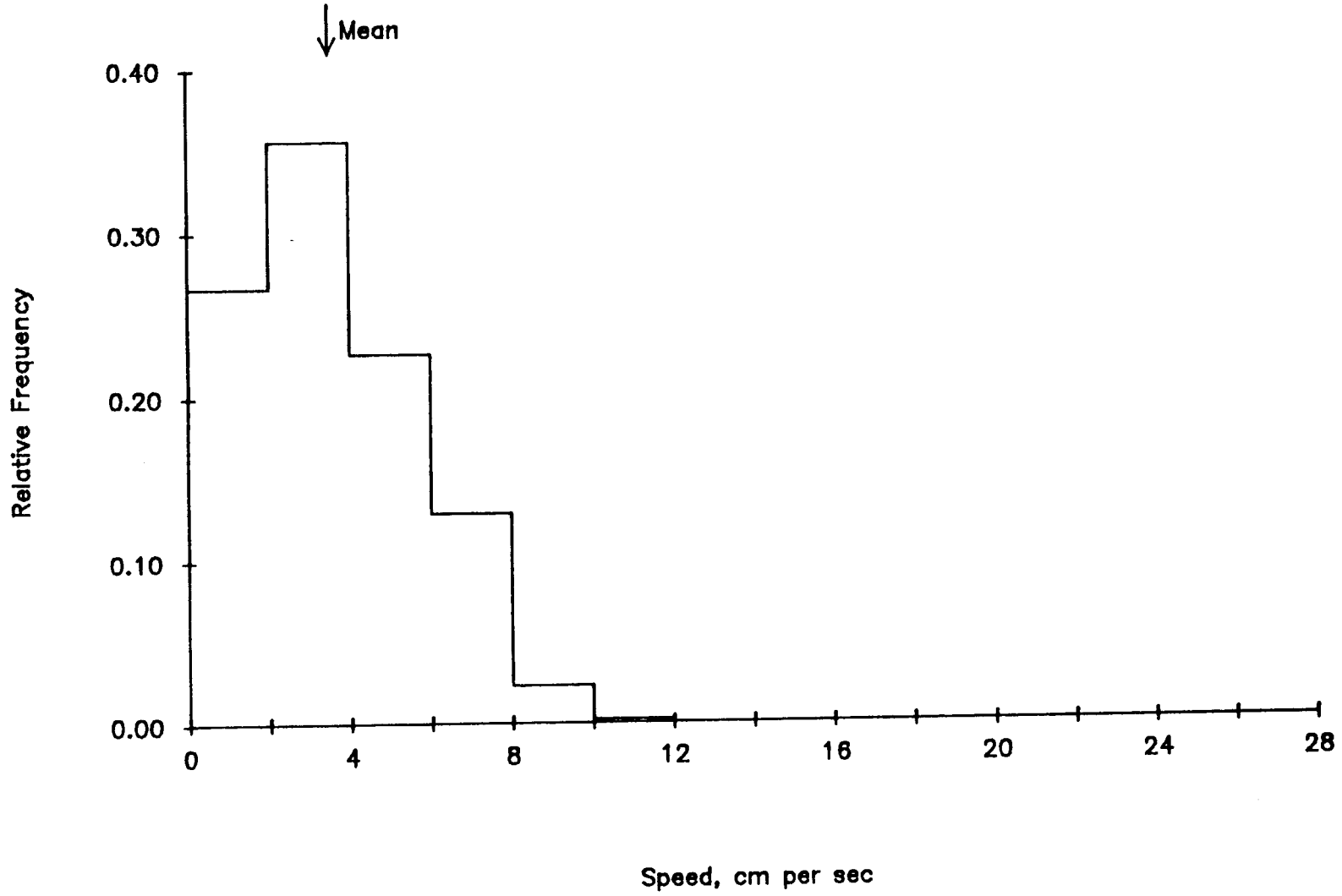

4800 M at Nares–II. 21 Sep 84 – 21 Nov 85. Tape 7161/3.

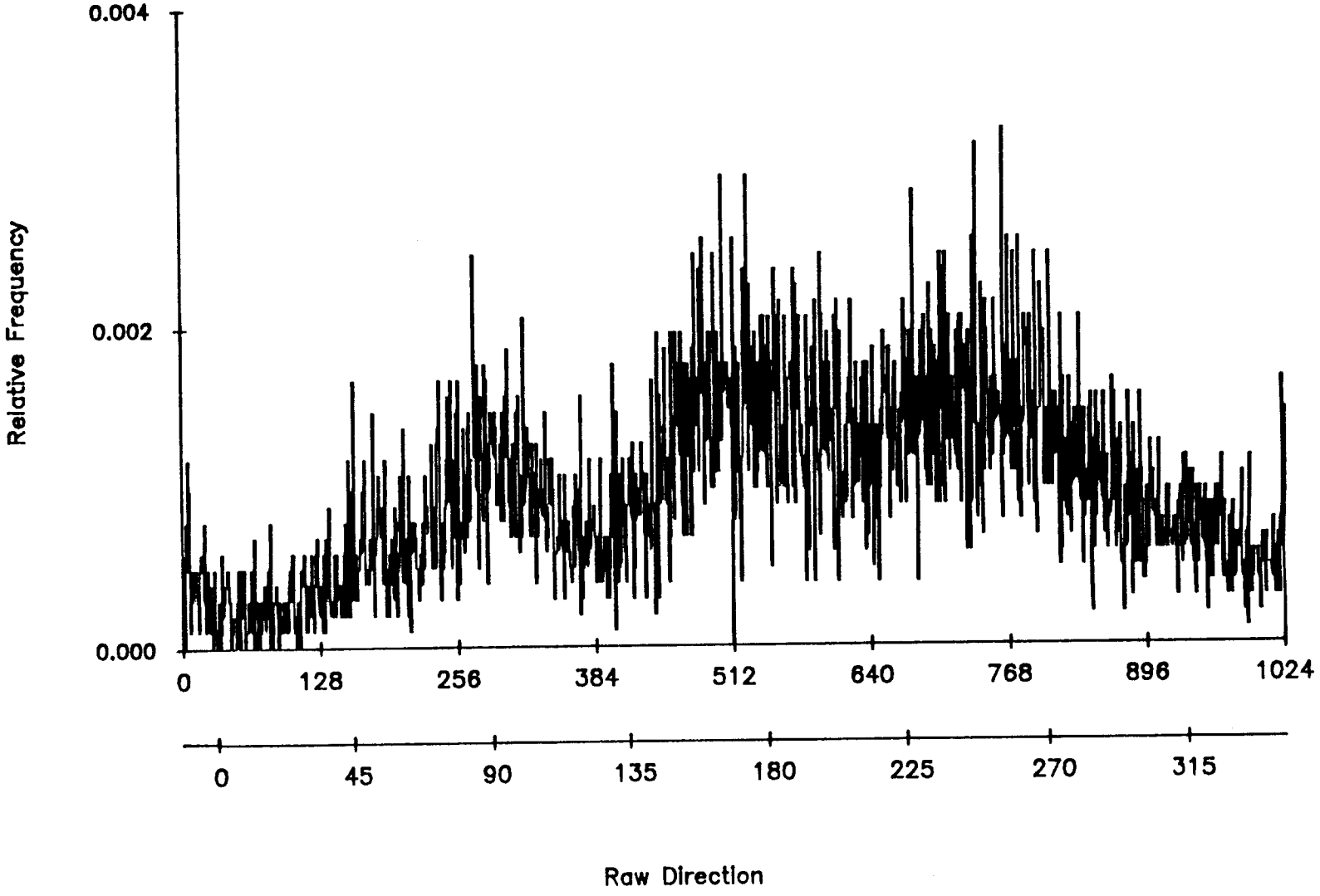

4800 M at Nares–II. 21 Sep 84 – 21 Nov 85. Tape 7161/3.

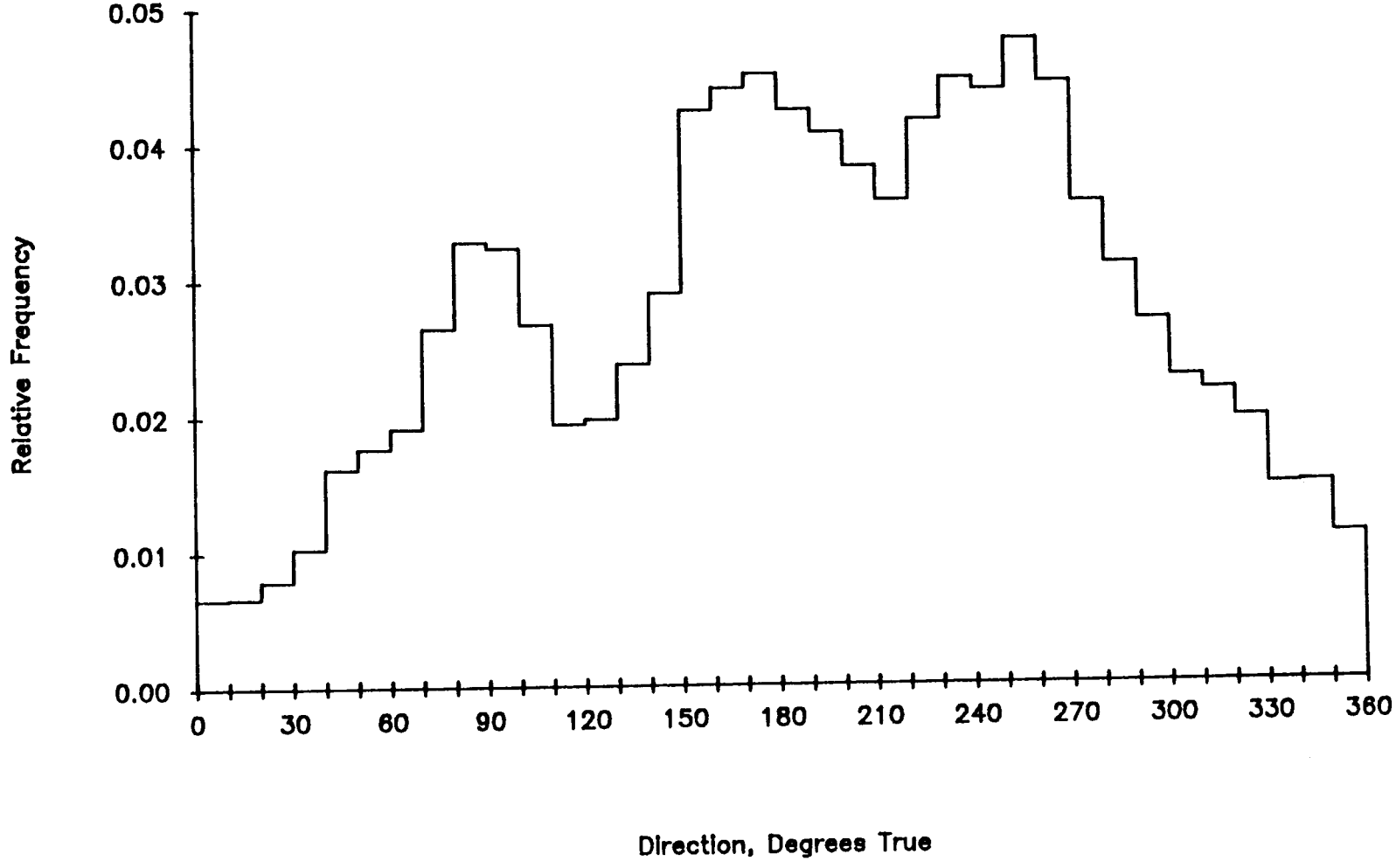

4800 M at Nares–II. 21 Sep 84 – 21 Nov 85. Tape 7161/3.

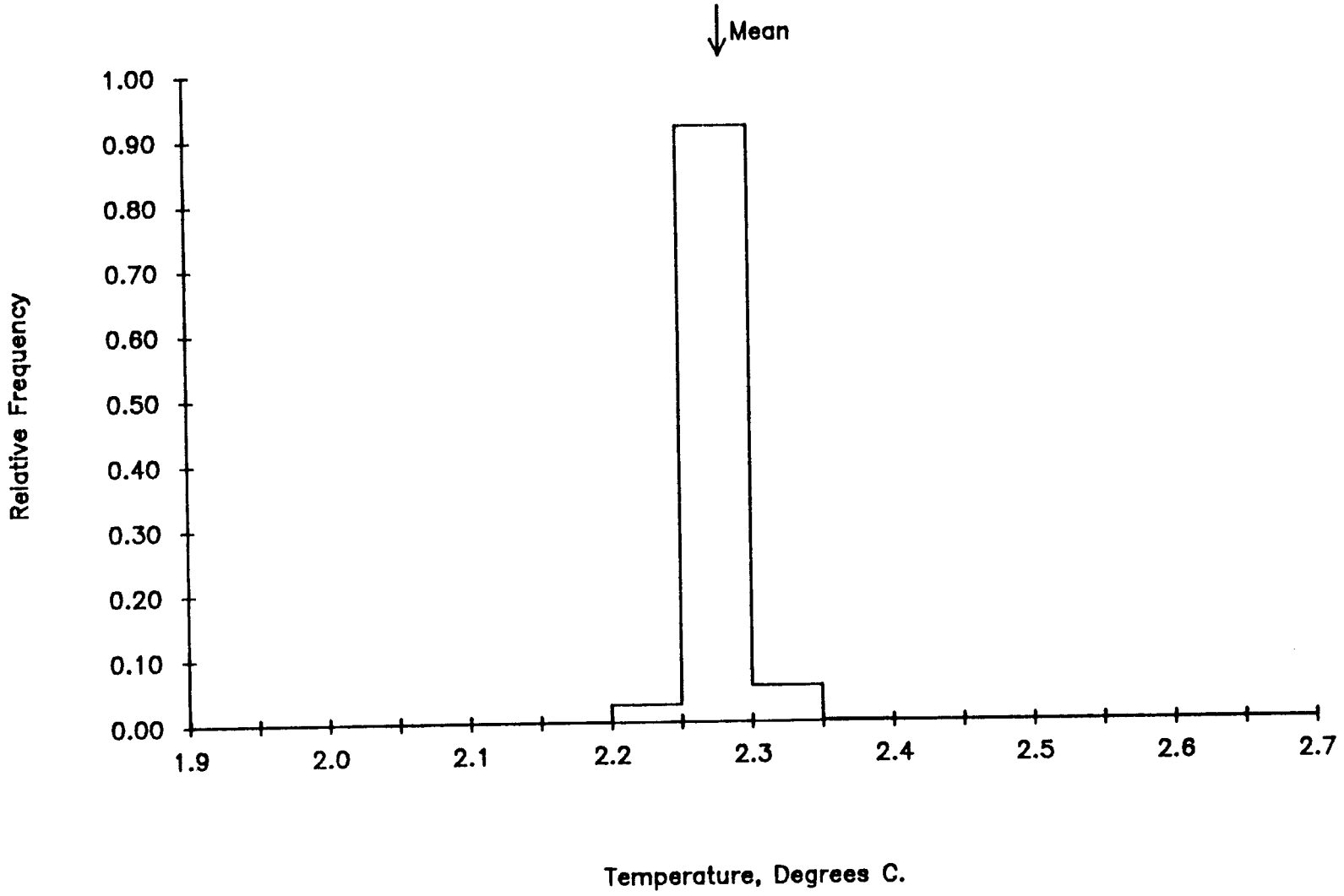

4800 M at Nares–II. 21 Sep 84 – 21 Nov 85. Tape 7161/3.

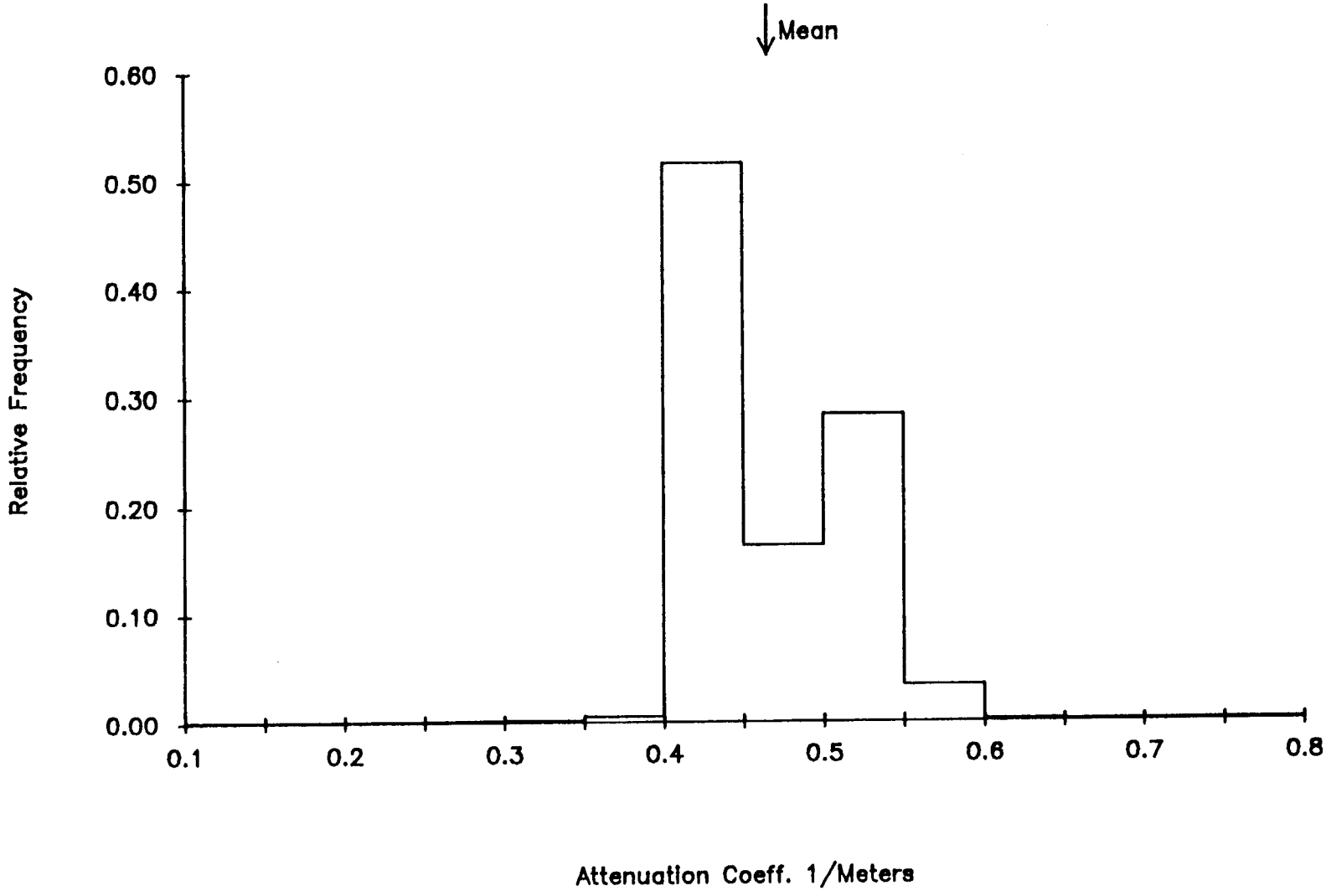

.P DATA AT NARES-II, 5800 METERS
LINE 1 THRU END OF FILE

	MEAN	SD	SKEWNESS	KURTOSIS	MIN	MAX	LENGTH
S	3.41	2.15	0.62	3.16	0.80	13.50	7827
U	-0.72	2.73	0.07	2.85	-8.60	8.10	7827
V	-0.42	2.85	-0.66	4.07	-13.30	7.60	7827
T	2.08	0.01	0.54	2.55	2.06	2.11	7827
A	0.45	0.04	0.25	2.07	0.36	0.54	7827

EDDY KE = 7.78 7827 POINTS

HEAT FLUX U = -0.01 7827 POINTS

HEAT FLUX V = -0.01 7827 POINTS

MOMENTUM FLUX = -0.65 7827 POINTS

.LLP DATA AT NARES-II, 5800 METERS
LINE 1 THRU END OF FILE

	MEAN	SD	SKEWNESS	KURTOSIS	MIN	MAX	LENGTH
U	-0.72	2.28	-0.07	2.46	-6.62	4.86	1296
V	-0.44	2.32	-1.15	5.07	-10.31	5.11	1296
T	2.08	0.01	0.75	2.67	2.06	2.10	1296
P	0.45	0.04	0.25	2.06	0.38	0.53	1296

EDDY KE = 5.29 1296 POINTS

HEAT FLUX U = -0.01 1296 POINTS

HEAT FLUX V = -0.01 1296 POINTS

MOMENTUM FLUX = -0.49 1296 POINTS

5800 Meters at Nares-II. 21 Sep 84 - 13 Aug 85. Tape 4921/15.

FIRST 5 LINES:

2100	21	9	84	0.8	63	0.7	0.3	2.10	0.0	0.381	1
2200	21	9	84	0.8	38	0.5	0.6	2.09	0.0	0.381	2
2300	21	9	84	0.8	78	0.7	0.2	2.09	0.0	0.381	3
0	22	9	84	0.8	71	0.7	0.2	2.09	0.0	0.381	4
100	22	9	84	0.8	93	0.7	0.0	2.09	0.0	0.381	5

LAST 5 LINES:

1900	13	8	85	7.3	345	-1.9	7.1	2.08	0.0	0.529	7823
2000	13	8	85	6.4	341	-2.1	6.0	2.08	0.0	0.529	7824
2100	13	8	85	5.8	343	-1.7	5.6	2.08	0.0	0.529	7825
2200	13	8	85	5.2	343	-1.5	5.0	2.08	0.0	0.529	7826
2300	13	8	85	4.9	350	-0.9	4.8	2.08	0.0	0.529	7827

	MIN	MEAN	MAX	SD	NUM
SPEED, CM/SEC	0.80	3.41	13.50	2.15	7827
U, CM/SEC	-8.60	-0.72	8.10	2.73	7827
V, CM/SEC	-13.30	-0.42	7.60	2.85	7827
TEMP, DEG C	2.06	2.08	2.11	0.01	7827
ATTEN. C. 1/M	0.36	0.45	0.54	0.04	7827

THIS RECORD IS SHORT DUE TO A LEAK WHICH DEVELOPED IN ONE OF THE TRANSMISSOMETER ELECTRICAL PASS THROUGHS. IT ALSO APPEARS THAT THE TRANSMISSOMETER UNDERWATER UNIT LEAKED AT DEPTH, WHICH MAY ACCOUNT FOR THE LARGE OFFSET IN ATTENUATION COEFFICIENT SEEN ON 15 MAR 85. NO CORRECTIONS WERE APPLIED TO PROCESSED ATTENUATION COEFFICIENT.

5800 M at Nares-II. 21 Sep 84 - 13 Aug 85. Tape 4921/15.

FREQUENCY TABLE FOR CURRENT SPEED

LOWER BOUND	UPPER BOUND	FREQUENCY	RELATIVE FR.
0.00	2.00	2322	0.296665
2.00	4.00	2510	0.320685
4.00	6.00	1996	0.255015
6.00	8.00	796	0.101699
8.00	10.00	158	0.020187
10.00	12.00	39	0.004983
12.00	14.00	6	0.000767
14.00	16.00	0	0.000000
16.00	18.00	0	0.000000
18.00	20.00	0	0.000000
20.00	22.00	0	0.000000
22.00	24.00	0	0.000000
24.00	26.00	0	0.000000
26.00	28.00	0	0.000000

MEAN	3.41260
STANDARD DEVIATION	2.15027

5800 M at Nares-II. 21 Sep 84 - 13 Aug 85. Tape 4921/15.

FREQUENCY TABLE FOR CURRENT DIRECTION

LOWER BOUND	UPPER BOUND	FREQUENCY	RELATIVE FR.
0	10	89	0.011371
10	20	105	0.013415
20	30	161	0.020570
30	40	147	0.018781
40	50	138	0.017631
50	60	161	0.020570
60	70	172	0.021975
70	80	170	0.021720
80	90	161	0.020570
90	100	163	0.020825
100	110	157	0.020059
110	120	157	0.020059
120	130	184	0.023508
130	140	174	0.022231
140	150	130	0.016609
150	160	188	0.024019
160	170	214	0.027341
170	180	232	0.029641
180	190	277	0.035390
190	200	284	0.036285
200	210	219	0.027980
210	220	231	0.029513
220	230	241	0.030791
230	240	245	0.031302
240	250	293	0.037435
250	260	329	0.042034
260	270	359	0.045867
270	280	408	0.052127
280	290	420	0.053660
290	300	417	0.053277
300	310	323	0.041267
310	320	232	0.029641
320	330	209	0.026702
330	340	173	0.022103
340	350	118	0.015076
350	360	146	0.018653

5800 M at Nares-II. 21 Sep 84 - 13 Aug 85. Tape 4921/15.

FREQUENCY TABLE FOR TEMPERATURE

LOWER BOUND	UPPER BOUND	FREQUENCY	RELATIVE FR.
1.70	1.75	0	0.000000
1.75	1.80	0	0.000000
1.80	1.85	0	0.000000
1.85	1.90	0	0.000000
1.90	1.95	0	0.000000
1.95	2.00	0	0.000000
2.00	2.05	0	0.000000
2.05	2.10	6782	0.866488
2.10	2.15	1045	0.133512
2.15	2.20	0	0.000000
2.20	2.25	0	0.000000
2.25	2.30	0	0.000000
2.30	2.35	0	0.000000
2.35	2.40	0	0.000000
2.40	2.45	0	0.000000
2.45	2.50	0	0.000000

MEAN	2.07959
STANDARD DEVIATION	0.01086

5800 M at Nares-II. 21 Sep 84 - 13 Aug 85. Tape 4921/15.

FREQUENCY TABLE FOR ATTENUATION COEFFICIENT

LOWER BOUND	UPPER BOUND	FREQUENCY	RELATIVE FR.
0.10	0.15	0	0.000000
0.15	0.20	0	0.000000
0.20	0.25	0	0.000000
0.25	0.30	0	0.000000
0.30	0.35	0	0.000000
0.35	0.40	1224	0.156382
0.40	0.45	2865	0.366041
0.45	0.50	2594	0.331417
0.50	0.55	1144	0.146161
0.55	0.60	0	0.000000
0.60	0.65	0	0.000000
0.65	0.70	0	0.000000
0.70	0.75	0	0.000000
0.75	0.80	0	0.000000

MEAN	0.44885
STANDARD DEVIATION	0.04082

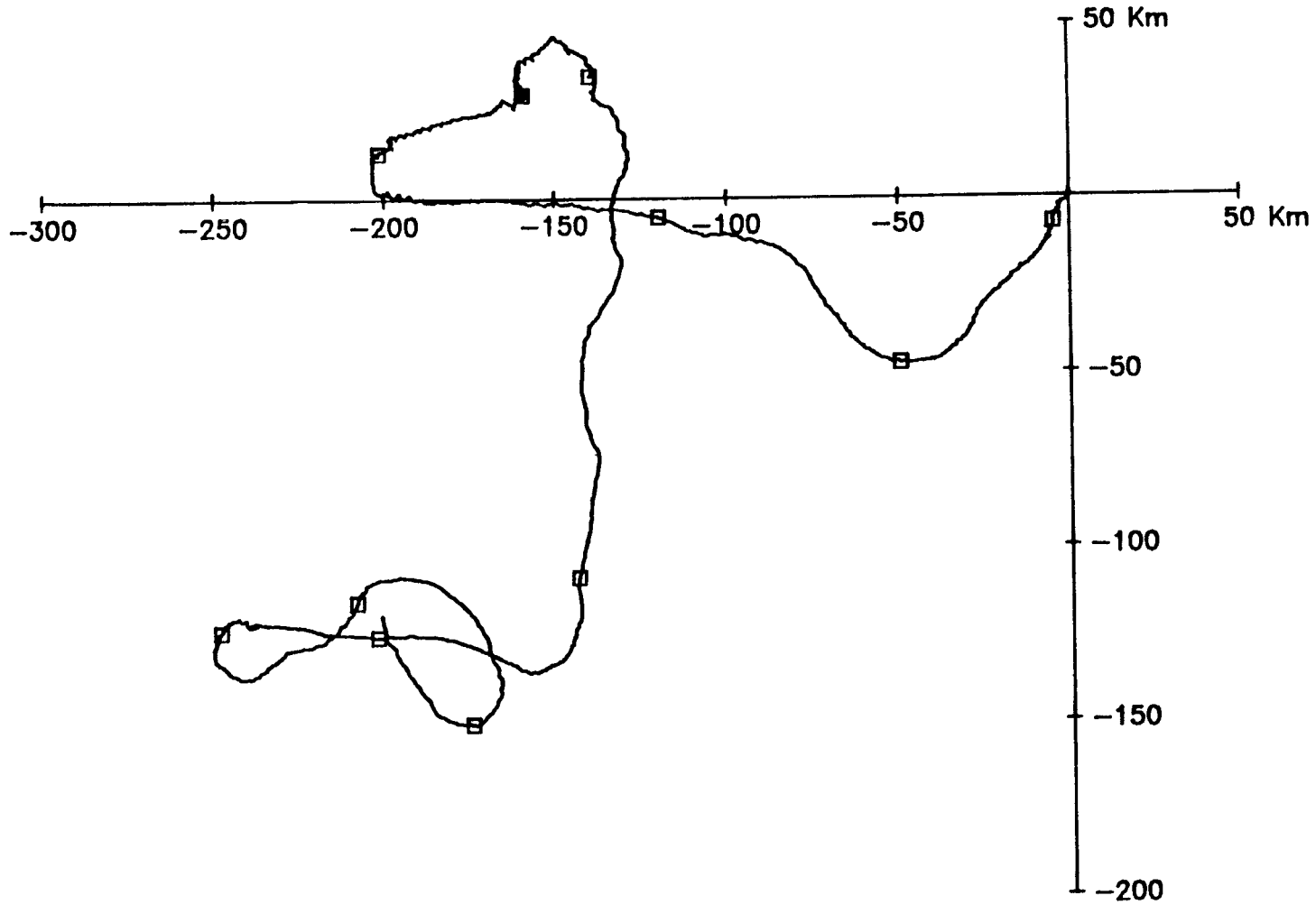

5800 M at Nares-II. 326.1 days starting 2100 21 Sep 84.

5800 M at Nares–II. 21 Sep 84 – 13 Aug 85. Tape 4921/15.

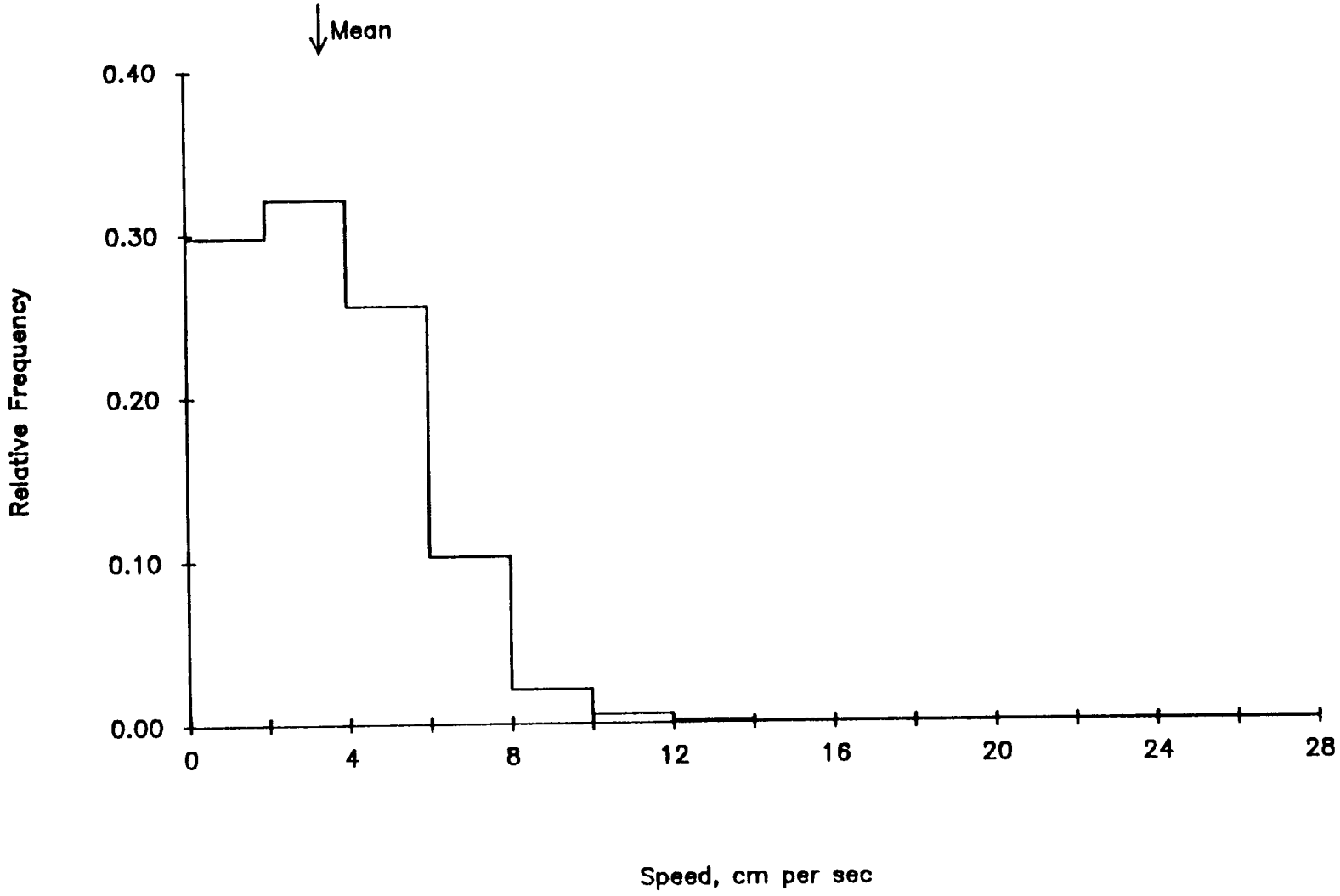

5800 M at Nares–II. 21 Sep 84 – 13 Aug 85. Tape 4921/15.

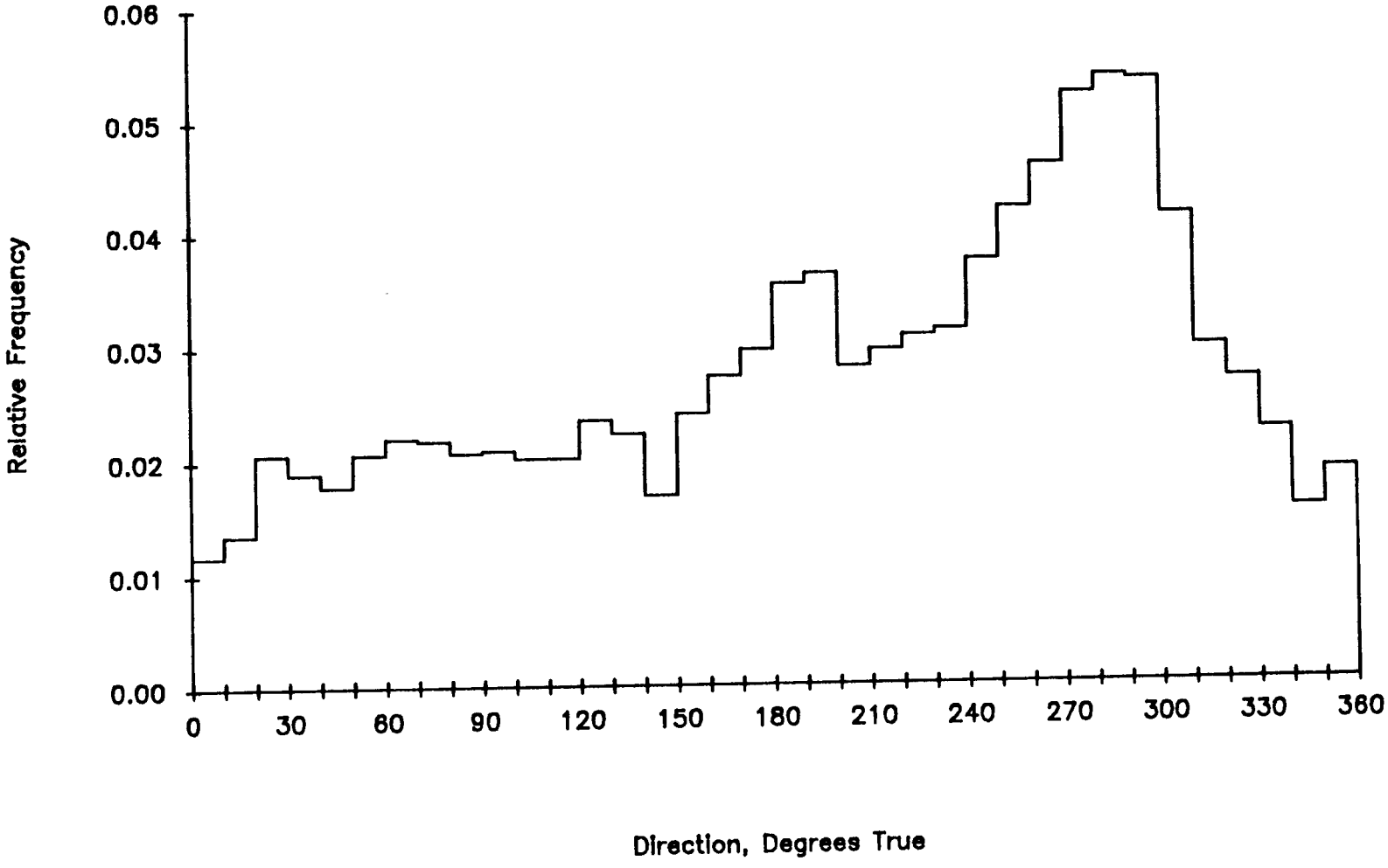

5800 M at Nares–II. 21 Sep 84 – 13 Aug 85. Tape 4921/15.

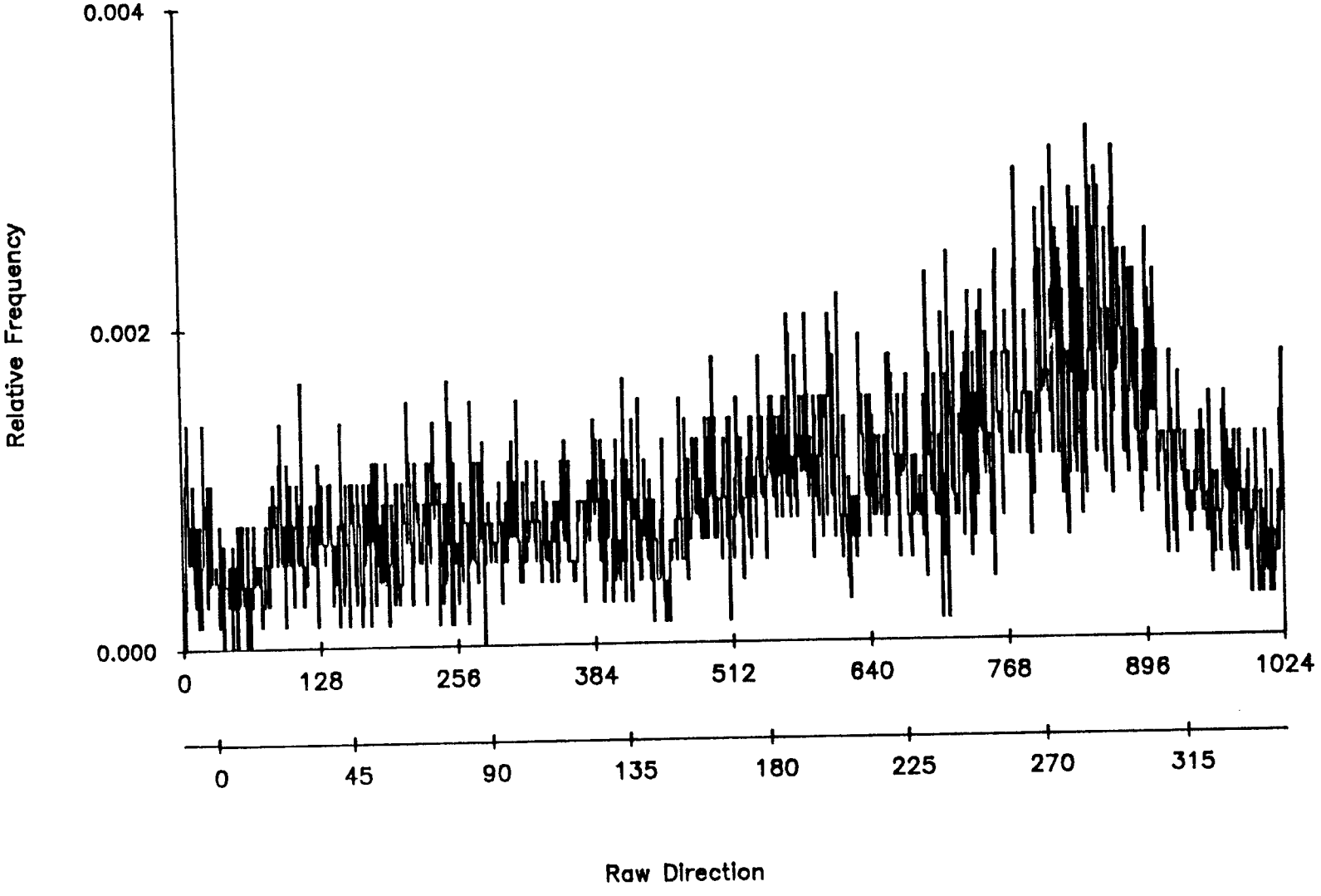

5800 M at Nares-II. 21 Sep 84 – 13 Aug 85. Tape 4921/15.

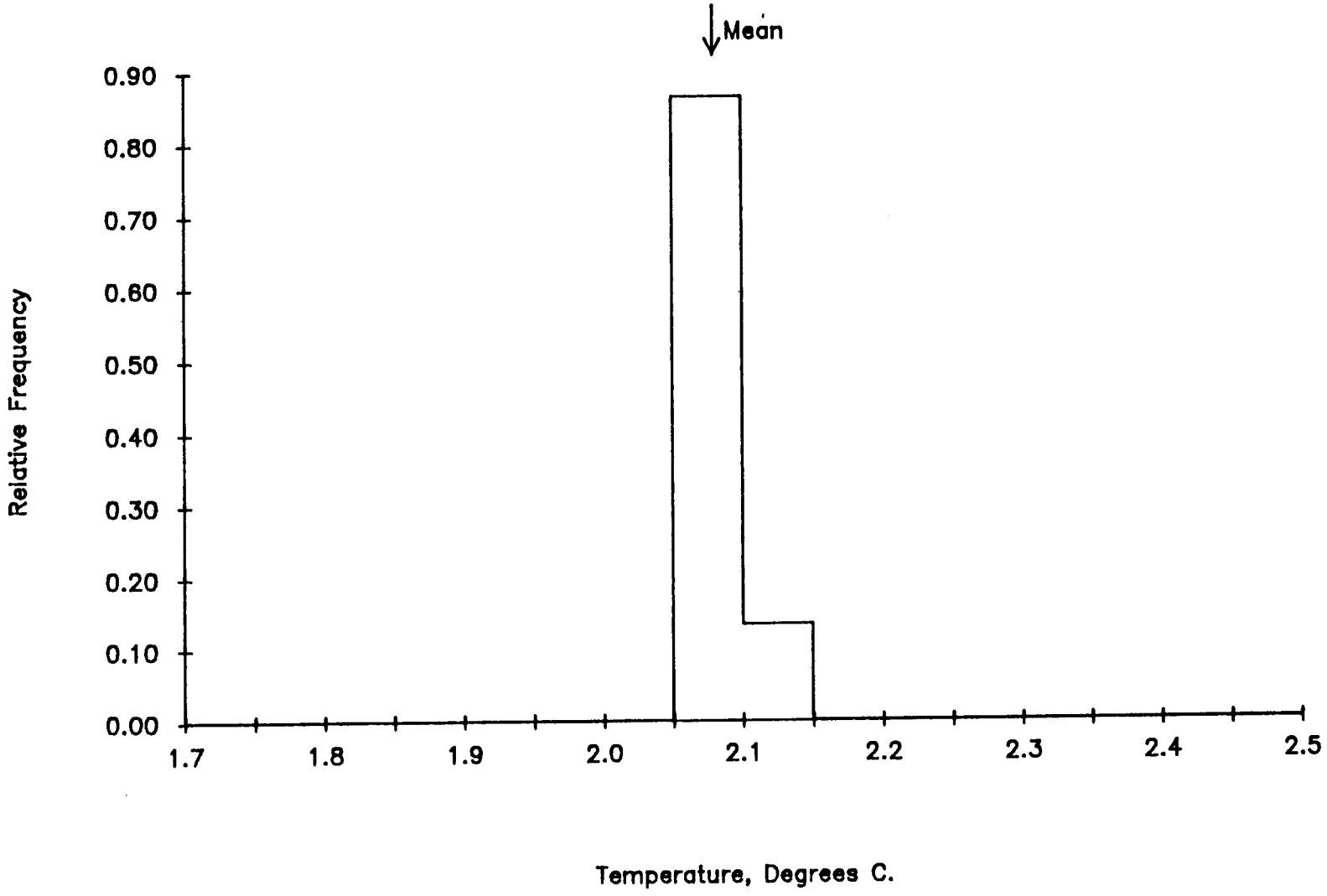

5800 M at Nares-II. 21 Sep 84 – 13 Aug 85. Tape 4921/15.

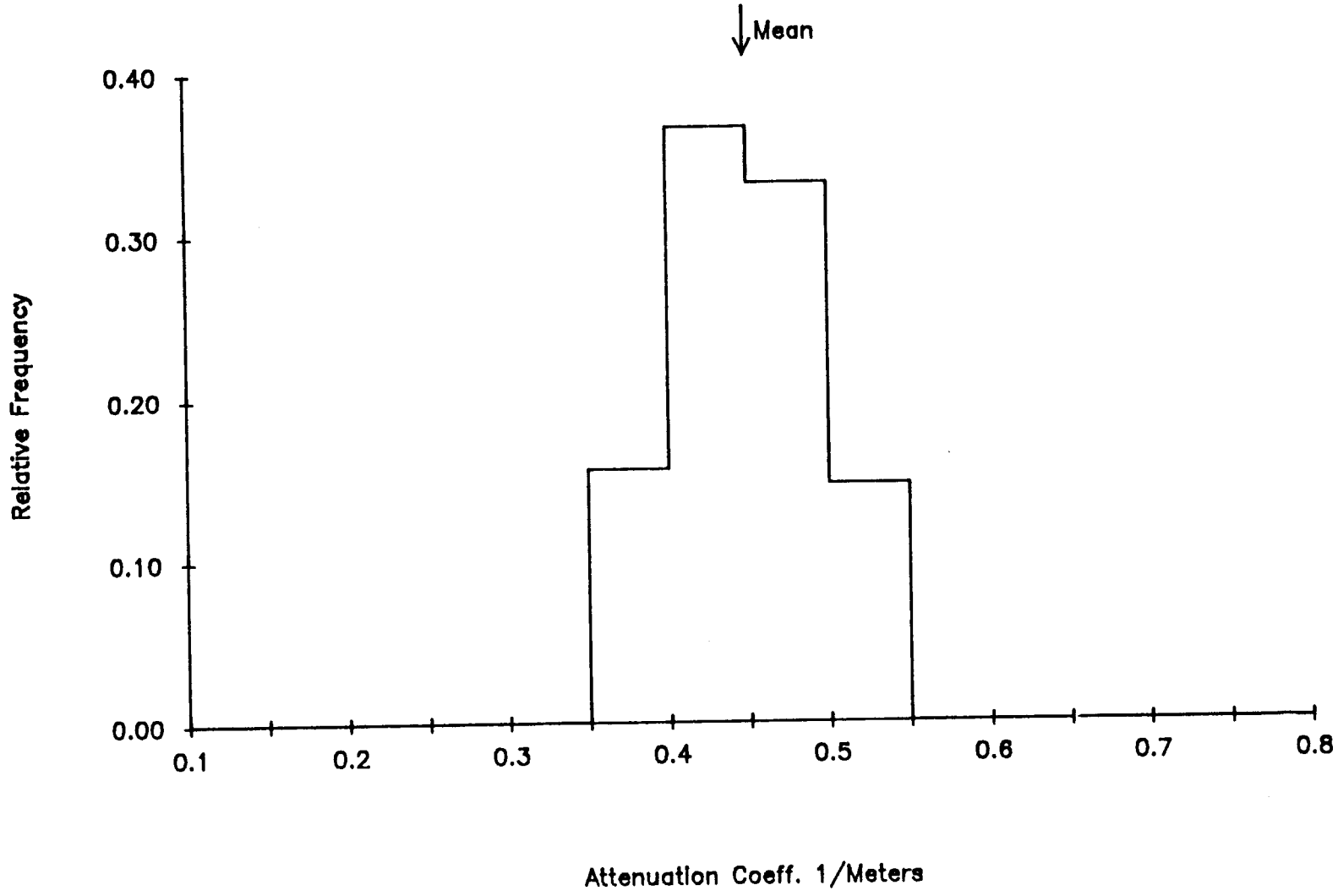

APPENDIX F

RADIOCHEMICAL STUDIES AT THE NARES ABYSSAL PLAIN:

FIELD STUDIES, NOVEMBER 15,

N. D. LIVINGSTON, L. D SUPPRENANT AND W. R. CLARKE

FINAL TECHNICAL REPORT

SUBSEABED DISPOSAL PROGRAM

CONTRACT 32-5713

with

Sandia National Laboratories

Albuquerque, New Mexico

Hugh D. Livingston, Lolita D. Surprenant and William R. Clarke

Woods Hole Oceanographic Institution

Woods Hole, Massachusetts 02543

September 1986

Nares Abyssal Plain Field Studies - November 1985

The decision to terminate the Subseabed Disposal Program occurred during our FY1986 research program. The impact of this decision for our laboratory was to restrict our activities to those involved with the 9-15 November 1985 cruise to the Nares Abyssal Plain on R/V ENDEAVOR - as outlined as Task 1 of the contract. This report is consequently limited to an account of the sample collection activities on this cruise and does not include any shore-based analytical results - since these analyses were postponed indefinitely because of the termination decision.

The objectives of our laboratory on this cruise were as follows:

1) To deploy and test newly developed wire-deployed in-situ pumping systems for particle and soluble actinide collection.

2) To test and evaluate the performance of different filters and chemisorber systems (for both actinide and cesium isotope collection).

3) To collect a series of samples at different depths to obtain more detailed information on the distribution of fallout radionuclides at depths not sampled in 1984 - to enable more definition of various features of the profiles.

4) To deploy prototype passive chemical monitors (PCM) on the Nares-3 mooring set by the Oregon State University group.

We were more fortunate than other cruise participants in that we were able to realize a major fraction of these objectives on ENDEAVOR-137. The cruise was made especially difficult because of the bad weather encountered which prevented deployment of the mooring on our leg and made the gear deployment and recovery more difficult. The loss of the CTD package, while disastrous for that program itself, only meant a loss of a supporting hydrographic data set for our samples - but we have the data collected in 1984 at the Nares site - so the major hydrographic characteristics are well described (assuming inter-annual differences are not present).

1. Test Deployments of New In-Situ Pumps

Only two of four new pumps were ready for testing on this cruise - the remainer of the in-situ pumping program was completed using three pumps of an older design. The new pumps are lighter, more stable, easier to move and secure, and offer greater access for installation of plumbing fixtures, filter housings, flow-meters, etc. The start and stop controls of the new pumps were activated by built-in electronic timers - instead of the separate pinger/timer controls in the older design. After some teething problems, these functioned well and represent a significant improvement over the older design in respect to flexibility and precision. There were some handling problems with the new pumps related to deploying them on 1/2" wire in bad weather. We expect that some minor modifications to the techniques used to rig the equipment as it is hung on the wire will be able to eliminate the problems encountered. The

deepest sample collected on the cruise, 5720m (Table 1), was collected with a pump in the new design. The volume pumped (1972 liters) and flow-rate (8.2 liters/minute) were the highest subsurface values obtained on this cruise. We are satisfied that the new design performed properly in the field and that the new series of four such pumps extends the overall sampling capability by this method.

2. Filters and chemisorbers

Three types of filters were used on this cruise. They were:

a) Polypropylene wound-fiber filter cartridges (1μm)-(POLY)

b) Cotton wound-fiber filter cartridges (1μm)-(COTTON)

c) Thin Sheet Membrane Cartridges (9.6μm)-(TSM)

The two wound-fiber cartridges are the same nominal pore size. Previous work had suggested that the cotton filters collected a higher fraction of the total concentration of radionuclides at any given depth. Filters were deployed at different depths and in various combinations (Table 1) to be able to assess the effect of the filter used on the nuclide partition observed between the dissolved and particulate phases. One issue which was of particular interest was the following: It is possible that the higher particulate radionuclide fraction collected by the cotton filters was not simply a result of more efficient collection of the particulate phase. It may be that the reason for the extra activity collected by the cotton filter was by direct absorption from the dissolved phase. The cotton fibers themselves may act as absorbers or the residual dust or soil particles entrained in the fiber may be active surfaces.

Finally, one surface sample was collected using a thin sheet membrane filter. These filters are supposed to be both inert (with respect to absorption properties) and highly effective in collection of small particles by filtration at high flow-rates and volumes. The limited time and weather conditions prevented us from collection of additional subsurface filter samples using this type filter.

Four types of MnO_2 absorbers were used. These were used as shown in Table 1. They were as follows: polypropylene cartridges impregnated with MnO_2 as used in 1984 (POLY); the same absorber but prepared without removing the anti-wetting agent - a tedious, time-consuming process (POLY-no-prefx); cotton filters loaded with pre-formed MnO_2 at sea; and polyurethane foam plugs (2" X 1.5") impregnated by soaking in saturated $KMnO_4$ solutions for 5 minutes.

All of these varieties were designed to optimize actinide collection in one way or another. The use of the filters prepared without removal of the anti-wetting agent was simply an operational convenience. The cotton absorbers were used to discover their effectiveness in collection of Pu - as appeared to have been observed in work in the Pacific. However, the form of fallout Pu may not be the same in the Atlantic and Pacific so it was considered necessary

Two manuscripts have been prepared for submission for publication. They are as follows:

1. Livingston, H. D. and J. K. Cochran, 1986. Determination of transuranic and thorium isotopes in ocean water: in solution and in filterable particles. J. Radioanal. Nucl. Chem., submitted.

2. Cochran, J. K., H. D. Livingston, D. J. Hirschberg and L. D. Surprenant, 1986. Natural (^{232}Th, ^{230}Th and ^{228}Th) and anthropogenic (^{239,240}Pu, ^{241}Am) distributions in the Northwest Atlantic. Earth Planet. Sci. Lett., to be submitted.

A copy of the first manuscript is attached to this report, and a copy of the second one will be forwarded when the final version for submittal is completed.

EN137 TABLE 1

DEPTH (METERS)	VOLUME (LITERS)	RATE (L/min.)	PF	MnO2	Cs	CAST	PUMP #
3	2574.2	8.6	TSM	Cotton	Yes	S-1	Ship's SW Supply
3	3350.5	9.8	POLY+ Cotton+	POLY	No	S-2	" " "
3	1319.1	4.2	POLY	FOAM++	No	S-3	" " "
3	1050.3	5.5	Cotton	POLY- no-prefx***	No	S-4	" " "
3	1179.0	2.9	POLY	FOAM++	No	S-5	" " "
350	26.5	.2	POLY	POLY	Yes	1	5
460	828.9	2.8	POLY	FOAM++	Yes	2	3
550	1584.8	5.3	POLY+ Cotton+	POLY	No	2	2
560	221.8	.7	Cotton	Cotton	No	2	1
660	1738.1	5.8	POLY+ Cotton+	POLY	No	4	2
1250	1958.7	6.5	POLY	POLY	No	4	1
3500	617.7	>2.1*	POLY	FOAM++	Yes	4	3
5720**	1972.4	8.2	POLY	POLY	Yes	3	5

*: pump un-plugged during cast, pumping time uncertain.
**: depth determined acoustically, others by wire out.
***: anti wetting agent not removed.
+: two filters in series, poly first.
++: Polyurathane foam.

to test this at the Nares site. A trade-off with the use of the impregnated cotton cartridges is that although they may be more efficient at Pu collection, they contain high Th blanks which limits their usefulness when Th is being measured simultaneously with transuranics. The polyurethane foam plugs are very easy to prepare - so if they were effective in actinide collection, they would represent a substantial savings in time spent in preparing the absorbers for use at sea.

The final new type of absorber tested was a cesium isotope collector. Although copper ferrocyanide has been used in various ways to absorb cesium from seawater, it has never been used on filter cartridges. This offered potential for high flow-rate absorption performance because of the high surface areas available. The copper ferrocyanide was prepared by filtering it after precipitation from mixing solutions of copper sulfate and potassium ferrocyanide. The filter cartridge used was the polypropylene wound-fiber type. It was found that it was necessary to dry the cartridge at 80°C for the precipitate to be retained when seawater was passed through it. Although we expect that these cartridges would function fairly well in terms of Cs collection, we have subsequently refined and improved these techniques. We now use a cotton filter cartrige as a matrix which we find to retain the precipitate more effectively and leads to higher collection efficiences. Another advantage of this matrix is that it does not deform during drying. This problem sometimes led to mechanical losses in absorbers of the polypropylene type. The current stage of development of these absorbers is such that volumes up to about 3000 liters may be processed before the absorber becomes saturated. During processing, at flow-rates up to 6 liters per minute, the efficiency of cesium collection decreases from an initial value around 90% to about 60% after 2000 liters have been processed.

3. Additional Depth Sampling at Nares

Some additional depths were sampled on this cruise to add to the detail obtained from the 1984 cruise. Five depths in the range 350-660m were the most concentrated detail. In addition, the 1250m sample would help define the fallout maximum noted at 1500m in 1984. Finally, two deep samples were obtained. These samples were expected to be especially valuable in respect of confirming the presence of a deep ^{137}Cs tracer signal. This is an important indication of advective ventilation of the deep water. Because of the very large volumes processed through the new style cesium collectors, this signal should be measurable with confidence and precision. It had been our hope to collect almost three times as many samples from various depths at Nares. However, the combination of bad weather, pump malfunctions, and handling constraints lead to many fewer samples being collected than planned.

4. Passive Chemical Monitors (PCMs)

The basic concept of passive chemical monitoring is to devise a chemical matrix which can be deployed in the ocean at a position where potential radiation leaks from waste disposal operations might occur. Generally such locations might be monitored on infrequent research cruises to the site. If suit-

able PCM's are developed which collect specific nuclides slowly from the dissolved phase of seawater, they could potentially detect episodic releases which might be missed on periodic monitoring cruises. In effect, they would provide an integrated record over time of the ambient levels of the nuclides being monitored. The uptake of specific species would be normalized to a naturally present species in the local environment which also was collected by the PCM. The type of PCM tested at Nares is a sheet of polyurethane foam impregnated with MnO_2 (by a technique similar to that described above for the polyurethane filter plugs). Manganese dioxide can collect a range of metals with high particle reactivities - including the lanthanides and actinides. The idea is that ^{230}Th can be used to monitor the volume of water processed by the PCM - since its ambient concentration is measurable. Other species detected by the PCM would then be measured relative to ^{230}Th - after suitable correction for differential rates of uptake by different radioelements. At the Nares site we intended to test this concept throughout the water column using ^{230}Th and ^{241}Am to demonstrate feasability. From our 1984 studies, we know the distributions of both nuclides throughout the water column. We would use the amount of ^{230}Th collected by the PCM to convert the ^{241}Am collected to a concentration value. This in turn can be compared with the expected value from our previous studies.

Seven PCMs were attached to the NARES-3 mooring at depths ranging from 750m to 5796m. The positions on the mooring are shown in Figure 1. It was our intention to analyze these samples following the eventual recovery of the mooring. Presently the collapse of the program has made the recovery plans uncertain and the future of this study cloudy. We plan on storing the samples until new funding can be raised to continue this work.

Publications and Presentations

Ironically, the program has stopped at a time when we had just begun to present some of the results of our actinide scavenging studies at meetings and in the scientific literature. There are many unanswered questions and additional measurements required and, in addition, several papers which can be written on the basis of the work completed so far.

The methodology of actinide collection and particle partition determination has been presented at two meetings in 1986. These were as follows:

1. American Geophysical Union - Ocean Sciences Meeting, New Orleans, LA (February 1986): Livingston, H. D., J. K. Cochran, L. D. Surprenant and D. J. Hirschberg, 1985. Actinide distributions and particle associations in the North American Basin. Eos 66(51): 1293.

2. International Conference on "Low-Level Measurements of Actinides and Long-Lived Radionuclides in Biological and Environmental Samples," Lund, Sweden (June 1986): Livingston, H. D. and J. K. Cochran, 1986. Determination of transuranics and thorium isotopes in ocean water: in solution and in filterable and sinking particles.

Abstracts of these papers are attached to this report.

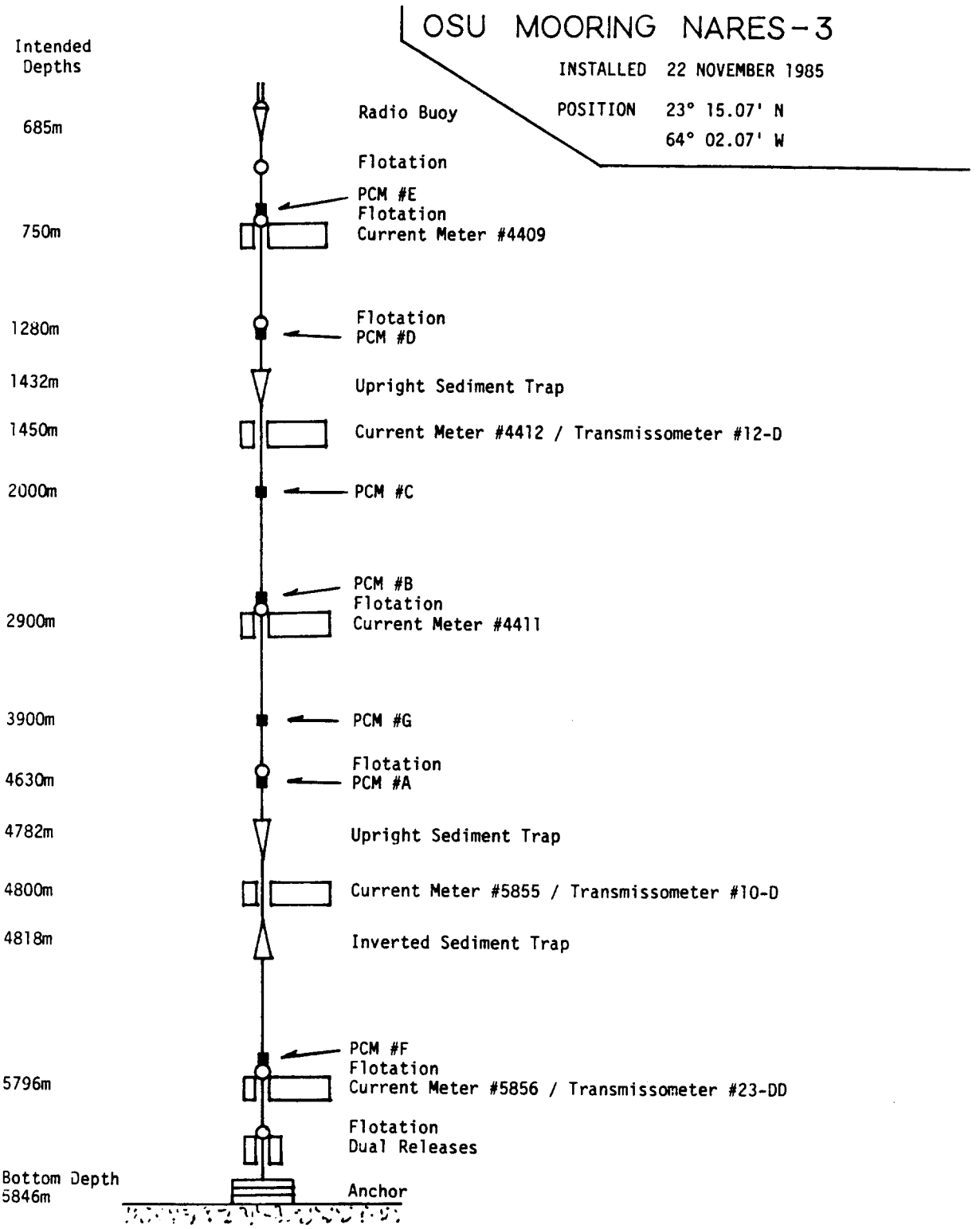
OSU MOORING NARES-3
INSTALLED 22 NOVEMBER 1985
POSITION 23° 15.07' N
64° 02.07' W
Intended Depths
685m
Radio Buoy
Flotation
750m
PCM #E
Flotation
Current Meter #4409
1280m
Flotation
PCM #D
1432m
Upright Sediment Trap
1450m
Current Meter #4412 / Transmissometer #12-D
2000m
PCM #C
2900m
PCM #B
Flotation
Current Meter #4411
3900m
PCM #G
4630m
Flotation
PCM #A
4782m
Upright Sediment Trap
4800m
Current Meter #5855 / Transmissometer #10-D
4818m
Inverted Sediment Trap
5796m
PCM #F
Flotation
Current Meter #5856 / Transmissometer #23-DD
Flotation
Dual Releases
Bottom Depth
5846m
Anchor

LOW-LEVEL MEASUREMENTS OF ACTINIDES AND LONG-LIVED RADIONUCLIDES IN BIOLOGICAL AND ENVIRONMENTAL SAMPLES

LUND, SWEDEN
JUNE 9-13, 1986

ORGANIZED BY:

RADIOBIOLOGY DIVISION
UNIVERSITY OF UTAH, U.S.A.

DEPARTMENT OF RADIATION PHYSICS
UNIVERSITY OF LUND, SWEDEN

HEALTH, SAFETY, AND ENVIRONMENT DIVISION
LOS ALAMOS NATIONAL LABORATORY, U.S.A.

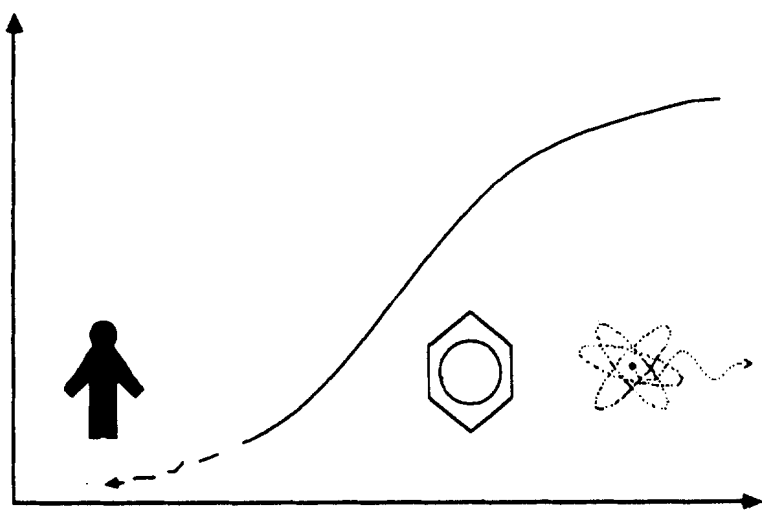

SPONSORED BY:

NATIONAL INSTITUTE OF RADIATION PROTECTION
STOCKHOLM, SWEDEN

SWEDISH NATIONAL SCIENCE RESEARCH COUNCIL

U.S. ENVIRONMENTAL PROTECTION AGENCY

U.S. DEPARTMENT OF ENERGY

21. Determination of Transuranic and Thorium Isotopes in Ocean Water: in Solution and in Filterable and Sinking Particles.

H.D. Livingston and J.K. Cochran

Woods Hole Oceanographic Institution
Woods Hole, MA 02543 (U.S.A.)

Studies on the oceanic distribution of the actinides are often limited, particularly in the deep ocean, by analytical limitations in the determination of the very low concentrations present. This problem is exacerbated when actinide partition is measured between dissolved and particle-associated phases. Techniques of higher analytical sensitivity or sampling developments which substantially increase the amounts of actinides available for analysis yield improvements in the quality of such measurements. We describe recent sampling techniques which have permitted high-quality determination of actinide concentrations in Atlantic Ocean waters, at depths down to about 6000 m, in both soluble phases: suspended particulate phases; and large-settling particle phases.

The actinides represented include the natural series isotopes ^{228}Th, ^{230}Th, and ^{232}Th, and the fallout transuranics $^{239,240}Pu$ and ^{241}Am. We sampled dissolved and suspended particle phases using wire-mounted electrical pumping systems which have processed samples of up to 4000 liters, at flow rates of 7 liters per minute. The suspended particles were first removed by filtration through 1μm wound polypropylene-fiber cartridges. Thorium and Am isotopes were then collected by absorption from the filtrate on two MnO_2-coated fiber cartridges in series. We collected large-settling particles at four sequential intervals annually in 0.5 m^2 diameter sediment traps deployed at various depths. Analyses of the actinide content of this material provided data on the fluxes of each actinide delivered to the deep ocean on large sinking particles.

This paper presents data from various locations in the Western North Atlantic which demonstrate the effectiveness of the sampling techniques in the development of a meaningful data set. The data speak to the nature of the processes which control the movement of these nuclides in the ocean, including physical mixing processes, and those which involve geochemical scavenging and vertical transport in association with oceanic particles.

Actinide Distributions and Particle Associations in the North American Basin

H. D. Livingston,[1] J. K. Cochran,[2] L. D. Surprenant,[1] and D. J. Hirschberg[2]

ABSTRACT

Distributions of reactive actinides have been measured in solution, suspended particles, settling particles and sediments at the Hatteras and Nares Abyssal Plains. The data permit a comparison of transient and steady state particle tracer distributions - fallout transuranics and Th isotopes respectively. We discuss data from water column samples collected by 1) in situ pumps which filtered 1000-2000 ℓ through 1 μm wound-fiber cartridge prefilters ("particulate"), then two MnO_2 coated fiber cartridges in series ("dissolved") and 2) Niskin bottles ("total"). Radiochemical analyses showed that each MnO_2 cartridge absorbed Th and ^{241}Am (but not Pu) efficiently (~83%) at flow rates up to 7 ℓ/min. The distributions of fallout Pu and ^{241}Am reflect transport primarily by physical processes of ventilation (traced here by ^{137}Cs) despite significant transport in association with settling particles. The major fraction of fallout transuranics is still at depths shallower than 2000 m. Th isotope distributions result from their differing modes of input or production and the net effects of scavenging. ^{228}Th concentrations reflect the distribution of ^{228}Ra and are highest in near-surface and near-bottom waters; ^{230}Th is relatively more depleted in the upper ocean with values increasing to 0.8 dpm/1000 ℓ towards the bottom; ^{232}Th activities are controlled by the concentrations of suspended particles. Amongst the factors which affect the partition of these actinides between "particulate" and "dissolved" phases of the water column are 1) chemical reactivity, 2) half-life 3) concentration of suspended particles. The particle association characteristics observed for these actinide tracers show increasing particle reactivities (as percentage filterable) lying in the ranges; Pu: 0.3-1.6, ^{241}Am: 5-11, ^{228}Th: 2-26, ^{230}Th: 5-40, ^{232}Th: 11-100.

Eos 66(51): 1293 (1985)

APPENDIX G

NARES ABYSSAL PLAIN SEDIMENT FLUX STUDIES,

FY 1986 ANNUAL REPORT, J. DYMOND AND R. W. COLLIER

1986 ANNUAL REPORT
SUBSEABED DISPOSAL PROGRAM

SUMMARY OF FIELD ACTIVITIES AND SAMPLES COLLECTED

Contract 32-5716

with

Sandia National Laboratories

Albuquerque, New Mexico

Jack Dymond and Robert W. Collier
College of Oceanography
Oregon State University
Corvallis, OR 97331

May, 1986

NARES ABYSSAL PLAIN SEDIMENT FLUX STUDIES

Mooring NAP-2.

On 21 September, 1984, a mooring ("NAP-2") was deployed at 23°14.5'N, 64°02.1'W with an approximate bottom depth of 5835 meters. This mooring contained 6 upward looking traps (@ 720, 1420, 2870, 3785, 4770, 5780 meters) and two inverted traps (@ 2900 and 4800 meters). This mooring was successfully recovered on 21 November, 1985. The details of this recovery and the samples are given below.

Mooring NAP-3.

On 22 November, 1985, another shorter trap mooring ("NAP-3") was deployed. The mooring was similar in design to NAP-1 and has two normal traps at 750 and 4800 meters and an inverted trap at 4830 meters.

Recovery results from NAP-2.

The NAP-2 mooring was deployed from the R/V Endeavor on 21 September, 1984. This was on of the most detailed moorings ever deployed and its recovery and instrument performance were very good. The mooring was in the water for 426 days. The following table summarizes the timer settings and recovery notes:

cup#	start date	total days
1	9/21/84, 8/30/85	7 + 83 = 90
2	9/28/84	84
3	12/21/84	84
4	3/15/85	84
5	6/7/85	84

(recovered 21 November, 1985.)

Recovery Notes - NAP-2

720 meters	(recovery normal, timer worked)
1420	(recovery normal, timer worked)
2820	(recovery normal, timer worked)
2900 [inv.]	(cup 1 washed out on recovery, timer worked)
3785	(changer failed, open to cup 2, bulk sample)
4770	(recovery normal, timer worked)
4800 [inv]	(cup 1 washed out on recovery, timer worked)
5780	(changer failed when timer flooded, open to cup 2, bulk sample)

All samples are currently located at the OSU Core Lab in an unprocessed, unsplit form. We hope to be able to do basic processing work ASAP to stabilize these valuable samples. As always, we will make splits and data available to other investigators as time and funds permit.

APPENDIX H

RADIOCHEMICAL STUDIES AT THE NARES ABYSSAL PLAIN: NATURAL RADIONUCLIDE RESORTS

J. K. Cochran, O. J. Hirshbert and Mark Dornblaser

1986

Final Report

Sandia Contract 32-5712

Radiochemical Studies at the Nares Abyssal Plain: Natural Radionuclide Results

J. Kirk Cochran, David J. Hirschberg
and Mark Dornblaser

Marine Sciences Research Center
State University of New York
Stony Brook, New York 11794-5000

Contents

I. Introduction

This report describes work accomplished during FY 85 on samples of sea water and bottom sediments collected at the Nares Abyssal Plain. We participated in the November 1985 cruise (EN-137) aboard the R/V ENDEAVOR to the Nares Abyssal Plain. Water samples were collected by in situ pump and by hydrocast. The former were taken for analysis of Th isotopes, Pu and ^{241}Am, but the analyses have not been carried out this year due to reductions in funding. The hydrocast samples were taken for in situ radon, and the initial analyses were made aboard the ship. Details on the collection and analysis of samples from the cruise are given in Section II.

Sediment studies completed this year involved samples collected in September, 1984 aboard the R/V ENDEAVOR (EN-121) and in February, 1984 by the R/V TYRO. This work forms the bulk of a Master's thesis by Mark Dornblaser. The results are summarized in Section III and the thesis manuscript is included as Appendix A.

Two manuscripts have been prepared this year in collaboration with Dr. Hugh Livingston. The first involves the details of the in situ pumping and subsequent laboratory analyses and has been submitted to the Journal of Radioanalytical and Nuclear Chemistry. This manuscript is included as Appendix B. The second manuscript describes the initial pump results at Nares. We expect to submit it during Fall, 1986, to Earth and Planetary Science Letters.

II. Cruise Report EN-137, San Juan to San Juan, Puerto Rico

Geochemical sampling during R/V ENDEAVOR Cruise EN-137 consisted of in situ pumping, deployments of passive chemical monitors (PCM's) on OSU moorings and water casts for bottom radon. Personnel for Leg I included K. Cochran (SUNY), D. Hirschberg (SUNY), L. Surprenant (WHOI) and W. Clarke (WHOI). Mr. Hirschberg remained on board for Leg II. The original cruise plan called for all geochemistry to be accomplished during Leg I. Severe weather forced the PCM deployments and radon casts to be moved to Leg II and reduced the number of pump samples taken on Leg I. This report details the in situ pumping and radon casts.

A. In Situ Pumps

The in situ pumps sample large volumes of sea water for reactive chemical species, particularly the Th isotopes, Pu and ^{241}Am. Sea water is pumped through a cartridge prefilter to separate the particles, then through chemically treated cartridges which extract dissolved radionuclides from solution. Our goals for the pumping were 1) to compare the retention of particles on membrane and cotton and polypropylene wound fiber prefilters, 2) to assess the efficiency of extraction of Pu from solution onto different manganese oxide substrates and at different flow rates and 3) to add to the pumping system a cartridge designed to scavenge dissolved ^{137}Cs. Table 1 lists the samples recovered on four pump casts at Nares.

B. Passive chemical monitors (PCM's)

These are rectangular pieces of polypropylene foam which have been soaked in a hot $KMnO_4$ solution to coat them with MnO_2. They are designed to passively adsorb radionuclides from sea water during their deployment. Analysis of the foam after retrieval permits assessment of nuclide concentrations and activity ratios. For cruise EN-137, PCM's were prepared in Dr. Hugh Livingston's laboratory and were deployed on the current meter/sediment trap mooring set out during Leg II. Figure 1 shows the depths of deployment. At the time of this report, the mooring remains deployed and no PCM analyses have been made.

C. Radon casts

Radon sampling was originally planned using 10 liter Niskin bottles on the CTD. The loss of this instrument and the rough weather on Leg I forced us to reschedule the radon casts for Leg II and to use 30 liter Niskin bottles hung on the hydrowire. Two such hydrocasts were made, emphasizing sampling in the bottom ~400 meters. A CTD cast using 5 liter bottles was made in the bottom 1000 meters and bottles were combined to make 10-15 liter samples. Table 2 lists samples taken for radon.

Subsequent inspection of the radon and nutrient data revealed that cast 1 had pre-tripped near the bottom, but not in the bottom 100 meters as intended. Because temperature data were limited, we do not know the precise depths of these samples.

Initial radon extractions were performed on board the ship by circulating He through the samples. The radon was stripped from solution, collected on charcoal and subsequently transferred to a scintilation cell for counting. A few of the water samples were returned to the laboratory for ^{226}Ra analysis. ^{222}Rn and ^{226}Ra were allowed to reach secular equilibrium, and the radon was extracted and counted following the procedure outlined above. The blank-corrected data are given in Table 3. Excess ^{222}Rn is evident in the bottom 150 m and Figure 2 shows the profile. Samples from cast 1 are excluded from Table 3 because the cast pre-tripped. Because casts 2 and 3 were designed to sample higher in the water column, data coverage is not the optimium in the bottom 100 m. Nevertheless, a trend of increasing excess ^{222}Rn is seen toward the sea floor, and the values agree well with previous TTO measurements.

Figure 3 shows a semi-log plot of excess ^{222}Rn vs. depth above the bottom. From such a plot, it is possible to calculate the vertical eddy diffusion coefficient. The approach taken assumes that, in steady state, mixing is balanced by radioactive decay:

$$K_z \frac{\partial^2 C}{\partial z^2} - \lambda C = 0 \qquad (1)$$

The solution to eq (1) is

$$C = C_o \exp\left[-\left(\frac{\lambda}{K_z}\right)^{1/2} z\right] \qquad (2)$$

Where C = activity of excess ^{222}Rn at depth z
C_o = activity of excess ^{222}Rn at the sea floor
λ = decay constant for ^{222}Rn
K_z = vertical eddy diffusion coefficient
z = depth above the bottom.

Applying eq (2) to the data in Figure 2 gives a value for K_z of 39 cm^2/sec. In comparison, values calculated for TTO stations 20, 22 and 24 range from 5 to 73 cm^2/sec. Station 24 corresponds to the Nares-1 site and the value of 73 cm^2/sec is similar to that of 39 cm^2/sec measured here. It should be kept in mind that ^{222}Rn reaches a steady state in about two weeks and there may be significant temporal changes in eddy diffusion when profiles are measured years apart.

III. Sediment Studies

Sediment studies which were begun last year and have been completed this year have focused on 1) the chronologies of particle mixing by organisms and accumulation of Nares sediments and 2) the construction of radionuclide mass balances. This work forms the basis of the Master's thesis of Mr. Mark Dornblaser and is attached as Appendix A. This section summarizes briefly the results of that study.

Additional analyses of ^{210}Pb and ^{226}Ra were made on box core subcores collected by the R/V TYRO in February, 1984. Previous analyses of these cores indicate that excess ^{210}Pb decreases rapidly below the sediment-water interface and the additional results presented in Appendix A confirm this pattern; ^{210}Pb and ^{226}Ra appear to be in equilibrium by 4-5 cm depth in the cores. Particle mixing coefficients have been calculated from the new data and the range of values, .01-.17 cm^2/y, remains near the low end for deep-sea sediments.

Radiochemical and other solid phase analyses (bulk density, Fe, Mn content) were made on gravity core GC-1 collected in September, 1984 on the R/V ENDEAVOR. The core has excess ^{230}Th present throughout its 170 cm length but the activities are low and erratic. Moreover, ^{226}Ra is deficient with respect to its parent ^{230}Th even at depths of 170 cm. This suggests that the core represents a series of turbidite which have been deposited during the past 10,000 years. The average sediment accumulation rate is ~20 cm/ky, a value in agreement with Kuijpers' (1985) results and consistent with the location of the core in the path of turbidity flows in the Nares Abyssal Plain (see Appendix A, Figure 1).

Depending on the organic content of a turbidlite, oxidation of the organic matter can cause oxidation fronts to be set up in the sediments. Manganese and migrating ^{226}Ra are trapped at these oxidation fronts and core GC1 shows a good example of such a feature at ~40 cm depth.

The second goal in this study has been the evaluation of radionuclide mass balances. At Nares, this is perhaps best done for ^{210}Pb and involves balancing removal of ^{210}Pb from the water column with the fluxes measured in sediment traps and in bottom sediments. Removal of ^{210}Pb from the water column is estimated at ~70 atoms/cm^2/min. In comparison only 16 atoms/cm^2/min are collected in a sediment trap at 4832 m and sediment fluxes are 7-14 atoms/cm^2/min. Thus it appears that only about 20% of the ^{210}Pb removed from the water column is accumulating at Nares; the remainder must be transported away and is probably removed at ocean boundaries such as mid-ocean ridges or the continental shelf-slope.

For ^{230}Th, the situation is similar in that the sediment traps record less than the removal from the overlying water column. In this case the figure is ~80%. We do not believe that this represents a trapping efficiency less than 100% because Bacon et al. (1985) report similar values for different type traps deployed near Bermuda. Rather, the lower values reflect scavenging removal of some of the ^{230}Th at sites away from the Nares Abyssal Plain.

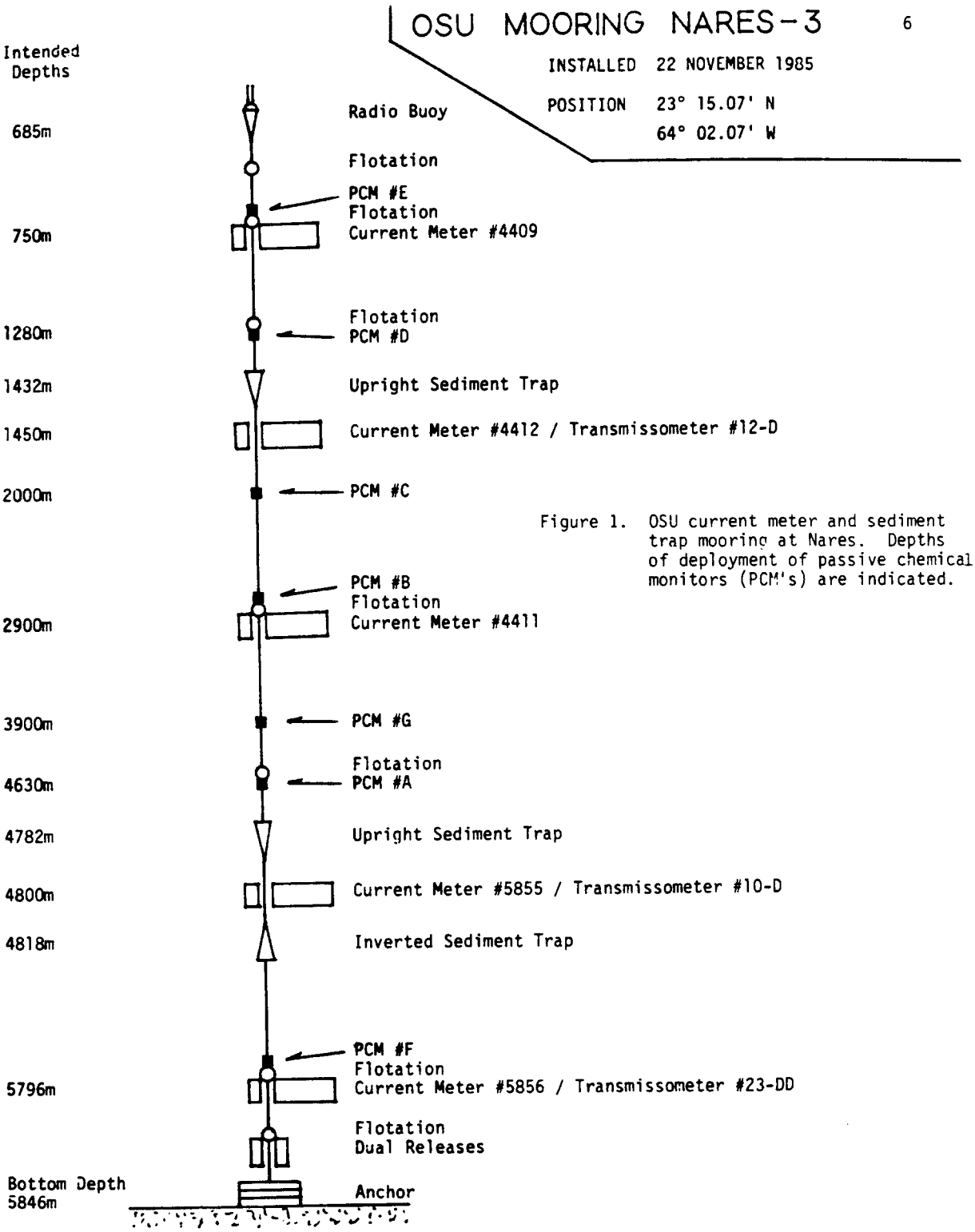

Figure 1. OSU current meter and sediment trap mooring at Nares. Depths of deployment of passive chemical monitors (PCM's) are indicated.

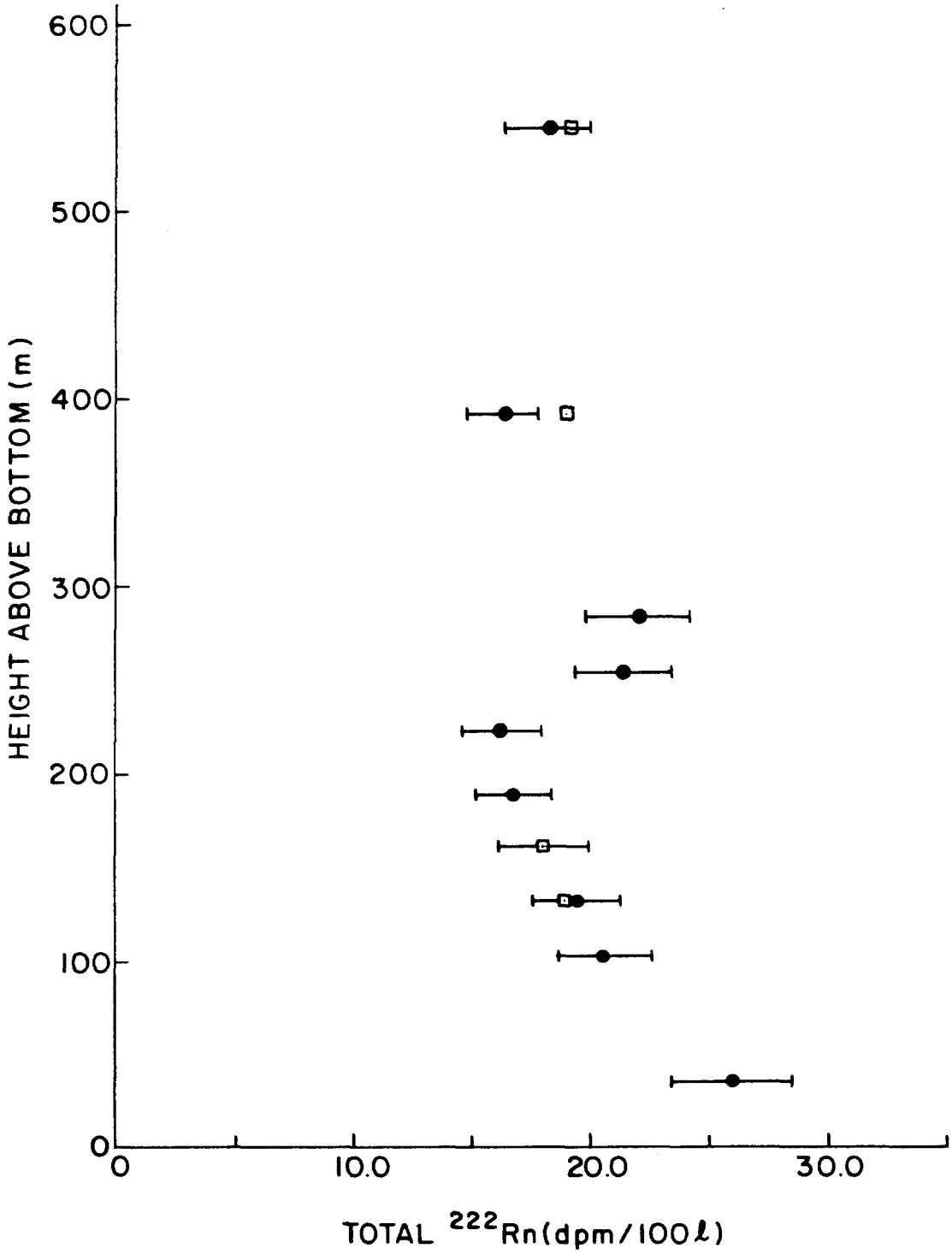

Figure 2. ^{222}Rn activity plotted against height above bottom at the Nares Abyssal Plain.
Solid circles = in situ ^{222}Rn activity
Open squares = ^{226}Ra activity

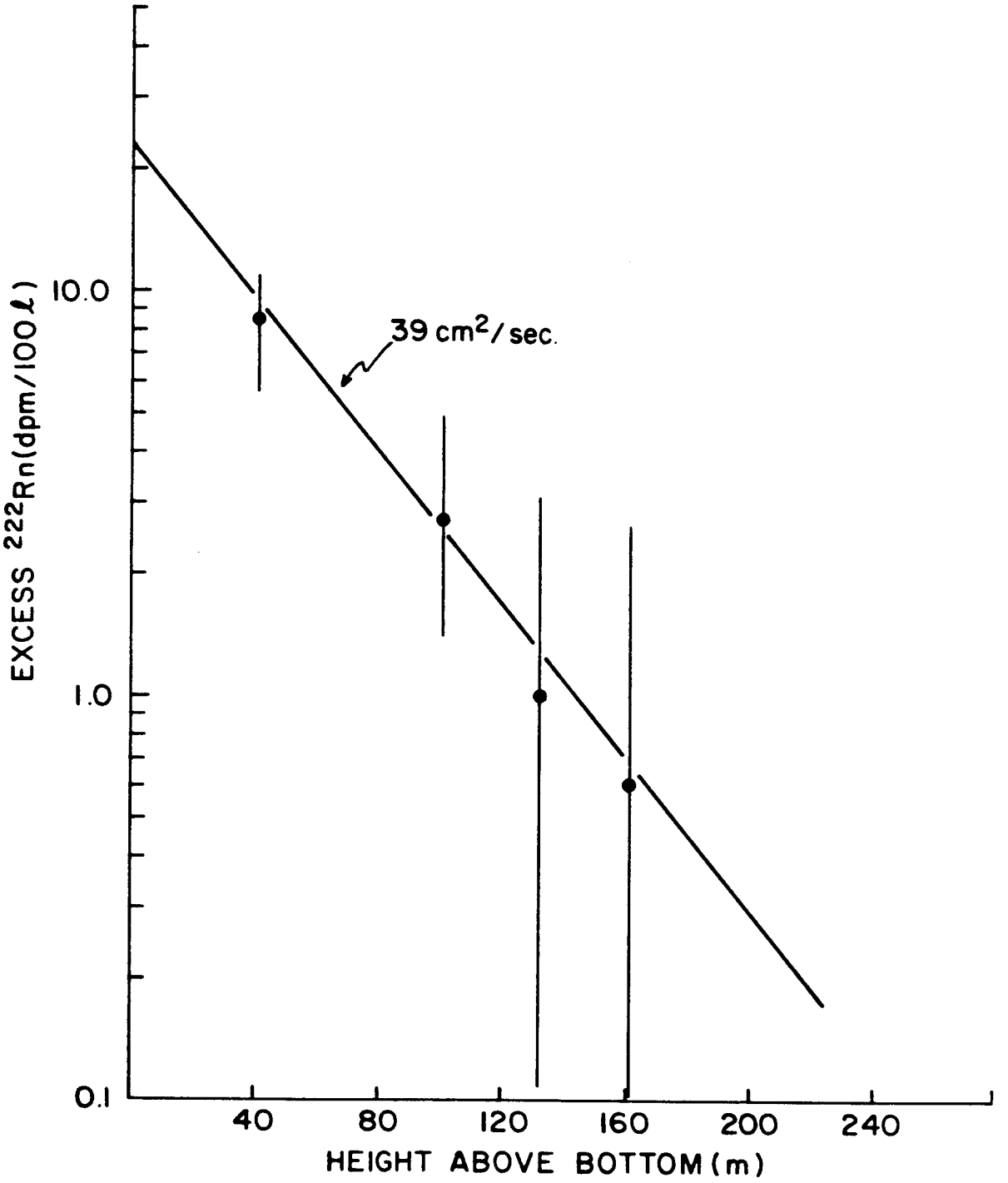

Figure 3. Excess ^{222}Rn vs. height above bottom at Nares. Vertical eddy diffusion coefficient calculated from the data is 39 cm^2/sec.

Table 1. In situ pump samples taken during EN-137 Leg I.

Cast	Depth (m)	Volume (ℓ)	Prefilter Type**	MnO_2 Filter Type**	Cs
1	350	27.1	Poly	Poly	Yes
2	460	848.1	Poly	Foam	Yes
2	550	1622.5	Poly+Cotton	Poly	No
2	560	227.1	Cotton	Cotton	No
3	5670	-	Poly	Poly	Yes
3	5720	2019.3	Poly	Poly	Yes
4	660	1779.4	Poly+Cotton	Poly	No
4	1250	2005.3	Poly	Poly	No
4	3500	632.4	Poly	Foam	Yes
S-1	3	2635.4	TSM	Cotton	Yes
S-2	3	3430.1	Poly+Cotton	Poly	No
S-3	3	1350.4	Poly	Foam	No
S-4	3	1075.3	Cotton	Poly	No
S-5	3	1207.1	Poly	Foam	No

* Surface water samples using deck pump.
** Filter key: Poly = wound polypropylene fiber cartridge, cotton = wound cotton fiber cartridge, TSM = membrane filter.

Table 2. Water casts for radon.

Cast	Bottle Depth*	Cast Information
1	5834 (11) 5824 (21) 5814 (31) 5804 (41) 5794 (51) 5779 (66) 5764 (81) 5749 (96)	23°18'93"N, 63°57'92"W 2136 11/20/85 local time Bottom depth = 5845 m 30 liter Niskin bottles
2	5832 (13) 5802 (43) 5772 (73) 5742 (103) 5712 (133) 5682 (163) 5652 (193) 5622 (223) 5592 (253) 5562 (283)	23°17'75"N, 64°10'05"W 1830 11/24/85 local time Bottom depth = 5845 m
3	4950 (895) 5149 (696) 5300 (545) 5449 (396)	23°12'88"N, 64°07'71"W 1130 11/25/85 local time 5 liter Niskins on rosette with CTD

* Values in parentheses are depths above bottom (m).

Table 3. Nares in situ radon data.

Depth (m)	Meters above bottom	^{222}Rn (dpm/100ℓ)	^{226}Ra (dpm/100ℓ)
4950	895	13.3±1.3	15.0±1.5
5149	696	15.5±1.6	n.m.
5300	545	18.4±1.8	19.0±1.9
5449	396	16.4±1.6	19.0±1.9
5562	283	22.2±2.2	n.m.
5592	253	21.4±2.1	n.m.
5622	223	16.3±1.6	n.m.
5652	193	16.9±1.7	n.m.
5682	163	18.1±1.8	17.5±1.0
5712	133	19.5±1.9	18.5±1.0
5742	103	20.7±2.1	n.m.
5802	43	26.5±2.6	n.m.

n.m. = not measured

¤

Appendix A

Sediment Chronologies and Radionuclide Mass Balances on the Nares Abyssal Plain

Mark Dornblaser

Fall 1986

Abstract:

Excess ^{230}Th activities were recorded throughout the length of a gravity core collected on the Nares Abyssal Plain. Activities were low and erratic, suggesting that the sedimentary sequence is comprised of a series of rapidly deposited turbidites separated by poorly-defined layers of pelagic sedimentation. ^{230}Th and ^{226}Ra are in disequilibrium as deep as 170cm, suggesting that the entire length of the core has been deposited within the last 10,000 years. This indicates an overall accumulation rate as great as 10-20 cm/ky. ^{210}Pb and ^{230}Th balances were made by comparing water column removal to measured sediment trap fluxes and sediment inventories. The sediment trap collected 29% of the expected ^{210}Pb flux and 80% of the expected ^{230}Th flux. The sediments recorded 12% of the ^{210}Pb and 15% of the ^{230}Th. It is concluded that ^{210}Pb and ^{230}Th are removed from the ocean interior by horizontal transport and scavenged at ocean boundaries.

I. Introduction

A wide variety of chemical, physical, and biological processes affect particles sinking through the water column from the surface until they are buried in the sediments. Chemical species undergo transformations between organic and inorganic forms and dissolved and particulate forms, as well as adsorption and desorption reactions and oxidation state changes, and are affected by physical processes such as eddy diffusion and advective transport. Once a particle reaches the sediments it can be affected by such processes as bioturbation, resuspension, and sediment winnowing and focussing.

The purpose of this study has been to investigate both the processes that transform and transport particulate matter and the rates of removal of reactive chemical species from the oceans. The long term objective of this kind of research is to understand the flux of materials on the scale of the world's oceans. To reach such an end, we must first identify the controlling processes and measure their rates. Fortunately, the processes involved may be approached from an analytical standpoint with the use of radioisotopic disequilibrium studies. The radionuclides commonly used in these studies are known as "particle-reactive" nuclides. They exhibit an affinity for particles, and it is this trait that makes them so useful in the study of oceanic processes. In order to describe and measure the removal of radionuclides from the water column, information is needed on fluxes through the water column, the partitioning between

particles and solution, and the quantities of radionuclides in sea floor sediments. One can calculate these "inventories" by integrating their activity profiles over the sediment column. Inventory differences between cores provide information about spatial heterogeneities in particle fluxes and physical reworking (Aller and DeMaster, 1984).

In this research, sediment core, sediment trap, and seawater samples from the western North Atlantic have been analyzed for uranium and thorium series nuclides. Sediment cores yield information on sedimentation rates and the depth and rate of biological stirring. Bioturbation is important in that surface sediment stirring determines benthic fluxes to the water column and modifies the material preserved in the sediments. For many elements, benthic fluxes can be large enough to greatly impact global chemical mass balances (National Research Council, 1984). Sediment traps and seawater samples provide information on mass and nuclide fluxes through the water column. These water column nuclide fluxes provide data on biological cycling as well as chemical and physical cycling since it has been shown that the radionuclide fluxes covary with the total material fluxes (Bacon, 1984; Deuser, 1984; Bacon et al., 1985).

One of the most useful aspects of this type of research is that the data may be brought together to construct a geochemical balance for the radionuclides. Measured sediment trap fluxes and sediment inventories may be compared to the water column fluxes expected from the known radionuclide inputs. If the fluxes do not balance, much can be learned about such things as benthic

regeneration (Dymond, 1984), sediment trap efficiencies, and horizontal transport (Buesseler et al., 1985).

Knowledge of the deep sea geochemistry of metals has become increasingly important as nations such as the United States have begun considering the possibility of using deep sea sediments as a repository for high level radioactive waste (Nozaki et al., 1981). Radionuclides such as ^{230}Th are useful in developing models for removal of heavy metals because of their constant input and particle reactivity. It is hoped that this research will increase the understanding not only of materials cycling in general but also of processes specifically relevant to a region that is under consideration as a high level radioactive waste repository.

A. Study Area

The Nares Abyssal Plain (NAP) is located north of Puerto Rico in the western North Atlantic (Figure 1). It extends about 800 km from east to west and about 200-400 km from north to south (Thomson et al., 1984). It is bordered to the north by the Bermuda Rise and to the south by the Greater Antilles Outer Ridge. Its depth ranges from 5800 m to nearly 6000 m with an eastward sloping sea floor having a gradient of about 1:4000 (Tucholke, 1980). The NAP is essentially flat and is interrupted only by occasional basement highs and volcanic peaks (Shipley, 1978). One of the most interesting features of the NAP is that the sediments often exhibit a layered sequence corresponding to two main types of clay. One is a brown clay, considered pelagic in origin, and the other is a coarse grey clay, considered to be

turbiditic in origin (Shipley, 1978).

B. Geochemistry of Radioisotopes

The naturally occurring radionuclides of interest in this research belong to the uranium and thorium decay series. Following is a brief discussion of their geochemical behavior and their uses in this project.

1. Uranium

The uranium isotopes of interest are primordial ^{238}U ($t_{1/2}=4.5x10^9y$) and ^{234}U ($t_{1/2}=2.5x10^5y$). Uranium is present in solution as uranyl carbonate ($UO_2(CO_3)_3^{4-}$), which is formed during chemical weathering and enters the ocean through river input. Since uranyl carbonate is quite soluble, the uranium isotopes have a long residence time in the ocean, on the order of 400,000 years. This allows the use of their daughters as tracers of oceanic processes because the activity of uranium is essentially constant. The uranium isotopes are used to correct their daughters' activities to that which is unsupported from uranium decay. They are also important in tracing the deposition of turbidites in deep sea cores. The oxidation of organic carbon from bottom water oxygen proceeds from the tops of the turbidites downwards. Uranium redistributes itself to form a concentration peak below the oxidation front, and it is this marker that aids in the detection of turbidites.

2. Thorium

The thorium isotopes of interest are primordial ^{232}Th ($t_{1/2}$=1.4x10^{10}y) and ^{230}Th ($t_{1/2}$=7.5x10^{4}y). Very little ^{232}Th is found in seawater. Some mobilization of thorium occurs during weathering, but most of the thorium that enters the ocean by way of rivers is in particulate form (Cochran, 1982a). ^{230}Th also enters the ocean through in situ decay of its parent, ^{234}U. Thorium is a particle reactive element and it is quickly taken up by particles and removed from the water column via settling (Bacon and Anderson, 1982). This process was referred to by Goldberg (1954) as "scavenging". The major scavenging processes include adsorption, co-precipitation with Mn and Fe oxides, ion exchange, and incorporation into the shells of plankton (Cochran, 1982a; Riley and Chester, 1971).

One of the major uses of ^{230}Th is as a chronometer for determining deep-sea sediment accumulation rates. Due to its long half-life, ^{230}Th retains measurable levels of activity deep into the sediments (assuming sedimentation rates on the order of cm/ky). All radioactive isotopes decay exponentially according to the following equation:

$$A = A^{o}e^{-\lambda t} \qquad (1)$$

where A is activity, A^{o} is initial, or surface activity, λ is the decay constant, and t is time. For deep sea sediments, t in eq. (1) can be replaced by x/s (assuming a constant sediment accumulation rate and porosity), where x is the depth in the sediment and s is the sedimentation rate. Replacing t in eq. (1) and solving, one obtains

$$\ln(A) = \ln(A^{o}) - \lambda(x/s) \qquad (2)$$

Equation (2) is a straight line on a plot of $\ln(A)_{xs}$ vs. depth, with a slope of $-\lambda/s$. (The subscript xs refers to excess activity, that which is unsupported from the parent nuclide.) Since λ is known, all one has to do to obtain the sedimentation rate is measure ^{230}Th activities with depth in a core and plot them. There are, however, three assumptions made when using this method (Turekian and Cochran, 1978): 1)the activity at the sediment/water interface (A^o) is constant, 2)the sedimentation rate and the flux of ^{230}Th to the sediment/water interface are constant, and 3)there is no chemical migration of thorium. According to Bonatti et al. (1971), thorium is not affected by diagenetic mobility. Furthermore, for a given site in the deep sea, the other assumptions are generally valid (at least on a thousand year time scale) unless the sediment record has been affected by the deposition of turbidites. As will be discussed later, this appears to be the case for much of the NAP, thus making it exceedingly difficult to derive any meaningful sedimentation rates.

Another useful piece of information obtained from ^{230}Th activity profiles in sediments is the depth of continuous mixing by benthic organisms (Cochran, 1982b). Benthic fauna rework the upper few centimeters of deep sea sediments on a time scale that is rapid relative to the half-life of ^{230}Th. The mixing process alters the activity profile such that the ^{230}Th activity remains virtually constant over the depth in which the mixing occurs (Cochran and Krishnaswami, 1980). Thus one can read the depth of continuous mixing from the ^{230}Th profile.

Given ^{230}Th sediment trap data it also may be possible to calibrate the collection efficiency of sediment traps. Because the uranium concentration in seawater is constant, one can predict what the measured flux of ^{230}Th should be. One simply integrates the ^{234}U activity over the height of the water column. Any discrepancies between the measured and theoretical fluxes can be attributed to trapping inefficiencies, assuming horizontal transport to be negligible (Knauer et al., 1979; Brewer et al., 1980). It will be shown in a later section, however, that this may not be a valid assumption for the area under consideration.

Lastly, sediment inventories of ^{230}Th can be calculated from a sediment activity profile. As previously stated, these inventories can be used, along with water column flux calculations, to construct a geochemical balance for the nuclide. If the transport of thorium on sinking particles is primarily vertical, then inventories should balance fluxes, assuming the fluxes are constant over large time periods. It has recently been shown, however, that horizontal transport can be a major removal mechanism of particles from the deep sea (Anderson et al., 1983b). Other processes that can contribute to deviations from a balance include sediment focussing, winnowing, or bottom transport of sediments by turbidites (Cochran and Osmond, 1976).

3. Radium

The radium isotope of interest is ^{226}Ra ($t_{1/2}$=1622y). Some radium enters the oceans via rivers, but most of it enters the ocean from ^{230}Th decay and recoil in the sediments (Cochran, 1982a). In marine sediments, $^{226}Ra/^{230}Th$ activity ratios are

typically less than one near the sediment/water interface due to the diffusion of ^{226}Ra into the overlying water. The activity ratio grows to one at depth in the sediment (Cochran and Krishnaswami, 1980). Radium activities are used to calculate the unsupported activities of its daughters, such as ^{210}Pb.

4. Lead

The major lead isotope of interest is ^{210}Pb ($t_{1/2}$=22.3y). A significant source of ^{210}Pb to the surface ocean is the atmosphere, where it is produced from the decay of ^{222}Rn. Rivers supply ^{210}Pb to the oceans in the particulate phase and it is also produced in situ from the decay of ^{226}Ra (through ^{222}Rn). ^{210}Pb, like ^{230}Th, is a particle reactive isotope. Its residence time in the deep sea is on the order of 15-100 years (Spencer et al., 1981).

$^{210}Pb_{xs}$ gradients in deep-sea sediments can be used to determine particle mixing rates. The most common approach to measuring such rates treats the mixing process like eddy diffusion. As in the case of ^{230}Th, a geochemical balance may be constructed for ^{210}Pb, using sediment trap, water column, and sediment inventory data. Since both ^{230}Th and ^{210}Pb are particle reactive, a comparison of the results obtained from each set of budget calculations provides information on horizontal vs. vertical transport of radionuclides on different time scales.

II. Methods

A. Gravity core

One 2 m gravity core (GC-1) was obtained from the Nares Abyssal Plain (cruise EN-121, September 1984) at 5800 m (see Figures 1 and 2). The core was cut into four 50 cm sections and frozen for storage. The sections were split vertically. One set of sections was used to obtain samples and the other set remained frozen. Initially, 12 randomly spaced samples were withdrawn from the core with an open-ended 30 cc syringe. In order to insert the syringe, the core had to be slightly thawed, but was returned to the freezer immediately after sampling. Volumes of the samples withdrawn were noted and later used to calculate dry densities. The samples were weighed, placed in 250 ml acid washed Pyrex beakers, and put in an oven at 80°C to dry overnight. The samples were then reweighed, ground by hand, stored in plastic bags, and then analyzed for radionuclides as described below. Aliquots of these samples were sent to Oregon State University for radiochemical, trace metal, and organic carbon analysis. Later in the course of research, additional samples were taken from GC-1 for iron and manganese analysis.

B. Box Cores

Box cores were collected during the February 1984 cruise of the R/V Tyro (see Figure 2). A 10 cm diameter subcore of each box core was shipped to Woods Hole Oceanographic Institution (WHOI). There each subcore was sampled in 1-2 cm increments. The samples

were dried at 110°C, ground, and preliminary nondestructive ^{210}Pb and ^{226}Ra assays were made at WHOI (Cochran and Livingston, 1985) using a planar germanium detector for ^{210}Pb and a coaxial Ge(Li) detector for ^{226}Ra. Approximately 0.5 g of sediment was then reserved for radiochemical analyses of ^{210}Pb, ^{226}Ra, Th, and U isotopes at SUNY, Stony Brook.

C. Sediment Traps

Sediment trap samples were collected from cruise EN-121 of the R/V Endeavor. The trap mooring consisted of two upward-looking sediment traps (at 1463m and 4832m) and one downward-facing trap (at 4862m) (Dymond and Collier, 1986). The traps were of the standard 5-cup OSU design (Moser et al., 1986). Each cup sampled for approximately 80 days; total deployment time was thirteen months. Analyses of NAP sediment trap samples were carried out by David Hirschberg of SUNY, Stony Brook. The analytical procedures for the samples are the same as those described for sediments below (Krishnaswami and Sarin, 1976; Flynn, 1968; Livingston et al., 1975).

D. Radiochemical Procedure

The radiochemical analysis for sediments is based on the ^{210}Po method described in Krishnaswami and Sarin (1976). A ^{208}Po tracer (SBP6, 0.5ml) and 0.5 ml of a $^{232}U/^{228}Th$ tracer were added to 0.5g of dried sediment. The samples were then dissolved in HCl, HNO_3, and HF acids. The samples were brought up in 50 ml of 1.5 N HCl in preparation for ^{210}Pb analysis. Polonium was auto-

plated onto silver disks according to the method of Flynn (1968). Ascorbic acid was added to the samples to reduce iron and prevent it from plating. The samples were plated for three hours in an 80°C water bath. The polonium was counted on a Canberra Quad Alpha Spectrometer, Model 7404. In order to calculate the activity of the polonium from the counts measured on the spectrometer, the following equation is used:

$$A_{210} = (C_{210}/C_{208}) \times A_{208}/\exp(-\lambda t) \times (v/m) \qquad (3)$$

where: A_{210} = activity of ^{210}Po at time of plating (dpm/g)

(C_{210}/C_{208}) = ratio of ^{210}Po counts to ^{208}Po counts, corrected for background

A_{208} = activity of ^{208}Po at midpoint of counting (dpm/g)

λ = decay constant for ^{210}Po

t = time between counting and plating

v = volume of tracer used

m = mass of sample

Errors represent 1σ counting statistics.

The sample solutions remaining after the plating of polonium were saved for ^{226}Ra analysis by a standard ^{222}Rn emanation technique (Mathieu, 1977). The solutions were purged with He for 30 minutes to remove any radon present in the sample. The solutions were then allowed to sit for at least two weeks to let radium and radon grow into secular equilibrium. At that time He was recirculated through the solution for 30 minutes to extract dissolved radon from the sample. The radon was adsorbed onto an

activated charcoal column at -60°C in an isopropanol/dry ice bath. The column was heated in an oven at 475°C to drive the radon off the column and into an evacuated glass scintillation cell. At this point the cells were allowed to sit for about three hours until ^{222}Rn came into secular equilibrium with its short-lived daughters ^{218}Po and ^{214}Po. The activity of the cell was then counted on an Applied Techniques Co. Dual Radon Counter model DRC-MK-6. Finally, the activity was calculated from the following equation:

$$A_{226} = [\{cpm/3(1-\exp(-\lambda t_1))(\exp(-\lambda t_2))E\}-B]/m \quad (4)$$

where: A_{226} = activity of ^{226}Ra (dpm/g)

cpm = counts per minute

λ = decay constant for ^{222}Rn

t_1 = time between extraction and purging

t_2 = time between counting and extraction

E = counting efficiency

B = blank

m = sample mass

Counting efficiencies for each cell and counter combination were determined by runs of an NBS ^{226}Ra standard. Blank determinations were made on distilled water blanks extracted like samples. Blank and efficiency values have been entered into a computer program designed to simplify the ^{226}Ra activity calculations. From repeated laboratory measurements, overall experimental errors are approximately 10%.

Following ^{226}Ra analysis, HNO_3 and H_2O_2 were added to the sample solutions to decompose the ascorbic acid. The samples were brought up to 30 ml with 8 N HCl in preparation for addition to

ion exchange columns, which separate uranium from thorium. The 10 ml columns were filled with AG1X8 100-200 mesh anion resin and conditioned with 50 ml of 8 N HCl. The samples were then added and the columns were washed with 65 ml of 8 N HCl; the eluted thorium fraction was saved for further purification. Uranium was eluted from the columns in 70 ml of .02 N HCl. The thorium fraction was taken to dryness, treated with aqua regia and 8 N HNO_3, and finally brought up to 30 ml with 8 N HNO_3 prior to addition to a thorium clean-up column. For this column, the resin was conditioned with 50 ml of concentrated HNO_3. Then the sample was added, the column was washed with 65 ml of 8 N HNO_3, and finally the thorium was eluted with 70 ml of 8 N HCl.

The uranium fraction was taken to dryness and dissolved in 10 ml of 8 N HNO_3 prior to addition to uranium clean-up columns. The resin was conditioned as with the thorium-clean up columns. The sample was added, the columns were washed with 20 ml of 8 N HNO_3, and finally uranium was eluted with 70 ml of .02 N HCl.

The purified uranium and thorium fractions are plated onto stainless steel disks following the method of Livingston et al. (1975). The samples were plated for two hours at 1 amp. After plating, the disks were placed in the Canberra Quad Alpha Spectrometer for counting.

After counting, ^{232}Th and ^{230}Th activities can be calculated using the following equations. They are written for ^{232}Th, but the procedure for ^{230}Th is the same:

$$A_{232} = (C_{232}/C_{228}) \times A_{228} \times (v/m) \quad (5)$$

where: A_{232} = activity of ^{232}Th (dpm/g)

(C_{232}/C_{228}) = ratio of ^{232}Th counts to ^{228}Th counts, corrected for background. ^{228}Th counts are also corrected for ^{224}Ra decays which occur in ^{228}Th peak energies and for natural ^{228}Th in the sample.

A_{228} = activity of ^{228}Th at the time of U/Th separation (dpm/ml)

v = volume of tracer used

m = mass of sample

The activities of ^{238}U and ^{234}U are calculated (after counting) according to the following equations. Here again, both isotopes' activities are calculated in the same manner:

$$A_{238} = (C_{238}/C_{232}) \times A_{232} \times (v/m) \quad (6)$$

where: A_{238} = activity of ^{238}U (dpm/g)

(C_{238}/C_{232}) = ratio of ^{238}U counts to ^{232}U counts, corrected for background

A_{232} = activity of ^{232}U at time of counting (dpm/ml)

v = tracer volume used

m = mass of sample

E. X-radiographs

Radiographs of frozen GC-1 sections were made using Kodak SB panoramic dental X-ray film and a tungsten X-ray source. The X-ray film was placed directly under the core liner and the X-ray

source was set about 1 m from the film. Exposure time was approximately 0.5 sec.

F. Iron and Manganese

GC-1 was analyzed for the metals Mn and Fe with standard atomic absorption techniques. In preparation for AA analysis, 0.1 g amounts of sample were completely dissolved in HCl, HNO_3, and HF. In addition to the GC-1 samples that were analyzed, two replicates of NBS SRM 1645 River Sediment and one sample of Canadian MESS-1 Marine Sediment were run.

For Mn analysis, the dissolved samples were brought up to 100 ml (in volumetric flasks) with 1.5 N HCl. An NBS Mn stock standard of 1000 ppm was used to make up standards of 0.5, 1.0, 1.5, 2.5, and 3.0 ppm. From these standards, a standard curve was generated from which a regression equation was determined to calculate sample concentrations. The standards and samples were run on a Perkin Elmer model 5000 Atomic Absorption Spectrophotometer. For Mn, the samples were run with the background corrector and a coarse screen was used to block part of the lamp energy.

The sample solutions were diluted prior to the Fe runs. Five ml of the solutions were brought up to 100 ml with 1.5 N HCl. An NBS stock solution of 1000 ppm was used to make standards of 1.0, 2.0, 3.0, 4.0, and 5.0 ppm. As with Mn, a standard curve was generated to determine sample concentrations. The background corrector was used for Fe as well.

G. Water Column

Nine water column samples from the NAP were analyzed for ^{210}Pb. The samples were collected from cruise EN-121 of the R/V Endeavor by paired 30 L Niskin samplers. The paired samples were combined into Delex containers and acidified on board. The samples were then shipped to WHOI. Approximately 4 L of each sample was saved for analysis at MSRC, SUNY, Stony Brook. To each sample was added 0.2 ml of the ^{208}Po tracer SBP6, 0.5 ml of Galena Pb carrier, and 2.0 ml of an Fe carrier (5.0 g $FeCl_3*6H_2O$ in 100 ml 8 N HCl). The pH of the samples was then raised to about 7-8 with NH_4OH to precipitate the lead. The precipitates were collected and dissolved in 50 ml 1.5 N HCl. Polonium was plated from these solutions according to the procedure previously described for sediments.

^{226}Ra analyses of a few NAP deep water samples were also carried out by David Hirschberg of MSRC by the ^{222}Rn emanation technique (Mathieu, 1977). In order to determine the removal of ^{210}Pb from the water column a complete ^{226}Ra profile was needed. The ^{226}Ra profile was calculated from silica data (GEOSECS Station 32) since it has been shown that ^{226}Ra and Si covary (Bacon et al., 1976). The equation used to calculate ^{226}Ra values was: Ra (dpm/100kg) = 6.91 + .217*Si (um/kg) (Bacon et al., 1976).

III. Results

Tables 1 and 2 present radiochemical data and activity ratios for Box Core 32. The radiochemical data for the remaining box cores are given in Table 3. ^{210}Pb and $^{210}Pb_{xs}$ values for all box cores have been decay corrected to the time of collection. Excess ^{230}Th in BC32 exhibits a relatively constant activity in the upper few centimeters and then drops significantly (see Figure 6). Excess ^{210}Pb activities for this core drop dramatically from the sediment/water interface downwards. The activity ratios for BC32 (Table 2) present the expected trends. $^{210}Pb/^{226}Ra$ activity ratios decrease to one and $^{226}Ra/^{230}Th$ activity ratios increase to one. Table 3 indicates an order of magnitude variability in surficial excess ^{210}Pb activities. Excess ^{210}Pb profiles of the cores used to calculate mixing coefficients are plotted in Figure 3. The mixing coefficients determined for the NAP cores fall at the low end of the range of 0.04-0.4 cm^2/y calculated by DeMaster and Cochran (1982) for Atlantic, Pacific, and Antarctic Ocean cores.

Radiochemical data and activity ratios for GC-1 are given in Tables 5 and 6, respectively. In Figure 4 the $^{230}Th_{xs}$ profile is presented, along with sediment color and X-ray information. Excess ^{230}Th is calculated by subtracting the measured ^{234}U activity from the measured ^{230}Th activity. This represents the activity of ^{230}Th which is unsupported from the decay of its parent, ^{234}U. Similarly, excess ^{210}Pb is calculated as the measured ^{210}Pb activity minus the measured ^{226}Ra activity. The

problem with this calculation of excess ^{210}Pb is that it ignores the possibility of ^{222}Rn migration out of the sediments (Cochran, 1985). However, since in situ ^{222}Rn data are not available, excess ^{210}Pb is calculated relative to ^{226}Ra. Cochran (1985) found that such a simplification did not drastically affect the calculation of mixing coefficients and in this study all but one of the mixing coefficients are estimated to be within a factor of two of what they would be using ^{222}Rn to calculate excess ^{210}Pb.

Iron and manganese data for GC-1 are given in Table 7 and plotted in Figure 5, along with organic carbon data. In Table 7, standard deviations of the analyses of five replicate samples at the 97-99 cm depth interval were applied to all other depths as a percent error. The NBS concentration recorded in the table is an average of two replicates. The manganese profile in Figure 5 shows a large maximum at 40 cm and consistently lower values deeper in the core. The iron profile is more erratic, with values falling in the range of 2-6%. Organic carbon content averages 0.2-0.3% with a maximum at 88 cm.

The sediment inventory data for ^{210}Pb in all cores is found in Table 9. Inventories were determined by integrating the activity of excess ^{210}Pb with depth. For these calculations, a dry bulk density of 0.78 g/cm^3 was used. This was the density determined for the uppermost sample in GC-1 (Table 5). In the cases where the excess ^{210}Pb activities did not decrease to near zero in the intervals sampled (BC09, BC15, and BC25), extrapolations were made to calculate inventories by fitting curves to the profiles. In core BC32, continuous intervals were

not sampled for ^{210}Pb. Therefore, intermediate activities were interpolated linearly from surrounding activities in order to calculate the inventory.

IV. Discussion

A. Sediments

1. Particle Mixing Rates

Tables 1 and 3 present the radiochemical data used to calculate particle mixing rates. The data indicate an order of magnitude range in the surficial excess ^{210}Pb activities measured. The possible reasons for the observed variability are as follows: 1)there is actual variability in the ^{210}Pb activity of the sediments being deposited, 2)there is a loss of the uppermost section of the core due to recovery problems, and 3)there is spatial variability in the particle mixing rate. The sedimentary environment of the NAP is complex (Thomson et al., 1984; Carpenter et al., 1983; Cochran and Hirschberg, 1985). The NAP is subject to periods of turbiditic as well as pelagic sedimentation, and sediment winnowing and focussing is a common occurrence (Duin, 1985). Thus there probably is some spatial variability in the ^{210}Pb being deposited. It also appears that there may have been some problems with the recovery of the box cores resulting in the loss of core tops (Kirk Cochran, pers. comm.).

Radionuclide profiles used to calculate particle mixing rates are typically described with a steady state vertical advection diffusion model (DeMaster and Cochran, 1982; Cochran, 1985). Biological mixing does not always transport particles in an eddy diffusion-like manner, but the method is useful because it allows the comparison of mixing rates in different sedimentary

environments and on different time scales. The general equation that describes the system can be written as follows (Cochran, 1985):

$$\frac{\partial}{\partial t}[\rho A] = \frac{\partial}{\partial t}[\rho D_B \frac{\partial A}{\partial z}] - \frac{\partial}{\partial z}[\rho SA] - \lambda \rho A \qquad (7)$$

where: t = time (y)

ρ = dry bulk density (g dry sed/cm^3 wet sed)

A = excess activity (dpm/mass dry sed)

z = depth (cm)

D_B = particle mixing coefficient (cm^2/y)

S = sedimentation rate (cm/y)

λ = decay constant (y^{-1})

Since sediment accumulation does not generally contribute to the distribution of shorter-lived nuclides such as ^{210}Pb in the deep sea, the accumulation term in the above equation can be ignored. Equation 7 is then solved for ^{210}Pb, assuming steady state, constant D_B in the mixed zone, constant ρ, and the conditions $A = A_o$ at $z = 0$ and A goes to zero as z goes to infinity. The solution is as follows:

$$A = A_o \exp[-z(\lambda/D_B)^{1/2}] \qquad (8)$$

There are many assumptions involved in using eq. (8), but it allows the calculation of mixing rates that can easily be compared for various locations and environments. Given the stated assumptions, this equation is appropriate as long as excess ^{210}Pb decreases to small values within the mixed zone. From the excess ^{230}Th profile in Figure 6 it appears that the mixed zone may extend down to 4-5 cm. Tables 1 and 3 confirm that for the box cores used to calculate mixing coefficients, excess ^{210}Pb does decrease to low values within this zone.

Figure 3 shows excess ^{210}Pb profiles for five box cores that were used to determine particle mixing coefficients. The profiles for box cores 9 and 15 were not used to calculate a mixing coefficient because the excess activities recorded for the 2-3 cm intervals were actually greater than those recorded for the 1-2 cm intervals. This could occur with the filling in of burrows with surficial sediment, and according to core descriptions burrows were evident in all cores. Cochran and Livingston (1984) calculated mixing coefficients for the same box cores but without the benefit of having activities recorded for the 2-3 cm intervals (and the 4-5 cm interval for BC32). A comparison of their results to those of this study is given in Table 4. The additional samples run in this study generally resulted in slight increases in the D_B values of Cochran and Livingston (1984). There is better than an order of magnitude range in the mixing coefficients. Thus, even though the possibility of variable ^{210}Pb deposition has not been ruled out, it is believed that the results indicate real variability of particle mixing on the NAP. Since the deep sea is typically characterized by a low abundance and high diversity of fauna and displays a variability in benthic biomass of about an order of magnitude (Turekian et al., 1978), this conclusion is not unreasonable.

2. Longer Term Chronologies: Gravity Core 1

The Nares Abyssal Plain (NAP) is an area of deposition of distal turbidites (Thompson et al., 1984; Carpenter et al., 1983). The geochemical and X-ray data presented here are

consistent with these findings. Although excess ^{230}Th is present throughout the length of the core (Table 5, Figure 4), the profile does not display a smooth decrease in $^{230}Th_{xs}$ activity with depth. Activities for GC-1 vary irregularly with depth and are low compared to other cores from the NAP (Carpenter et al., 1983). Dry bulk densities for GC-1 are large for deep sea pelagic sediments (Kirk Cochran, pers. comm.).

The sedimentary sequence in GC-1 on the NAP consists of alternating layers of brown and grey sediments (Figure 4). The brown sediments are thought to be slowly accumulating pelagic clays whereas the grey clays are thought to be the result of rapidly depositing turbidites (Thomson et al., 1984). Both clays have the same terrigenous origin (Shipley, 1978; Carpenter et al., 1983). Color changes in GC-1 were difficult to detect due to ice crystal formation on the sediments. It does appear that two major grey clay sections exist in the sequence (Figure 4), but the color boundaries cannot necessarily be taken as the true boundaries of the turbidites. One reason for this is that sediments have been observed to change color between the time cores are collected and the time they are described in the laboratory (Shipley, 1978). Another reason is that redox reactions associated with organic matter diagenesis in turbidites often cause color changes. Upon deposition, the oxidation of organic carbon in turbidites proceeds from the tops of the turbidites downwards. The rate at which the front moves is determined by both the reducing capacity of the sediment (the amount of organic carbon) and the balance between the diffusive fluxes of reductants (Mn^{2+} and Fe^{2+}) and oxidants (O_2 and NO_3^-)

(Wilson et al., 1986). When the fluxes are equal, the front no longer descends into the turbidite. As sediment continues to accumulate above, the level of zero oxidant concentration then travels upwards through the sediment, maintaining a constant distance from the sediment/water interface.

An association of authigenic uranium with organic carbon in marine sediments is well known (Mangini and Dominik, 1979), and it has been shown that uranium may be mobilized to form a concentration peak below the oxidation front (Colley and Thompson, manuscript). Isotopic differentiation between ^{234}U and ^{238}U has been seen, and this is thought to be caused by a preferential migration of ^{234}U in the (VI) oxidation state across the redox front following its in situ production from ^{238}U in the (IV) oxidation state (Colley et al., 1984). The uranium peaks are sometimes useful in confirming the presence and location of turbidites. However, uranium peaks may not be seen in turbidites with low organic carbon contents (<0.5%). As can be seen in Table 5, the organic carbon content throughout GC-1 is relatively low (Dymond and Collier, 1986). In the case where organic-poor turbidites are deposited, the redox front moves downwards too quickly to allow the uptake of uranium from seawater and its subsequent enhancement below the front. Alternately, if the oxidation of organic matter in the turbidite is complete, the sediments may appear organic-poor when in fact they were organic-rich at the time of deposition. Unless all material being deposited has the same organic fraction, however, this is unlikely. Even in once organic-rich layers where oxidation is

complete, enough organic carbon should be preserved to prevent the labelling of the layer as "organic-poor" (Muller and Suess, 1979). The highest organic carbon contents were recorded in the same section of the core that the highest uranium activities were found, at 88 and 98 cm (see Table 5). The uranium activities at these depths, although significantly greater than surrounding acitivies, do not indicate a "peak" of the magnitude seen in most organic-rich turbidite sections (Colley et al., 1984).

Manganese and iron are two other elements that may become mobilized and travel across the redox front (e.g. Bonatti et al., 1971). In contrast to uranium, however, manganese and iron become enriched in the upper oxidized zone (Colley and Thompson, manuscript). Mn^{2+} and Fe^{2+} may diffuse across the front, where they can be oxidized and precipitated in a narrow depth interval (Wilson, 1986). This process may not develop to any great extent if turbidites are deposited too frequently or production rates of the elements is too low. From the Mn and Fe profiles for GC-1 (Figure 5) it appears that total Fe has not been very active diagenetically. On the other hand, any diagenetic signals that might be present are probably hidden, due to the fact that much of the Fe is structural and is therefore not involved in diagenetic reactions. The variations observed are probably the result of variations in the depositional flux over time or a change in the sediment composition.

A large spike in Mn is evident at 40 cm. Carpenter et al. (1983), working on a core from the Kane Fracture Valley at the eastern end of the NAP, found a similar spike in Mn at around 40 cm. They concluded that this feature is diagenetic since the high

solid phase Mn values were measured close to the depth at which Mn begins to increase in the pore waters. In addition to Mn, the similarity between the ^{230}Th profile for the core sampled by Carpenter and his coworkers and that of GC-1 is remarkable. Both profiles show low surface activities, as well as similarly spaced sections of higher activities throughout the cores. Carpenter et al. (1983) described their grey clay sequence as extending from 50-160 cm. The grey clay sequences from GC-1 are contained in that same interval. It may be that the two sites where these cores were collected, although a few hundred kilometers away from each other, lie along a major depositional path for turbidites (Figure 1).

It has been shown that low excess ^{230}Th activities are recorded in turbidite sequences (Thomson et al., 1984; Carpenter et al., 1983). Low activities are expected when a sediment section moves, is mixed, and redeposited (Thompson et al., 1984). Also, sediments underlying a shallow water column such as the Hatteras shelf (see discussion below) should have lower activities than those found in the deep sea because in situ production of ^{230}Th from its parent ^{234}U would be less. Yet it appears (Figure 4) that both low and high excess ^{230}Th activities are found in grey clay sequences. In order to explain this, one must look at the source of the turbidites.

According to Tucholke (1980), the major sources of turbidity currents to the NAP are distal flows from the Hatteras Canyon and Abyssal Plain that enter the NAP through the Vema Gap (see Figure 1). There are a number of pieces of evidence that support the

idea that turbidity flows travel in a more or less easterly direction across the NAP. Duin (1985) mapped the sediment thickness above the shallowest high-amplitude seismic reflection for various sites on the NAP and found a gradual decrease in the thickness of this layer from the west to the east and northeast. Kuijpers (1985), contouring the cumulative thickness of silt intervals across the plain, found the same result. He also found an increase in average grain size toward the western part of the NAP region.

The fact that both low and high excess ^{230}Th activities are found within turbidite sequences raises questions about the depositional source. Turbidity flows might also originate from the Bahama Banks, travelling to the NAP through the Cat Gap, or from the Silver Abyssal Plain, flowing between the Antilles Outer Ridge and the Caicos Outer Ridge (Figure 1). Anderson et al. (1983a) calculated high in situ scavenging rates of ^{230}Th at ocean margins relative to the open ocean. If one considers horizontal advection, then ocean margins can act as a sink for ^{230}Th produced in the open ocean. Bacon and Rosholt (1982), working on the Bermuda Rise, found that the rate of ^{230}Th accumulation was approximately nine times its production in the water column. If such an area with excess inventories was the source of turbidity flows to the NAP, the deposition of sediments with elevated ^{230}Th activities could result.

Both multiple sources and various layers of sediment from the same source can cause variations in the excess ^{230}Th deposited on the NAP. Deposited sediment that was originally part of the upper few centimeters of the sediment column will contain

relatively high excess ^{230}Th activities while deposited sediment that was originally deep in the sediment column will contain relatively low activities. One should also consider the possibility that there may be smaller turbidity flows cutting across the NAP from the Bermuda Rise, the Antilles Outer Ridge, or more regional topographic highs. The NAP has been found to be a complex sedimentary environment, containing many narrow migratory silt dispersal paths (Kuijpers, 1985). It has been shown that cores within a few miles of each other with no apparent change in elevation can vary from pelagic to turbiditic (de Lange, 1985). Sediment focussing has also been shown to be common on the NAP, occurring every few nautical miles on the average (Duin, 1985). The distal parts of major turbidity currents from the west along with migrational and local flows have apparently formed a braided pattern of meandering dispersal paths (Kuijpers and Duin, 1985).

X-ray data from GC-1 (Figure 4) suggest the frequent deposition of relatively small amounts of turbiditic sediment rather than large infrequent deposits as the color scheme might first suggest. The layers identified in Figure 4 are more dense than the surrounding material. In areas known for the deposition of turbidites, these high density layers are usually associated with the sand-sized fraction laid down at the beginning of a depositional event (Freeman, 1985). But if the only major source of turbidites to the NAP is the Hatteras shelf then only fine-grained sediments would reach the central NAP. If, on the other hand, some of the deposits were the result of smaller, more

regional flows, then the high densities could be explained by large grains, the rapid compaction of layers deposited over a relatively short time scale, or a difference in the water content of the flows.

By looking at the relationship between various isotopes, one can get an idea of the stability of the area over various time scales. The data for GC-1 (Tables 5 and 6) suggest that ^{210}Pb and ^{226}Ra are in equilibrium (within the counting uncertainty) throughout the length of the core. Since these isotopes should be in equilibrium after about five half-lives of the daughter ^{210}Pb (approximately 100 y), this finding is expected. The fact that the isotopes are in agreement adds reliability to the radiochemical procedures. Had the upper few centimeters of sediment in GC-1 been sampled, they probably would have indicated excess ^{210}Pb, as shown in the box cores. There is an excess of ^{226}Ra relative to ^{210}Pb at 40 cm. As was previously discussed, this is the same depth at which the manganese spike was located. The attraction of radium for manganese oxides is well known (Kadko, 1980). ^{226}Ra mobilized in the sediments via recoil associated with the decay of its parent ^{230}Th has apparently precipitated out with the manganese oxides on the oxidized side of a relict redox boundary. The deficiency of ^{210}Pb at this depth must be due to the migration of ^{222}Rn away from the Mn/^{226}Ra spike.

An examination of ^{230}Th and ^{226}Ra data (Tables 5 and 6) indicates intervals of both equilibrium and disequilibrium for this parent/daughter isotope pair. ^{230}Th and ^{226}Ra are in equilibrium in the 117-119 cm and 134-136 cm intervals. Much of

the rest of the core appears to be in disequilibrium with respect to these isotopes. Diffusion of ^{226}Ra out of the core can affect the upper 20-30 cm of sediment (Cochran and Krishnaswami, 1980; Cochran, 1980). The excess in ^{226}Ra over ^{230}Th at 39-41 cm probably reflects the trapping of ^{226}Ra by manganese. At other depths, the disequilibrium is probably the result of variable $^{226}Ra/^{230}Th$ ratios in turbiditic sequences. Since these isotopes should reach equilibrium within about five half-lives of the daughter ^{226}Ra (8100 y), this suggests that much of GC-1 has been affected by the rapid deposition of turbidites, separated by poorly-defined periods of pelagic sedimentation. This conclusion is in agreement with that of Kuijpers (1985), who found that within the sedimentary sequence, sections of strictly pelagic sediments were rare.

Given the extent to which GC-1 has been affected by the deposition of turbidites, the determination of a pelagic sedimentation rate is impossible. Proper use of the ^{230}Th method requires that the sedimentation rate and ^{230}Th flux be constant with time, or at least change in a monotonic fashion, and it is evident that this is not the case at the GC-1 site. From the radiochemical data, however, it is possible to get an idea of the overall sediment accumulation rate. Since ^{230}Th and ^{226}Ra are in disequilibrium as deep as 170 cm, it appears that the entire length of the core must have been deposited within the last 10,000 years. Thus the average sediment accumulation rate could be as great as 10-20 cm/ky. This is consistent with the findings of Kuijpers (1985), who mapped sedimentation rate indices on the

NAP based on seismic data. He found generally higher rates to the north and west and lower rates to the south and east. Rates for the area near the GC-1 site were on the order of decimeters/ky.

Figure 6 presents an excess ^{230}Th profile for Box Core 32 (BC32), taken to the SW of GC-1 (see Figure 2). Kuijpers (1985) found no evidence of turbidites deposited in this box core and the profile does not suggest the presence of turbidites. Indeed, $^{226}Ra/^{230}Th$ activity ratios in BC32 (Table 2) follow a predictable pattern and increase to about one by 30 cm. Therefore a pelagic sedimentation rate has been calculated for this core and found to be 0.17 cm/ky. Kuijpers (1985), using a calcium carbonate spike which he interpreted as corresponding to an age of 10,000 years BP, calculated a sedimentation rate for BC32 of 2.5-3.0 cm/ky. The difference between this rate and that calculated from the ^{230}Th profile may be due to Kuijpers' (1985) approximation of the age corresponding to the $CaCO_3$ spike. The rate calculated in this study is in better agreement with the 0.5 cm/ky rate calculated by Cochran and Livingston (1984) for BC02 from the excess ^{230}Th profile. Although the rate at BC02 is higher than for BC32, BC02 is located to the NW of BC32 (Figure 2), and sedimentation rates appear to decrease to the south and east in this region (Duin, 1985).

B. Radionuclide Balances

1. ^{210}Pb Balance

a. Water Column Removal

Nares water column ^{210}Pb and ^{226}Ra data are given in Table 8 and plotted in Figure 7. As was previously stated, the ^{226}Ra

profile was calculated from GEOSECS silica data using the method of Bacon et al. (1976). The deep water ^{226}Ra values generated from this method agree well with the values determined directly from NAP deep water. Given the errors associated with the ^{226}Ra values, only the NAP ^{226}Ra value at 4950 m is significantly less than its corresponding value generated from silica data. Even this difference is relatively small. The total flux of ^{210}Pb removed from the water column is determined by adding the atmospheric flux of ^{210}Pb to that obtained from the deficiency with respect to ^{226}Ra. Turekian et al. (1983) determined depositional fluxes of ^{210}Pb in New Haven, Connecticut and Bermuda to be 22.1 dpm/cm^2 and 38.4 dpm/cm^2, respectively. For the purposes of these calculations, an intermediate value of 30 dpm/cm^2 will be used. The in situ removal of ^{210}Pb is calculated by integrating the deficiency of ^{210}Pb with respect to ^{226}Ra. This flux is 37.2 dpm/cm^2, resulting in a total flux of ^{210}Pb through the water column of 67.2 dpm/cm^2.

b. Sediment Trap Fluxes

The annual flux of ^{210}Pb measured in a sediment trap at 4832 m on the NAP (Cochran and Hirschberg, 1985) was 15.8 dpm/cm^2. This compares well with the 15.7 dpm/cm^2 collected in a sediment trap at 4000 m on the Hatteras Abyssal Plain (see Table 5, Cochran and Hirschberg, 1984) and the 11.2 dpm/cm^2 collected by Bacon et al. (1985) near Bermuda at 3200 m. The ^{210}Pb measured on the NAP amounts to only 29% of the ^{210}Pb input to this depth. Earlier it was stated that radionuclides can be used to calibrate

sediment traps because frequently it is possible to construct exact geochemical balances for them (Knauer et al., 1979; Brewer et al., 1980). However, such calculations are meaningless when horizontal transport is thought to occur. The latter process will be discussed further below.

2. Sediment Inventories

Table 9 presents sediment inventories for ^{210}Pb on the NAP. The inventories vary by more than a factor of five. This is not surprising, considering the complexity of the sedimentary environment in this region and possible coring difficulties. No apparent relationship exists between the inventories and the core locations. Druffel et al. (1984), after studying several cores from a single site in the north central Pacific, found that even short-term tracers had significantly different profiles and inventories from core to core. Aller and DeMaster (1984) reached a similar conclusion following their work on cores in the Panama Basin.

C. Horizontal Transport

1. ^{210}Pb

The average excess ^{210}Pb sediment inventory for this area of the NAP is 7.83 dpm/cm^2. This represents only 12% of the ^{210}Pb input from the overlying water column and atmosphere. The sediment trap collected more ^{210}Pb than the sediments, but both fell quite short in recording the flux through the water column. An important point to make with regard to these comparisons is that different time scales are represented by the different flux

measurements. Water column removal measurements represent only one point in time. Sediment trap fluxes have been calculated from one years worth of sample collection. And sediment inventories reflect a much longer time scale. Interannual variations not recorded in the sediment trap fluxes and any time scale variations in water column removal fluxes will introduce uncertainties in the construction of geochemical balances. However, since long term water column and sediment trap data are unavailable, the balances are constructed with the limited data that is available.

In spite of this problem, it appears that ^{210}Pb is released to solution before it reaches the sediments (or deep sediment traps) and is transported horizontally away from the ocean interior to some other location, most likely the continental margins. Other researchers have recorded similar results. Bacon et al. (1976), failing to find significant vertical gradients in particulate ^{210}Pb in the deep sea, proposed that horizontal transport was carrying ^{210}Pb away from the ocean interior. Buesseler et al. (1985) collected excess ^{210}Pb inventory data along the U.S. North Atlantic shelf and slope. Deep sea inventories only recorded 45% of the expected ^{210}Pb flux while shallow water (<2000m) sediments recorded inventories that were greater than expected. Although Buesseler et al. did not believe that the excess inventories along the North American margin can completely account for the deficiencies observed in deep sea sediments, they did suggest that horizontal transport is removing ^{210}Pb away from the deep ocean interior. Bacon et al. (1985)

recorded a sediment trap ^{210}Pb flux in the Sargasso Sea that was only 30% of that which was expected and reached a similar conclusion. Buesseler et al. (1985) suggested that the eastern margin may be acting as a sink for ^{210}Pb. This is not unreasonable, since sediment surpluses in ^{210}Pb have been recorded along the eastern Pacific margins. It appears that strong upwelling and lateral transport result in an increased advective supply (and thus removal) of ^{210}Pb (Carpenter et al., 1981; Carpenter et al., 1982). Another possible sink could be the Mid-Atlantic Ridge, where ^{210}Pb sediment inventories are also greater than expected based on water column production (Nozaki et al., 1977).

It is thought that for ^{210}Pb, scavenging via uptake at ocean boundaries is at least as important a removal mechanism as scavenging by the vertical flux of particles in the ocean interior (Spencer et al., 1981; Anderson et al., 1983b; Bacon, 1984). ^{210}Pb could be preferentially scavenged at ocean margins by several mechanisms, including 1)co-precipitation with Mn and Fe oxides forming at the sediment/water interface, 2)resuspension (physical or biological) from the sediments resulting in increased adsorptive surfaces, and 3)increased scavenging due to greater primary production and higher particle flux (Bacon, 1984; Anderson et al., 1983a; Thomson and Turekian, 1976).

At this point it is not clear which of these factors, or others, is most important. However Spencer et al. (1981) calculated the extent to which boundary removal may be important. They modelled the dissolved ^{210}Pb distribution in the north equatorial Atlantic Ocean including a term for boundary

scavenging. The relative importance of sinks included in the model was 55% by radioactive decay, 25% by biological uptake, 12% by in situ adsorption, and 8% by boundary uptake. Both Bacon et al. (1976) and Cochran et al. (1983) showed that the distribution of $^{210}Pb/^{226}Ra$ activity ratios away from oceanic margins was consistent with horizontal eddy diffusion and boundary uptake.

Unfortunately, very little ^{210}Pb inventory data exist for boundary areas surrounding this region of the western North Atlantic. It is therefore difficult to determine where the ^{210}Pb is transported to from the deep sea above the NAP. Earlier it was stated that large excesses of ^{230}Th had been found on the Bermuda Rise (Bacon and Rosholt, 1982). Although it is true that the partitioning between vertical and horizontal transport pathways will probably be different for different elements (Thomson et al., 1984), the chemical behavior of ^{230}Th and ^{210}Pb is similar. Perhaps the sediments of the Bermuda Rise also hold excess inventories for ^{210}Pb.

2. ^{230}Th

As ^{230}Th and ^{210}Pb behave similarly, it is of interest to construct a geochemical balance for ^{230}Th as well as ^{210}Pb. The water column production of ^{230}Th may be calculated from the uranium content and the $^{234}U/^{238}U$ activity ratio in seawater (3.3 ug/L and 1.14, respectively). The resulting production of ^{230}Th is 1367 dpm/cm^2 for a water column of 4832 m. A sediment trap at 4832 m on the NAP collected 1096 dpm/cm^2 of ^{230}Th. This is similar to values of 652 dpm/cm^2 collected at 3694 m in the

Sargasso Sea by Brewer et al. (1980) and 1291 dpm/cm^2 collected at 5367 m in the Sargasso Sea by Spencer et al. (1978).

To complete the ^{230}Th balance a sediment inventory must be calculated. This is more difficult for ^{230}Th than for ^{210}Pb on the NAP, since the deeper excess ^{230}Th profiles are more likely to be affected by turbiditic sedimentation. In the series of cores examined in this study, it appears that only BC32 can be used to calculate a sediment inventory. The excess ^{230}Th profile of BC32 (Figure 6) shows decreasing activities and the ^{226}Ra/^{230}Th activity ratio (Table 2) steadily increases to about one by 30 cm. A sediment inventory was calculated according to the following equation:

$$^{230}Th_{xs} \text{ inventory } (dpm/cm^2) = \rho S A_o/\lambda \qquad (9)$$

where: ρ = sediment dry bulk density, here taken to be 0.78 g/cm^3, for reasons explained previously

S = mean sediment accumulation rate, determined from Figure 6 to be 0.17 cm/ky

A_o = surface $^{230}Th_{xs}$ activity, taken from Table 1 to be 16.66 dpm/g

λ = ^{230}Th decay constant (9.2 x 10^{-6} y^{-1})

Substituting the values into equation 9 gives an inventory of 240 dpm/cm^2.

The results indicate that the sediment trap collected 80% of the water column production to 4832 m while the sediments only received 15% of the water column production to 5800 m (1647 dpm/cm^2). Cochran and Hirschberg (1984) constructed a ^{230}Th balance for the Hatteras Abyssal Plain. The results were similar

to those of this study, in that the sediment trap collected 77% of the input and the sediments collected 13% of the input. Thomson et al. (1984) found a shortfall of approximately 40% in the sediment inventories of three cores on the NAP. Bacon et al. (1985) recorded a deficiency in sediment trap fluxes and concluded that only two-thirds of the ^{230}Th production was vertically removed from the water column.

As with ^{210}Pb, it appears that ^{230}Th in the ocean interior is subject to horizontal transport, perhaps in association with particles. It is thought that the sinks for ^{230}Th lie along ocean margins (Anderson et al., 1983a), but the direction of transport out of this area is unclear. DeMaster (1981) found large accumulations of ^{230}Th in Antarctic sediments and he attributed them to horizontal transport from other oceans. Closer to the NAP, Bacon and Rosholt (1982) recorded nine times the expected ^{230}Th in sediments on the Bermuda Rise. While it is true that only one core was used to calculate a ^{230}Th sediment inventory and it is not certain that this core was unaffected by the deposition of turbidites, the gathering evidence supports the idea that ^{230}Th is horizontally carried away from the ocean interior.

V. Summary and Conclusions

The purpose of this project has been twofold; to examine and describe the history of sedimentation on the Nares Abyssal Plain and to construct geochemical balances in this region for the radionuclides ^{210}Pb and ^{230}Th. Towards the first end, extensive radiochemical work was done on a gravity core (GC-1) from the central NAP. The data revealed a complex sedimentary sequence. An excess ^{230}Th profile did not show a regular decrease in activity with depth, but rather indicated zones of high and low activity. Evidence of two relict redox fronts exists. The first occurs at 40 cm in GC-1, where a large diagenetic spike in solid phase manganese is observed. There is a corresponding excess in ^{226}Ra at this depth, and it is believed that ^{226}Ra mobilized in the sediment precipitated out with the manganese oxides that formed on the oxidized side of the redox boundary. The second possible redox front is located around 88 cm in the core, where elevated uranium activities and organic carbon concentrations (but no anomalous Mn) exist. In addition to the above findings, it has been shown that ^{230}Th and ^{226}Ra are in disequilibrium for most of the length of GC-1. These pieces of information, together with X-ray and core color data, suggest that the observed sedimentary sequence is the result of periods of turbiditic deposition. This conclusion is consistent with that of Thomson et al. (1984). It appears that the entire length of GC-1 has been affected by rapidly deposited turbidites. Sediment sequences of strictly pelagic origin are not evident. The source of these turbidites is

apparently the Hatteras shelf, with flows entering the NAP by way of the Vema Gap (Shipley, 1978; Tucholke, 1980) (Figure 1). There may also be smaller, more regional flows arising from the north on the Bermuda Rise or from the south on the Antilles Outer Ridge that complicate the sedimentary picture.

Given the erratic excess ^{230}Th profile determined for GC-1, no meaningful pelagic sedimentation rate could be calculated from this core. The radiochemical data indicate an overall sediment accumulation rate of up to 10-20 cm/ky. Box Core 32 did not appear to be affected by the deposition of turbidites, and a pelagic sedimentation rate of 0.17 cm/ky was calculated for this core. Other box core data were used to calculate particle mixing coefficients. Coefficients for five cores ranged from 0.01-0.23 cm^2/y.

The second goal of this study, the construction of geochemical balances for ^{210}Pb and ^{230}Th, compared water column removal, sediment trap fluxes, and sediment inventories. For ^{210}Pb, the sediment trap recorded only 29% of the expected flux and the sediments collected only 11% of the expected flux. Other researchers have recorded similar deficiencies (Buesseler et al., 1985; Bacon et al., 1985) and it is concluded that ^{210}Pb is being removed from the ocean interior by horizontal transport and carried to ocean boundaries, where it is scavenged through co-precipitation with Mn and Fe oxides, resuspension, and increased particle fluxes due to higher primary productivity. A deficiency in the excess ^{230}Th sediment inventory (15%) was also recorded, which suggests that this isotope is also horizontally transported

away from the ocean interior. The fact that the sediment trap collected 80% of the expected ^{230}Th but only 29% of the expected ^{210}Pb suggests that ^{210}Pb is more easily returned to solution during its descent through the water column.

REFERENCES

Aller, R.C. and D.J. DeMaster. 1984. Estimates of particle flux and reworking at the deep-sea floor using 234-Th/238-U disequilibrium. Earth and Planetary Science Letters. 67:308-318.

Anderson, R.F., M.P. Bacon and P.G. Brewer. 1983a. Removal of 230-Th and 231-Pa at ocean margins. Earth and Planetary Science Letters. 66:73-90.

Anderson, R.F., M.P. Bacon and P.G. Brewer. 1983b. Removal of 230-Th and 231-Pa from the open ocean. Earth and Planetary Science Letters. 62:7-23.

Bacon, M.P., D.W. Spencer and P.G. Brewer. 1976. 210-Pb/226-Ra and 210-Po/210-Pb disequilibria in seawater and suspended particulate matter. Earth and Planetary Science Letters. 32:277-296.

Bacon, M.P. and J.N. Rosholt. 1982. Accumulation rates of 230-Th, 231-Pa, and some transition metals on the Bermuda Rise. Geochimica et Cosmochimica Acta. 46(4)651-666.

Bacon, M.P. and R.F. Anderson. 1982. Distribution of thorium isotopes between dissolved and particulate forms in the deep sea. Journal of Geophysical Research. 87(C3)2045-2056.

Bacon, M.P. 1984. Radionuclide fluxes in the ocean interior. In: Global Ocean Flux Study: Proceedings of a workshop. National Academy Press. Washington, D.C. pp. 180-205.

Bacon, M.P., C.-A. Huh, A.P. Fleer and W.G. Deuser. 1985. Seasonality in the flux of natural radionuclides and plutonium in the deep Sargasso Sea. Deep-Sea Research. 32(3)273-286.

Bonatti, Enrico, D.E. Fisher, O. Joensuu and H.S. Rydell. 1971. Postdepositional mobility of some transition elements, phosphorus, uranium and thorium in deep sea sediments. Geochimica et Cosmochimica Acta. 35:189-201.

Brewer, P.G., Y. Nozaki, D.W. Spencer and A.P. Fleer. 1980. Sediment trap experiments in the deep North Atlantic: isotopic and elemental fluxes. Journal of Marine Research. 38(4)703-728.

Buesseler, K.O., H.D. Livingston and E.R. Sholkovitz. 1985. 239,240-Pu and excess 210-Pb inventories along the shelf and slope of the northeast USA. Earth and Planetary Science Letters. 76:10-22.

Carpenter, M.S.N., S. Colley, H. Elderfield, H.A. Kennedy, J. Thomson and T.R.S. Wilson. 1983. Geochemistry of the near surface sediments of the Nares Abyssal Plain. Institute of Oceanographic Sciences. Report no. 174. 66 pp.

Carpenter, R., J.T. Bennett and M.L. Peterson. 1981. 210-Pb activities in and fluxes to sediments of the Washington continental slope and shelf. Geochimica et Cosmochimica Acta. 45:1155-1172.

Carpenter, R., M.L. Peterson and J.T. Bennett. 1982. 210-Pb-derived sediment accumulation and mixing rates for the Washington continental slope. Marine Geology. 48:135-164.

Cochran, J.K. and J.K. Osmond. 1976. Sedimentation patterns and accumulation rates in the Tasman Basin. Deep-Sea Research. 23(3)193-210.

Cochran, J.K. 1982a. The oceanic chemistry of the U- and Th-series nuclides. In: Uranium Series Disequilibrium: Applications to Environmental Problems, M. Ivanovich and R.S. Harmon, eds. Clarendon Press. Oxford. pp. 384-430.

Cochran, J.K. 1982b. The use of naturally occurring radionuclides as tracers for biologically related processes in deep sea sediments. In: The Environment of the Deep Sea, Rubey Volume II, W.G. Ernst, J. Morin, eds. Prentice Hall. pp. 55-72.

Cochran, J.K. 1980. The flux of 226-Ra from deep-sea sediments. Earth and Planetary Science Letters. 49:381-392.

Cochran, J.K. and S. Krishnaswami. 1980. Radium, thorium, uranium, and 210-Pb in deep-sea sediments and sediment pore waters from the north equatorial Pacific. American Journal of Science. 280:849-889.

Cochran, J.K., M.P. Bacon, S. Krishnaswami and K.K. Turekian. 1983. 210-Po and 210-Pb distributions in the central and eastern Indian Ocean. Earth and Planetary Science Letters. 65:433-452.

Cochran, J.K. 1985. Particle mixing rates in sediments of the eastern equatorial Pacific: evidence from 210-Pb, 239,240-Pu and 137-Cs distributions at MANOP sites. Geochimica et Cosmochimica Acta. 49:1195-1210.

Cochran, J.K. and D.J. Hirschberg. 1984. Radiochemical studies in support of the low level waste ocean disposal program (East Coast site). Final Report. Sandia contract 58-3521. 28 pp.

Cochran, J.K. and H.D. Livingston. 1984. Radiochemical studies of Nares Abyssal Plain sediments. Manuscript.

Cochran, J.K. and D.J. Hirschberg. 1985. Radiochemical studies at the Nares Abyssal Plain: natural radionuclide results. 1985 Annual Report. Sandia Nat'l Lab. Contract 25-8717. 29 pp.

Cochran, J.K. and H.D. Livingston. 1985. Radiochemical studies of Nares Abyssal Plain sediments. In: Geological Studies of the Southern Nares Abyssal Plain, western North Atlantic: Progress Report 1984, A. Kuijpers, ed. Ministry of Economic Affairs of the Netherlands. pp. 95-106.

Colley, S. and J. Thompson. Recurrent uranium relocations in distal turbidites emplaced in pelagic conditions. Manuscript.

Colley, S., J. Thompson, T.R.S. Wilson and N.C. Higgs. 1984. Post-depositional migration of elements during diagenesis in brown clay and turbidite sequences in the North East Atlantic. Geochimica et Cosmochimica Acta. 48:1223-1235.

de Lange, G.J., J. Ebbing, T. van Zessen and M. van Alphen. 1985. Chemical composition of interstitial water in cores from the Nares Abyssal Plain (western North Atlantic). In: Geological Studies of the Southern Nares Abyssal Plain, western North Atlantic: Progress Report 1984, A. Kuijpers, ed. Ministry of Economic Affairs of the Netherlands. pp. 81-94.

DeMaster, D.J. 1981. The supply and accumulation of silica in the marine environment. Geochimica et Cosmochimica Acta. 45:1715-1732.

DeMaster, D.J. and J.K. Cochran. 1982. Particle mixing rates in deep-sea sediments determined from excess 210-Pb and 32-Si profiles. Earth and Planetary Science Letters. 61:257-271.

Deuser, W.G. 1984. Seasonality of particle fluxes in the ocean's interior. In: Global Ocean Flux Study: Proceedings of a workshop. Nat'l Academy Press. Washington, D.C. pp. 221-236.

Druffel, E.R.M., P.M. Williams, H.D. Livingston and M. Koide. 1984. Variability of natural and bomb-produced radionuclide distributions in abyssal red clay sediments. Earth and Planetary Science Letters. 71:205-214.

Duin, E.J.Th. 1985. Geophysics of the southern Nares Abyssal Plain, western North Atlantic. In: Geological Studies of the Southern Nares Abyssal Plain, Western North Atlantic, Progress Report 1984, A. Kuijpers, ed. Ministry of Economic Affairs of the Netherlands. pp. 5-38.

Dymond, J. 1984. Sediment traps, particulate fluxes, and benthic boundary layer processes. In: Global Ocean Flux Study: Proceedings of a workshop. Nat'l Academy Press. Washington, D.C. pp. 260-284.

Dymond, J. and R. Collier. 1986. 1985 Annual Report: Subseabed Disposal Program. Sandia Nat'l Lab. Contract 25-8715. 23 pp.

Flynn, W.W. 1968. The determination of low levels of 210-Po in environmental materials. Analytica Chimica Acta. 43:221-227.

Freeman, T.J. 1985. Nondestructive bulk density measurement of cores from the Nares Abyssal Plain. In: Geological Studies of the Southern Nares Abyssal Plain, Western North Atlantic, Progress Report 1984, A. Kuijpers, ed. Ministry of Economic Affairs of the Netherlands. pp. 113-118.

Goldberg, E.D. 1954. Marine geochemistry 1, chemical scavengers of the sea. Journal of Geology. 62:249-265.

Kadko, D. 1980. A detailed study of some uranium series nuclides at an abyssal hill area near the East Pacific Rise at 8°45'N. Earth and Planetary Science Letters. 51:115-131.

Knauer, G.A., J.H. Martin and K.W. Bruland. 1979. Fluxes of particulate carbon, nitrogen, and phosphorus in the upper water column of the North East Pacific. Deep-Sea Research. 26:97-108.

Krishnaswami, S. and M.M. Sarin. 1976. The simultaneous determination of Th, Pu, Ra isotopes, 210-Pb, 55-Fe, 32-Si and 14-C in marine suspended phases. Analytica Chimica Acta. 83:143-156.

Kuijpers, A. 1985. Sediments of the southern Nares Abyssal Plain, western North Atlantic. In: Geological Studies of the Southern Nares Abyssal Plain, Western North Atlantic, Progress Report 1984, A. Kuijpers, ed. Ministry of Economic Affairs of the Netherlands. pp. 39-74.

Kuijpers, A. and E.J.Th. Duin. 1985. A sedimentation model for the southern Nares Abyssal Plain, based on sediment cores and 3.5 kHz echo-character. In: Geological Studies of the Southern Nares Abyssal Plain, Western North Atlantic, Progress Report 1984, A. Kuijpers, ed. Ministry of Economic Affairs of the Netherlands. pp. 75-80.

Livingston, H.D., D.R. Mann and V.T. Bowen. 1975. Analytical procedures for transuranic elements in seawater and marine sediments. In: Analytical Methods in Oceanography, T.R.P. Gibb, ed. pp. 125-138.

Mangini, A. and J. Dominik. 1979. Late Quaternary sapropel on the Mediterranean Ridge: U-budget and evidence for low sedimentation rates. Sedimentary Geology. 23:113-125.

Mathieu, G.G. 1977. 222-Rn and 226-Ra technique of analysis. Prog. Rep. ERDA Contract Ey 76-S-02-2185.

Moser, J.C., J. Dymond and K. Fischer. 1986. Multiple sampling OSU sediment trap: Technical design and function. Submitted to Limnology and Oceanography.

Muller, P.J. and E. Suess. 1979. Productivity, sedimentation rate, and sedimentary organic matter in the oceans-I. Organic carbon preservation. Deep-Sea Research. 26A:1347-1362.

National Research Council. 1984. Global Ocean Flux Study: Proceedings of a workshop. Nat'l Academy Press. Washington, D.C. 360 pp.

Nozaki, Y., J.K. Cochran and K.K. Turekian. 1977. Radiocarbon and 210-Pb distribution in submersible-taken deep-sea cores from project FAMOUS. Earth and Planetary Science Letters. 34:167-173.

Nozaki, Y., Y. Horibe and H. Tsubota. 1981. The water column distributions of thorium isotopes in the western North Pacific. Earth and Planetary Science Letters. 54:203-216.

Riley, J.P. and R. Chester. 1971. Introduction to Marine Chemistry. Academic Press. New York. 465 pp.

Shipley, T.H. 1978. Sedimentation and echo characteristics in the abyssal hills of the west-central North Atlantic. Geological Society of America, Bulletin. 89:397-408.

Spencer, D.W., P.G. Brewer, A. Fleer, S. Honjo, S. Krishnaswami and Y. Nozaki. 1978. Chemical fluxes from a sediment trap experiment in the deep Sargasso Sea. Journal of Marine Research. 36(3)493-523.

Spencer, D.W., M.P. Bacon and P.G. Brewer. 1981. Models of the distribution of 210-Pb in a section across the north equatorial Atlantic Ocean. Journal of Marine Research. 39(1)119-138.

Thomson, J. and K.K. Turekian. 1976. 210-Po and 210-Pb distributions in ocean water profiles from the eastern South Pacific. Earth and Planetary Science Letters. 32:297-303.

Thomson, J., M.S.N. Carpenter, S. Colley and T.R.S. Wilson. 1984. Metal accumulation rates in northwest Atlantic pelagic sediments. Geochimica et Cosmochimica Acta. 48:1935-1948.

Tucholke, B.E. 1980. Acoustic environment of the Hatteras and Nares Abyssal Plains, western North Atlantic Ocean, determined from velocities and physical properties of sediment cores. Journal of the Acoustical Society of America. 68(5)1376-1390.

Turekian, K.K., J.K. Cochran and D.J. DeMaster. 1978. Bioturbation in deep-sea deposits: rates and consequences. Oceanus. 21(1)34-41.

Turekian, K.K. and J.K. Cochran. 1978. Determination of marine chronologies using natural radionuclides. In: Chemical Oceanography, Vol. 7, J.P. Riley and R. Chester, eds. Academic Press. New York. pp. 313-360.

Turekian, K.K., L.K. Benninger and E.P. Dion. 1983. 7-Be and 210-Pb total deposition fluxes at New Haven, Connecticut and at Bermuda. Journal of Geophysical Research. 88(C9)5411-5415.

Wilson, T.R.S., J. Thompson, D.J. Hydes, S. Colley, F. Culkin and J. Sorenson. 1986. Oxidation fronts in pelagic sediments: diagenetic formation of metal-rich layers. Science. 232:972-975.

Depth in core (cm)	^{232}Th	^{230}Th	$^{230}Th_{xs}$	^{238}U	^{234}U	$^{210}Pb^{*}$	^{226}Ra	$^{210}Pb_{xs}^{*}$
0-1	3.61±.34	18.20±1.25	16.66±1.25	1.60±.10	1.54±.10	11.43±.82	3.23±.32	8.20±.76
1-2	3.46±.34	16.11±1.15	14.72±1.15	1.54±.10	1.39±.10	6.55±.71	3.66±.37	2.89±.61
2-3	4.43±.57	18.78±2.15	17.39±2.15	1.69±.10	1.39±.10	7.26±.77	4.41±.44	2.85±.63
4-5	3.65±.49	15.49±1.59	14.02±1.59	1.54±.10	1.47±.10	5.59±.82	4.93±.49	0.66±.66
6-7	3.09±.20	13.60±0.70	12.13±0.71	1.53±.10	1.47±.10	5.87±.91	5.79±.58	0.08±.70
10-12	2.88±.50	12.49±1.49	11.00±1.49	1.49±.10	1.49±.10		6.58±.66	
18-20	3.01±.42	10.67±1.16	9.06±1.16	1.61±.10	1.61±.10		6.60±.66	
28-32	3.11±.34	4.39±0.42	2.99±0.43	1.54±.10	1.40±.10		5.62±.56	

Table 1: Radiochemical data for Nares Abyssal Plain sediments.
Core BC32: 22°13.9'N, 63°15.5'W
Date collected: February 1984
Water depth: 5800 m
Activities are expressed in dpm/g
* Decay corrected to the time of collection

Depth in core (cm)	$^{230}Th_{xs}/^{232}Th$	$^{210}Pb/^{226}Ra$	$^{234}U/^{238}U$	$^{226}Ra/^{230}Th$
0-1	4.61±.56	3.54±.43	0.96±.09	0.18±.02
1-2	4.25±.53	1.79±.27	0.90±.09	0.23±.03
2-3	3.93±.70	1.65±.24	0.82±.08	0.23±.03
4-5	3.84±.67	1.13±.20	0.95±.09	0.32±.05
6-7	3.93±.34	1.01±.19	0.96±.09	0.43±.05
10-12	3.82±.84		1.00±.09	0.53±.08
18-20	3.01±.57		1.00±.09	0.62±.09
28-32	0.96±.17		0.91±.09	1.28±.18

Table 2: Activity ratios for Nares Abyssal Plain sediments.
Core BC32: 22°13.9'N, 63°15.5'W

Table 3: Radiochemical Data for Nares Abyssal Plain Sediments. Box core results. Activities are expressed in dpm/g
* Corrected to time of collection

Depth in core (cm)	^{210}Pb*	^{226}Ra	$^{210}Pb_{xs}$*
BC 08: 23°32.8'N, 64°30.2'W			
0-1	15.8±0.7	2.9±0.1	12.9±0.7
1-2	5.4±0.2	3.3±0.1	2.1±0.2
2-3	3.9±0.3	3.3±0.1	0.6±0.3
BC 09: 23°12.0'N, 64°45.4'W			
0-1	7.5±0.3	3.9±0.1	3.6±0.3
1-2	5.0±0.2	3.5±0.1	1.5±0.2
2-3	5.5±0.3	3.4±0.1	2.1±0.3
BC 15: 23°16.7'N, 63°53.6'W			
0-1	6.1±0.2	3.2±0.1	2.9±0.2
1-2	4.4±0.1	3.9±0.1	0.5±0.1
2-3	4.3±0.3	3.5±0.1	0.8±0.3
BC 18: 22°41.5'N, 63°27.3'W			
0-1	5.0±0.2	3.7±0.1	1.3±0.2
1-2	5.0±0.1	4.0±0.1	1.0±0.1
2-3	4.6±0.3	4.0±0.1	0.6±0.3
BC 23: 23°01.4'N, 64°13.6'W			
0-1	11.5±0.4	2.7±0.1	8.8±0.4
1-2	4.9±0.3	3.1±0.1	1.8±0.3
2-3	3.8±0.3	3.3±0.1	0.5±0.3
BC 25: 22°57.7'N, 64°10.5'W			
0-1	8.5±0.4	3.0±0.1	5.5±0.4
1-2	4.7±0.2	3.0±0.1	1.7±0.2
2-3	4.6±0.3	3.5±0.1	1.1±0.3

Note: The 0-1 and 1-2 cm depth interval results are from Cochran and Livingston (1984).

Table 4: Mixing Coefficients in Nares Abyssal Plain Sediments

	Mixing Coefficient (cm^2/y)				
	BC08	BC18	BC23	BC25	BC32
Cochran and Livingston (1984)	.01	.17	.01	.03	.06
This study	.01	.23	.02	.05	.08

Depth in core (cm)	Dry bulk density*	$\%H_2O$	Percent Org. C.	^{232}Th	^{230}Th	$^{230}Th_{xs}$	^{238}U	^{234}U	^{210}Pb	^{226}Ra
6.5-8.5	0.78	46.3	.32	3.73±.41	7.99±.75	6.52±.76	1.62±.10	1.47±.10	4.15±.14	3.91±.39
19-21	0.91	42.4	.31	3.21±.19	4.50±.28	2.71±.32	1.67±.16	1.79±.16	5.20±.17	5.07±.51
29-31	0.92	45.4	.30	3.25±.49	5.17±.74	3.83±.75	1.59±.16	1.34±.09	3.40±.12	3.25±.33
39-41	0.95	36.9	.26	3.02±.49	3.73±.57	2.31±.58	1.77±.16	1.42±.10	7.97±.24	9.48±.95
57-59	0.72	48.7	.24	3.48±.73	5.33±1.05	3.71±1.05	1.60±.10	1.62±.10	3.30±.14	3.32±.33
74-76	1.07	36.5	.28	2.86±.18	3.60±.19	1.77±.25	1.71±.16	1.83±.16	2.82±.11	2.94±.29
87-89	0.65	53.0	.44	4.49±.35	6.60±.52	4.74±.53	2.17±.17	1.86±.10	3.93±.16	4.49±.45
97-99	0.87	41.5	.34	3.08±.26	8.27±.54	6.04±.55	2.25±.10	2.23±.10	4.05±.24	4.29±.43
117-119	1.10	32.4	.13	2.53±.18	2.09±.10	0.70±.13	1.47±.09	1.39±.09	2.08±.16	2.02±.20
134-136	1.22	34.8	.29	2.62±.18	2.28±.18	1.05±.20	1.45±.10	1.23±.09	2.27±.15	2.65±.27
150-152	0.69	49.6	.31	3.14±.34	3.24±.34	1.86±.35	1.66±.16	1.38±.09	2.94±.21	2.08±.21
166-168	0.78	47.1	.26	3.29±.26	4.70±.28	3.32±.32	1.61±.16	1.38±.16	3.18±.19	3.67±.37

Table 5: Radiochemical data for Nares Abyssal Plain sediments.
Core GC1: 23°12.0'N, 63°58.5'W
Date collected: September 1984
Water depth: 5800 m
Activities are expressed in dpm/g
* g dry sediment/cm^3 wet sediment
Organic carbon data are from Dymond and Collier (1986)

Depth in core (cm)	$^{230}Th_{xs}/^{232}Th$	$^{210}Pb/^{226}Ra$	$^{234}U/^{238}U$	$^{226}Ra/^{230}Th$
6.5-8.5	1.75±.28	1.06±.11	0.91±.08	0.49±.07
19-21	0.84±.11	1.03±.11	1.07±.14	1.13±.13
29-31	1.18±.29	1.05±.11	0.84±.10	0.63±.11
39-41	0.76±.23	0.84±.09	0.80±.09	2.54±.46
57-59	1.07±.38	0.99±.11	1.01±.09	0.62±.14
74-76	0.62±.10	0.96±.10	1.07±.14	0.82±.09
87-89	1.06±.14	0.88±.10	0.86±.08	0.68±.09
97-99	1.96±.24	0.94±.11	0.99±.06	0.52±.06
117-119	0.28±.06	1.03±.13	0.95±.08	0.97±.11
134-136	0.40±.08	0.86±.10	0.85±.09	1.16±.15
150-152	0.59±.13	1.41±.17	0.83±.10	0.64±.09
166-168	1.01±.13	0.87±.10	0.86±.13	0.78±.09

Table 6: Activity ratios for Nares Abyssal Plain sediments.
Core GC1: $23^{o}12.0'N$, $63^{o}58.5'W$

Table 7: Iron and Manganese Data for Nares Abyssal Plain Sediments. Core GC1: 23°12.0'N, 63°58.5'W

Depth in core (cm)	Mn (ppm)	Fe (%)
6.5-8.5	1372±27	5.73±.17
19-21	2768±55	5.89±.18
22.5-24.5	1488±30	4.55±.14
29-31	883±18	5.84±.18
39-41	4830±97	4.45±.13
43-45	1202±24	4.01±.12
57-59	881±18	6.37±.19
61-63	959±19	3.43±.10
67-69	528±11	4.12±.12
70-72	495±10	2.59±.08
74-76	653±13	3.77±.11
82-84	571±11	2.40±.07
87-89	766±15	5.91±.18
97-99	651	3.53
"	681	3.83
"	642 Ave: 656±13	3.60 Ave: 3.61±.11
"	653	3.54
"	655	3.56
102-104	718±14	5.59±.17
117-119	598±12	3.21±.10
127-129	909±18	5.67±.17
131-133	937±19	5.51±.17
134-136	728±15	3.78±.11
150-152	1020±20	4.90±.15
154-156	979±20	4.65±.14
158-160	762±15	2.55±.08
166-168	1179±24	5.32±.16

Standards		Ref. Value		Ref. Value
NBS	813±16	785±97	10.27±.31	11.30±1.2
MESS-1	508±10	513±25	2.33±.07	3.03±.17

Table 8: ^{210}Pb and ^{226}Ra in seawater, Nares Abyssal Plain

Depth (m)	^{210}Pb (dpm/100kg)[1]	^{226}Ra (dpm/100kg)[2]
834	12.2±1.0	-
1060	7.9±1.0	-
1442	7.1±0.7	-
2550	9.2±2.2	-
3331	7.5±0.7	-
4124	6.4±0.6	-
4950	-	14.59±1.46*
4994	6.1±0.6	-
5300	-	18.48±1.85*
5449	-	18.48±1.85*
5681	7.6±0.6	-
5682	-	17.02±0.97**
5712	-	18.00±0.97**
5788	6.8±0.5	-

1 ^{210}Pb samples were taken in September 1984 (R/V Endeavor cruise EN-121). Location: 23°12.0'N, 63°58.9'W

2 ^{226}Ra samples were taken in September 1985 (R/V Endeavor cruise EN-137). Sample analyses were done by D. Hirschberg, MSRC, SUNY

* Location: 23°12.9'N, 64°7.7'W

** Location: 23°17.8'N, 64°10.1'W

Table 9: ^{210}Pb Sediment Inventories, Central NAP

Box Core	Inventory (dpm/cm^2)
*BC 02	9.54
BC 08	12.12
BC 09	6.24
BC 15	3.35
BC 18	2.26
BC 23	8.66
BC 25	6.79
BC 32	13.65
Average:	7.83
Sediment trap (4832 m):	15.80
Removal from water column:	67.20

* Radiochemical analysis was done by Cochran and Livingston (1984).

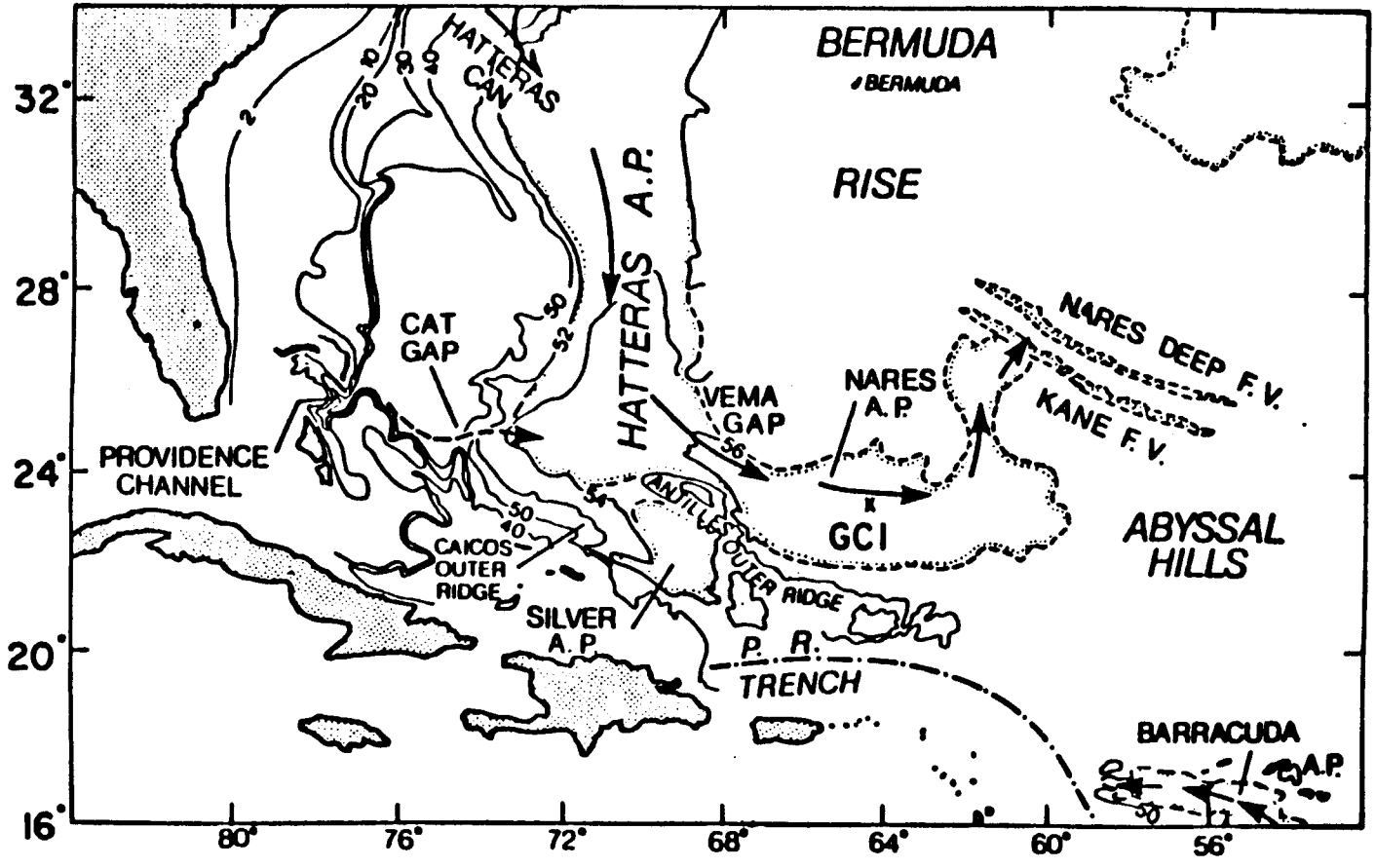

Figure 1: Map of western North Atlantic showing study area and location of Gravity Core 1. Arrows indicate turbidity paths. Reprinted with permission from B. E. Tucholke (1980).

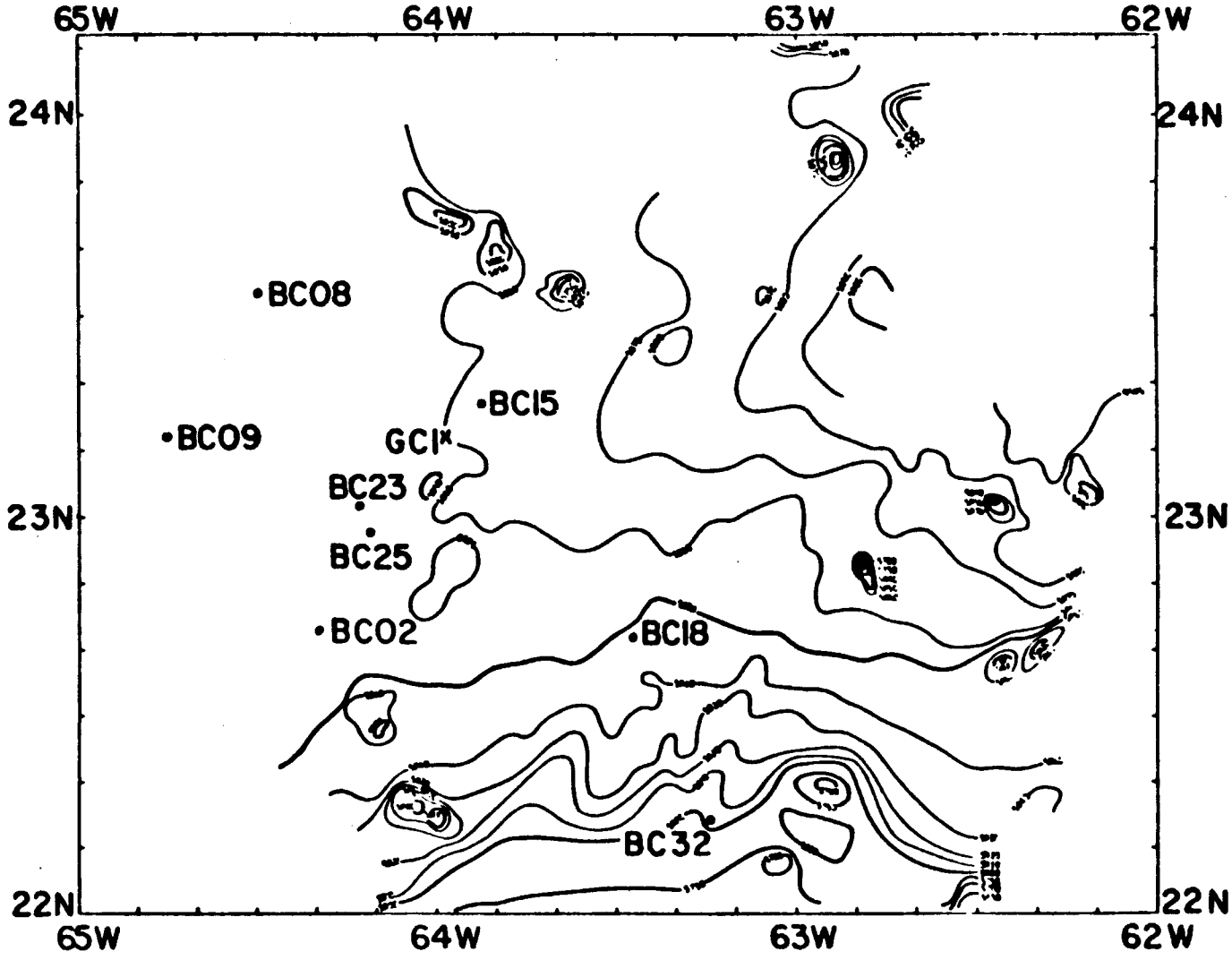

Figure 2: Bathymetric map of central Nares Abyssal Plain showing locations of box cores and gravity core. From Duin (1985).

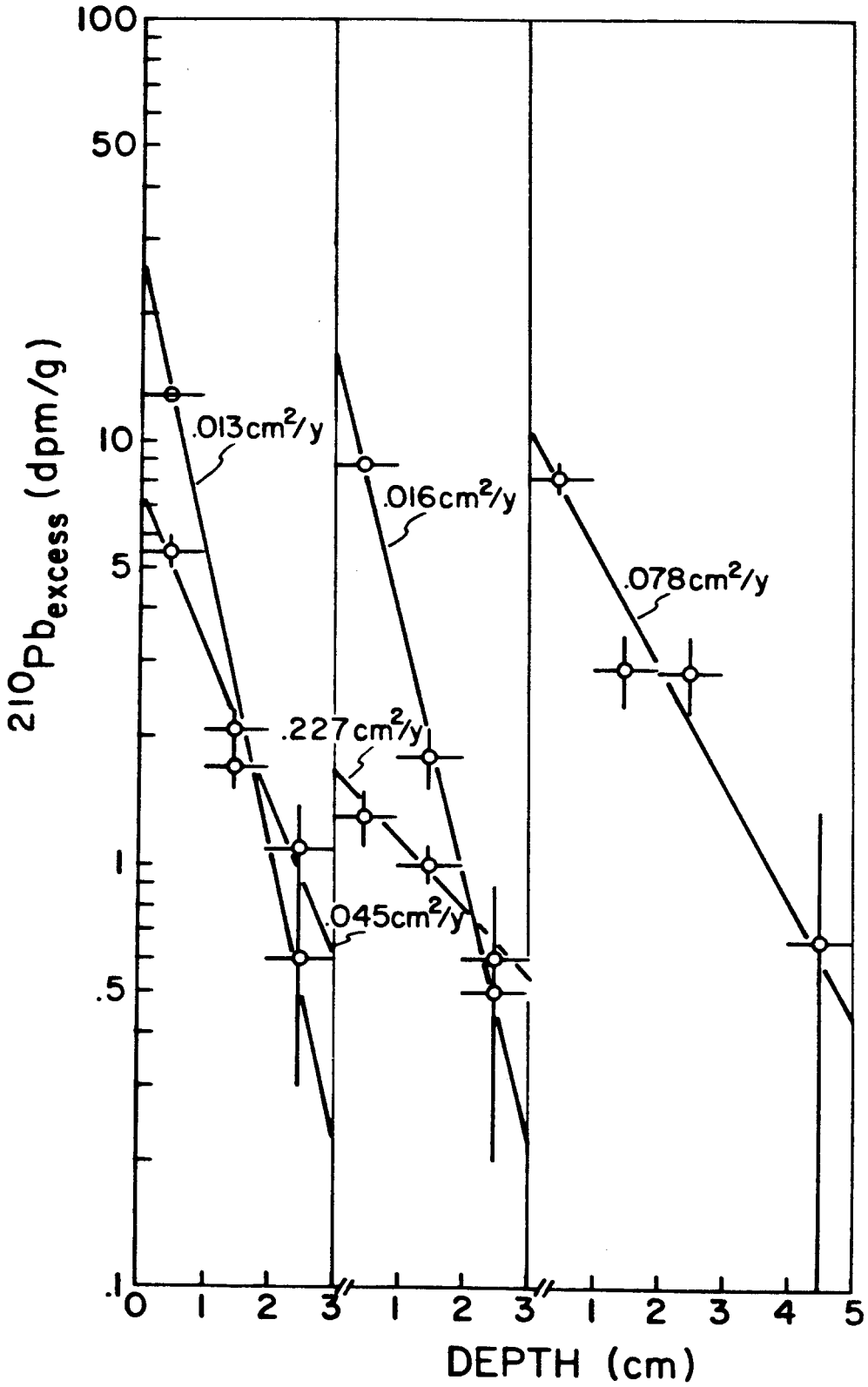

Figure 3: $^{210}Pb_{excess}$ profiles for box cores. Mixing coefficients (D_B) were calculated from the slopes of best fit lines. Decay corrected to the time of correction.

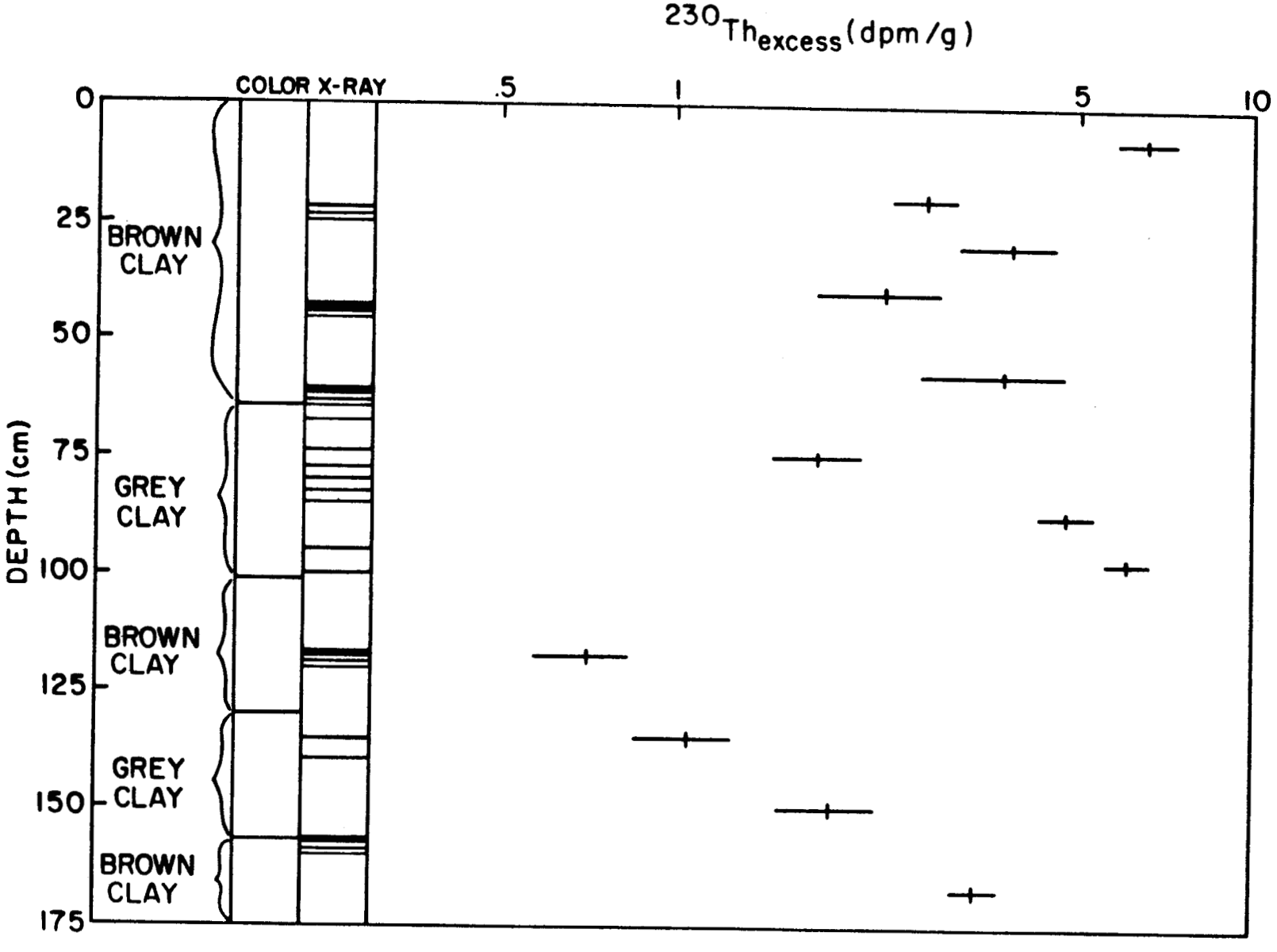

Figure 4: $^{230}Th_{excess}$ profile for Gravity Core 1, along with color and X-ray information. Shading in the X-ray sequence indicated higher density sediment layers.

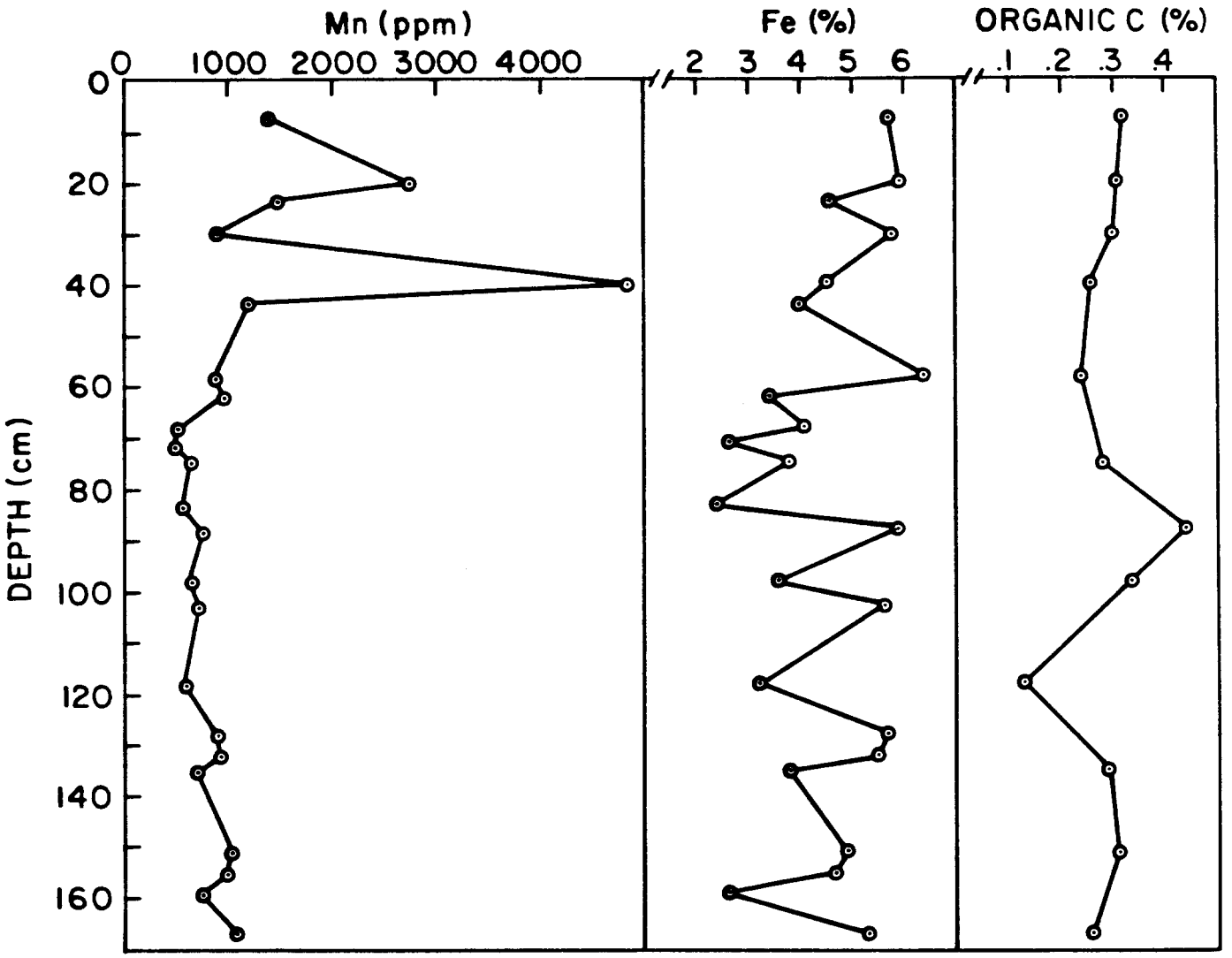

Figure 5: Manganese, iron, and organic carbon profiles for Gravity Core 1. Organic carbon data are from Dymond and Collier (1986).

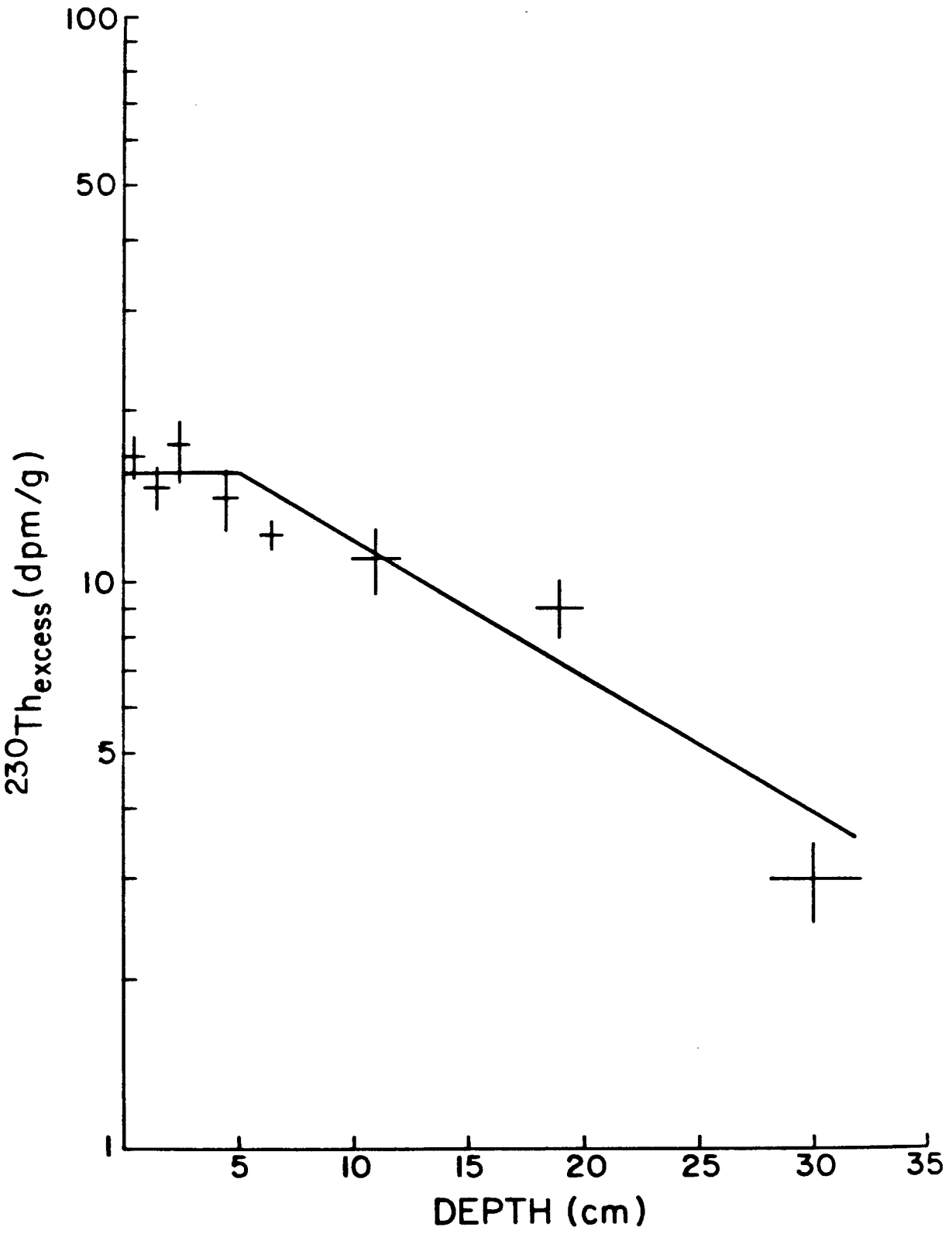

Figure 6: $^{230}Th_{excess}$ profile for BC32.

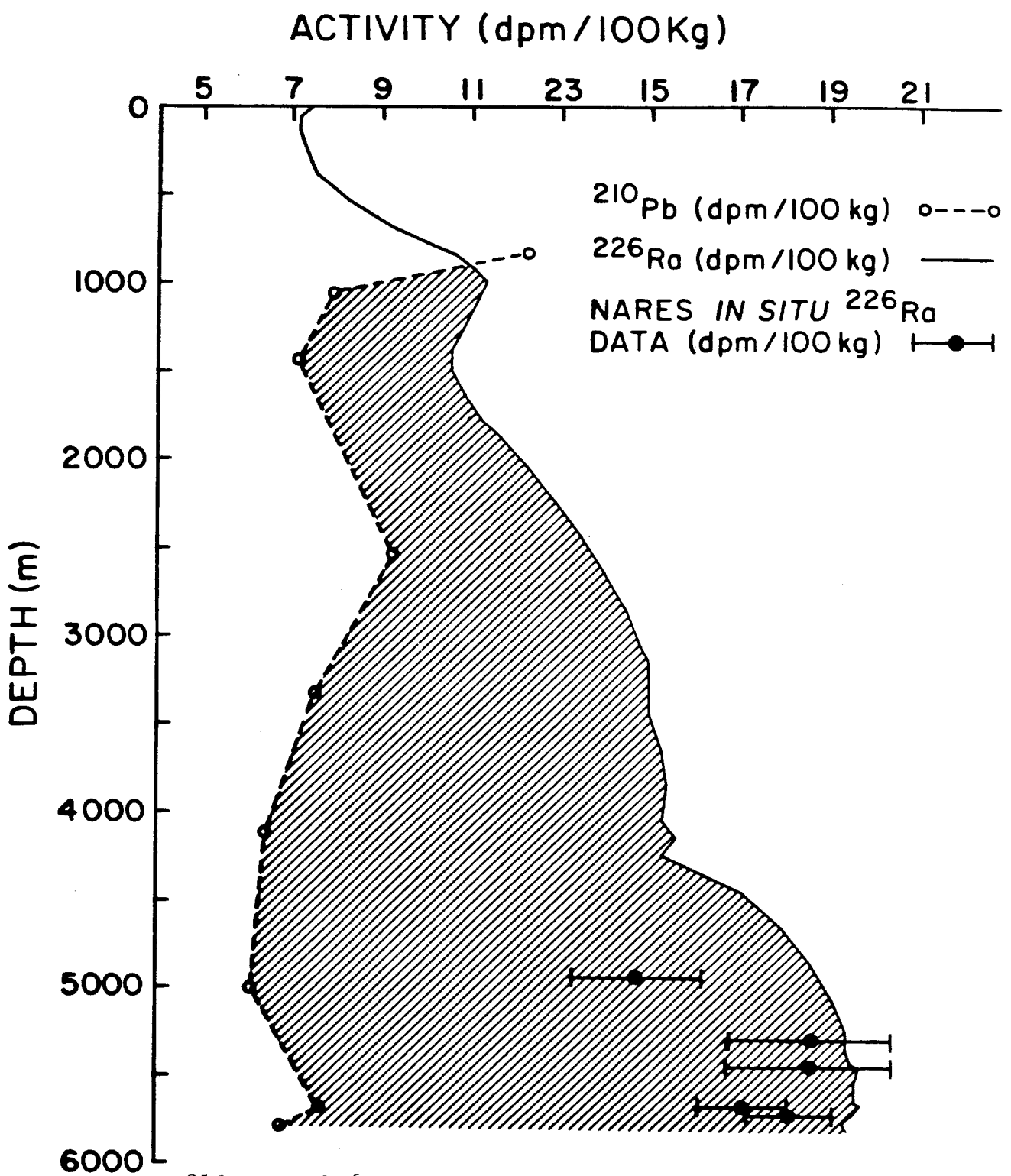

Figure 7: ^{210}Pb and ^{226}Ra seawater profiles for NAP. ^{226}Ra profile was generated from silica data (GEOSECS station 32) using the equation Ra = 6.91 + .217*Sil (Bacon et al., 1976). Hatched area was used to calculate the ^{210}Pb flux through the water column.

Appendix B

Determination of Transuranic and Thorium Isotopes in Ocean Water: in Solution and in Filterable Particles.

H. D. Livingston

Woods Hole Oceanographic Institution, Woods Hole, MA 02543, U.S.A.

and

J. K. Cochran

State University of New York, Stony Brook, NY 11794, U.S.A.

Submitted to
JOURNAL OF RADIOANALYTICAL AND NUCLEAR CHEMISTRY

9/25/86

Determination of Transuranic and Thorium Isotopes in Ocean Water: in Solution and in Filterable Particles.

H. D. Livingston

Woods Hole Oceanographic Institution, Woods Hole, MA 02543, U.S.A.

and

J. K. Cochran

State University of New York, Stony Brook, NY 11794, U.S.A.

A sensitive technique for the measurement of dissolved and particulate actinide concentrations and water column distributions is described. Pu, Am, and Th isotopes are collected using large-volume, wire-mounted electrical pumping systems. Particles were removed by filtration, and actinides by absorption on MnO_2-coated filters. The very large volumes processed (up to 4000 liters) result in very sensitive and precise concentration measurements after analyses of the samples by standard radiochemical and alpha spectrometric techniques.

Introduction

Studies of the oceanic distributions of reactive elements have direct relevance to the nature of the "scavenging" process which removes such substances from the oceans. The actinide elements represent a useful

group for studies of oceanic scavenging because they span a range of chemical reactivities, have well characterized source functions and include both steady state and transient radionuclide tracers. The former are naturally occurring members of the U and Th decay series. The latter are the transuranics introduced to the oceans chiefly by the global fallout of debris from atmospheric nuclear weapons tests.

Recent developments of scavenging models, based on radionuclide studies, have emphasized the interconnected roles played by large, rapidly sinking particles and small, slowly sinking particles on reactive nuclide transports and removal (Bacon et al. 1985). Equilibria (or disequilibria) and transformations between the various particle types and seawater are likely to be critical components to actinide scavenging processes. The standing crop of suspended small particles represents the major particulate reservoir in oceanic water masses and is in dynamic equilibrium with the dissolved phases and large sinking particle phases. The large particle/small particle interaction is likely to be relatively complex and involves both particle aggregation and disaggregation.

For many of the actinides, oceanic concentrations of both particle and solution phases are low enough on a volume basis to make their measurement difficult. To some extent, this limitation has been overcome by the development of highly sensitive analytical techniques such as low level alpha spectrometry (on radiochemically purified actinide isolates) or mass spectrometry (for plutonium isotopes). In our studies, the low concentration limitation has been overcome by the use of sampling techniques which collect enough actinide bearing material from the various phases to permit reliable measurement by 'state of the art' analytical

techniques.

The sampling technique for the small particle and soluble phases uses electrically powered, wire-mounted pumps to collect particulate actinides on filters and solution phase actinides on MnO_2 impregnated absorbers. This technique is essentially a modification of the one described by Mann et al. (1984) and used in North Pacific transuranic studies by Livingston et al. (1986). The critical modification is the use of inert polypropylene fiber filter cartridges for filtration and as a support for the MnO_2 absorber phase - instead of the cotton fiber cartridges used in the above studies. This change was a consequence of the cotton fiber cartridges having unacceptable blank levels of Th isotopes. As noted by Mann et al. (1984), it has not been possible to load preformed MnO_2 on polypropylene fiber filter cartridges. We used an alternative MnO_2 impregnation technique following Moore (1976) but somewhat modified (A. P. Fleer, personal communication). This technique involves the bonding to the fibers of MnO_2 formed by their exposure to a solution of $KMnO_4$.

Methods

Our actinide scavenging studies have been conducted at two locations in the Western North Atlantic. The first location is at the Nares Abyssal Plain at about 23°12'N, 63°59'W; the second is at the Hatteras Abyssal Plain at about 32°46'N, 70°50'W. Both of these locations are in the interior of the North Atlantic Basin and are oceanographic settings fairly typical of a mid-gyre, i.e. oligotrophic, with low particle fluxes and suspended particle concentrations.

The suspended particulate and dissolved actinides were sampled using electrically powered pumping systems attached to the ship's hydro-wire or

trawl-wire. These are battery-powered pumps and we have deployed as many as five systems simultaneously at different water depths. The older version of the pumping system is a modification of a design previously reported (Winget et al., 1982). The modification involves the replacement of the previously used Jabsco Products pump with a more reliable Flotec pump (Model R2, Flotec Inc., Norwalk, California, U.S.A.) which operates effectively using substantially less electrical power than the Jabsco pump. Because of the lower power requirements of this pump we designed a newer version of this pumping system which is smaller, lighter and has greater flexibility in designing configurations of filters and absorbers. The pumps are manufactured by Oceanic Industries Inc., Monument Beach, Massachusetts, U.S.A. The start and stop controls are controlled by pre-set timers mounted in each system.

The filters and MnO_2 absorbers are based on 1μm filter cartridges (AMF Cuno, Microwynd II cartridge #DPPPY), mounted inside their housings as used by Mann and Casso (1984) as prefilters. The sequence of components consists of four units connected in series. A prefilter first collects suspended particles. Two MnO_2 impregnated filter cartridges then adsorb actinides from the filtered water stream. Finally, the stream exits through a flow meter which provides a measure of the volume of water processed. The efficiency of actinide absorption by the MnO_2 absorbers is determined from the relative amounts collected on each absorber by the method described by Mann et al., (1984). Basically the collection efficiency is derived from the relationship:

$$\text{Collection Efficiency} = 1 - \frac{\text{Activity on 2nd absorber}}{\text{Activity on 1st absorber}}$$

As noted above, blank problems for Th isotopes forced us to use polypropylene fiber filter cartridges instead of the cotton fiber type used previously when only transuranic nuclides were being measured (Mann et al., 1984; Livingston et al., 1986). The technique for impregnating the filter cartridge with MnO_2 is rather time-consuming because of the necessity of removal of an anti-wetting surfactant. This is achieved by successive soakings in strong detergent and NaOH and HCl baths (each 1.0M). Following this treatment the cartridges were washed with distilled water and left in a saturated, hot $KMnO_4$ solution for 24 hours and again thoroughly rinsed with distilled water. At sea, water was pumped through the systems at flow-rates generally at the high end of the 2-7 liters/minute used. Sample sizes collected at these flow-rates ranged up to 4000 liters.

All samples were analyzed radiochemically by essentially standard radiochemical methods. Each cartridge sample was first dried at 110°C then ashed at 450°C for about 24 hours. The ash was dissolved in about 200ml of HNO_3 (8.0M) in the presence of ^{229}Th, ^{243}Am and ^{242}Pu chemical yield tracers. Following addition of $NaNO_2$ (0.1g per 10ml solution) to oxidise Pu, the solution was passed through an anion exchange resin (20ml column; Biorad AG 1x8, 50-100 mesh). Th and Pu were retained and were eluted with HCl (12M) and HCl/NH_4I (12M; 0.03M), respectively. Am passes through this column and was retained for further purification. Th was subsequently purified on a smaller anion exchange column. Pu and Am were further purified and all actinides electroplated as described by Livingston et al.,(1975) and measured by alpha spectrometry.

Results and discussion

Generally, we found that the MnO_2 absorbers which were used to collect dissolved actinides were very effective for the Th isotopes and ^{241}Am. From other experiences we know that they are equally effective in lanthanide isotope collection but seem to be less effective for elements which form stable complex species in seawater. Pu in particular is not collected efficiently or predictably (presumably due to its existence in complexed, higher oxidation states in seawater) - in contrast with our experience in the North Pacific using MnO_2 loaded cotton fiber filter cartridges (Livingston et al., 1986) where high Pu collection efficiencies were obtained. In Table 1 we list the collection efficiencies for Th and Am absorption during twelve deployments at various depths at the two sites where we have made these studies. The collection efficiencies tend to co-vary and average about 83%-84% based on all the data we have obtained. Given this result it should be theoretically possible to analyze both cartridges in combination - since collectively they absorb more than 97% of the total dissolved Th or Am concentrations. This approach would appear feasable and would represent a worthwhile savings in radiochemistry effort.

The fractions of the total actinide concentrations in the ocean at different depths which were associated with the filtered particulate phase are shown in Table 2, together with the observed range and median of the various observations. The total concentration of each actinide was the sum of those found in the filtered and particulate phases. For $^{239,240}Pu$, the total concentration could not be derived by this method since Pu was not effectively absorbed by the MnO_2 absorbers. The total concentration

was derived from $^{239,240}Pu$ profiles measured in large volume water samples collected at the same locations and times as the in-situ pump deployments.

The range of values found for all the actinides is quite wide. Some of this variability comes from inclusion of near-surface or near-bottom data. The higher suspended particulate concentrations in the euphotic zone or benthic boundary layers favor the increased actinide proportions in the particle phase. The differences between the median values, on the other hand, result from real chemical reactivity differences. For example, the median ^{241}Am particle association of 7.5% is close to an order of magnitude higher than the Pu median value. ^{230}Th and ^{228}Th show similar partition between particulate and dissolved phases. The ^{230}Th median value of 16% is possibly significantly greater than the 12.5% value observed for ^{228}Th. On the other hand, ^{232}Th is clearly much more associated with water column particles. This difference relates to the very different sources of ^{228}Th, ^{230}Th and ^{232}Th in the ocean. The former two, produced by radiogenic decay of dissolved radium and uranium, show lower particulate association. ^{232}Th is derived from the input of terrigenous particles in which much of the Th is in mineral phases which do not become involved with absorption/desorption equilibria.

We have included depth profiles of the total and particle associated concentrations of ^{241}Am and ^{230}Th in our two study locations. These are intended to demonstrate the high quality of low level actinide data which has been obtained using the large volume filtration/chemisorption technique. The full data set will be published in a forthcoming paper on actinide scavenging in the northwest Atlantic (Cochran et al., 1986). The particulate and total concentrations of ^{241}Am are plotted against depth in

Figure 1. It should be noted that the concentration scale for particulate ^{241}Am is one tenth that of the total activity scale. The corresponding ^{230}Th data are shown in Figure 2. Here the data from the two sites are plotted separately and both particulate and total concentrations are shown on the same scale.

The total concentrations of ^{241}Am and ^{230}Th in these water columns do not exceed 0.4 and 1.0 dpm/m^3 respectively (7 and 17 mBq/m^3). The particulate concentrations range about one order of magnitude lower concentration. At these concentrations, it would not be possible to have obtained sufficient analytical sensitivity without the use of the large volume in-situ pumping technique. Two features point up the sensitivity of this approach. Both are in line with the principle of oceanographic consistency referred to by Moore in a discussion of chemical oceanographic data produced by the GEOSECS program (Moore, 1984). This stated that trace constituents followed the patterns of the more abundant constituents (such as nutrients). Additionally, trace constituent patterns often characterize the various water masses in which they are measured. The first feature is the uniformity of both particulate and total concentrations of ^{241}Am and ^{230}Th in deep water. This occurs at depths greater than 2000m and is in the relatively homogeneous North Atlantic Deep Water. The second feature derives from the similarity in the shapes of the particulate and total (or, as inferred, dissolved) nuclide depth distributions. This is the situation one would expect to see with respect to the partition between the dissolved and particulate phases if some kind of equilibrium existed between the phases and there was little variation in suspended particulate concentrations throughout much of the water column. This

latter proviso is generally true of the northwest Atlantic except in surface or bottom waters where higher particle concentrations are frequently present (Brewer et al., 1976).

Acknowledgements

The field programs, equipment development and laboratory analyses were completed thanks to the skillful efforts of W. R. Clarke, D. J. Hirschberg and L. D. Surprenant. We thank the officers and crew of R. V. Endeavor for their help and cooperation on the cruises involved in theses studies.

The work at the Woods Hole Oceanographic Institution and at S.U.N.Y. (Stony Brook) was supported under contracts 25-8712 and 25-8717 respectively from Sandia Laboratories. This support is acknowledged with our thanks. This is Contribution Number 6309 from the Woods Hole Oceanographic Institution and Contribution Number 538 from the Marine Sciences Research Center.

REFERENCES

M.P. Bacon, C.-A. Huh, A.P. Fleer and W.G. Deuser, Deep-Sea Res., 32 (1985) 273.

P.G. Brewer, D.W. Spencer, P.E. Biscaye, A. Ganley, P.L. Sachs, C.L. Smith, S. Kadar and J. Fredericks, Earth Planet. Sci. Lett., 32 (1976) 393.

J.K. Cochran, H.D. Livingston, D.J. Hirschberg, L.D. Surprenant, Natural (^{232}Th, ^{230}Th, ^{228}Th) and anthropogenic (^{239,240}Pu, ^{241}Am) actinide distributions in the Northwest Atlantic, Earth Planet. Sci. Lett., submitted.

S. Honjo, J. Connell, P. Sachs, Deep-Sea Res., 27 (1980) 745.

H.D. Livingston, R.F. Anderson, Nature, (1983) 303, 228.

H.D. Livingston, D.R. Mann, S.A. Casso, D.L. Schneider, L.D. Surprenant, V. T. Bowen, J. Environ. Radioactivity (1986) in press.

H.D. Livingston, D.R. Mann, V.T. Bowen, In "Analytical Methods in Oceanography" (T.R.P. Gibb, ed.), Am. Chem. Society (1975) p. 124.

D.R. Mann, S.A. Casso, Mar. Chem., 14 (1984) 307.

D.R. Mann, L.D. Surprenant, S.A. Casso, Nuclear Instruments and Methods in Phys. Res., 223 (1984) 235.

W.S. Moore, Deep-Sea Res. 23 (1976) 647.

W.S. Moore, Nuc. Inst. Meth. in Phys. Res., 223 (1984) 459.

J.C. Moser, J. Dymond, K. Fischer, Multiple sampling OSU sediment trap: technical design and function. Limnol. Oceanog. (1986) submitted.

C.L. Winget, J.C. Burke, D.L. Schneider, D.R. Mann, Woods Hole Oceanographic Institution Technical Report (1982) WHOI-82-8.

TABLE 1

Manganese Dioxide Absorber Collection Efficiencies in Field Studies

Deployment No.	Collection Efficiency (%)	
	Thorium	Americium
1	69	71
2	73	83
3	73	85
4	80	76
5	84	94
6	85	92
7	85	72
8	86	92
9	86	92
10	87	96
11	91	95
12	93	97

TABLE 2

Fraction (%) of Total Water Actinide Concentration in Filterable Particulate Phase

^{232}Th	^{230}Th	^{228}Th	^{241}Am	$^{239,240}Pu$
51	40	7.9	25	--
50	16	9.0	9.3	0.3
59	24	24	6.9	--
--	6.0	14	7.7	1.1
62	13	21	3.1	--
--	5.0	2.0	5.3	1.6
46	16	6.0	6.5	--
61	25	7.0	7.4	3.2
11	12	7.4	11	0.4
19	11	14	9.3	0.4
49	13	22	11	1.0
60	19	22	6.1	0.6
--	7.6	14	5.3	1.4
--	31	26	8.9	1.4
--	13	11	6.0	0.9
--	38	11	15	1.0
11-62[1]	5-40[1]	2-26[1]	3-25[1]	0.3-3.2[1]
50.5[2]	16[2]	12.5[2]	7.5[2]	1.0[2]

1 - Range; 2 - Median

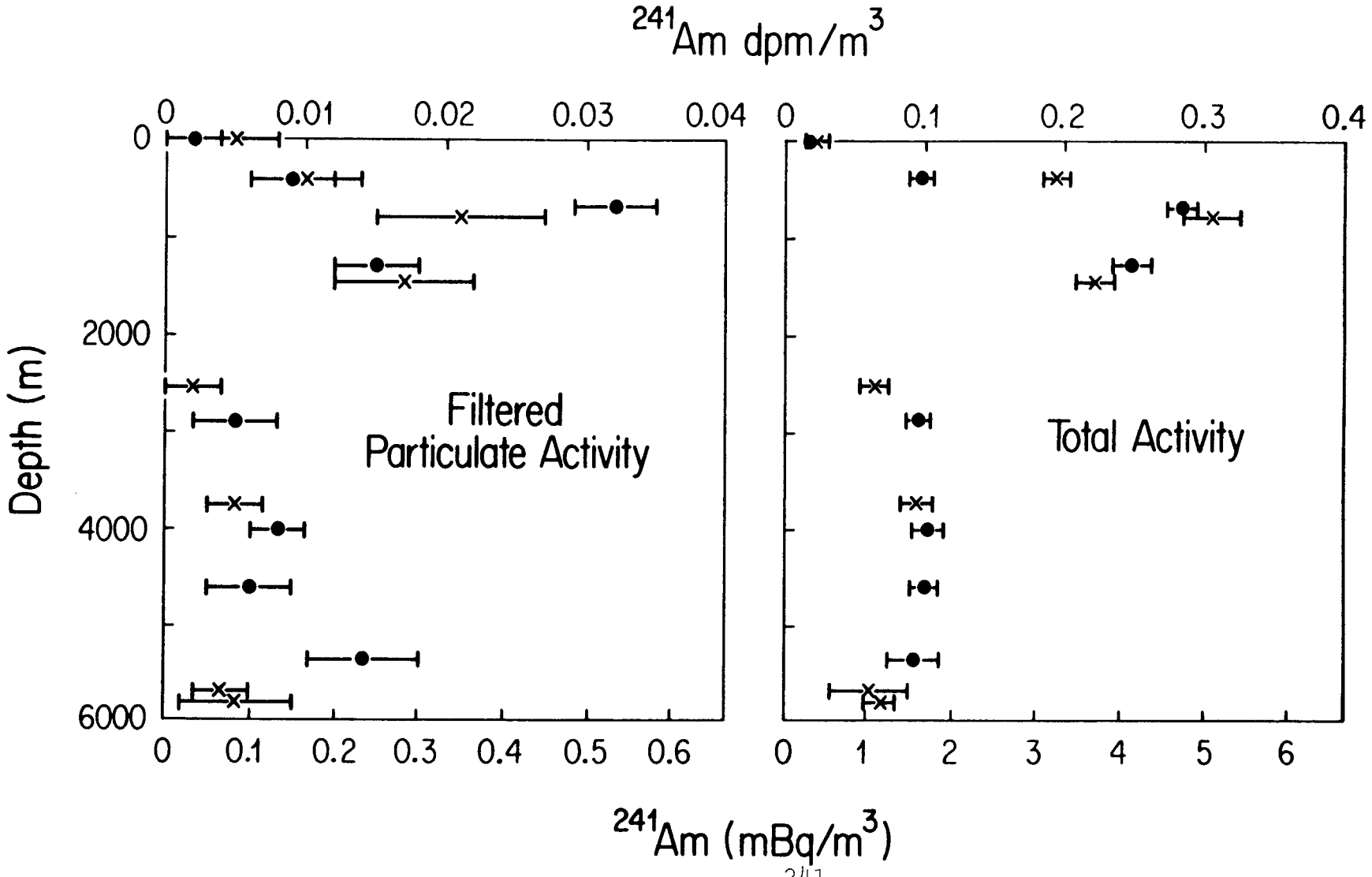

Figure 1: Particulate and total concentrations of ^{241}Am in the northwest Atlantic Ocean. Hatteras Abyssal Plain data are indicated by solid circles (●) and Nares Abyssal Plan data by crosses (X); particulate concentrations are plotted in the left-hand panel, total concentrations (dissolved and particulate) in the right-hand panel.

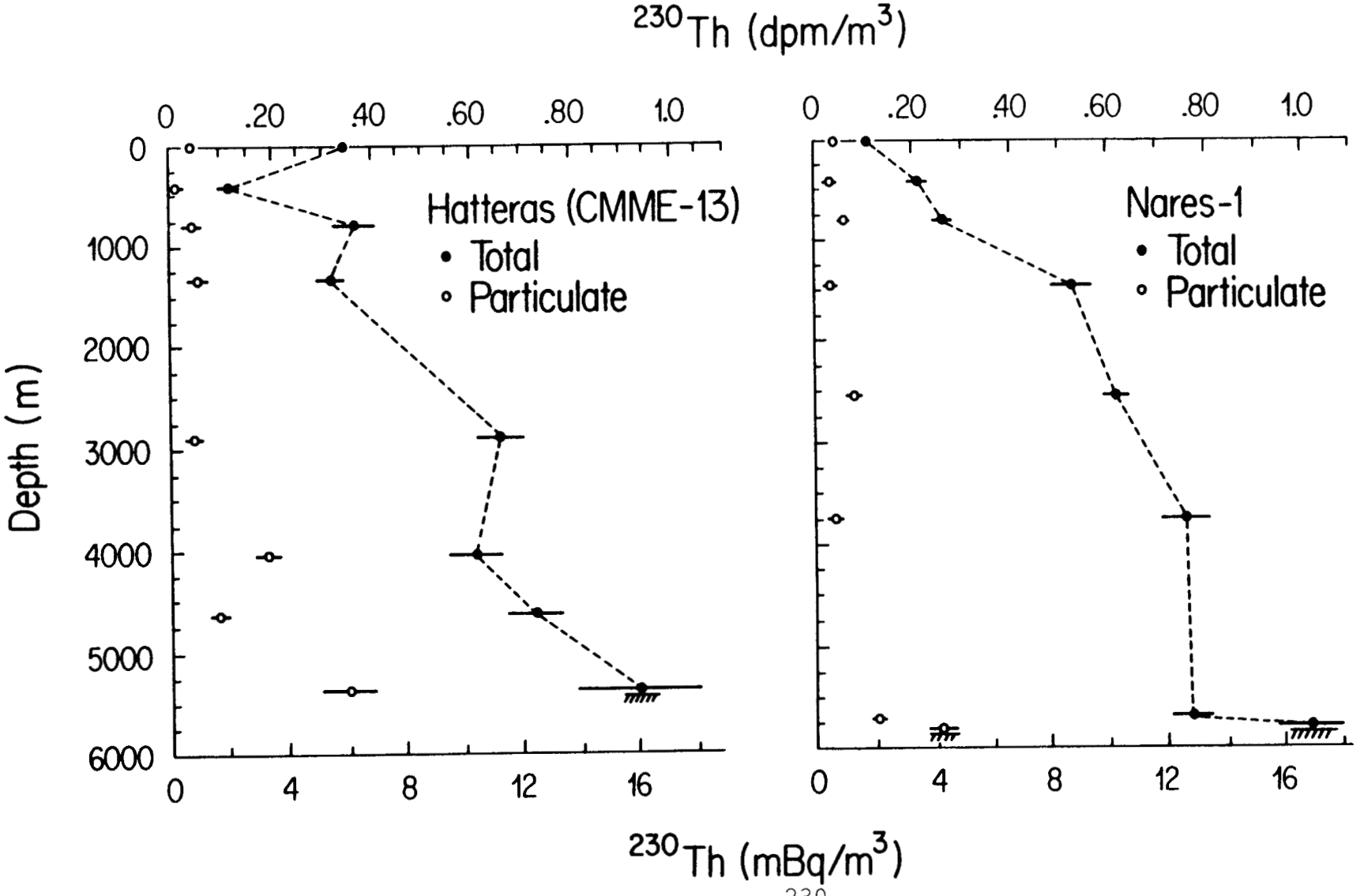

Figure 2: Particulate and total concentrations of ^{230}Th in the northwest Atlantic Ocean. Hatteras Abyssal Plain data are on the left-hand panel; Nares Abyssal Plain data are on the right-hand panel.

APPENDIX I

NARES III MOORING RECOVERY MESSAGE

J. Simpkins and K. Brooksforce

Posted: Wed Nov 5, 1986 7:23 PM EST Msg: CGIG-2706-6975
From: RV.ENDEAVOR
To: D.PILLSBURY
Subj: NARES 3

Mooring released at 12:54 3 Nov 86. Required 9 hours to recover in moderate weather, 8' seas, 15 knt winds. Could not hear the releases with the ranging receiver possibly due to poor conditions. Used the PDR as a substitute.
The releases checked out o.k. on deck. 4 Aanderaas o.k. RCM at 4800m flooded after 6 months via passthrough and is a total write-off, transmissometer also leaked. I am soaking the tape in fresh water and hope it can be read. The extra deep transmissometer seems o.k.

Sending the data tapes home in the current meters.
Sediment trap at 1435m stopped on cup 4. Trap at 4785m stopped on cup 3. Trap at 4815m had cup 4 broken.

Please tell Lolita Suprenant of W.H.O.I. that the ship will dock at Woods Hole 15 or 16 Nov prior to the end of cruise. Regret to inform her that 7 of the PCMs were missing due to tie-wrap failure. PCM G at 3900m o.k.
Bahamas port stop cancelled. ETA at URI still 16 Nov.
Regards Jay & Kathryn

DISTRIBUTION:

Harvard University (2)
Division of Applied Sciences
Attn: Allan R. Robinson
Pierce Hall
Cambridge, MA 02138

University of Washington (6)
Department of Oceanography
Attn: J. Smith
P. Jumars
G. R. Heath
P. B. Rhines
S. Riser
A. Nowell
WB-10
Seattle, WA 98195

University of Washington (2)
Applied Physics Laboratory
Attn: T. Ewart
M. Gregg
1013 N.E. 40th St.
Seattle, WA 98105

Woods Hole Oceanographic Institute (10)
Attn: M. Bacon
H. Bryden
N. Hogg
C. D. Hollister
W. J. Jenkins
H. D. Livingston
M. S. McCartney
B. Tucholke
F. Sayles
R. Schmitt
Woods Hole, MA 02543

Webb Research Corporation
Attn: D. C. Webb
769 Palmer Ave
Falmouth, MA 02540

University of Rhode Island (7)
Department of Oceanography
Attn: D. R. Kester
R. Mukherji
H. Rossby
A. Driscoll
K. Hinga
M. Wimbush
Kingston, RI 02881

Atlantic Oceanographic Laboratory (5)
Bedford Institute of Oceanography
Attn: M. Bewers
G. Needler
G. Vilks
A. Clarke
B. Hargrave
PO Box 1006
Dartmouth, Nova Scotia
B2Y 4A2
CANADA

Columbia University (4)
Lamont-Doherty Geological Observatory
Attn: P. E. Biscaye
H. J. Simpson
D. E. Hayes
R. Anderson
Palisades, NY 10964

Pacific Marine Environmental Lab/NOAA
Attn: S. P. Hayes
3711 15th Ave. NE
Seattle, WA 98105

Scripps Institution of
Oceanography (12)
Attn: R. Hessler
M. M. Mullin
R. L. Salmon
K. L. Smith
A. A. Yayanos
F. N. Spiess
V. C. Anderson
P. P. Niiler
J. L. Reid
R. Davis
L. Armi
C. Cox
La Jolla, CA 92093

Oregon State University (3)
School of Oceanography
Attn: D. Pillsbury
W. Pearcy
T. Beasley
Corvallis, OR 97331

Bettis Atomic Power Laboratory (2)
Attn: C. A. Detrick
J. L. Rider
PO Box 79
West Mifflin, PA 15122

DISTRIBUTION (Cont):

Texas A&M University
Department of Oceanography
Attn: W. Nowlin
College Station, TX 77843

Princeton University (4)
Geophysical Fluid Dynamics Lab/NOAA
Attn: M. D. Cox
G. Mellor
K. Bryan
J. Sarmiento
Princeton, NJ 08540

Yale University
Department of Geology and Geophysics
Attn: K. Turekian
221 KGL
New Haven, CT 06520

Battelle Pacific Northwest Laboratory
Attn: W. L. Templeton
PO Box 999
Richland, WA 99352

Naval Oceanographic Office
Attn: A. Lowrie
Code 7221
NSPL Station, MS 39522

National Center for Atmospheric
Research (3)
Attn: F. R. Bretherton
W. R. Holland
A. J. Semtner
Boulder, CO 80307

JK Associates, Ltd.
Attn: J. Kelly
3408 Bonnie Rd
Austin, TX 78703

W. Simmons (5)
PO Box 412
Woods Hole, MA 02543

University of Rhode Island
Department of Civil Engineering
Attn: A. J. Silva
Kingston, RI 02281

Bowdin College
Environmental Studies Program
Attn: E. P. Laine
Brunswich, ME 04011

US DOE (2)
Office of Civilian Radioactive Waste
Management RW-24
Attn: C. R. Cooley
C. Heath
Washington, DC 20545

US DOE
Albuquerque Operations Office
Attn: W. Forster
PO Box 5400
Albuquerque, NM 87115

US Congress
Office of Technology Assessment
Attn: W. D. Barnard
Washington, DC 20510

Battelle Memorial Institute (2)
Battelle Project Management Division
Attn: R. Best
B. Rawles (ONWI Library)
505 King Ave. C 20545
Columbus, OH 43201

Office of Science & Technical Policy
Natural Resources & Commercial Services
Attn: P. M. Smith
Washington, DC 20500

H. Herrmann
50 Congress St., Room 1045
Boston, MA 02109

Johns Hopkins Applied Physics Lab. (2)
Attn: R. Henrick
C. Saraban
Johns Hopkins Road
Laurel, MD 20707

National Ocean Science Admin.
Attn: A. Malahoff
6001 Executive Blvd
Rockville, MD 20852

MAFF Directorate of Fisheries
Research (4)
Fisheries Laboratory
Attn: R. Dickson
P. Gurbutt
H. Hill
J. Shepherd
Lowestoft, Suffolk, NR33 OHT
UNITED KINGDOM

DISTRIBUTION (Cont):

MAFF Fisheries Radiobiological Lab (2)
Hamilton Dock
Lowestoft, Suffolk
Attn: R. J. Pentreath
D. S. Woodhead
UNITED KINGDOM

Institute Oceanographic Sciences (10)
Attn: S. Thorpe
J. C. Swallow
W. J. Gould
M. Angel
M. Fasham
N. Merrett
A. Rice
J. Crease
A. S. Laughton
P. M. Saunders
Brook Road
Wormley
Godalming
Surrey
GU85UB
UNITED KINGDOM

Centre Oceanologique de Bretagne (4)
CNEXO
Attn: F. Madelain
M. Sibuet
R. le Suave
Y. Desaubies
BP No. 337-29273
Brest
FRANCE

Laboratoires International de Radioactivite Marine (7)
Agence Internationale de l'Energie Atomique Musee Oceanographique
Attn: S. W. Fowler
R. Cherry
R. Fukai
M. Heyraud
A. Walton (3)
MONACO

G. A. M. Webb
National Radiobiological Protection Board
Harwell
Didcot
OXCON OXLL ORQ
UNITED KINGDOM

Nederlands Institut voor Onderzoek der Zee
Attn: W. Helder
Postbus 59
Texel
THE NETHERLANDS

OECD Nuclear Energy Agency
Attn: E. Wallauschek
38 Bd Suchet
F75016 Paris 16e
FRANCE

Netherlands Energy Research Foundation
Division of Health Protection
Attn: A. W. van Weers
Esterduinweg 3 PO Box 1, 1755 2G
Petten, NH
THE NETHERLANDS

Radiological Protection and Safety Department
Attn: A. O. de Bettencourt
Estrada Nacional No. 10
Sacavem
PORTUGAL

Swedish Meteorological and Hydrological Institute
Attn: B. Vasseur
Folkborgsvagen 1
S-60236 Norrkoping
SWEDEN

F. Nyffeler
Universite de Neuchatel
Lab Geologie
11 Rue Emile Argand
2000 Neuchatel
SWITZERLAND

W. Feldt
Isotopen Laboratorium der Bundesforschungsanstalt fur Fisherei
Wustland 2
D-2000 Hamburg 55
FEDERAL REPUBLIC OF GERMANY

Laboratoire de Geologie
Ecole Normale Superieure
Attn: J. C. Gaury
46 Rue D'Ulm
75230 Paris CEDEX 05
FRANCE

DISTRIBUTION (Cont):

Deutsches Hydrographisches Institut (4)
Attn: E. Mittelstaedt (2)
D. Schulte
H. Kaulsky
Postfach 220
2000 Hamburg 4
FEDERAL REPUBLIC OF GERMANY

CED
Joint Research Centre (2)
Attn: C. N. Murray
F. Girardi
Ispra Establishment
21020 Ispra (Varese)
ITALY

Marine Sciences Research Center
SUNY
Attn: K. Cochran
Stony Brook, NY 11794

Dept. of Earth & Planetary Sciences
Attn: J. M. Edmond
Massachusetts Institute of Technology
Cambridge, MA 02139

Commission Communautes Europeens (2)
200 rue de la Loi
Attn: A. Cricchio
K. Schaller
B-104 9
Bruyettes, Belqique

Dept. of Oceanography
Attn: C. Garrett
Dalhousie University
Halifax, Nova Scotia
CANADA

Pacific Marine Environmental Lab/NOAA
Attn: B. A. Taft
3711 15th Ave. SE
Seattle, WA 98105

Dept. of Oceanography
Attn: G. L. Weatherly
Florida State University
Tallahassee, FL 32303

Skidaway Institute of Oceanography (2)
Attn: L. B. Atkinson
K. Bush
PO Box 13687
Savannah, GA 31416

1510 J. W. Nunziato
1511 D. K. Gartling
1511 L. A. Mondy
1512 D. C. Reda
1512 K. L. Erickson
1530 L. W. Davison
1543 J. L. Krumhansl
5163 D. F. McVey
6330 R. W. Lynch
6300 W. D. Weart
6334 D. R. Anderson (25)
6334 S. G. Bertram
6334 L. H. Brush
6334 D. P. Garber
6334 L. S. Gomez (2)
6334 E. S. Hertel
6334 R. D. Klett
6334 S. L. Kupferman (10)
6334 M. G. Marietta (2)
6334 C. M. Percival
7530 T. B. Lane
8024 M. A. Pound
3141 C. M. Ostrander (5)
3151 W. L. Garner
3154-3 C. H. Dalin (28)
For DOE/TIC (Unlimited Release)